UNIVERSITY OF LIVERPOOL

Expression and regulation of key lysosomal effectors in RPE cells – Implications for Age-related Macular Degeneration (AMD)

Umar Sharif

Thesis submitted in accordance with the requirements of the University of Liverpool for the degree of Doctor in Philosophy

November 2015

Doctor of Philosophy Declaration

I hereby declare that this dissertation is a record of work carried out in the Institute of Ageing and Chronic Disease at the University of Liverpool during the period of December 2011 to November 2015. This dissertation is original in content except where otherwise stated.

November 2015

.....

(Umar Sharif)

The work presented in this thesis is dedicated to my parents, Tariq Mamood and Rubina Kausar. Without your unconditional love and support, I would not have been able to achieve what I have today. I am honoured to have you as my parents and love you with all my heart. Thank you for everything.

A special dedication also goes out to my two sisters and my younger brother, who believed in me and kept me going through the hard times.

Last but not least, a special dedication goes out to my late uncle, Shabbir Hussain, who passed away in July, 2015. You will always be missed and loved. I hope I have made you proud!

Acknowledgements

First and foremost, all praise and thanks to Almighty God as due to His blessings, I have been able to complete this research successfully. The PhD study that I undertook around 4 years ago has been the most challenging and significant academic challenge I have ever faced. I sincerely would like to express my appreciation to everyone who has contributed either directly or indirectly to help my dream become a reality.

I would like to express my sincere appreciation and gratitude to my supervisor, Dr Luminita Paraoan. Her selfless time, continuous support and motivation helped me pull through and achieve my goal. Her patience, vast knowledge and guidance have not only made me a better scientist, but more importantly a better human being. I could not have asked for a better supervisor. I would also like to thank Professor Simon Harding and Professor Ian Grierson. You were always there when needed and the experience and advice that you gave was always very valuable. I would also like to thank the team at Leeds Institute of Biomedical and Clinical Sciences such as Professor Chris Inglehearn and Dr Manir Ali, for giving up time and allowing me the opportunity to broaden my scientific horizons through the genetics work that was performed in collaboration. I have to thank all the exudative AMD patients that donated their blood and allowed this genetic research to be conducted.

A special thanks to my laboratory colleagues such as Dr Joe Butler, Dr Paul Kay, Dr Raheela Awais, Dr Christopher Myerscough, Sam McDonnell, Wasu Supharattanasitthi and Nur Musfirah Ahmed. The work, the ideas we shared and the time we spent together was amazing and something I will treasure for the rest of life. I know I have made a special group of friends. Also, people such as Dr George Sakellariou, Dr Kevin Hamill and Tiago Ramos were always there as a source of encouragement for me. The advice and help provided was always appreciated.

I would also like to thank all my friends that helped me remain focused on goal of achieving my PhD. There are so many of you but a special mention goes to Mohamad Madi, who began his own journey towards a PhD degree at a similar time to me. Your encouragement, help and time we spent together during these past years will remain close to my heart and I will always see you my big brother.

Last but not least, I would like to show my appreciation to my parents, two sisters and younger brother, who always supported me in helping me fulfil my potential – Always know that everything I am today is ultimately due to you.

Table of contents

List of figures

Chapter 1 – Introduction

Chapter 2 – Materials and Methods

Chapter 3 – Expression and activity regulation of cathepsins in RPE cells

Chapter 4 - Analysis of the genetic association between the cysteine protease inhibitor CST3 and exudative AMD

List of tables

Chapter 2 – Materials and Methods

Chapter 3 – Expression and activity regulation of cathepsins in RPE cells

Chapter 4 - Analysis of the genetic association between the cysteine protease inhibitor CST3 and exudative AMD

List of abbreviations

Retinal pigmented epithelium	(RPE)
Photoreceptor outer segments	(POS)
Extracellular matrix	(ECM)
Interphotoreceptor matrix	(IPM)
Bruch's membrane	(BrM)
Reactive oxygen species	(ROS)
Inner collagenous layer	(ICL)
Elastic layer	(EL)
Outer collagenous layer	(OCL)
Choriocapillaris basement membrane	(CbM)
Blood retina barrier	(BrM)
Bicarbonate	(HCO_3^-)
Glucose transporters	(GLUT)
Carbon dioxide	(CO_2)
Retinal pigment epithelium specific protein	(RPE-65)
Age-related macular degeneration	(AMD)
Alzheimer disease	(AD)
N-retinylidene-N-retinylethanolamine	(A2E)
Fibroblast growth factors	(FGF)
Insulin-like growth factor-I	(IGF-I)
Platelet epithelial derived factor	(PEDF)
Matrix metalloproteinase	(MMP)

Inhibitor of matrix metalloproteinase	(TIMP)
Vascular endothelial growth factor	(VEGF)
Choroidal neovascularisation	(CNV)
Proteoglycans	(PG)
Glycosaminoglycan	(GAG)
Advanced glycation end products	(AGEs)
Carboxymethyl lysine	(CML)
Carboxyethyl lysine	(CEL)
Basal linear deposits	(BlinD)
Messenger ribonucleic acid	(mRNA)
Deoxyribonucleic acid	(DNA)
Ubiquitin carboxyterminal hydrolase-1	(UCHL-1)
Oligosaccharryltransferase-48	(AGE-R1)
80K-H	(AGE-R2)
Galectin-3	(AGE-R3)
Receptor for AGEs	(RAGE)
Mitogen-activated protein kinase	(MAPK)
Nuclear factor kappa B	(NF-κB)
Interleukin 1β	(IL-1β)
Interleukin 18	(IL-18)
Polycyclic aromatic hydrocarbons	(PAHs)
Genome wide association study	(GWAS)
Complement factor H	(CFH)

Pleckstrin homology domain containing family A member 1	(PLEKHA1)
Age-related maculopathy susceptibility 2	(ARMS2)
High-temperature requirement A serine peptidase 1	(HTRA1)
Apolipoprotien E	(ApoE)
Basal laminar deposits	(BlamD)
Oxygen	(O_2)
Adenosine triphosphate	(ATP)
Hydrogen peroxide	(H_2O_2)
Nicotinamide adenine dinucleotide phosphate	(NAPDH)
Ubiquitin proteasome system	(UPS)
Lysosome-associated membrane proteins	(LAMPs)
Chaperone-mediated autophagy	(CMA)
Trans-Golgi network	(TGN)
Synaptotagmin VII	(Syt VII)
Sphingomyelinase	(aSMase)
Lysosomal membrane permeabilization	(LMP)
L-Leucyl-L-leucine methyl ester	(LLOMe)
Cysteine	(Cys)
Histidine	(His)
Aspartic acid	(Asp)
Threonine	(Thr)
Glycine	(Gly)
Serine	(Ser)

Endoplasmic reticulum	(ER)
Mannose-6-phosphate	(M6P)
Single nucleotide polymorphism	(SNP)
Multivesicular bodies	(MVB)
Cellular retinaldehyde-binding protein	(CRALBP)
Dulbecco's modified Eagle's medium	(DMEM)
Fetal calf serum	(FCS)
Matrigel™	(MG)
Phosphate buffered saline	(PBS)
Double-distilled water	(ddH_2O)
Sodium dodecyl sulfate-polyacrylamide gel electrophoresis	(SDS-PAGE)
Bovine serum albumin	(BSA)
Enhanced chemilumininescent	(ECL)
Glyceraldehyde 3- phosphate dehydrogenase	(GAPDH)
7-methoxycoumarin-4-acetic acid	(MCA)
Amino-4-trifluoromethyl coumarin	(AFC)
Relative fluorescent unit	(RFU)
Potassium permanganate	($KMnO_4$)
3-amino-9-ethylcarbozole	(AEC)
Region of interest	(ROI)
Tris-borate-EDTA	(TBE)
Deoxynucleotide triphosphates	(dNTPs)
Polymerase chain reaction	(PCR)

Exome Sequencing Project	(ESP)
Dideoxyribonucleotide triphosphates	(ddNTPs)
Microtubule-associated protein light chain	(LC3)
Serine residue at position 536	(Ser536)
Analysis of Variance	(ANOVA)
Hardy Weinberg Equilibrium	(HWE)
Odds ratios	(OR)
6-hydroxydopamine	(6-ODHA)
Quinolinic acid	(QA)
High mobility group box 1	(HGMB1)

List of publications

Butler, J.M., **Sharif, U.**, Ali, M., McKibbin, M., Thompson, J.P., Gale, R., Yang, Y.C., Inglehearn, C., and Paraoan, L. (2015). A missense variant in CST3 exerts a recessive effect on susceptibility to age-related macular degeneration resembling its association with Alzheimer's disease. Human genetics **(Joint first author)** (Published article in appendix 2).

List of published abstracts/presentation and international meetings

L. Paraoan, **U. Sharif**, P. Kay, I. Grierson, Y.C. Yang, S.P. Harding,
Effects of advanced glycation end-products (AGEs) on retinal pigment epithelial (RPE) cells lysosomal function: implications for age-related macular degeneration (AMD). Association for Research in Vision and Ophthalmology (ARVO) 2015, Denver, Colorado, USA

U. Sharif, J.M. Butler, Y.C. Yang, S.P. Harding, L. Paraoan
Cysteine proteases expression and secretion by retinal pigmented epithelium (RPE). Association for Research in Vision and Ophthalmology (ARVO) 2014, Orlando, Florida, USA

P. Kay, **U. Sharif**, Y.C. Yang, L. Paraoan
Aging alter the proteolytic activity of human retinal pigment epithelium – implications for the pathogenesis of age-related macular degeneration.
International Society for Eye Research (ISER) 2012, Berlin, Germany

Luminita Paraoan, Paul Kay, **Umar Sharif**, Paul Hiscott, Donna Gray, Arvydas Maminishkis, Yit C. Yang
AGEs decrease cystatin C secretion and alter its polarity in the retinal pigment epithelium – contribution to age-related retinal proteolytic imbalance. Healthy Ageing: From Molecules to Organisms Conference 2015, Cambridge, UK

Abstract

The retinal pigmented epithelium (RPE) is a monolayer of highly specialised polarised post-mitotic cells that help maintain retinal homeostasis. Accumulation of advanced glycation end products (AGEs), a phenomenon of the ageing process, in RPE and Bruch's membrane (BrM) contribute to the development of age-related macular degeneration (AMD), the leading cause of blindness in the western world. AGEs induced oxidative insult which causes proteins to misfold and become dysfunctional. Removal of misfolded dysfunctional proteins by the lysosome is critical for cell survival.

Key effectors of lysosomal enzymatic activity are cathepsins. In addition to lysosomal function, cathepsins also exert extracellular functions. Cathepsins activity is regulated by endogenous inhibitors and the balance between proteases and their inhibitors regulate several crucial cellular processes such as autophagy, apoptosis and extracellular remodelling. The most abundantly expressed protease inhibitor from the RPE is cystatin C. In addition, cystatin C, an inhibitor of cathepsins B, L and S, is susceptible to age-related alterations. Furthermore, the polymorphism rs1063049 in the cystatin C gene (CST3) is genetically associated with susceptibility to exudative AMD.

The understanding of the effects of ageing on the balance between cathepsins and their inhibitors and how dysregulation could contribute to pathological changes associated with AMD is of crucial importance. Therefore, the overall aim of this present study is: 1) to investigate the endogenous expression and secretion of cathepsins B, L and S in RPE cells; 2) to assess the impact of age-related stresses on expression/processing and activity of cathepsins and 3) to further investigate the genetic association of CST3 with exudative AMD.

Immunoblot and immunohistochemical (IHC) analysis confirmed the presence cathepsins B, L and S in RPE cells. In addition, immunoblot analysis of conditioned media detected the presence of cathepsins B, L and S, indicative of their secretion. RPE cells exposed to AGEs exhibited alterations in cathepsin L, which showed decreased protein and activity levels. Finally, the genetic analysis study showed that the rs1063049 was associated with exudative AMD in a recessive manner.

The results presented in this thesis showed that cathepsins are susceptible to age-related changes in RPE cells. Alterations of cathepsins may impair important lysosomal processes such as autophagy, which may influence the age-related dysfunction of RPE. In addition, the genetic association of CST3 gene with exudative AMD further supports that proteolytic dysregulation involving cathepsins and cystatin C is a crucial event that contributes to RPE dysfunction and subsequent development of disease states such as AMD.

Chapter 1 - Introduction

1.1 - The Eye

1.1.1 Overview of the structure and function of the human eye

The eye is the organ that provides the sense of vision by converting light waves into electrical impulses that are passed onto the brain for analysis as visual images. The eye is located in a pear shaped cavity of the skull known as the 'orbit' (Snell and Lemp, 1998). The orbit contains openings that allow blood vessels and nerves such as the optic nerve to pass through it. The orbit also contains fatty tissue which offers protection to the eye, and extra ocular muscles which help regulate movement (Hogan et al., 1971; Snell and Lemp, 1998). The human eye itself is not a perfectly shaped sphere but rather a two-piece unit which consists of a smaller anterior sphere (corneal unit) fused to a larger posterior sphere (sclerotic unit). Both corneal and sclerotic units are connected together by a ring called the limbus. The corneal unit makes up a 1/6th of the eye shape whilst the remaining 5/6th is made up of the sclerotic unit (Bron et al., 1997; Snell and Lemp, 1998) (Figure 1.1).

The eyeball is made up by three coats: the external, the middle (uvea) coat and the innermost coat (Bron et al., 1997; Snell and Lemp, 1998). The external coat, which consists of the cornea and sclera, protects the eye from damage as it is strong and rigid. The middle coat (uvea) consists of the ciliary body and the iris as well as blood vessels such as the choroid which provide nutrition to the eye. The innermost coat of the eye consists of the delicate neuroretina where light is received and converted into electrical impulses for generation of vision. Together, the outer and middle coats of the eye work to protect and maintain the delicate neuroretina (Bron et al., 1997). Within the ocular layers, transparent gelatinous fluids called the aqueous humour and vitreous body exist (Bron et al., 1997). The aqueous humour is a clear fluid contained in the space between the cornea and the lens. The vitreous body is present behind the lens and makes contact with the retina. The vitreous is much larger than the aqueous humour and occupies around 4/5th of eyeball volume. A major function of these

transparent fluids is to exert pressure and help maintain eye shape (Bron et al., 1997; Snell and Lemp, 1998).

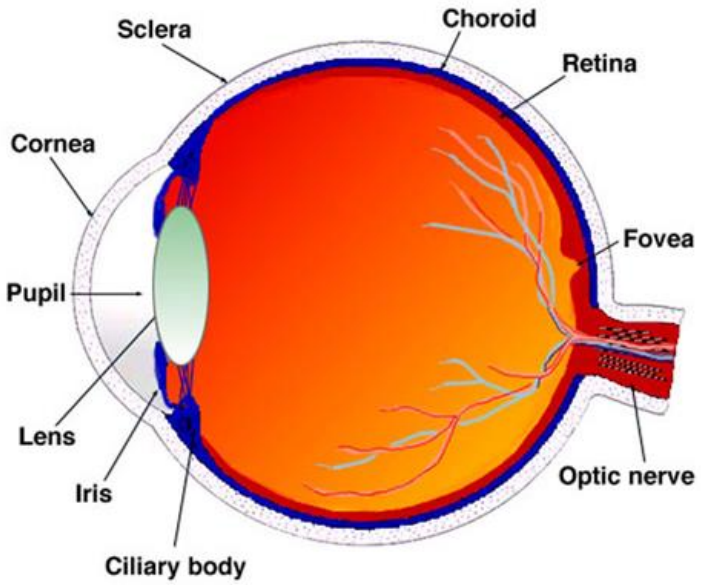

Figure 1.1: Gross anatomy of the human eye in a vertical sagittal section. The 3 coats of the eye are visible: The cornea and sclera together form the outer coat of the eye. The middle later (blue) consists of blood vessels such as the choroid. The innermost layer (red) consists of the retina, of which the fovea represents the central region (http://webvision.med.utah.edu/imageswv/sagitta2.jpeg).

The cornea is a transparent specialised tissue whose primary function is to allow the passage of light into the eye. The cornea is an avascular tissue that contains collagen fibrils specially packed in a homogenous manner. The cornea forms the principal refractive tissue and along with the lens, helps focuses light onto the retina. The cornea is responsible for approximately 70% of the light refraction and this high refractive power is due to the convex external surface and concave internal surface (Bron et al., 1997). Once light is refracted by the cornea, it moves through the aqueous humour to reach the iris, the pupil and then the lens, where light is refracted further.

The iris, a thin circular structure, functions as a shutter that regulates the amount of light reaching the interior of the eye by controlling the size and diameter of the pupil (Hogan et al., 1971; Snell and Lemp, 1998). The ciliary body, which lies behind the iris, is a specialised ring of tissue consisting of

ciliary muscles and ciliary processes. The ciliary body is attached to ciliary zonules from which the lens is suspended. Ciliary processes are involved in producing aqueous humour while the ciliary muscles change the refractive power of the lens.

The lens is a transparent, biconvex structure with an elliptical shape that has the ability to change which helps refract and focus light. By changing shape, the lens is able to alter the focal distance of the eye therefore being able to focus on objects at different distances. In order to see short distance objects, the ciliary muscles contract making the lens rounder which shortens the focal distance. For far distance objects, the ciliary muscles relax and flatten the lens which increases focal distance. The eye is considered to be divided into anterior and posterior segments at the position of the lens (Bron et al., 1997; Hogan et al., 1971). Light refracted by the lens will then pass through the vitreous body and arrive at the neuroretina region. The vitreous body allows the unhindered passage of light and contains phagocytic cells which help remove unwanted debris from the visual field (Purves, 2012).

The passage of light thus far can be summarised as follows: The transparent cornea significantly refracts light as it enters the eye after which it passes uninterrupted through the aqueous humour and the pupil. Light is again refracted at the lens where it then passes through the vitreous body without any interference and arrives at the neuroretina region.

1.1.2 Neuroretina

The neuroretina is a thin sensory tissue that internally is in contact with the vitreous body and externally attached to the retinal pigmented epithelium (RPE) monolayer, which together make up the retina. The retina covers the posterior eye and extends as far anteriorly into a region known as the ora seratta. The retina has 10 distinct layers, 9 of which are neuronal and make up the neuroretina (Bron et al., 1997; Snell and Lemp, 1998) (Figure 1.2). The central region of the neouretina is called the macula lutea, which is a yellow blood vessel-free spot and in its centre is the fovea. The fovea is a small central depression of approximately 5mm in diameter and is composed

of a type of photoreceptor known as cones that are important for central vision (Curcio et al., 1990).

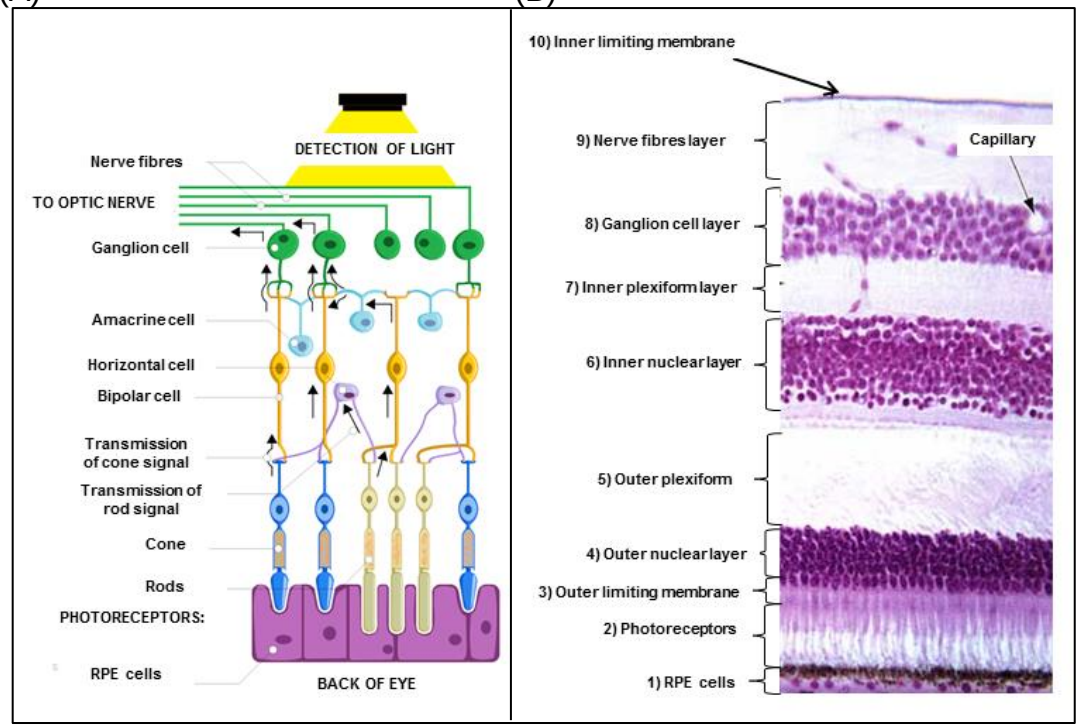

Figure 1.2: Cell types and layers that constitute the retina. (A) A diagrammatic representation of the different cell types found in the retina including the photoreceptor cells, bipolar, amacrine and ganglion cells. (B) A histological section diagram showing the 10 different layers that make up the retina (Picture adapted from https://www.pinterest.com/pin/518547344564805253/).

The 3 main types of neuronal cells found in the retina are the photoreceptors, bipolar cells and ganglion cells. A three-neuron chain of photoreceptor-bipolar-ganglion cells is the main route that information flows from the photoreceptors to the optic nerve. In addition, two other types of neurons, horizontal and amacrine cells, are also responsible for lateral interactions within the retina (Purves, 2012; Snell and Lemp, 1998).

In the retina, there are two main types of photoreceptors: the rods and cones. The rods are responsible for low light vision whereas the cones are responsible for colour vision and high visual acuity. Photoreceptors are made up of two parts: the inner segment, which contains the nucleus and synaptic terminals that come in contact with bipolar cells and an outer

segment, that lies adjacent to the epithelial RPE layer and contains the photosensitive pigment (Snell and Lemp, 1998). When light is absorbed by the photosensitive pigment in the outer segments of photoreceptors, a signalling cascade is initiated that leads to a change of cellular membrane potential (Ridge et al., 2003). This membrane potential change causes the release of neurotransmitters from the photoreceptor synapses to bipolar cells. The synapsis between the photoreceptors terminals and bipolar cells occurs in the outer plexiform layer. The cell bodies of the photoreceptors and the bipolar cells lie in the outer nuclear layer and inner nuclear layer respectively. The bipolar cells then make synaptic contacts with dendritic processes of ganglion cells in the inner plexiform layer. The axons of the ganglion cells form the optic nerve and carry information to the brain for image processing (Purves, 2012).

The retina is arranged in an inverted manner i.e. the retinal neurons are situated in between the lens and the photoreceptors. This arrangement can be considered as disadvantageous as retinal neurons can scatter some light and therefore lead to loss of light and image blur. A better option may be to place the neurons behind the photoreceptors so that they are out of the way of incoming light. However, there are many advantages of why the vertebrate eye has evolved in an inverted manner such as being a space-saving mechanism. It is believed that the space-saving mechanism is advantageous as it allows relatively large eyes to fit into a small head (Kroger and Biehlmaier, 2009). To overcome the light scattering effects of the inverted arrangement, the retina contains cells such as Müller cells which act as light guides. Muller cells pick up visual information and guide it undistorted through the neuronal cells to the photoreceptors therefore minimising loss of signal (Franze et al., 2007). In addition to space-saving, evolution places photoreceptors in close proximity with the RPE layer. The RPE has a special relationship with the photoreceptors and is involved in many important functions that help maintain retina homeostasis.

1.2 - Retinal pigmented epithelium (RPE) and Bruch's membrane (BrM)

The RPE is a specialised monolayer of polarised cells that make contact with the photoreceptor outer segments (POS). The RPE consists of post-mitotic hexanocuboidal epithelial cells that play a critical role for protection, survival and function of photoreceptors (Strauss, 2005; Zinn and Marmor, 1979). RPE functions that help maintain retinal homeostasis include establishment of an outer blood-retina barrier, transport of nutrients between the choroid and photoreceptors, phagocytosis of spent POS, role in the visual cycle, and absorption of scattered and reflected light (Bok, 1993; Strauss, 2005) (RPE functions are described in detail in section 1.2.3). Typically, the apical surface of an epithelium faces an open lumen but the RPE differs as its apical surface is in immediate contact with an extracellular matrix (ECM) known as the interphotoreceptor matrix (IPM) (Hollyfield, 1999; Rohlich, 1970). The highly specialised photoreceptors are surrounded by the IPM establishing a close structural interaction with the RPE (Tien et al., 1992). On the basal side, the RPE cells are in contact with an underlying basement membrane called the Bruch's membrane (BrM). The importance of the BrM in eye physiology is highlighted by its strategic position and by the functions that it carries out. The BrM, along with the RPE, forms a selective barrier that helps separate the neuroretina from the choroidal blood and controls diffusion of molecules between the RPE and choroid (Booij et al., 2010). The BrM is also involved in helping RPE cells adhere, migrate and differentiate (Del Priore et al., 2002; Del Priore and Tezel, 1998; Gong et al., 2008). Thus, in normal physiology, the RPE along with the BrM serves vital functions for the integrity of the retinal health and abnormalities could lead to specific disease development.

1.2.1 - Anatomy of the RPE

The RPE monolayer has a cobblestone appearance and it extends from the optic nerve to the boundaries of the retina known as the ora seratta. Interestingly, RPE cells are uniquely adapted to different functional requirements of a certain region (Burke and Hjelmeland, 2005). The RPE

cells in the macula region measure about 14μm in diameter, 12μm tall and are more densely packed with approximately 4500 cells/mm^2 appearing tall and narrow. Moving towards the periphery, cells appear wider and flatter with a diameter of 60μm seen in cells at the ora seratta. Also in the periphery, cells become less densely packed with approximately 1500 cells/mm^2 (Hogan et al., 1971; Panda-Jonas et al., 1996).

RPE cells have a cuboidal shape and differentiate into polarised cells where organelles are found in specific areas of the cells. RPE subcellular structure examination shows the presence of a nucleus around 12μm in diameter located in the basal aspect of the cell. RPE cells located in the ora seratta are often multinucleated (Hogan et al., 1971). The RPE cells also contain many mitochondria, located between the basal membrane and nucleus, reflecting their high metabolic capacity. Viewed by electron microscopy, mitochondria in the RPE appear to be around 0.5μm in length (Hogan et al., 1971). RPE cells are susceptible to oxidative insult due to their high metabolic activity as well as the fact that they are situated in a highly oxidising environment and exposed to high levels of visible light (Beatty et al., 2000). The RPE cells contain an array of antioxidants such as catalase and superoxide dismutase that help protect them against oxidative damage (Newsome et al., 1994). In addition, the presence of melanosomes granules (~2μm long) at the apical side contributes to the protective mechanisms that exist in RPE cells against oxidative insult (Bron et al., 1997; Rozanowska et al., 1999). The apical membrane of RPE also forms two types of specialised microvilli: long microvilli (5-7μm) that contribute to epithelial transport and shorter microvilli that project into the IPM to form sheaths around rod and cone photoreceptor outer segments (Bok, 1993). The apical surface of RPE cells carry out the daily phagocytosis of exhausted POS tips (Strauss, 2005).

The basolateral surface is connected to a specialised acellular layer BrM separating the RPE from the choriocapillaries (Hogan et al., 1971). The basal surface membrane displays convoluted infoldings that help attach the RPE to the BrM as well as increasing the surface area for metabolic

exchange and secretion with the underlying blood supply (Zinn and Marmor, 1979) (Figure 1.3).

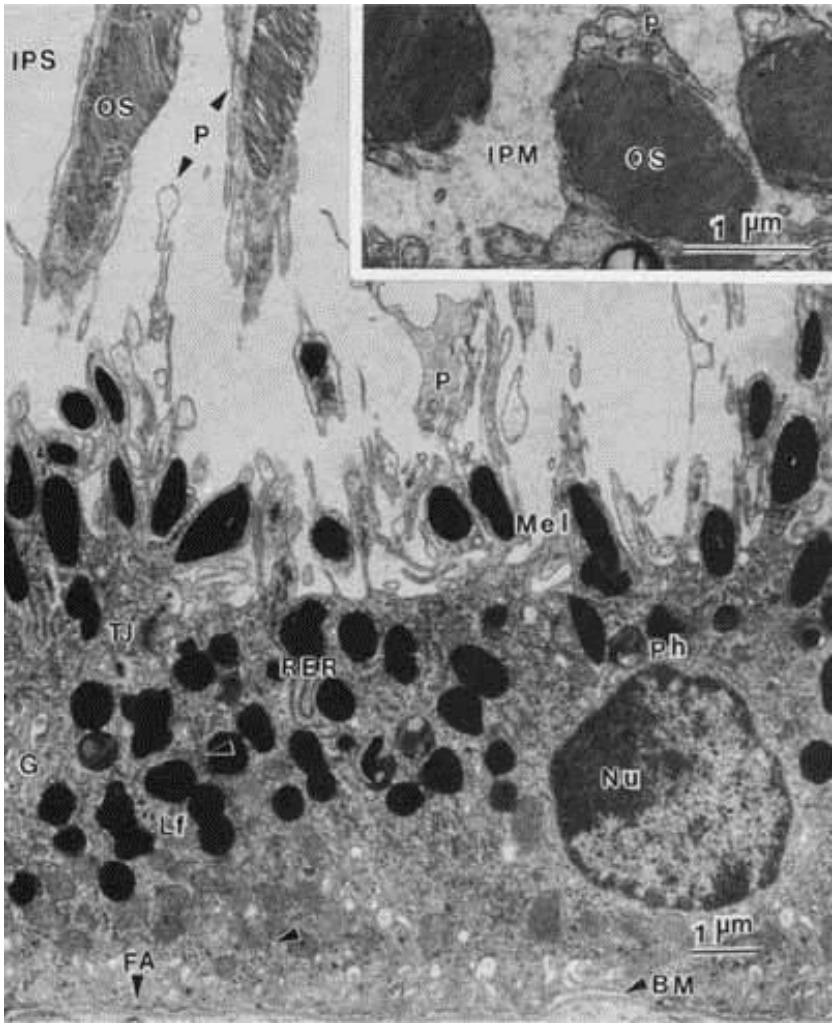

Figure 1.3: Transmission electron microscopy image of RPE in transverse plane. Features of an RPE cell include: the nucleus containing a nucleolus (Nu) is basally located; focal adhesions (FA) connecting the cell to the basement membrane (BM); apical surface contains microvilli processes (P) that extend into the interphotoreceptor space (IPS) which envelopes the distal part of photoreceptor outer segments (OS). Inset: Cross section of OS encircled. Note interphotoreceptor matrix (IPM) presence. Two types of pigments including melanin (Mel), located apically, and lipofuscin (Lf) located more basally, are observed. In addition, the presence of the rough endoplasmic reticulum (RER), Golgi apparatus (G), Phagolysosomes (Ph) and lysosomes are also observed in the RPE cells. (http://www.oculist.net/downaton502/prof/ebook/duanes/pages/v7/ch021/006f.html)

1.2.2 – Anatomy of BrM

The human BrM is a thin five layered acellular ECM that lies strategically between the RPE and the choriocapillaries. This five layered structure comprises of: (1) basement membrane of the RPE, (2) inner collagenous layer (ICL), (3) a porous elastic layer (EL), (4) outer collagenous layer (OCL) and (5) the outermost basement membrane of choriocapillaries endothelial cells (Hogan, 1961).

The basement membrane of the RPE – In humans, the RPE basement membrane is a 0.14-0.15µm thick continuous layer that contains specific collagen IV isoforms such as α1, α2, α3, α4 and α5 (Chen et al., 2003), fibronectin (Pauleikhoff et al., 1992), laminins 1 and 5 (Aisenbrey et al., 2006), heparan sulphate and chondroitin/dermatan sulphate (Hewitt et al., 1989).

Inner collagenous layer (ICL) - The ICL of the human BrM is around 1.4µm in diameter and is made up of 60nm thick fibres of collagens I, III and V arranged in a multi-layered lattice structure (Booij et al., 2010). The collagen lattice also contains biomolecules such as the negatively charged proteoglycans dermatan sulphate and chondroitin sulphate (Hewitt et al., 1989).

Elastic layer (EL) - Linear elastin fibres arranged in several stacked layers criss-cross to form the 0.8µm EL sheet of the human BrM. This sheet has an interfibrillar spacing of 1µm to allow diffusion and shape distortion. The EL extends from the optic nerve right through to the ciliary body (Booij et al., 2010). Along with the elastin fibres, other molecules such as collagen VI and fibronectin exist in the EL. Also, collagen fibres from the ICL and the OCL can cross into the EL (Booij et al., 2010). In other tissues, elastin fibres bind to anti-angiogenic proteins such as endostatin (Miosge et al., 1999). In relation to the BrM, this anti-angiogenic property of elastin may help prevent vascular growth in to the sub-retinal space. Interestingly, the EL from human BrM is 3-6 times thinner in the macula and possibly explains why choroidal neovascularisation (CNV) is more frequent in this region (Booij et al., 2010).

The outer collagenous layers (OCL) - Components of the OCL are largely the same as those found in the IC. However the OCL is not as thick as the ICL (0.7µm thickness) (Booij et al., 2010).

Choriocapillaris basement membrane (CBm) – Human CbM is mainly composed of collagen type IV, V and VI, laminins and heparan sulphate (Booij et al., 2010). Collagen VI is a CbM specific component and could be involved in the anchoring of BrM to choroid (Marshall et al., 1994). It is also proposed that collagen IV in the CbM is involved in inhibition of endothelial cell migration into the BrM (Roberts and Forrester, 1990).

1.2.3 - Functions of RPE

The RPE, along with the BrM, lies at the interface between the neuroretina and the choriocapillaries, where it is involved in important functions that help maintain retinal homeostasis. RPE functions are presented below along with the supportive properties of BrM (Figure 1.4).

Edited version

Figure 1.4: Summary of RPE functions essential for retinal homeostasis. Functions include absorption of scattered light, phagocytosis of POS and involvement in the visual cycle (Picture taken from Strauss, 2005).

1.2.3.1 – Blood retina barrier (BRB) and transport properties

Tight-junctions between neighbouring RPE cells together with the underlying BrM which provides physical support to the RPE, form the outer blood retina barrier (Ban and Rizzolo, 2000; Crane and Liversidge, 2008; Konari et al., 1995). The barrier separates the retina from the choroid as well as acting as a semi-permeable molecular sieve which regulates the access of nutrients and elimination of waste products (Booij et al., 2010). In one direction, the RPE is involved in the movement of ions and water from the subretinal space to the blood while, in the other direction, the RPE helps with the transport of nutrients such as glucose from the blood to the photoreceptors. The RPE monolayer is classified as a tight epithelium as paracellular resistance is 10 times higher than the transcellular resistance (Miller and Steinberg, 1977a, b). Therefore, the movement of molecules such as glucose and water is regulated by a series of membrane transporters or pumps (Stamer et al., 2003; Strauss, 2005).

For example, a large quantity of water is produced in the retina as a by-product of metabolic turnover in neurons and photoreceptors. Moreover, due to intraocular pressure in the vitreous body, water moves into the retina (Hamann, 2002; Strauss, 2005). This water in the retina needs to be removed. Water found in the inner retina is removed by Müller cells, with water in the sub-retinal space removed by the RPE. The movement of water occurs via the transcellular transport path in RPE cells, which is facilitated by a membrane protein known as Aquaporin-1 as well as the activity of Cl^- and K^+ pumps (Stamer et al., 2003; Strauss, 2005). The RPE cells are also involved in the removal of metabolic end products such as lactic acid from photoreceptors. Lactic acid removal by RPE requires an apical transmembrane potential and transepithelial transport of bicarbonate (HCO_3) to control intracellular pH. This allows HCO_3^- to regulate the direction of transport of lactic acid from the subretinal space to the blood (Strauss, 2005).

In the other direction, RPE cells transport nutrients from the blood into the retina. Various specific membrane receptors on the apical and basal surface

of the RPE aid in this process. For example, the apical and basal surfaces of RPE cells contain a large amount of glucose transporters (GLUT) such as GLUT1 and GLUT3 which allow inducible and constitutive glucose transport respectively (Strauss, 2005). Other substances that are transported by the RPE include taurine and docosahexaenoic, both of which are needed for photoreceptor cells (Bazan et al., 1992; Miller and Steinberg, 1976). Also retinol (vitamin A), an important molecule for photoreceptors, is transported by the RPE. Retinol is used in the visual cycle, a process described in section 1.2.3.2.

As molecules are exchanged between the RPE and choroid, they pass through the BrM on route. The BrM is acellular in nature and therefore diffusion is mainly a passive process. Diffusion of molecules across the BrM depends on its molecular composition which is influenced by factors such as age and location in the retina (Grindle and Marshall, 1978). Diffusion also depends on hydrostatic pressure on either side of the BrM and concentration of specific biomolecules and organic ions (Grindle and Marshall, 1978). Thus, any changes to the composition of the BrM will affect its diffusion properties which in turn will compromise the function of RPE cells and retina.

In summary, biomolecules that pass through the BrM from the choroid to the RPE include lipids, vitamin A, oxygen, nutrients, pigment precursors as well as anti-oxidant components (Booij et al., 2010). These molecules are taken up by RPE cells from the choroid via the BrM or bind to the BrM and are needed for structural and functional integrity of the photoreceptor-RPE complex. Molecules such as oxidized lipids and cholesterols, carbon dioxide (CO_2), ions and water along with metabolic waste from the visual cycle and electrophysiological waste from photoreceptors or RPE passes from the RPE to the choroid via the BrM (Booij et al., 2010; Strauss, 2005).

1.2.3.2 – RPE role in phagocytosis of outer segments (POS)

As photoreceptors contain a high amount of photosensitive molecules and exposed to intense level of light, an accumulation of photo-damaged

proteins and lipids occurs. Therefore, an increase of toxic substances within the photoreceptors occurs each day. These light-induced toxins could hinder light transduction as this process depends on the proper structure and function of proteins, retinal and membranes of photoreceptors. Maintaining excitability of photoreceptors is of upmost importance, and in order to do this, POS undergo a continuous regeneration process which involves the RPE. POS are constantly renewed by photoreceptors shedding old POS which are phagocytosed by RPE cells, where they are degraded in the lysosomal apparatus (Strauss, 2005). The importance of RPE cells in phagocytosis of shed POS is highlighted by the degeneration of photoreceptors in Royal College of Surgeon rats (RCS) (Bok and Hall, 1971). The RCS rats carry a mutation that causes defects in the normal phagocytic capacity of RPE cells leading to malfunction in POS renewal and subsequent visual cell death (Bok and Hall, 1971). The process of phagocytosis of POS by RPE cells and their degradation within the lysosomal apparatus is described further in section 1.3.1.3.

1.2.3.3 – The role of the RPE in visual cycle

In addition to POS phagocytosis, RPE cells play an important role in the visual cycle. The visual cycle is the process by which a photon of light is converted into an electrical signal. Processing of visual information begins with the detection of light by the photoreceptors. The photoreceptors involved in vision are rods and cone cells which use a derivative of all-trans-retinol (vitamin A), called 11-cis-retinal, to help detect light and begin the process of phototransduction. This process occurs via a photosensitive pigment called opsin to which the chromophore 11-cis-retinal is covalently linked. Both rods and cones differ in relation to amino acid sequence of opsin and therefore this determines the wavelength of light that is efficiently absorbed by the different photoreceptors. The visual cycle process in rod cells is described briefly below in order to highlight the role RPE cells play in this process.

Rhodopsin is a light sensitive receptor found in rod photoreceptors that consists of a molecule called opsin covalently bound to 11-cis-retinal. The

absorption of a photon by the opsin causes isomerisation of 11-cis-retinal into all-trans-retinal which induces a conformational change in opsin. This change results in formation of metarhodopsin, an active form of opsin, which initiates a phototransduction cascade leading to the hyperpolarisation of the cell (Hofmann, 1999; Okada et al., 2001). The electrical signal is then passed onto the optic nerve through the visual pathway into the visual cortex of the brain, where perception of vision is made. The active form of rhodopsin is inactivated by binding to a molecule called arrestin which then causes release of all-trans-retinal. Rhodopsin will eventually bind with 11-cis-retinal so it can function again by absorbing light. All-trans-retinal is reduced to all-trans-retinol in the cytosol of the photoreceptors. As photoreceptors lack the cis-trans isomerase for conversion of all-trans-retinal into 11-cis-retinal, the reisomerasation step occurs in the RPE (Baehr et al., 2003).

The conversation of all-trans-retinol to 11-cis-retinal involves the action of three enzymes found in the RPE cells, lecithin:retinol transferase (LRAT), retinal pigment epithelium-specific protein (RPE-65) and 11-cis-retinol dehydrogenase (RDH5). Following uptake into RPE cells, all-trans-retinol is transferred to the first enzyme, LRAT, by the cellular retinoid binding protein (CRBP) (Saari et al., 1982). LRAT is involved in the esterification of all-trans-retinol to a fatty acid from membrane phosphatidylcholine to generate all-trans retinly esters (Saari and Bredberg, 1989). The esters generated by the first enzymatic reaction are the substrates for the next step of the visual cycle which involves the RPE65 enzyme. The RPE65 enzyme facilitates the simultaneous hydrolysis and isomerisation of the ester substrates to yield 11-cis-retinol (Redmond et al., 1998). The third enzyme, RDH5, facilitates the oxidation of 11-cis-retinol to 11-cis-retinal, after which the 11-cis-retinal is transported back to the photoreceptors where it will bind with opsin to form the new light sensitive molecule (Driessen et al., 1995; Strauss, 2005).

In addition to the RPE regenerating 11-cis-retinal for photoreceptors, RPE cells are able to spatially buffer ions such as K^+ to help maintain photoreceptor excitability (Strauss, 2005). Light stimulation of photoreceptors causes events that eventually lead to a decrease in K+ ions

concentration in the sub-retinal space. This disturbance is compensated for by the RPE in the following way: decreased K^+ ions cause the apical membrane of RPE to become hyperpolarised which leads to the activation of K^+ channels. This results in K^+ ions being pumped back into the sub-retinal space. The ability for RPE cells to compensate in changes in ion composition is similar to glial cells and helps in maintaining photoreceptor visual function (Strauss, 2005).

1.2.3.4 - RPE secretion

On either side of the RPE are two different microenvironments (apical – photoreceptor region; basal – BrM and choroidal blood supply), which require different proteins for structural and functional maintenance. The RPE secrete a variety of growth factors and proteins such as fibroblast growth factors (FGF-1, FGF-2 and FGF-5), insulin-like growth factor-I (IGF-I), platelet epithelial derived factor (PEDF), vascular endothelial growth factor (VEGF) as well as matrix metalloproteinase (MMP-2) and inhibitor of matrix metalloproteinases (TIMPs) (Kay et al., 2013; Strauss, 2005). Examples of proteins secreted specifically from the apical and basolateral side of RPE and their function are described below.

Apical secretion - At its apical side, the RPE is in contact with IPM. The IPM is important in providing an attachment between photoreceptors and RPE and therefore maintaining the integrity and structure of the IPM is crucial for retina homeostasis (Hollyfield, 1999; Rohlich, 1970). Examples of proteins secreted apically by RPE cells are MMP-2 and TIMP-1 (Padgett et al., 1997). MMPs are zinc-containing proteases that play an important role in ECM turnover. Regulation of MMPs activity is tightly regulated and includes functional inhibition through interactions with TIMPs. MMPs/TIMPs are suggested to play a role in IPM turnover as well involvement in the degradation of POS which signals their readiness for phagocytosis by RPE cells (Padgett et al., 1997). PEDF is also secreted from the apical side of the RPE (Becerra et al., 2004; Maminishkis et al., 2006). PEDF gives neurotropic support to the photoreceptor region and provides a non-

angiogenic environment for the retinal region (Cayouette et al., 1999; Dawson et al., 1999).

Basolateral secretion - Examples of proteins secreted from the basal side of the RPE include endothelin I, VEGF and cystatin C. Endothelin I is a vasoactive protein thought to mediate both vasoconstriction and vasodilation via interactions with endothelin receptors in smooth muscle cells (Kedzierski and Yanagisawa, 2001). In relation to the RPE, endothelin I secretion is predominantly from the basal side making it possible that endothelin I activate receptors in the choriocapillaries and regulate blood flow (Narayan et al., 2004). VEGF is a pro-angiogenic growth factor secreted from the basal side of the RPE (Maminishkis et al., 2006). VEGF is involved in preventing endothelial cell death and is essential for an intact choriocapillaris endothelium (Burns and Hartz, 1992). As VEGF is pro-angiogenic, its secretion is tightly regulated to stop concentrations from exceeding normal levels where it can induce vascularisation (Kwak et al., 2000; Spilsbury et al., 2000). In addition to endothelin I and VEGF, the most abundantly RPE expressed protease inhibitor cystatin C is also predominantly secreted basolaterally. Cystatin C is thought to be mostly involved in extracellular proteolytic control on the basolateral side of the RPE (Paraoan et al., 2001).

1.2.3.5 - Anti-oxidant properties of RPE

During life, RPE cells are exposed to high intensity of light and high oxygen levels which create an environment prone to photo-oxidation and ROS generation (Winkler et al., 1999). ROS are reactive species that contain one or more unpaired electrons in their outer orbits and are molecular oxygen derived molecules which include oxygen-centred radicals such as superoxide anion and hydroxyl radical and non-radical reactive derivatives of oxygen such as hydrogen peroxide (H_2O_2) and singlet oxygen (Zorov et al., 2014).

Sources of oxidative insult for the RPE are diverse. Due to facing the blood supply of the choriocapillaris, RPE cells are subjected to a very high tension of oxygen (O_2) (Alder and Cringle, 1985). There is high blood flow rate in the choriocapillaris with a measurement of 1400ml per min per every 100g of

tissue. The venous blood supply from choriocapillaris is 90% O_2 saturation (Plafker et al., 2012). Therefore, the high blood flow rate along with high oxygen saturation creates an ideal oxidising environment for ROS generation. Light exposure can also be a significant source of ROS generation for the RPE. Although the cornea and lens filter out most of the damaging constituents of solar radiation, the retina is still exposed to intense focal light which contains the blue part of the solar spectrum (Young, 1988). Blue light exposure causes photoxidation of RPE molecules and increase intracellular ROS levels (Rozanowska et al., 1995).

As RPE cells are highly metabolically active, they contain an enriched mitochondria population to help meet the high energy requirements of these cells (Hogan et al., 1971). Energy is accumulated in the form of adenosine triphosphate (ATP) that is produced by the process of oxidative phosphorylation, which occurs in the inner membrane of the mitochondria of cells (Beatty et al., 2000). However, this process, which is vital for cell metabolism, also leads to a generation of high amounts of ROS (Murphy, 2009). The ROS that are produced damage the mitochondria and affect its function (Cui et al., 2012; Richter, 1992). Also, ROS from the mitochondria is released into the cytoplasm which could then go an act on neighbouring mitochondria causing amplification of ROS levels (Zorov et al., 2014). ROS-induced damage of the mitochondria will affect the ability of RPE cells to meet its metabolic demands. Oxidants such as H_2O_2 also react with iron in lysosomes in a process referred to as Fenton reaction which helps generate further ROS. Some of the oxidation products also help in forming lysosomal lipofuscin (Lipofuscin is described in more detail in section 1.2.4.1) (Terman et al., 2010). In addition, phagocytosis of POS is also attributed to producing ROS (Miceli et al., 1994).

Under normal physiological conditions, cellular damage by ROS is neutralised by the collective effects of endogenous antioxidant defence mechanisms. As mentioned previously, RPE cells contain a pigment called melanin which serves a photoprotective role by absorption of scattered light as well as scavenging free radicals and ROS (Rozanowska et al., 1999;

Sarna et al., 2003). In addition, RPE cells also contain a wide range of anti-oxidants such as catalase, glutathione peroxidase, superoxide dismutase as well as vitamins C and E which scavenge and decompose ROS (Winkler et al., 1999). The enzyme superoxide dismutase is involved in the catalysis of the superoxide radical into less damaging species of H_2O_2 and oxygen (McCord and Fridovich, 1988). H_2O_2, a non-radical ROS, is toxic to cells as it can form radical ROS such as hydroxyl radical (Puppo and Halliwell, 1988). Therefore, H_2O_2 must also be broken down and this involves the antioxidant property of catalase as well as glutathione peroxidase (Dominguez et al., 2010; Jurkovic et al., 2008). When the balance between ROS levels and anti-oxidant levels is lost i.e. levels of ROS exceed antioxidant capacity, during ageing or in pathological conditions, a situation known as oxidative stress arises (Costa and Moradas-Ferreira, 2001).

1.2.3.6 – The importance of RPE interaction with BrM

The ability of the RPE monolayer to perform its many functions is dependent on its interaction with the BrM. RPE cells adhere via integrins to the BrM (Aisenbrey et al., 2006; Del Priore et al., 2002; Del Priore and Tezel, 1998). Integrins are a group of membrane proteins and mediate RPE-BrM adhesion by binding to molecules present in the BrM such as laminin 5 and collagen IV (Aisenbrey et al., 2006). Indeed, RPE cells overexpressing integrins increase their adhesion to BrM compared to normal RPE cells (Fang et al., 2009).

Alterations in the adhesion of RPE cells to the BrM may impact critical RPE functions. Age-related alterations of ECM affect the adhesion of cells (Haucke et al., 2014). Interestingly, RPE cells cultured on aged-BrM show a decrease in POS phagocytic ability (Sun et al., 2007). In addition, RPE cells cultured on an advanced glycation end products (AGEs) modified matrix display RPE polarity impairment (Kay et al., 2014). The accumulation of advanced glycation end products (AGEs), an age-related phenomenon, is described in section 1.2.4.3. Taken together, the evidence shows that defects in the BrM may contribute to reduced RPE cell adhesion with subsequent impact on critical cellular functions.

1.2.4 – Age-related changes of RPE and BrM

With age, the RPE and its surrounding environment such as the BrM undergo structural changes that lead to vision decline. Given the important roles of the RPE and BrM in maintenance of retinal homeostasis, the age-related loss of melanin in RPE, accumulation of lipofuscin and AGEs as well as other changes such as BrM thickening ultimately lead to photoreceptor dysfunction and the onset of diseases such as age-related macular degeneration (AMD).

AMD is the leading cause of irreversible, severe loss of vision in the elderly population in the developed world (Bressler et al., 2003; Smith et al., 2001). Approximately 50 million people suffer from AMD worldwide and this number is predicted to increase 3 fold over the next 20 years, highlighting AMD as a major public health issue (Gehrs et al., 2006; Gordois et al., 2012). The macula, a specialised region found in the central region of the retina responsible for high acuity and colour vision, undergoes pathological changes resulting in severe loss of central vision. Deterioration of central vision in AMD, therefore, severely impacts the quality of life. AMD is described in further detail in section 1.4.

1.2.4.1 - RPE ageing

Many studies have looked at how RPE cell density changes with age. In 1989, Dorey et al investigated the impact of age on RPE density in patients of different ethnicities (Dorey et al., 1989). It was observed that RPE cell density decreases with age (Dorey et al., 1989). Another study showed that ageing RPE cell density decreases at an annual rate of 0.3% (Panda-Jonas et al., 1996). As the rate of RPE loss is greater than that of photoreceptor loss, the metabolic load upon each RPE cell increases on a yearly basis (Dorey et al., 1989).

In addition to RPE loss, many morphological age-related changes occur in RPE cells. Changes include increase in cell diameter due to cells spreading to fill spaces left by dead cells, hyper and hypopigmentation, loss of cell shape, hyperplasia with areas of multi-layered cells and atrophy of RPE cells

(Boulton and Dayhaw-Barker, 2001). At the apical end of the RPE cells, microvilli change from being long and thin and become shorter and thicker with age and the intimate contact between POS and microvilli of the RPE is therefore reduced (Katz and Robison, 1984). A decrease in efficient POS phagocytosis and subsequent POS degradation with age also occurs which is indicated by a reduction of phagosome material in aged RPE cells in parallel with the age-related changes in microvilli (Katz and Robison, 1984). Changes also occur at the basolateral side of the RPE where infoldings decrease and become irregular with age. This causes a decrease in surface area for metabolic and waste exchange between the RPE and choroid as well as RPE connections with the BrM being compromised which in turn contributes to defects in molecule transport (Mishima and Hasebe, 1978; Mishima and Kondo, 1981).

There are also age-related changes of RPE pigmentation. A decline in total pure melanin granules is observed in RPE cells with age (Feeney-Burns et al., 1984; Weiter et al., 1986). Between the early and late decades, melanin levels decline by about 35% and this decrease results in a reduction of light absorption and a reduction of anti-oxidant capacity in RPE cells (Boulton and Dayhaw-Barker, 2001). In addition, remaining melanin does not function properly resulting in further loss of protection and increased photo-oxidation (Sarna et al., 2003; Schmidt and Peisch, 1986). This loss of true melanin correlates with the fusion of melanin with lysosomes and lipofuscin resulting in melanolysosomes and melanolipofuscin granules respectively (Feeney-Burns et al., 1984). Melanolysosomes, which most likely represent melanin in the process of being degraded, have a loss of a typical cigar shape structure. The origin of melanolipofuscin is not clear however, they are thought to arise from the fusion of melanin and lipofuscin granules (Feeney, 1978). Melanolysosomes, melanolipofuscin and lipofuscin accumulate with age resulting in an overall decrease in cytoplasmic volume in the RPE. These pigments are photosensitive and generate free radicals and ROS (Feeney-Burns et al., 1984).

Lipofuscin, also known as the ‘age-pigment’ is a yellowish brown material that accumulates in many post-mitotic cells over time such as neurons, cardiac myocytes and RPE cells (Sparrow and Boulton, 2005; Yin, 1996). In RPE cells, lipofuscin accumulates with age eventually leading to occupation of up to 19% of cytoplasmic volume by the ninth decade (Feeney-Burns et al., 1984). For many cells, lipofuscin originates from degradation of exhausted organelles via autophagy. However, for RPE cells a major source of lipofuscin generation also occurs by phagocytosis and degradation of POS (Boulton et al., 1989; Feeneyburns and Eldred, 1983; Katz, 1989).

The formation of lipofuscin is a complex process for which two theories exists. The first theory suggests that prior to phagocytosis by RPE cells, POS are oxidised and cannot be completely degraded by lysosomal enzymes (Kaemmerer et al., 2007; Kennedy et al., 1995). Indeed, lipofuscin granules contain proteins that are damaged by lipid peroxidation-derived modifications (Schutt et al., 2003; Schutt et al., 2002). The process of lipid peroxidation involves the action of oxygen-derived free radicals on polyunsaturated fatty acids oxidised molecules. Major lipid peroxidation products, such as malondialdehyde (MDA) and 4-hydroxynonenal (HNE), are able to covalently attach to residues within proteins (Esterbauer et al., 1991). Furthermore, when modified POS containing oxidised molecules are fed to cultured RPE cells, a resistance to degradation by lysosomal proteases occurs (Kaemmerer et al., 2007). In addition, modified POS exert an inhibitory effect on degradation of normal POS by RPE lysosomes (Kaemmerer et al., 2007). This indicates that lysosomal enzyme activity may be compromised by the presence of oxidised molecules which causes a reduction of lysosomal degradative capacity which subsequently increases the accumulation of undegraded material. The second theory states that a decrease in lysosomal degradative ability, due to age-related alterations in lysosomal enzymatic activity, contributes to lipofuscin generation. This notion is supported by the knowledge that inhibition of lysosomal proteases results in decreased POS degradation and accumulation of lipofuscin-like debris (Rakoczy et al., 1994). Taken together, accumulation of lipofuscin is a

possible interplay between degradation-resistant molecules as well as alterations in lysosomal protease activity.

Although a major source of generation of lipofuscin in RPE cells is through the phagocytosis of POS, the composition of lipofuscin remains an area of research interest. Analysis shows that lipofuscin is an aggregate of oxidised lipids, bisretinoids and a small amount of protein (Ng et al., 2008). A main component of lipofuscin is the bis-retinoid, N-retinylidene-N-retinylethanolamine (A2E) (Eldred and Lasky, 1993). A2E is generated from all-trans-retinal and ethanolamine, both of which are components of photoreceptor POS (Liu et al., 2000; Ren et al., 1997; Sakai et al., 1996; Wu et al., 2013). A2E exerts adverse effects on RPE cells such as activating complement pathway and therefore causing inflammation (Zhou et al., 2006). A2E also inhibits isomerohydrolase in the visual cycle which results in a disruption of 11-cis-retinal supply to the retina subsequently leading to photoreceptor dysfunction (Moiseyev et al., 2010). Additionally, A2E activates the retinoic acid receptor and cause induction of pro-angiogenic VEGF which may predispose the RPE environment to CNV (Iriyama et al., 2008).

Lipofuscin is also known to produce ROS, which consequently provides oxidative insult and causes cellular damage (Rozanowska et al., 1998; Shamsi and Boulton, 2001). In a study conducted by Rozanowska et al, lipofuscin is shown to have greater O_2 uptake compared to melanin (Rozanowska et al., 1995). The photoactivation of lipofuscin leads to the generation of ROS such as singlet oxygen, superoxide anion and H_2O_2 (Rozanowska et al., 1995). Lipofuscin is also thought to have an ability to provide a redox-surface by integrating oxidatively liable iron (Boulton et al., 1989; Feeneyburns and Eldred, 1983; Hohn et al., 2010; Katz, 1989). Due to the presence of iron in lipofuscin, it allows the production of ROS to be sustained independently from the mitochondria (Hohn et al., 2010). ROS are countered by endogenous anti-oxidant systems. However with age, these defensive systems are diminished and cause further oxidative burden upon the RPE. For example, catalase activity decreases in ageing and in AMD

eyes (Liles et al., 1991). An increase in ROS accompanied by a decrease in endogenous antioxidant systems results in oxidative stress, a condition associated with RPE dysfunction and development of diseases such as AMD (Jarrett and Boulton, 2012).

1.2.4.2 - BrM Ageing

The BrM also undergoes many age-related changes throughout life which in general include an increase in thickness, reduced capacity for filtration of biomolecules and molecular and structural changes (Moore and Clover, 2001; Ramrattan et al., 1994). Alterations of the BrM biophysical properties lead to dysfunction of RPE and photoreceptors and subsequent development of eye diseases. As the BrM ages, a decrease in soluble collagen content from 100% in the first decade to approximately 40-50% in the ninth decade occurs (Karwatowski et al., 1995). This increase in insoluble collagen arises from collagen cross-linking that has a negative effect on BrM permeability and changes the nature of the ECM by increasing strength whilst decreasing elasticity which may affect filtration. Insoluble collagen network becomes less susceptible to RPE collagenase degradation and may result in inefficient turnover of BrM components (Karwatowski et al., 1995).

Turnover of other components of the BrM such as the proteoglycans are also affected with age (Hewitt et al., 1989). Proteoglycans (PG) are proteins that are heavily glycosylated and are the ‘glue’ of extracellular matrices such as the BrM. PGs are made up of a core protein which is linked covalently to glycosaminoglycan (GAG) chains. In the BrM, 58% of PGs are of the heparan sulphate kind which is predominantly primarily found in RPE and choroidal basement membranes. The remaining 42% of PGs found in the BrM are made up of the chondroitin sulphate or dermatan sulphate which link with collagen fibrils (Hewitt et al., 1989; Inatani and Tanihara, 2002). Newly synthesised PGs are made up of 25% heparan sulphate and 75% chondroitin sulphate/dermatan sulphate and this ratio remains relative stable throughout life. Over the age of 70, however there is a small size shift where PGs increase in size indicating an inability of cells to process core proteins

as normal (Hewitt et al., 1989). The BrM in eyes from retinitis pigmentosa and diabetic retinopathy showed that heparan sulphate becomes the predominant PG at levels of 55-64% compared to control eyes (Hewitt et al., 1989; Hewitt and Newsome, 1985). Taking into account the filtration properties of PGs in BrM, changes in the negatively charged filled environment may hinder movement of molecules.

Calcium is also deposited in the BrM which causes calcification, the presence and extent of which increases with ageing (van der Schaft et al., 1992). A significant correlation between BrM calcification and exudative AMD has been observed (Spraul et al., 1999). The calcification of the BrM makes it more brittle and more susceptible to breaks (Spraul et al., 1999). Along with calcium, there is an accumulation of iron and zinc deposits that occur on the ageing BrM (Booij et al., 2010). A significant pathological change in the BrM is the progressive accumulation of lipids in the BrM (Pauleikhoff et al., 1990; Sheraidah et al., 1993). The accumulation of lipids renders the BrM hydrophobic over time and therefore impedes the diffusion of molecules between the RPE and choroidal vessels.

1.2.4.3 – Accumulation of advanced glycation end products (AGEs) in RPE/BrM and links to oxidative stress

An important phenomenon that occurs with age is the accumulation of advanced glycation end products (AGEs). AGEs are toxic by-products of non-enzymatic Maillard reactions between reducing sugars with deoxyribonucleic acid (DNA), proteins and lipids (Baynes, 2001; Monnier et al., 1992). The formation of AGEs is related to reactions with glucose, various α-oxaloaldehydes such as glycolaldehyde and lipid peroxidation products (Baynes, 2001). AGE formation involves the following steps:

1) Initial Schiff base formation: For example the aldehyde group of the glucose molecule combines with an amino group of amino acids (arginine or lysine molecules) present in proteins. This process involves a double bond forming between the carbon of the aldehyde group from the glucose and the nitrogen from the amino group.

2) Amadori product formation: Further rearrangement of hydrogen atom from the hydroxyl group adjacent to the carbon-nitrogen double bond moves to nitrogen atom to form a ketone known as Amadori product.

3) AGEs formation: The Amadori products are oxidised and dehydration reactions results in irreversible forms of protein bound AGEs.

The first two steps of the Maillard reaction are reversible whilst the last step is non-reversible (Kandarakis et al., 2014) (Figure 1.5).

Edited version

Figure 1.5: AGEs formation: Maillard reaction between glucose and amino group present in proteins. Initially there is a formation of an unstable Schiff base. Further arrangements leads to a more stable Amadori product which subsequently gets oxidised and forms cross-linked AGE product (Picture taken from Kandarakis et al., 2014)

Products of metabolism such as α-oxaloaldehydes like glycolaldehyde, methylglyoxal and glyoxal are reactive intermediates for AGEs formation and exist at high amounts in cells exposed to elevated glucose levels (Glomb and Monnier, 1995; Thorpe and Baynes, 2003). Glycolaldehyde as well as glyoxal can undergo Maillard reactions to give rise to AGEs products such as carboxymethyl lysine (CML) (Glomb and Monnier, 1995). Thus, α-oxaloaldehydes such as glycolaldehyde are an important source of intra- and extracellular AGEs.

Over 20 AGE adducts have been reported such as CML, carboxyethyl lysine (CEL), pentosidine and crossline (Kandarakis et al., 2014). In general, AGEs are known to accumulate on long lived structures such as collagens and lens

crystallins (Kumar et al., 2007; Monnier et al., 1992; Sajithlal et al., 1998). The rate of AGEs accumulation is enhanced in situations of poor glucose use and increased oxidative stress (Miyata et al., 1997; Semba et al., 2010). AGEs are linked with the acceleration of the ageing process and age-related diseases such as diabetes mellitus, Alzheimer disease (AD) and AMD (Baynes, 2001; Ishibashi et al., 1998; Sasaki et al., 1998; Semba et al., 2010; Sensi et al., 1995).

In the eye, AGEs are observed in cornea, lens, vitreous, neuroretina, RPE, BrM as well as the optic nerve (Cheng et al., 2002; Nagaraj et al., 2012; Stitt, 2005). In particular, the RPE cells and BrM are at high risk of formation of AGEs as the outer retina, being rich in glucose and lipid, provides an environment prone to oxidation. AGEs are increased in RPE and BrM from aged eyes and AMD patient eyes (Glenn et al., 2009; Handa et al., 1999; Howes et al., 2004; Ishibashi et al., 1998; Schutt et al., 2003). Furthermore, AGEs also constitute a major portion of proteins found in lipofuscin granules in RPE (Schutt et al., 2003). Lipofuscin components such as A2E can also contribute to AGEs formation. A2E photo-degradation causes release of methylglyoxal, which can react with proteins and produce AGEs (Wu et al., 2010). RPE function is also affected by basal linear deposits (BlinD) and drusen (described in further detail in section 1.4.1), both of which accumulate between the RPE and BrM and contain AGEs (Handa et al., 1999; Ishibashi et al., 1998). As there is a direct relationship between the RPE and BrM, AGEs deposition on the BrM may be partially attributed to RPE dysfunction and subsequent atrophy and degeneration of photoreceptor.

AGEs such as CML and pentodine accumulate in the BrM and choroid with age and promote the breakdown of the RPE-BrM-choroid complex (Handa et al., 1999). Choroidal endothelial cell proliferation and VEGF up-regulation, both of which are involved in development of CNV in wet AMD, are shown to be induced by AGEs (Hoffmann et al., 2002). Moreover, experimental models that mimic BrM ageing show RPE dysfunction can be induced by glycation reactions of basement membrane proteins. For example, exposure

to nitrite or AGEs-modified ECM proteins causes a reduction in RPE cell attachment and survival (Wang et al., 2005). In addition, RPE cells grown on an AGEs-modified matrix show an increase in lipofuscin accumulation and reduced lysosomal degradative capacity potentially as a result of down-regulation of mRNA expression of cathepsin S, cathepsin G and cathepsin D (Glenn et al., 2009). Lysosomal activity is of upmost importance in RPE as it is involved in turnover of damaged molecules and organelles as well as POS digestion. Dysfunction of this system leads to an accumulation of non-degradable material such as lipofuscin which itself has shown to impair the degradative capacity of the lysosomes (Shamsi and Boulton, 2001). In addition, proteins such as the deubiquitinating enzyme ubiquitin carboxyterminal hydrolase-1 (UCHL-1) are also affected in RPE cells upon AGEs exposure (Glenn et al., 2012).

It is believed that AGEs exert their biological effects on processes such as gene expression via binding to AGE receptors (RAGEs) as well as through RAGE-independent mechanisms. AGEs accumulate and colocalises with their receptors which are expressed in many different cell types such as macrophages (Vlassara et al., 1986), monocytes (Festa et al., 1998), vascular smooth muscle cells (Sano et al., 1999) and vascular endothelial cells (Stitt et al., 1999). AGE receptors include oligosaccharryltransferase-48 (AGE-R1), 80K-H (AGE-R2), galectin-3 (AGE-R3) and receptor for AGEs (RAGE) (Li et al., 1996; Vlassara et al., 1995). In the RPE, immmunolabelling for RAGE on human eye from normal and early/late stage AMD patients show an increase in RAGE levels with age whilst RPE cells from early stage and late stage AMD display intense RAGE immmunolabelling (Howes et al., 2004). Furthermore, RAGE expression increases in RPE cells exposed to AGEs (Howes et al., 2004). AGE-R1, AGE-R2 and AGE-R3 are all expressed by the RPE, with exposure to AGEs causing a significant increase in mRNA levels for AGE-R1 and AGE-R2 (McFarlane et al., 2005). These receptors of AGE-binding proteins are thought to form complexes on plasma membranes and are involved in removal and breakdown of AGEs or induction of specific intracellular signalling cascades (Thornalley, 1998; Vlassara and Bucala, 1996).

AGE-RAGE receptor complex can trigger p21 (ras)-dependent mitogen-activated protein kinase (MAPK) pathway which leads to nuclear translocation of nuclear factor kappa B (NF-κB) (Lander et al., 1997). NF-κB is a transcriptional factor for expression of important pro-inflammatory cytokines genes such as interleukin 1β (IL-1β) and interleukin 18 (IL-18) (Hiscott et al., 1993; Suk et al., 2001). Both IL-1β and IL-18 are synthesised as precursor which require proteolytic maturation via the action of caspase-1 which must first be activated by multiprotein complexes known as inflammasomes (Mariathasan and Monack, 2007). Indeed, RAGE receptor activation induces gene expression of pro IL-1β and pro IL-18 via NF-κB (He et al., 2012). Notably, inflammation is thought to play a major role in the pathogenesis of AMD (Telander, 2011). It is likely that AGEs contribute to age-related RPE dysfunction and subsequent AMD development by causing up-regulation of pro-inflammatory cytokines via binding to RAGE receptor and activating NF-κB pathway. In addition to regulating pro-inflammatory cytokine gene expression, NF-κB activation also plays a central role in RAGE dependent up-regulation of secretion of the pro-angiogenic molecule VEGF (Ma et al., 2007). In contrast to the activation of RAGE receptor, other AGEs binding receptors seem to have a protective role. For example, AGE-R3 is shown to be protective for RPE cells against the effects of AGEs, as overexpression of AGE-R3 reduces VEGF expression following AGEs exposure (McFarlane et al., 2005).

The expression of other genes in the RPE is also effected by AGEs exposure. For example, the mRNA for a prostaglandin transporter involved in transporting prostaglandin D-2 synthase is downregulated in RPE cells exposed to AGEs (Glenn et al., 2009). As prostaglandin D-2 synthase is involved in prevention of ROS formation, AGEs effecting its expression indicates a link of AGEs with oxidative stress (Garg and Chang, 2004). Interestingly, AGEs formation is accelerated in oxidative stress environments (Miyata et al., 1997). Moreover, accumulating evidence shows that AGEs themselves elicit oxidative stress generation in various cell types such as mesangial cells (Scivittaro et al., 2000), neouroblastoma cells (Wang et al., 2015a) as well as in RPE cells (Wang et al., 2015b).

AGEs cause oxidative stress by binding and activating the RAGE receptor (Wang et al., 2015a; Wang et al., 2015b). AGE-RAGE signalling induces mitochondria ROS production (Basta et al., 2005). RAGE activation also increases ROS production via activation of nicotinamide adenine dinucleotide phosphate (NAPDH) oxidase (Thallas-Bonke et al., 2008). An important factor that contributes to RPE dysfunction and leads to development of diseases such as AMD is oxidative damage. As RPE cells have high metabolic activity as well as being exposed to high oxygen consumption and intense levels of light throughout life, their structural and functional integrity is under threat by oxidative stress (Winkler et al., 1999). Sources that contribute to the generation/increase of intracellular ROS (described previously in section 1.2.3.4) cause biomolecules such as proteins to mis-fold which subsequently causes cellular dysfunction (Beatty et al., 2000; Grune et al., 2004). Removal of toxic misfolded and damaged proteins from the cell is critical for cell survival, particularly in post-mitotic cells such as the RPE as an accumulation of damaged dysfunctional proteins are destructive for the cells (Kopito, 2000).

1.3 - Proteolytic function of RPE cells

Throughout the life of cell proteins are constantly synthesised and degraded (Goldberg and Dice, 1974). There are many systems in place within eukaryotic cells that take care of protein degradation and two important ones are: 1) the ubiquitin proteasome system (UPS) which degrades many short and long-lived proteins and abnormal intracellular proteins; and 2) the lysosomal system which degrades cell organelles, membrane proteins and endocytosed proteins (Ciechanover, 2005; Hershko and Ciechanover, 1998). In RPE cells, the lysosomes possess a multifunctional capacity to handle proteins destined for degradation as they are critical regulators of endocytosis, phagocytosis and autophagy (Lakkaraju, 2012; Strauss, 2005; Wang et al., 2009b). The RPE cells are post-mitotic cells which makes the lysosomal system critically important in the protein turnover as it has to maintain efficiency throughout life. A decline in system efficiency would therefore lead to the build-up misfolded proteins and aggregates subsequently causing cellular dysfunction.

1.3.1 Lysosomes and proteolysis in RPE

The biological concept of lysosomes was first coined in 1955, when Christian De Duve et al, discovered a distinct group of lytic bodies or granules that contained acidic hydrolases, when initially looking at the effects of insulin on isolated liver tissue (De Duve et al., 1955). Today it is known that lysosomes are key membrane-enclosed organelles controlling cellular proteolysis. Lysosomes are found in the cytosol where they appear as dense bodies with a perinuclear pattern (Appelqvist et al., 2013b). Lysosomes are usually spherical in shape and are typically >1µm in size surrounded by a 7-10nm phospholipid bilayer (Appelqvist et al., 2013b; Saftig et al., 2010). The lysosomal membrane has high carbohydrate content due to membrane proteins being greatly glycosylated. Around 25 lysosomal proteins have been recognized such as lysosome-associated membrane proteins (LAMPs) 1 and 2 (Eskelinen et al., 2003; Lubke et al., 2009).

Lysosomes are virtually found in all eukaryotic cells, except for red blood cells, with the main function of the lysosomes being involved in the

degradation of macromolecules. Components that are destined for the degradation reach the lysosomes via different mechanisms such as autophagy for intracellular material and endocytosis for ingested exogenous material. These organelles contain a variety of hydrolases (approx. ~60) such as nucleases, lipases and proteases which collectively cause the degradation of all kinds of molecules (Appelqvist et al., 2013b; Saftig and Klumperman, 2009). The acidic pH of the lysosome (pH 4.5-5.0) helps in loosening the structures of macromolecules as well as being important for the optimal activity of enzymes (Mindell, 2012). This leads to the enzymes being able to degrade macromolecules down to their monomeric forms inside of lysosomes. In addition to being involved in the degradation of macromolecules, recent research has identified lysosomal involvement in a number of functions such as secretion, signalling energy metabolism and plasma membrane repair, demonstrating that the lysosome is a dynamic organelle central in maintaining cell homeostasis (Settembre et al., 2013).

1.3.1.1 – Autophagy

Autophagy is a general term used for pathways in which cytoplasmic materials are delivered to the lysosome for degradation. Autophagy can be divided into three types known as microautophagy, chaperone-mediated autophagy (CMA) and macroautophagy (Mizushima and Komatsu, 2011; Yang and Klionsky, 2010) (Figure 1.7). The microautophagy pathway involves the engulfment of cytoplasm at the surface of the lysosomes (Li et al., 2012). In CMA, substrate proteins that harbour specific recognition sites translocate across the lysosomal membrane with the help of chaperone molecules and the lysosomal receptor LAMP-2A (Kaushik and Cuervo, 2012). Macroautophagy involves the formation of an isolated membrane referred to as the phagophore (Yorimitsu and Klionsky, 2005). The phagophore expands and engulfs the target i.e. organelle to form a double-membrane structure (autophagosome) which subsequently fuses with the lysosome where contents are degraded by the lysosomal enzymes such as the cathepsins (Yorimitsu and Klionsky, 2005). Macroautophagy is the major type of autophagy and it has been extensively studied compared to the other

two forms. Therefore, from now on, the term autophagy will refer to macroautophagy.

In highly metabolically active cells such as RPE, where mitochondria turnover is very high, autophagy is a crucial system for maintenance of RPE homeostasis. Indeed, several lines of evidence show that autophagy occurs within RPE cells (Wang et al., 2009a; Wang et al., 2009b). Interestingly, an increase in mitochondrial damage and formation of ROS in aged-RPE suggests that removal of these oxidative damaged molecules is impaired (Jarrett and Boulton, 2012; Karunadharma et al., 2010). Improper digestion of substrates due to impaired autophagy or lysosomal function could contribute to accumulation of damaged organelles which consequently cause RPE dysfunction and AMD pathogenesis.

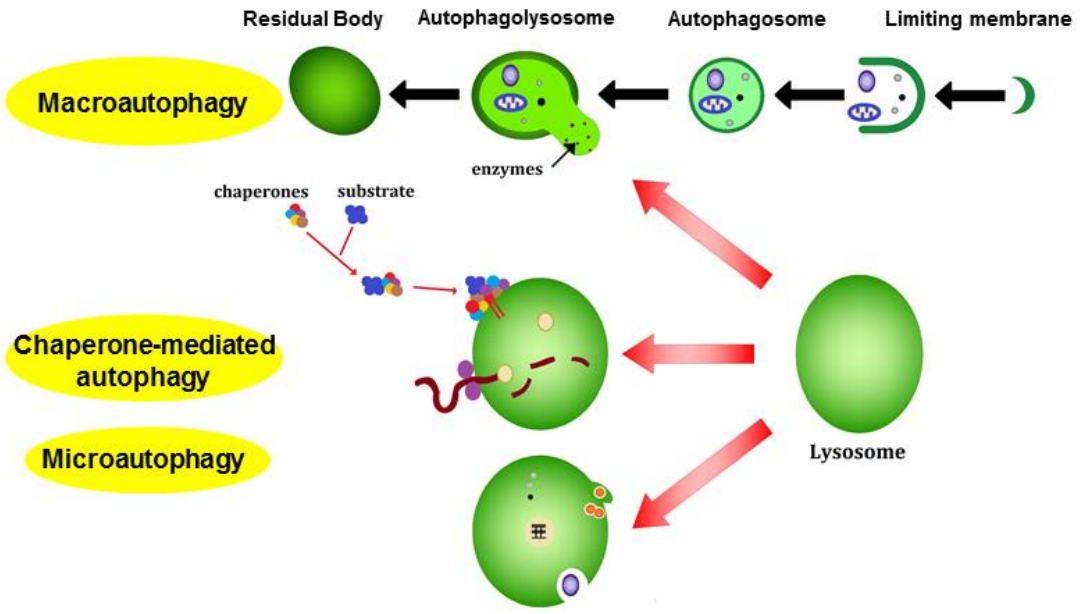

Figure 1.6: Different forms of autophagy: Autophagy is an important process in helping remove cellular debris such as damaged organelles. The three known types of autophagy are macro-autophagy, chaperone-mediated autophagy (CMA) and microautophagy.

1.3.1.2 – Endocytosis

Endocytosis is a cellular mechanism in which there is an uptake of material such as proteins, cell surface receptors and soluble molecules from the cell surface into the interior by endocytic vesicles. Two main types of endocytosis exist based on the size of the engulfed material – pinocytosis, which involves uptake of fluids and small solutes and phagocytosis, which is a characteristic of specialised cells that engulf larger particles like whole cells (Conner and Schmid, 2003). At least four mechanisms occur in the process of pinocytosis: macropinocytosis, caveolae-mediated endocytosis, clatherin-mediated endocytosis and clatherin/caveolae independent endocytosis (Conner and Schmid, 2003; Doherty and McMahon, 2009). Although there are mechanistic differences with the endocytic pathways, the lysosome represents the terminal stage for degradation for all types.

Components that have been endocytosed are firstly delivered to the early endosome, which functions as a sorting station, ensuring the separation of membrane proteins and receptors that will be utilised again from cargo and those that will be targeted to the lysosomes (Huotari and Helenius, 2011). Most proteins and receptors are sent back to the plasma membrane by the recycling endosomes (Huotari and Helenius, 2011). The recycling of membrane proteins from early endosomes back to the membrane represents the main membrane trafficking pathway in cells (Steinman et al., 1983). Material destined for degradation is kept within the early endosomes which converts into late endosomes through a series of fusion processes and exchange of material. Late endosomes contain acid hydrolases along with lysosomal membrane proteins (Appelqvist et al., 2013). In the late endosomes, further sorting of cargo material is carried out and transported to other organelles such as the trans-Golgi network (TGN). The TGN is involved in a trafficking material back and forth with the endosome as it removes endosomal components and delivers lysosomal material (Huotari and Helenius, 2011). The lysosome receives the cargo from late endosomes along with the new lysosomal hydrolases with membrane proteins coming from the TGN (Appelqvist et al., 2013).

The distinction between the different endosomes and the lysosomes is made to simplify the description of the endocytic pathway. In reality endocytosis is a complex pathway that has a continuous exchange of material between the different components of the pathway. Due to non-dividing nature of RPE cells, the endo-lysosomal system is under additional stress as it has to perform efficiently throughout life. One of the most important functions performed by the RPE is the phagocytosis and degradation of shed POS (Strauss, 2005). The process of POS is described next in section 1.3.1.3.

1.3.1.3 - Phagocytosis of photoreceptor outer segments (POS)

POS shedding and renewal along with the role of RPE cells in this process, was first described in the 1960's (Young, 1967; Young and Bok, 1969; Young and Droz, 1968). The renewal of POS with the help of RPE is important for the survival of photoreceptor cells. RPE cells are the most active phagocytic cells in the body and are involved in phagocytosis of POS on a daily basis (Bok, 1993; Strauss, 2005). An individual RPE cell maintains between 30-40 photoreceptors (Kaarniranta et al., 2013). Therefore, a huge metabolic burden upon the lysosomal system of an RPE cell exists.

POS phagocytosis occurs on the apical side of the RPE and once POS has been internalised, the formed phagosome moves to the basal side where its contents are digested. Important molecules such as docosahexaenoic and retinal are re-delivered to the photoreceptors (Bibb and Young, 1974; Bok, 1993). While the process of phagocytosis of POS by RPE is not completely understood at a molecular level, it has 4 distinct stages: (1) POS recognition and attachment (2) ingestion, (3) phagosome formation and lysosomal fusion and (4) degradation (Bosch et al., 1993).

Research into how POS attach to RPE cells has shown the involvement of vitronectin receptors such as αvβ3 and αvβ5 (Finnemann et al., 1997). Once POS are bound to receptors on RPE cells, signaling pathways are triggered which help to reorganize RPE plasma membrane and cause engulfment of POS. Phosphorylation is a common step in countless signaling pathways and in the case of POS engulfment, a role for focal adhesion kinase (FAK) is

shown (Finnemann, 2003). Once internalized, the phagosome that contains POS matures and fuses with the lysosome. Within the lysosomes, material is degraded by effector proteases such as the cathepsins. For example, roles for cathepsins D and S in degradation of POS have been shown (Rakoczy et al., 1997; Rakoczy et al., 1994). Proper functioning of lysosomal enzymes such as the cathepsins will ensure efficient POS degradation. Cathepsins are described further in section 1.3.2.

1.3.1.4 - Lysosomal exocytosis

In addition to being the terminal degradative compartment of processes such as autophagy and endocytosis within the cell, lysosomes are involved in a secretory pathway called lysosomal exocytosis. The process of lysosomal exocytosis is thought to occur in all cells and involves the movement of the lysosome towards the plasma membrane, where they fuse together (Jaiswal et al., 2002; Rodriguez et al., 1997). The fusion of the lysosome to the plasma membrane is driven by increased calcium concentration (Jaiswal et al., 2002; Rodriguez et al., 1997). Lysosomal exocytosis is involved in key processes such plasma membrane repair (Andrews, 2000, 2005).

Plasma membrane damage is a common event that occurs in cells, especially those under continuous mechanical stress such as muscle cells (McNeil and Khakee, 1992). Damage to plasma membrane can also occur via secreted pore-forming toxins by pathogens trying to gain access to the cell (Gonzalez et al., 2008). The restoration process of the damaged membrane is important for cell survival and depending on the damage, can be achieved within seconds up to a min (Steinhardt et al., 1994). Upon damage, calcium from the extracellular environment enters into the cell to initiate the repair of the membrane hole (Reddy et al., 2001). Calcium binds to and causes a conformational change of lysosomal membrane protein called synaptotagmin VII (Syt VII) which helps facilitate the fusion of the lysosome with the plasma membrane (Martinez et al., 2000). Translocation of the lysosome leads to the formation of a lysosomal patch which fuses with the plasma membrane and seals the damaged hole (McNeil, 2002). The process of exocytosis leads to the extracellular release of lysosomal

enzymes as well as the appearance of lysosome-associated membrane proteins i.e. LAMP-1 on the plasma membrane (Rodriguez et al., 1997). The lesion of plasma membrane that contains LAMP-1 is removed by endocytosis which helps promote and complete the resealing process. This endocytosis process is dependent on the action of an enzyme that was released by lysosomal exocytosis called acid sphingomyelinase (aSMase) (Tam et al., 2010). aSMase breaks down sphingomyelin, found in plasma membrane, into a waxy lipid known as ceramide. As the amount of ceramide increases it causes an inward bending of the membrane which helps in the endocytosis pathway (Holopainen et al., 2000).

In addition to lysosomal exocytosis contributing to membrane repair, it may act as a system to help clear accumulated debris within a cell where degradative mechanisms are impaired. In cultured kidney cells from a mouse model of metachromatic leukodystrophy, a lysosomal storage disease, intralysosomal storage material was delivered to the cultured medium via lysosomal exocytosis (Klein et al., 2005a). Furthermore, it has been shown that undigested outer segments discs and latex beads were exocytosed towards the basolateral surface of RPE (Matsumura et al., 1985; Peters et al., 2006). With age, the accumulation of debris lipofuscin in the RPE lysosomes along with accumulating drusen in the RPE basement membrane is observed. Malfunctioned lysosomal activity which is thought to play a role in lipofuscin generation may result in material that was initially destined to be degraded by the lysosomes, to leave the RPE via exocytosis and potentially contribute to drusen formation.

1.3.2 – Cathepsins - lysosomal effectors

In the lysosomal system, protein degradation comes as a result of combined action of numerous proteases. Lysosomes contains approximately 60 different hydrolases which collectively possess the capacity for both non-specific and specific degradation of macromolecules (Lubke et al., 2009). Major players that govern lysosomal function are the cathepsin family which include cysteine (Cys) proteases (B, C, F, H, K, L, O, S, V, W and X), the aspartic proteases cathepsin (D and E) and the serine cathepsins (A and G)

(Appelqvist et al., 2013b; Rossi et al., 2004). The three groups that cathepsins fall into are based on the amino acid found at the active site of the enzyme. Most cathepsins are predominantly endopeptidases while some, such as cathepsin X, are known to exhibit exopeptidase activity. Other cathepsins can exhibit dual endopeptidases/exopeptidase activity such as cathepsins B and H (Turk et al., 2002).

1.3.2.1 - Structure of cathepsins

The cysteine cathepsins comprise the largest group of cathepsins of which 11 human cathepsins (B, C, F, H, K, L, O, S, V, W and X) exist at a sequence level as well as being confirmed by bioinformatics analysis of the human genome (Rossi et al., 2004). All cysteine proteases share similar amino acid sequences and folds and are generally composed of a light chain connected to a heavy chain via disulphide bond. The enzymes are monomers with a molecular mass of around 30kDa, except for cathepsin C which in humans is a tetrameric protein with a molecular mass of 200kDa. Generally, cysteine proteases have a two domain structure: a left domain that consists of three α-helices and a right domain that is centred upon a β-barrel motif. The two domain structure opens up to form a V-shaped active site cleft which contains the reactive catalytic residues, cysteine (Cys) 25 and histidine (His) 159. The residues are located on opposite sides of the active site cleft in the left and right domain respectively. The two reactive residues form the thiolate-imidazolium ion pair which is important for enzymatic activity (Barrett et al., 2004; Guha and Padh, 2008; Turk et al., 2012).

Like cysteine proteases, mammalian aspartic proteases, such as cathepsin D and E, also share a high degree of sequence similarity and exhibit some key features. Conserved features include a triad of aspartic acid (Asp) threonine (Thr) and glycine (Gly) residues around two active site Asp residues (Asp residue 32 and 215). In addition, long stretches of sequence around the triads, such as Thr-Cys ‘flap’ regions around the active site, are highly conserved in aspartic proteases (Fusek and Vetvicka, 2005).

The structure of serine proteases such as cathepsin A has also been determined. Cathepsin A was shown to contain two domains – a core domain and a cap domain. The core domain contains the active site which is composed of a catalytic triad of Serine (Ser), His and Asp at positions 150, 429, 372 respectively (Kolli and Garman, 2014).

1.3.2.2 – Targeting and processing of cathepsins

Cathepsins are synthesised as inactive pre-pro enzymes containing a N-terminal signal peptide and a proregion. The N-terminal signal peptide is recognised by the signal recognition particle which allows the transport of the precursor cathepsin into the lumen of the rough endoplasmic reticulum (ER). The signal peptide is subsequently removed by a signal peptidase. On the other hand, the proregion helps with the proper folding of the cathepsin into a 3-D structure that is inactive and preserved at neutral pH. During transport to the Golgi apparatus, procathepsins undergo N-linked glycation where oligosaccharides are transferred to certain asparagine residues part of a consensus motif Asn-X-Thr/Ser (Braulke and Bonifacino, 2009). An addition of a mannose-6-phosphate (M6P) label to the pro-cathepsin also occurs. The M6P label binds to M6P-receptors in the TGN after which the enzyme-receptor complex exits and fuses with late endosomes. In the late endosomes, the mild acidic pH (6.0-6.5) causes dissociation of the pro-cathepsin from the M6P-receptor. The receptor is recycled back to the TGN, with enzymes processed into active proteases in the acidic environment of the late endosomes and lysosomes (Coutinho et al., 2012; Guha and Padh, 2008; Repnik et al., 2013). The targeting and processing of cathepsins is represented in a diagrammatic representation in figure 1.7.

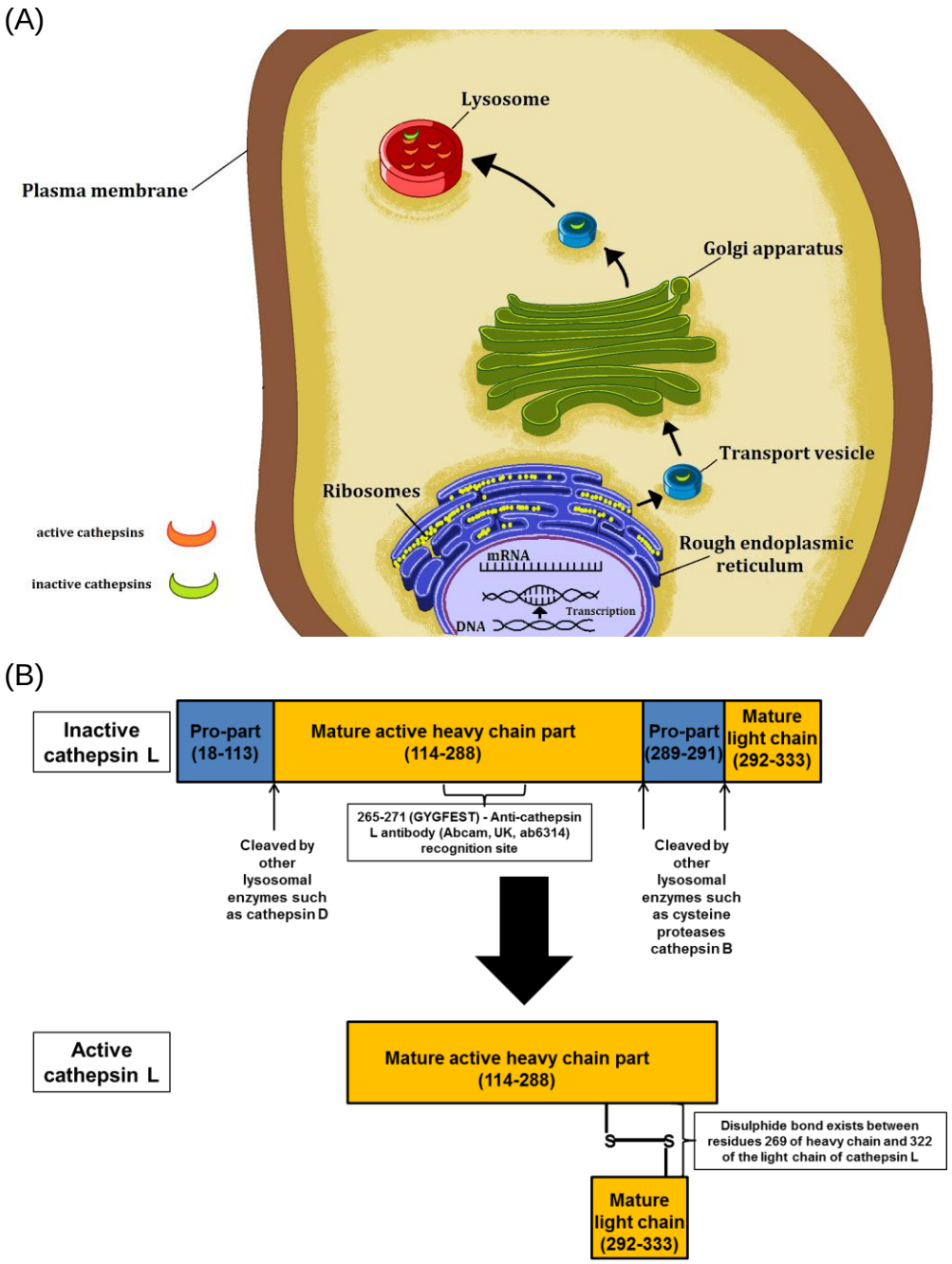

Figure 1.7: Cathepsins synthesis, targeting and processing. (A) Route of cathepsins synthesis and transport to the lysosomes within the cell. Once mRNA is produced, cathepsin synthesis occurs in the rough endoplasmic reticulum after which transportation to the Golgi apparatus occurs where cathepsins are labelled and sent to the lysosome. (B) Example of how cathepsin L is processed once it has been transported into the lysosome. Recognition site for antibody against cathepsin L used in this study (see methods section 2.2.3) is also shown.

1.3.2.3 - Mode of action of cathepsins

For cysteine proteases, the first step in their mode of action involves the thiol group of the cysteine residue undergoing deprotonation by the adjacent histidine residue. The substrate binds to the active site in an extended conformation where the substrate carbonyl carbon will undergo a nucleophilic attack from the deprotonated thiol from the Cys residue. This results in a release of amine fragment from the substrate and a thioester bond between the Cys thiol and the substrates carboxyl-terminus. Also the His residue is returned back to its deprotonated form. The thioester bond is hydrolysed which frees the enzyme and generates a carboxylic acid on the substrate (Guha and Padh, 2008).

Aspartic proteases in general are dimers of two identical subunits which form a monomeric bilobal structure enzyme (Fusek and Vetvicka, 2005). The general accepted mechanism for aspartic proteases is that the two Asp residues in the active side coordinate with one water molecule. One Asp residues abstracts a proton from the water which then enables the water to carry out a nucleophilic attack on the substrate carbonyl carbon of the scissile bond. This attack leads to the formation of an intermediate known as a tetrahedral oxyanion. This intermediate is unstable which causes protonation of the scissile amide resulting in the substrate being split into two (Suguna et al., 1987).

The mechanism of serine protease catalysis involves the Ser residue in active site carrying out a nucleophilic attack on the carbonyl carbon of the scissile bond of the substrate. Eventually through coordinated interactions with other residues within the active site and a water molecule, the breakdown of the substrate occurs (Hedstrom, 2002).

1.3.2.4 –The roles and functions of cathepsins

In general, it is in the acidic environment of the lysosomes where cathepsins are enclosed and carry out the bulk of proteolytic degradation. The cysteine cathepsins such as B, C, H and L and the aspartic cathepsin D are ubiquitously expressed and are the most abundant proteases in lysosomes

(Rossi et al., 2004). On the other hand, some cathepsins have specific cell and tissue-type expression highlighting the possibility of specific cathepsin functions. For example cathepsin K is highly expressed in bone cells such as osteoclasts where it is believed to participate in the process of bone resorption (Mandelin et al., 2006). Cathepsin K has an extracellular function in osteoclasts where, after secretion, it degrades the ECM component type I collagen. The genetic disease known as pycnodysostosis, which is caused by defective osteoclast function leading to impaired bone resorption, is linked to cathepsin K gene mutations (Gelb et al., 1996). Furthermore, a cathepsin K knock-out mouse model displays signs of osteoporosis i.e. bone fragility, which is believed to be due to impaired bone resorption by cathepsin K deficient osteoclast cells (Saftig et al., 1998). In addition to osteoclast function, cathepsin K is also important in fibroblast mediated collagen degradation (Everts et al., 2003). Fibroblasts are involved in the phagocytosis and lysosomal degradation of soft connective tissue collagen fibril (Everts et al., 1995). Cathepsin K contributes to the collagen degradation as its deficiency in pycnodysostosis leads to the accumulation of non-digested collagen material within the lysosomal apparatus of fibroblasts (Everts et al., 2003).

Other cathepsins such as B and L are also important for various physiological processes such as the development of bone, skin and hair (Potts et al., 2004; Roth et al., 2000). In its role in skin formation, cathepsin L is thought to be important in protein turnover during keratinocyte differentiation (Tanabe et al., 1991). Cathepsin L deficient mice present abnormalities such as skin epidermal skin epidermal hyperplasia, hair shaft fragmentation, gradual hair loss, and baldness (Potts et al., 2004). Also, mice deficient in cathepsin L along with cathepsin B display apoptotic neuronal loss and brain atrophy therefore demonstrating vital roles for cathepsins in maintenance of central nervous system (Felbor et al., 2002). Interestingly, neurodegeneration is preceded by the accumulation of lysosomal residual bodies in neurons indicative of impaired lysosomal function (Felbor et al., 2002).

Taken together, the above mentioned data shows that cathepsins are involved in vital functions such as ECM turnover as well as intracellular proteolytic function. In relation to RPE cells, alterations and/or impairment of cathepsin activity could have detrimental effects such as contributing to accumulation of undegraded material/lysosomal residual bodies, an event commonly seen in cells in ageing RPE. Also, cathepsin deficiency causes cell death, which could be of interest as atrophy of RPE cells occurs in degenerative diseases such as AMD.

As cathepsins are involved in processes such as ECM remodelling, this generally requires the relocation of cathepsins outside the lysosomes (Turk et al., 2012; Zuzarte-Luis et al., 2007). Extracellular function of cathepsins also demonstrates that cathepsins are able to remain active outside the lysosomes. To have optimal activity, be it inside the lysosome or outside, cathepsins generally require a reducing, slightly acidic environment as they can be irreversibly inactivated at neutral pH (Turk et al., 1995; Turk et al., 1993). An exception is cathepsin S which is active at neutral pH (Kirschke et al., 1989). Although cathepsins undergo inactivation at neutral pH they can remain active for a short amount of time and therefore in theory cause cleavage of substrates (Turk et al., 1995; Turk et al., 1993). In addition, acidification of the environment that cathepsins encounter can help to stabilise cathepsin activity (Gottlieb et al., 1995; Konttinen et al., 2002; Rozhin et al., 1994). Cathepsins may also be stabilised by binding to their substrates such as heparin (Almeida et al., 2001; Turk et al., 1993). Thus, cathepsins have the capability to remain active once outside the lysosome.

1.3.2.5 - Roles of cathepsins in the cytosol

In addition to their main function within the lysosomal compartment in protein degradation, cathepsins exert important roles within the cytosol such as involvement in apoptosis and inflammasome activation (Conus and Simon, 2008; Duewell et al., 2010; Rajamaki et al., 2010). A prerequisite for cathepsin release into the cytosol is lysosomal membrane permeabilization (LMP) (Conus and Simon, 2008). Although the mechanism by which LMP occurs is not fully understood, many agents that cause LMP have been

identified. Exogenous agents include $_L$-Leucyl-$_L$-leucine methyl ester (LLOMe) and hydroxycholoroquine (Boya et al., 2003; Uchimoto et al., 1999). Endogenous agents that induce LMP have also been described with an important category being ROS, which increase in oxidative stress conditions (Zdolsek et al., 1993). An increase in ROS production via hydrogen peroxide, through iron-catalysed Fenton reactions, is shown to induce LMP, the release of cathepsin D into the cytosol and cause cell death (Lin et al., 2010). In addition, in neutrophil cells, NAPDH-generated ROS causes LMP (Blomgran et al., 2007).

Evidence shows that LMP may be an early event that triggers apoptosis or may occur later on in the signalling cascade which amplifies the apoptotic signal (Repnik et al., 2012). The best characterised target of cathepsins in regards to apoptosis signalling is the pro-apoptotic Bcl-2 family member Bid (Repnik et al., 2012). Cathepsins, such as B, D, L and S can cleave Bid into its potent pro-apoptotic tBiD (Cirman et al., 2004). Cleavage of Bid into tBiD causes activation of other pro-apoptotic molecules such as Bax leading to release of cytochrome C from the mitochondria. Cytochrome C is then able to initiate the caspases cascade which causes cellular apoptosis. In addition to Bid, anti-apoptotic Bcl-2 proteins such as Bcl-2 and Bcl-X_L are also cathepsin substrates (Droga-Mazovec et al., 2008).

LMP also induce inflammasome activation (Hornung et al., 2008; Rajamaki et al., 2010). Inflammasomes are multiprotein complexes that initiate the inflammation process by activating caspase-1 which causes the proteolytic maturation of pro-inflammatory cytokines IL-1β and lL-18 (Mariathasan and Monack, 2007). Of interest, the NLRP3 inflammasome is expressed in RPE cells (Tseng et al., 2013). Destabilisation of lysosomes induced by LLOMe leads to activation of the NLRP3 inflammasome in RPE cells (Tseng et al., 2013). Furthermore, when cathepsin B and L are inhibited, lysosomal damage-induced inflammasome activation is blocked (Tseng et al., 2013). This suggests that cathepsins B/L are involved in causing NLRP3 activation.

Both inflammation as well as apoptosis are associated with RPE dysfunction and subsequent AMD development (Augustin and Kirchhof, 2009; Dunaief et

al., 2002). With age, an accumulative oxidative insult upon RPE cells due to the presence of initiators of stress such as AGEs as well as decreased anti-oxidant capacity, may induce LMP. Subsequently, cathepsins released into cytosol may participate in inflammasome and apoptotic activation.

1.3.2.6 - The role of cathepsins in extracellular matrix (ECM) degradation

ECM components such as fibronectin, laminins, proteoglycans and collagens are targets for cathepsin cleavage. Cathepsin B is able to degrade ECM components such as collagen type IV, fibronectin and laminin (Buck et al., 1992). Proteoglycans such as nidogens 1 and 2, involved in linking collagen type IV and laminin molecules together in basement membranes are also susceptible to cathepsin cleavage (Sage et al., 2012). Interestingly, both nidogen 1 and 2 are shown to be present within the BrM (Kunze et al., 2010). Cathepsins such as B, K, L and S also display elastinolytic activity (Turk et al., 2012). Furthermore, cathepsins are implicated in the process of angiogenesis (Pepper, 2001). For instance, cathepsin B can regulate the availability of endostatin, which is an angiogenic inhibitor critical for proper vascular structure development (Ferreras et al., 2000). Cathepsin B can cleave collagen XVIII, which is a protein in the vascular and epithelial basement membrane, into endostatin (Zatterstrom et al., 2000). Collagen XVIII has been shown to be present in the BrM of the retina (Fukai et al., 2002). Cathepsin L also shows ability to generate endostatin from collagen XVIII, in murine hemangioendothelioma (EOMA) cells (Felbor et al., 2000).

Taken together, cathepsins are able to act on different components of ECM which suggests a role in turnover as well as possible involvement in processes such as angiogenesis. It is conceivable that if uncontrolled cathepsin activity was found at the site of the BrM they could contribute to proteolytic degradation of the BrM and vascular outgrowth of choroidal vessels, events observed in AMD. Thus, due to their destructive properties, the regulation of cathepsins is crucial as uncontrolled behaviour could potentially have destructive effects.

1.3.3 - Regulation of cathepsin activity

Various cellular mechanisms are in place in order to prevent potentially harmful and uncontrolled proteolytic activity of cathepsins. Mechanisms include zymogen activation, environmental pH and endogenous inhibitors (Guha and Padh, 2008; Turk et al., 2012).

1.3.3.1 - Zymogen activation

Cathepsins are synthesised as inactive enzymes known as zymogens. In the main, propeptides chain folds on the surface of the enzyme run through the active-site cleft therefore blocking the active site and making it inaccessible to the substrate. In order to activate the enzyme, the N-terminal pro-domain is proteolytically removed by different proteases such as cathepsin D and cysteine proteases or autocatalytically due to acidic conditions (Turk et al., 2012). The autocatalytic activation of cathepsins is also accelerated in the presence of GAGs such as chondroitin sulfate and heparin (Caglic et al., 2007). Cathepsins can encounter GAGs in the lysosome, where GAGs recycling occurs (Caglic et al., 2007). GAGs are also present in the ECM where cathepsins have been shown contribute to conditions such as arthritis and cancer (Baici et al., 1995; Mohamed and Sloane, 2006). In addition to activating cathepsins, GAGs may help stabilise enzymes at neutral pH which may be important in the extracellular function of cathepsins (Almeida et al., 2001).

1.3.3.2 - Inhibitors of cathepsins - cystatin superfamily

The most important regulation of cathepsin protease activity is through their endogenous inhibitors such as the cystatin superfamily. The cystatin superfamily comprises of a group of homologous potent protease inhibitors and can be categorised into 3 major families: 1) stefins, 2) cystatins and 3) the kininogens (Barrett, 1986; Ochieng and Chaudhuri, 2010). From among this superfamily, cystatin C is the tightest binding inhibitor of cysteine proteases such as cathepsins B, L and S (Barrett, 1986; Turk and Bode, 1991).

1.3.3.3 - Cystatin C structure, biochemical characteristics and mechanism of inhibition

Cystatin C, the main member of the second major family of the cystatin superfamily, contains two-disulphide bridges (Barrett, 1987). The active cystatin C inhibitor protein is a 120 amino acid residue that has a molecular weight of ~13kDa. Cystatin C exhibits two inhibitory sites which confer a dual inhibitory property making it the tightest-binding inhibitor of cysteine proteases (Barrett et al., 1984; Turk and Bode, 1991).

Cystatin C functional studies have identified at least three regions vital for its inhibitory action: 1) in the N-terminal region there is an evolutionary conserved glycine (Gly) residue (Gly-11) with 3 preceding residues which help increase affinity for target enzymes; 2) the five amino acid residue at positions 55-59 (Gln-Val-Val-Ala-Gly) is involved in the formation of tight beta-hairpin loop crucial for binding cysteine proteases; 3) the pro-105-Trp106 region that anchors the inhibitor to the protease once the complex is made (Bjork et al., 1996; Hall et al., 1993; Paraoan et al., 2010; Rodziewicz-Motowidlo et al., 2009).

Cystatin C works via a two-step reversible inhibitory mechanism where initially a weak interaction is made followed by a conformational change (Barrett et al., 1984; Nycander et al., 1998). For example, the inhibition of cathepsin B by cystatin C occurs by an initial interaction which most likely involves binding of the N-terminal region of cystatin C to cathepsin B (Nycander et al., 1998). After the initial interaction of cystatin C, a conformational change occurs which helps displace structures of the cathepsin B and results in blockage of the active site and subsequent cathepsin inhibition (Nycander et al., 1998).

Interestingly, cystatin C can form inactive dimers and oligomers by ‘domain swapping’ (Janowski et al., 2001). Domain swapping is a process in which two proteins exchange a part of their structure to form dimers. Growth of dimers can occur by additional rounds to form oligomers which can eventually form toxic amyloid deposits (Wahlbom et al., 2007). The oligomerization of cystatin C is dramatically increased in the case of the

naturally occurring rare Leu68Gln (Icelandic) mutant variant. Autosomal dominant inheritance of this variant leads to hereditary cystatin C amyloid angiopathy (HCCAA) (Abrahamson, 1996; Palsdottir et al., 1988).

1.3.3.4 - Cystatin C expression and roles

Cystatin C was originally identified in human cerebrospinal fluid (CSF) and later in all other mammalian body fluids and tissues (Bobek and Levine, 1992; Turk et al., 2008). Notably, cystatin C is one of most abundantly expressed proteins from the RPE, being among the top 2% of all expressed genes in both human and mouse studies (Ida et al., 2004; Paraoan et al., 2000; Wistow et al., 2002). The cystatin C protein is synthesised as a precursor that contains a 26 amino acid long N-terminal signal peptide that targets the protein to the endoplasmic reticulum (ER)/Golgi secretory pathway (Abrahamson et al., 1987; Paraoan et al., 2001). In the RPE, cystatin C is secreted predominantly basolaterally towards the BrM and choriocapillaries (Paraoan et al., 2001).

The role of cystatin C is not fully characterized in the RPE. However, due to its strong inhibitory action on cysteine cathepsins as well as its presence in the extracellular environment, it is conceivable that cystatin C has the potential to modulate extracellular proteolytic activity such as matrix remodelling and turnover at its site of action. In addition to this, cystatin C can be internalised by cells where it is involved in the regulation of intracellular enzymatic activity. Notably, after uptake, cystatin C ends up in endo-lysosomal structures where it co-localises with target enzymes (Wallin et al., 2013). Furthermore, cellular uptake of cystatin C results in a decrease in enzymatic activity of targets such as cathepsin B (Wallin et al., 2013). Taken together, cystatin C may function as an extracellular inhibitor of its molecular targets as well as having possible involvement in intracellular regulation of lysosomal cathepsins. Maintaining a balance between cystatin C and cathepsins helps to potentially regulate several important processes such as ECM remodelling and important lysosomal functions. Interestingly, in ageing RPE, cystatin expression levels are altered (Kay et al., 2014). This

decrease with age could affect the balance of cystatin C with cathepsins and therefore, contribute to altered ECM turnover and lysosomal dysfunction.

1.3.4 – Implications of lysosomal dysfunction in RPE cells

The lysosomal apparatus of the RPE must eliminate a substantial amount of material received from POS degradation and the autophagy pathway. In order for the lysosome to work efficiently, a high level of activity from lysosomal enzymes is required. Therefore, the maintenance of the lysosome along with the functional enzymes such as the cathepsins is vital to help prevent the accumulation of damaged proteins in RPE (Kaarniranta et al., 2013; Ryhanen et al., 2009). Alterations of cathepsin activity in the RPE could have implications for important lysosomal processes such as POS degradation and autophagy and contribute to accumulation of cellular debris.

Interestingly, cathepsins are shown to be susceptible to age-related alterations. For example, an increase in cathepsin B and cathepsin D activity as well as a decrease in cathepsin L activity is seen in aged rat brain (Nakanishi et al., 1994). Cathepsin B protein and activity levels also increase in the livers of ageing rats (Keppler et al., 2000). Initiators of oxidative insult (ROS and AGEs) that accelerate cellular decline associated with ageing, also alter cathepsins levels. Cathepsin B, L and H activities significantly decrease in kidney proximal tubule cell line LLC-PK1 after AGEs exposure (Sebekova et al., 1998). Furthermore, exposure of vascular smooth muscle cells to AGEs causes autophagy inhibition at the autophagosome degradation phase via the down-regulation of cathepsin D protein expression (Ma et al., 2015). Autophagy suppression is reversed by overexpression of cathepsin D therefore showing the importance of normal cathepsin function in the autophagy process (Ma et al., 2015).

As oxidative stress is a major risk factor for RPE dysfunction and AMD development, exposure to ROS and AGEs may affect cathepsin activity in the RPE (Jarrett and Boulton, 2012). Indeed, cathepsin B, L and S gene expression increases in mouse RPE cells under oxidative stress conditions (Alizadeh et al., 2006). Furthermore, RPE cells exposure to AGEs causes a decrease in mRNA expression of lysosomal enzymes cathepsin S, cathepsin

G, acid phosphatase, β-galactosidase and β-mannosidase. Cathepsin D activity levels also decrease in RPE cells after AGEs exposure. These lysosomal changes may contribute to the decrease in POS degradation and increase in lipofuscin accumulation observed in RPE cells after AGEs exposure (Glenn et al., 2009).

In addition to POS degradation, alteration of cathepsins activity is likely to have adverse effects on the autophagy process which is involved in clearance of damaged organelles such as mitochondria. The mitochondria, as well as being a source for ROS generation, are also a target for ROS-induced damage i.e. mitochondria DNA damage (Kim et al., 2007). Damaged organelles fuse with lysosomes where they are degraded in the autophagy process (Kim et al., 2007). In an *in vitro* aged-RPE model in which mitochondria DNA damage is induced, a decrease in lysosomal activity, due to altered cathepsin D levels, occurs (Wang et al., 2009b). The decrease in lysosomal activity is likely to contribute to impaired autophagy response leading to an intracellular overload of molecules and organelle. Interestingly, a decrease in lysosomal activity was accompanied by increase in exosome markers which indicates increase exosome release (Wang et al., 2009b). Exosomes are 40-100nm vesicles that form through the endocytic pathway. Exosomes form by the inward invaginations of the membrane of endosomes leading to generation of multivesicular bodies (MVB). MVBs release their internal exosomes vesicles into the extracellular environment by fusing with the plasma membrane (Raposo and Stoorvogel, 2013). It may be that exosome release is an alternative mechanism by which the cells clear intracellular debris when lysosomal activity is compromised. The material that is released may contribute to the formation of extracellular deposits such as drusen. This is supported by the presence of intracellular proteins and exosome markers within drusen (Wang et al., 2009b).

Taken together, it is suggested that alterations of cathepsins cause lysosomal dysfunction which in turn contributes to accumulation of lipofuscin and drusen. Further study into the effects of ageing on the balance between cathepsins and their inhibitors and how dysregulation occurs will help gain a

better understanding on the pathological changes associated with RPE ageing and subsequent development of AMD.

1.4 - Age-related macular degeneration (AMD)

AMD is characterised by pathological changes that are primarily due to dysfunction and degeneration of RPE cells which subsequently lead to dysfunction of photoreceptor cells in the macula region. Along with the RPE and photoreceptor cells, changes are also observed in the BrM and the underlying choriocapillaries. AMD can be phenotypically divided into two forms: geographic atrophy (dry) and exudative (wet) types (Jager et al., 2008) (Figure 1.6).

Dry AMD accounts for approximately 85% of all AMD cases and is responsible for 10% of all vision loss linked with AMD. The development of dry AMD occurs over many years and therefore can go undetected in early stages (Bhutto and Lutty, 2012). A hallmark of early AMD is the presence of yellowish-white extracellular deposits called 'drusen' which accumulate between the basal surface of the RPE and the BrM (Bhutto and Lutty, 2012; Buschini et al., 2011). As dry AMD progresses, there is an atrophy of RPE cells and thinning of photoreceptors in the macula region leading to tissue death. Tissue loss causes patients to have blind spots in their central vision. Eventually as the disease progresses to the advanced stage, there is complete loss of central vision (Bhutto and Lutty, 2012). Currently there are no cures for the dry form of AMD.

A more rapid visual loss is caused by the wet form of AMD (Bressler et al., 1988). Wet AMD, is characterised by CNV, which is a migration of aberrant new choroidal blood vessel proliferation through the BrM into the space below the RPE (Bhutto and Lutty, 2012). The blood vessels that invade the sub-RPE space are highly permeable and leak fluid to cause haemorrhages, RPE/retinal detachment and distortion of vision (de Jong, 2006). The progression of wet AMD is very rapid and can potentially cause blindness within months (Munk et al., 2012). Although wet AMD only accounts for approximately 10-15% of all cases of AMD, it is responsible for 90% of vision loss associated with AMD (Donoso et al., 2006). Wet AMD can be treated to a certain extent with the use of anti-VEGF treatment that is intravitreally injected. Blocking VEGF helps reduce the growth of new abnormal blood

vessels, slowing down vision loss and in some cases, improvement of vision. It should be noted that not all patients respond to anti-VEGF treatment (Miller, 2010). Therefore, there is a need for better treatments which will only come through better biological understanding of AMD.

Edited Version

Figure 1.8: Pathological changes that occur in macula region in AMD. (A) Normal macula (B) dry form of AMD – drusen accumulation between RPE cells and BrM as well between RPE layer and photoreceptors. Atrophy of RPE cells, choroidal atrophy as well as thickening of BrM. Widespread atrophy leads to advanced stage geographic atrophy (not shown). (C) Wet form of AMD – characterised by CNV. New choroidal vessels break through gaps in BrM and grow below or within retina region causing disturbance of retina structure. CNV will eventually scar with permanent damage caused (Picture taken from Khandhadia et al., 2012).

1.4.1 - Hallmarks of AMD

As previously eluded to, the extracellular deposits of drusen are a hallmark of AMD. For diagnosis purposes, early AMD is recognised by the detection of drusen and /or pigmentation irregularities in the macula region by ophthalmoscopy (Seddon et al., 2006). Drusen accumulates between the RPE and the BrM, more specifically between the RPE basal lamina and the inner collagenous layer of the BrM (Hageman et al., 2001). Based on their appearance, drusen are classified as 'hard' or soft''. Hard drusen have a well-defined structure and are generally small whereas soft drusen are larger and have less-defined structures. Hard drusen can develop into soft drusen. The presence, number, size and confluency of drusen are risk factors for the progression of AMD (Klein et al., 2007). In particular, the presence of soft drusen is associated with higher risk of developing advanced AMD. When there are 8 or more hard drusen present, the incidence of soft drusen increases. This in turn increases the number and area of soft drusen and therefore leads to a higher risk of developing advanced AMD.

The composition of drusen is heterogeneous, but they are mainly composed of lipids such as unesterified and esterified cholesterol, phosphatidylcholine and fatty acids (Wang et al., 2010). In addition, drusen also contain other molecules such as apolipoproteins, AGEs and amyloid proteins such as Aβ (Buschini et al., 2011; Ishibashi et al., 1998). Although the origin of drusen is not fully understood, evidence suggests the RPE and the plasma are the most likely sources (Hageman et al., 2001; Wang et al., 2009b).

Other deposits that accumulate in the ageing retina are basal laminar deposits (BlamD), BlinD and reticular pseudodrusen. BlamD are located between the RPE plasma membrane and basal lamina. BlamD are heterogeneous material composed of long spaced collagen fibres and basal lamina proteins (Sarks et al., 2007). BlinD are located between the RPE basal lamina and the inner collagenous layers of the BrM (Curcio and Millican, 1999). On the other hand, reticular pseudodrusen deposits are located in the sub retina space between the apical surface of the RPE and the retina (Querques et al., 2014). Both BlinD and reticular pseudodrusen

have been associated with AMD (Bhutto and Lutty, 2012; Curcio and Millican, 1999; Zweifel et al., 2010). In addition, lipofuscin is also known to accumulate in RPE cells leading to dysfunction, as mentioned previously, and is associated with development of AMD (Dorey et al., 1989; Suter et al., 2000).

The accumulation of the above mentioned deposits can trigger unfavourable molecular events such as activation of complement cascade (Zhou et al., 2006) and oxidative damage (Rozanowska et al., 1995) that cause RPE dysfunction/death with subsequent photoreceptor loss leading to AMD.

1.4.2 - AMD aetiology

Although its pathogenesis is not fully understood, AMD is a complex late-onset multifactorial neurodegenerative disease that involves the interplay between genetic and environmental factors (Cai and McGinnis, 2012; Nowak, 2006).

1.4.1.1 - Genetic and Environmental Risk Factors in AMD development

Age is the greatest risk factor for AMD development but it is known that environmental and lifestyle factors also influence an individual's risk. A proven risk factor for development and progression of AMD is cigarette smoking (Velilla et al., 2013). Cigarette smoke contains a large amount of toxic compounds such as nicotine, cadmium and polycyclic aromatic hydrocarbons (PAHs). These compounds can cause damage by promoting molecular and pathological changes such as promoting angiogenesis and neovascularisation, inducing oxidative damage as well as promoting apoptosis of RPE cells (Velilla et al., 2013). Nicotine enhances the proliferation and migration of human choroidal and retinal arterial endothelial cells therefore showing vascularisation properties of cigarette smoke. Cadmium can accumulate in the RPE and choroid and cause an increase in reactive oxygen species (ROS) therefore inducing oxidative stress. Polycyclic aromatic hydrocarbons (PAHs) have toxic effects on RPE such as causing nuclear and mitochondrial DNA damage and RPE cell apoptosis (Patton et al., 2002; Sharma et al., 2008). Along with smoking other risk

factors such as alcohol intake (Chong et al., 2008) exposure to sunlight (Cruickshanks et al., 2001) and diet control (Seddon et al., 2001) have also been described to influence risk to AMD development.

A genetic component for AMD has been demonstrated by familial aggregation and twin studies. Familial aggregation studies have shown that there is a greater prevalence of AMD amongst first degree relatives of individuals with AMD compared with first-degree relatives of control individuals (Klaver et al., 1998b; Seddon et al., 1997). Furthermore, a higher concordance rate of AMD is observed between monozygotic twins compared to the concordance rate in dizygotic twins (Grizzard et al., 2003; Hammond et al., 2002; Klein et al., 1994; Meyers, 1994).

A significant breakthrough in understanding the genetic component of AMD came in 2005. Josephine Hoh and group reported a genome wide association study (GWAS) of 96 cases and 50 controls for polymorphisms associated with AMD (Klein et al., 2005b). From the 116,204 single nucleotide polymorphisms tested, a strong association of AMD with variants in and around the complement factor H (CFH) gene, which maps to chromosome 1q31, was identified (Klein et al., 2005). Other groups within the same year, using different approaches obtained similar results in which CFH gene was linked to AMD (Edwards et al., 2005; Hageman et al., 2005; Haines et al., 2005). Another locus shown to have strong association with AMD is in the chromosome 10q26 region. In the 10q26 region of association, at least 3 potential candidate genes for AMD association exist which are pleckstrin homology domain containing family A member 1 (PLEKHA1), age-related maculopathy susceptibility 2 (ARMS2- also known as LOC3877715) and high-temperature requirement A serine peptidase 1 (HTRA1) (Fisher et al., 2005; Jakobsdottir et al., 2005; Rivera et al., 2005).

A large set of candidate gene association studies have also revealed other genes linked to AMD. Candidate genes have been selected due to prior knowledge of their biology and/or pathways they are likely to be involved in. Apolipoprotien E (ApoE) was an early target as a candidate gene and this protein presents itself as three common isoforms E2, E3 and E4, which are

encoded by three alleles *ε2*, *ε3*, and *ε4* on the ApoE gene on chromosome 19q13.2 locus (Fritsche et al., 2009). The ApoE *ε2* is the strongest allele linked to increasing the risk of AMD whereas *ε4* allele carriers have the lowest risk of developing the disease (Klaver et al., 1998a). Other genes shown to be associated with AMD include manganese superoxide dismutase (Kimura et al., 2000), the ABCA4 gene (Allikmets and Consortium, 2000; Allikmets et al., 1997). Interestingly, a polymorphism in the cystatin C gene, CST3, which codes for the most abundant protease inhibitor in RPE cells, cystatin C, has also been implicated as a risk factor for exudative AMD in Caucasians (Zurdel et al., 2002).

Cystatin C is encoded by the CST3 gene, which is located on chromosome 20 (gene map locus 20p11.21) and contains three KspI single nucleotide polymorphism (SNP) at positions -157, -72 and +73 (Abrahamson et al., 1989; Balbin and Abrahamson, 1991). Due to strong linkage disequilibrium between the three SNPs, cystatin C presents two haplotypes called wild-type (haplotype A) and the variant B (haplotype B) (Finckh et al., 2000) (Figure 1.8). The polymorphism in the CST3 gene, that is associated with AMD, is the non-synonymous single nucleotide polymorphism (SNP) (rs1064039 – G73A) in the signal sequence which leads to an alanine (A) to threonine (T) substitution (A25T) at position 25 of the precursor protein (Balbin and Abrahamson, 1991; Balbin et al., 1993). Individuals homozygous for the variant have the greatest risk of disease (odds ratio (OR) = 3.03), while heterozygous individuals are not at increased risk (Zurdel et al., 2002). This indicates that the variant allele acts in a recessive manner for AMD. Interestingly, a meta-analysis of 8 association studies has also confirmed that the same rs1064039 SNP in the CST3 gene is associated with AD in Caucasians, with homozygous individuals for the variant allele at the greatest risk (OR = 1.73) (Hua et al., 2012). Similarly to its association with AMD, the variant allele acts in a recessive manner (Hua et al., 2012).

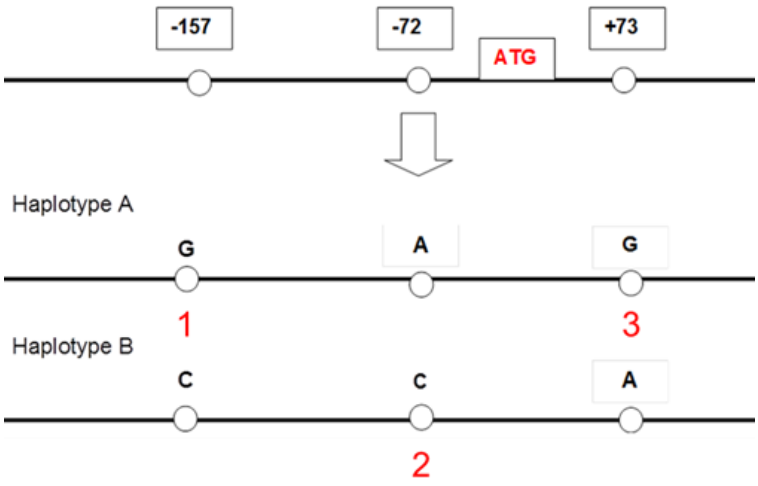

Figure 1.9: CST3 linkage disequilibrium of three KspI polymorphisms in 5' region of gene resulting in two haplotypes: wild-type (A) and variant (B). Two polymorphisms located 157 (**1**) and 72 (**2**) bases upstream from transcription start site (**ATG**) with one SNP 73 (**3**) bases downstream from the transcription start site.

Both AMD and AD are neurodegenerative disorders that share common features such as the presence of insoluble deposits at the sites of pathogenesis i.e. drusen of AMD and amyloid plaques of AD. Both drusen and amyloid deposits demonstrate some similarity in composition such as the presence of amyloid P, vitronectin and amyloid β peptide (Anderson et al., 2004; Mullins et al., 2000). In addition, both deposits also serve as chronic inflammatory stimulus which can contribute to atrophy of cells leading to disease development (Kurji et al., 2010; Liu et al., 2013; Rubio-Perez and Morillas-Ruiz, 2012). This suggests that common cellular mechanism may contribute to the pathogenesis of both AMD and AD. Notably, proteolytic dysregulation is considered to be implicated in AMD and AD pathogenesis (Hook et al., 2008; Kaarniranta et al., 2011).

As cystatin C is a potent protease inhibitor, it is believed to have an important role in proteolytic control in its sites of actions i.e. the BrM in relation to RPE. The A25T substitution has no effect of any of the protein domains involved in biochemical function of cystatin C but has consequences on processing and trafficking. In RPE cells, the A25T amino acid change in the signal peptide impairs the processing of cystatin C through the secretory pathway which leads to reduced secretion (Paraoan et

al., 2004). The significant impaired processing of cystatin C is believed to be dependent on the reduced hydrophobicity in the signal peptide due to the A25T substitution (Ratnayaka et al., 2007). In addition, the variant B cystatin C surprisingly associates with the mitochondria (Paraoan et al., 2004). In addition, reduction of cystatin C secretion is also observed from fibroblasts taken from AD donors homozygous for variant B when compared to fibroblasts from heterozygous or wild-type homozygous AD donors (Benussi et al., 2003). Furthermore, wild-type cystatin C is shown to be protective against AD development by inhibiting amyloid-beta deposition (Kaeser et al., 2007; Mi et al., 2007)

The fact that the same polymorphism in the CST3 gene has an identical recessive effect on both AMD and AD is very intriguing. Having a recessive effect suggests that a single wild-type allele will be able to compensate for the variant B form. Taking into account that cystatin C is a potent protease inhibitor of cathepsins, having one single copy of the wild-type will maintain proteolytic homeostasis. On the other hand, absence of both wild-type alleles may result in cystatin C/cathepsins imbalance and lead to proteolytic dysregulation. Altered levels of cystatin C in its sites of action in relation to the RPE, could allow uncontrolled cathepsin activity, which in turn contributes to dysregulation of proteolytic homeostasis in the retina region, RPE dysfunction and development of AMD.

1.5 - Aims of study

The evidence to date suggests that age-related stresses play a significant role in the dysfunction of RPE cells and the BrM. Given the importance of the lysosome system within the RPE, age-related alterations of lysosomal activity may have detrimental effects on processes such as autophagy and POS digestion resulting in accumulation of damaged molecules and organelles. The major lysosomal effectors cathepsins are susceptible to ageing and age-related stresses which can potentially lead to lysosomal dysfunction and impaired degradative ability of cells.

The main aim of this study was to investigate the influence of age-related stresses (ROS, AGEs) on the expression and activity of key lysosomal proteases, specifically the cathepsins. It was hypothesised that RPE cell exposure to age-related stresses will cause proteolytic imbalances by altering levels of key lysosomal cathepsin proteases, which in turn may affect important lysosomal processes such as autophagy and POS digestion subsequently causing RPE dysfunction and AMD progression.

The specific aims for this present study were:

1) To investigate the endogenous expression and secretion of key proteases cathepsins B, L and S in RPE cells.

2) To assess the impact of age-related stresses i.e. AGEs exposure and H_2O_2, on expression/processing and activity of cathepsins B, D, L and S. This was investigated to shed light on how with age, proteolytic control may change in RPE cells leading to subsequent cellular dysfunction.

3) To analyse the relationship between cathepsin L expression/accumulation and age in *ex vivo* human RPE cells.

4) To further investigate the genetic association between variant B cystatin C (SNP rs1064039 in CST3 gene) with exudative AMD.

Chapter 2 – Materials and Methods

2.1 - Cell Culture

2.1.1 – RPE cell lines

ARPE-19 cells have structural and functional properties that are characteristic of RPE cells *in situ* (Dunn et al., 1996). ARPE-19 cell line arose spontaneously from a primary culture of RPE cells from a 19 year old male donor. ARPE-19 cell line have a cobblestone appearance and also express CRALBP and RPE-65, both of which are synthesised by human RPE *in vivo* (Dunn et al., 1996).

D407 cell line, also a spontaneously transformed human RPE cell line, arose from a primary culture of RPE cells from a 12 year old male and exhibit high growth potential (Davis et al., 1995). Similar to ARPE-19 cells, when confluent, D407 cells also develop a cobblestone appearance. In addition, they also express CRALBP protein as well as cytokeratin 8 and 18, all of which are characteristic of RPE (Davis et al., 1995)

In this study, ARPE-19 and D407 cell lines were used to establish cultures of human RPE. Both ARPE-19 and D407 cell lines were cultured in a 1:1 mixture of Dulbecco's modified Eagle's medium and Ham's F12 Nutrient mixture (DMEM/F12) (Sigma-Aldrich, Dorset, UK) supplemented with 10% fetal calf serum (FCS) (Sigma-Aldrich,Dorset, UK) and 2mM L-glutamine (Sigma-Aldrich, Dorset, UK).

Routinely, cells were cultured in 75cm^2 (T75) culture flasks and incubated at 37^{o}C in a humidified 5% carbon dioxide atmosphere. Cells were fed every 2-3 days with fresh media until a confluent monolayer was formed. Cells were then passaged by first removing spent media, washing 2 times with 5ml phosphate buffered saline (PBS), and then adding 0.05% trypsin (Sigma-Aldrich, Dorset, UK) to cover the surface of the flasks (4ml). Cells with trypsin were incubated at 37^{o}C for 2-5 mins until cells detached from the surface (determined by light microscope). In order to neutralise the trypsin, 6ml of media was added after which the cell suspension was placed in a 15ml tube and centrifuged at 1000rpm for 3 mins. Supernatant was removed after which the cell pellet was re-suspended in 3ml media. 1ml of the re-

suspended cells was added to a T75 flask. Media was then added to give an overall volume of 10ml per flask and cells were incubated at 37^{o}C as described previously.

For all experimental procedures, unless stated otherwise, cells were cultured in 6-well plates as follows: cells were seeded at density between 5-25x10^{4} cells per well and cultured in appropriate media (2ml per well) between 7-10 days until a confluent monolayer was formed. Media was changed every 2-3 days. After the end of the experimental time, cell lysates and conditioned media (3 days old) were collected and stored at -20^{o}C until needed. Collection of cell lysates and conditioned media is described in section 2.2.1.

2.1.2 - Non-RPE cell lines

Throughout this study, non-RPE cell lines Hela, A549 and U87MG were also used as controls in experiments.

The Hela cell line is an immortalised cell line which was derived from human cervical cancer cells (Scherer et al., 1953). These cells were cultured in DMEM (Sigma-Aldrich, Dorset, UK) supplemented with 10% FCS and 2mM L-glutamine.

The A549 cell line, also an immortalised cell line, was derived from adenocarcinomic human alveolar basal epithelial cells (Giard et al., 1973). These cells were cultured in a 1:1 mixture of DMEM/F12 medium supplemented with 10% FCS and 2 mM L-glutamine.

In addition, U87MG, an immortalised human glioblastoma cell line, was also used. U87MG cells have epithelial like morphology and were derived from a 44 year old cancer patient (Ponten and Macintyre, 1968). These cells were cultured in Eagles Minimum Essentials Medium (EMEM) (Sigma, Dorset, UK) supplemented with 10% FCS and 2mM glutamine.

2.1.3 - Producing cell cultures upon control or AGEs-modified Matrigel^{TM}

Matrigel (MG) ^{TM} (BD Biosciences, Oxford, UK) is a solubilised basement membrane extract from Engelbreth-Holm-Swarm (EHS) mouse sarcoma cells. MG^{TM} contains many extracellular matrix proteins and has similar

constituents to that of the BrM. The principal components of MG^{TM} are structural proteins such as entactin, laminin, collagen IV and heparin sulphate proteoglycan along with growth factors which provide cultured cells an effective substrate for attachment, differentiation and proliferation (Hughes et al., 2010). MG^{TM} has been used by several groups such as Stitt et al to study the effect of AGEs upon cell culture systems by inducing the formation of AGE-adducts due to glycosylation of the matrix (Glenn et al., 2009; Stitt et al., 2004).

The procedure used in this study was based upon the one used by Stitt et al (Glenn et al., 2009; Stitt et al., 2004). For experimental procedures, both 6-well and 12-well plates were used. Described here are the volumes needed per well of a 12-well plate. Therefore, all volumes were re-scaled appropriately when a 6-well plate set up was used. Firstly, a 1:10 dilution of MG^{TM} in serum free 1:1 mixture of DMEM/F12 media was prepared and carefully added to each well (200µl) of a 12-well plate and evenly spread to ensure removal of bubbles. The MG^{TM} was allowed to polymerise at 37^{o}C for 1 hour to allow a gel to be formed. The gel, containing ECM proteins, mimicked the inner most layers of the BrM and on which RPE cells could be seeded and grown. To mimic an aged phenotype of BrM, AGEs modification of the MG^{TM} extract was done as previously described (Glenn et al., 2009; Stitt et al., 2004). Briefly, to induce the formation of AGEs adducts, MG^{TM} was incubated in the presence of 100mM glycolaldehyde (Sigma, Dorset, UK) (1ml per well) at 37^{o}C for 4 hours. Glycolaldehyde is a reactive intermediate known to cause the formation of the AGE adduct CML (Glomb and Monnier, 1995). CML has been shown to be involved in the pathogenesis of AMD as it was the first AGE to be found in AMD BrM and drusen (Ishibashi et al., 1998). CML has also been shown to stimulate neovascularisation *in vivo* (Okamoto et al., 2002).

The glycation reaction was terminated by rinsing the substrate twice with excess PBS before incubating with 50mM sodium borohydride (500µl) (Sigma, Dorset, UK) at 4^{0}C overnight. The following day, MG^{TM} was rinsed twice with excess PBS and was now ready for cells to be seeded upon it.

MG^{TM} that mimicked a young phenotype was prepared in the same way but instead of glycolaldehyde, MG^{TM} was incubated with PBS solution. The degree of AGEs modification and collagen cross-linking in this *in vitro* model has been previously described (Stitt et al., 2004). ARPE-19 and D407 cells were seeded upon control and AGEs-modified MG^{TM} at a cell density of 5x10^4 cells in appropriate media (1ml per well).

Each experiment was designed so that on one plate, there were three wells each for the control MG^{TM} (NA) and AGEs-modified MG^{TM} (A) for each cell type. Two time points of 1 and 2 week were used after seeding cells. For the 1 week experiments, both ARPE-19 and D407 cells were maintained in 1ml of 1:1 mixture of DMEM/F12 media supplemented with 10% FCS for the first four days after which media was switched to 1:1 mixture of DMEM/F12 supplemented with 2% FCS for the remaining time in order to help in the formation of stable RPE monolayers. For the 2 week cultures, only the ARPE-19 cell line was used. After the respective time points, cell lysates and media were collected and stored at -20^{o}C (described in section 2.2.1)

2.1.3 – Hydrogen peroxide (H_2O_2) treatment of ARPE-19 cells

ARPE-19 cells were seeded at a density of 1x10^4 cells into each well of a 6-well plate. Experiments were designed so that in each independent experiment, untreated control cells and cells treated with H_2O_2 (OxStress) were done in triplicate. Cells were cultured for 4 days in a 1:1 mixture of DMEM/F12 media supplemented with 10% fetal calf serum FCS and 2mM L-glutamine. On the fifth day, controls wells were treated with serum free 1:1 mixture of DMEM/F12 and test wells were treated with media containing the appropriate concentration of H_2O_2 for 24 hours. After the time point, media was removed and cell lysates were prepared and stored at -20^{o}C (described in section 2.2.1).

The 3-(4, 5-dimethylthiazol-2-yl)-2, 5-diphenyltetrazolium bromide tetrazolium (MTT) assay was used to determine an appropriate concentration of H_2O_2 that would not affect ARPE-19 cell viability. The MTT substrate, when incubated with cells, is converted into a purple coloured formazan product which is thought to be proportional to the amount of viable

cells, therefore also making the MTT assay a useful marker of cell viability (Riss et al., 2004). In this study, cell viability was measured using the Vybrant®MTT Assay kit (Invitrogen Ltd, Paisley, UK). ARPE-19 cells were seeded at a density of $2x10^4$ cells per well of a 96-well plate. Cells were incubated with different concentrations of H_2O_2 (50-500µM) at 37^oC for 4 hours. The media was removed from cells and replaced with 100µl of fresh media containing 0.5mg/ml MTT after which cells were incubated for 37^oC for 4 hours. After incubation, 75µl of media was removed carefully from each well after which 50µl of dimethyl sulfoxide (DMSO) was added to solubilise formazan produced from MTT by viable cells. The cells were then incubated at 37^oC for 10 mins after which absorbance was read at 540nm using a microplate reader (Benchmark™ Plus Microplate Spectrophotometer, BioRad, Hampstead, UK).

2.2 – Preparation of protein samples and immunodetection

2.2.1 - Preparation of cell lysates and media samples from cultures

The description below is for cell lysates prepared from a 12-well plate set-up. The volumes used were re-scaled appropriately when preparing samples from a 6-well plate set up. To prepare cell lysates, initially cells in culture were washed twice with excess PBS after which 400µl of 0.05% trypsin was added to each well. The cells were incubated at 37^{o}C for 3-5 mins until they were dislodged off the surface of the well. Once cells were dislodged, trypsin was neutralised by the addition of media (600µl). The 1ml cell suspension was placed in a 1.5ml Eppendorf tube and a cell count was carried out. 20µl of cell suspension was added under a coverslip to a chamber of a haemocytometer counting grid. The number of cells in the 4 areas of the central grid where counted and an average was calculated. The number was multiplied by 10^4 to give number of cells per ml.

After the cell count, the cell suspension was centrifuged at 1000rpm for 3 mins. Supernatant was removed and the cell pellet was placed on ice and resuspended in 200µl of Laemmli lysis buffer (Recipes for buffers and solutions that were used in this study are listed in the appendix 1). Conditioned media samples were prepared by the addition of 10X loading buffer (final concentration 2X). Both cell lysate and conditioned media samples were heated at 95^{o}C for 3-5 mins after which the samples were stored at -20^{o}C until needed for further analysis.

2.2.2 - Quantification of total protein in cell lysates and media

The total protein content of cell lysates and conditioned media samples of ARPE-19 and D407 cultures was determined by the Qubit® Protein Assay Kit using the Qubit® Flurometer 2.0 (Invitrogen Ltd, Paisley, UK). The protein assay kit provides a concentrated protein assay reagent, dilution buffer and pre-diluted BSA standards. All cell lysate samples were diluted 1:10 and media samples 1:20 with double-distilled water (ddH_2O) before carrying out the protein concentration reading using the manufacturer protocol.

Briefly, a stock Qubit™ working solution was prepared by diluting the Qubit™ protein reagent 1:200 in the dilution buffer. For protein measurement, a final volume of 200µl in each tube was recommended. In order to account for pipetting errors, a Qubit™ working solution was always prepared for 2 extra samples. As recommended by the manufacturer protocol, 10µl of standard sample was added to 190µl of working solution whilst 2µl of experimental sample was added to 198µl of working solution. After preparation, tubes were vortexed for 2-3 seconds and incubated at room temperature for 15 mins.

The Qubit® 2.0 Fluorometer machine used to take protein readings was calibrated using the 3 protein standards prepared. Once calibration was achieved, sample readings were taken. The machine calculated the stock solution concentration, which was then further multiplied by 10 for cell lysate samples or 20 for media samples, as they were previously diluted before the protein assay. The protein readings obtained were used to help calculate the volumes needed for each sample to load equal amount of proteins for relevant experiments.

2.2.3 - Sodium dodecyl sulfate-polyacrylamide gel electrophoresis (SDS-PAGE) and Western blot analysis for protein detection

Western blotting technique, also known as immunoblotting, was introduced by Towbin et al in 1979 (Towbin et al., 1992). Western blotting is a widely used technique in which detection of specific proteins in a sample is carried out. Proteins are separated by size through gel electrophoresis after which proteins are transferred to a solid support i.e. nitrocellulose membrane. This solid membrane is then probed with a specific antibody for protein detection (Renart et al., 1979).

After cell lysates and conditioned media were prepared, proteins were resolved by SDS-polyacrylamide gel electrophoresis alongside a protein molecular marker (PageRuler Prestained Protein Ladder, Thermo Scientific, Rockford, USA) using the Mini-PROTEAN 3 cell system (BioRad, Hampstead, UK). Gel electrophoresis was carried out at 90-130V for 1 hour

30 mins. After resolving, proteins separated on the gel were transferred onto a solid nitrocellulose membrane support (Sigma, Dorset, UK).

Before the transfer, the nitrocellulose membrane was soaked in transfer buffer for 10 mins. The gel was then placed on the membrane, and together sandwiched between 3 layers of filter paper and 1 sponge pad on each side. All components of the sandwich were submerged in transfer buffer with extra care taken to ensure no air bubbles were present between the layers. The transfer sandwich, after being enclosed in a cassette, was placed in an electrode module, with the resolving gel closest to the negative electrode and the membrane closest to the positive electrode. The electrode module was placed in a chamber which was submerged in transfer buffer. An ice block was placed within the chamber to help maintain a low temperature during the transfer. Electrophoresis was carried out at 100V for 1 hour and 30 mins.

After the transfer, the nitrocellulose membrane, which now contained the proteins from the original samples in the gel, was subjected to a Ponceau S stain to test transfer efficiency (Romero-Calvo et al., 2010). After this, the Ponceau S stain was removed by washing the membrane in 1X TBS for 10 mins after which the membrane was incubated in 50ml of blocking buffer for 90 mins with gentle agitation.

After blocking, the membrane was incubated with primary antibody overnight at $4^{o}C$ (list of primary antibodies - Table 2.1). Primary antibodies raised in rabbit were prepared in 5% bovine serum albumin (BSA) whereas primary antibodies raised in mouse were prepared in 5% milk blocking buffer. After incubation, the primary antibody was removed and the membrane was washed three times for 5 mins with wash buffer to remove unbound primary antibody. The membrane was then incubated with the appropriate secondary antibody at room temperature for 1 hour (Anti-Rabbit IgG (whole molecule)–Peroxidase antibody produced in goat (1:1000) OR Anti-Mouse IgG (whole molecule)–Peroxidase antibody produced in rabbit (1:2000), Sigma, Dorset, UK, both prepared in 5% milk blocking buffer). Unbound secondary antibody was then washed three times for 5 mins with wash buffer. Protein detection

was achieved using an enhanced chemilumininescent (ECL) substrate kit (SuperSignal West Pico Chemiluminescent substrate, Thermo Scientific, Rockford, USA), which measures horseradish peroxidase (HRP) activity from the antibodies. The ECL substrate kit contains ECL reagents 1 and 2 which were mixed in a 1:1 solution and applied to the membrane for 5 mins. The membrane was enclosed in a clear plastic sheet protector to prevent drying and was then imaged using the BioRad ChemiDOC^{TM} digital imager (BioRad, Hampstead, UK). Band intensity densitometric values were obtained using the BioRad Image Lab program. Glyceraldehyde 3-phosphate dehydrogenase (GAPDH) or α-tubulin protein detection was used to evaluate equal loading of samples unless stated otherwise.

Table 2.1: Primary antibodies used in the present study

Antibody	Type	Immungen information	Dilution
Anti-Cathepsin B (Abcam, UK, ab33538)	Rabbit polyclonal	Information not provided by datasheet.	1:500-1:1000
Anti-Cathepsin L (Abcam, UK, ab6314)	Mouse monoclonal	Recognises epitope within amino acid residues GYGFEST (265-271) of full length protein	1:500-1:1000
Anti-Cathepsin S (Abcam, UK, ab92780)	Rabbit polyclonal	Recognises epitope within residues 150 - 250 of Human Cathepsin S protein	1:500-1:000
Anti-Cathepsin D (BD Biosciences, UK, 610800)	Mouse monoclonal	Information not provided by datasheet.	1:500
Anti-NF-κB p65 (Abcam, UK, ab16502)	Rabbit polyclonal	Recognises epitope corresponding to residue 500 of NF-κB p65 protein	1:500
Anti-Phospho-NF-κB p65 (Ser536) (Cell Signalling, UK, 92H1)	Rabbit monoclonal	Antibody produced by immunizing animals with synthetic phosphopeptide corresponding to residues surrounding Ser536	1:500
Anti-IKB-α (Abcam, UK, [E130] ab32518)	Rabbit monoclonal	Information not provided by datasheet.	1:500
Anti-LC3-II (Cell Signalling, UK, (D11) 3868)	Rabbit monoclonal	Information not provided by datasheet.	1:500
Anti-GAPDH [6C5] (Abcam, UK, ab8245)	Mouse monoclonal	Information not provided by datasheet	1:30000
Anti- α-tubulin (Sigma-Aldrich, UK, T9026)	Mouse monoclonal	Information not provided by datasheet	1:5000

2.3 – Cathepsin activity assay

Cathepsin D, L and S activities were measured through the use of commercially available specific flourometric assays designed for quantitative measurement (Abcam, UK).

Samples used for activity measurement were prepared using manufacturer protocol. Briefly, at the respective time points for each experiment, media was removed and cells were washed twice with PBS. Cells were then trypsinised, centrifuged and collected as previously described in section 2.3.1. The cell pellet was resuspended in 200µl of respective cell lysis buffer from each kit and placed on ice for 10 mins. The samples were then centrifuged at 14,000g in a microcentrifuge for 5 mins. The supernatant was transferred to a new tube and the pellet was discarded. The sample was then diluted 1:10 before a protein content reading was carried out using the Qubit® 2.0 Fluorometer machine as described in section 2.2.2.

For the cathepsin D kit, an appropriate amount of sample was pipetted into each well and made up to 50µl solution using the respective cell lysis buffer. To this, 50µl of reaction buffer was added along with 2µl of 10mM preferred cathepsin D substrate (GKPILFFRLK(Dnp)-D-R-NH2) labelled with 7-methoxycoumarin-4-acetic acid (MCA). For a negative control, only buffer samples were used. Samples were then incubated at 37^{o}C for 1 hour. Samples that contained cathepsin D would cleave the substrate releasing fluorescence, which was quantified on a fluorescence plate reader at excitation wavelength 328nm and emission wavelength 460nm.

The cathepsin L and S kits worked in a similar way to the cathepsin D but this time a cathepsin-L preferred substrate sequence FR labeled with amino-4-trifluoromethyl coumarin (AFC) and cathepsin S synthetic substrate VVR-AFC to release free AFC were used respectively. Both these kits released fluorescence via the same label AFC therefore were quantified on a fluorescence plate reader using the same excitation wavelength 400nm and emission wavelength 505nm filters.

A line of best fit was made to predict the amount of protein needed to fall in the linear range (most sensitive area) for each kit used. RFU values were plotted against concentration of protein and data was analysed for fold change. The linear range of the kit was established when an approximate doubling of protein level coincided with doubling of relative fluorescent unit (RFU) values. The line of best fit helped determine amount of experimental sample protein needed for each kit.

2.4 - Immunohistochemistry and image analysis for quantification of cathepsin B, L and S protein from RPE cells

Immunohistochemistry (IHC) was performed on human donor eyes for which consent for research use had been obtained according to the ethical approval from the Liverpool Research Ethics Committee. Sections from one donor eye were used in the study conducted to determine the presence of cathepsin B, L and S in human RPE. A total of 32 different eyes were included in the study which investigated cathepsin L relative protein level and how levels are affected by age in RPE cells from posterior (opposite the cornea) and periphery (anterior to the equator of each globe, extending anteriorly until the middle point of the ora seratta and equator). The donors had no history of ocular disease and the age range for the eye set was 35-91 years old.

Paraffin wax embedded blocks of donor eyes were sectioned at 4µm using a rotary microtome (Leica RM2235, Milton Keynes, UK). Sections were then collected and adhered to coated microscope slides (Dako UK Ltd, Cambridgeshire, UK), and allowed to dry overnight at 37^{o}c.

2.4.1 – Removal of melanin pigment from RPE cells

Wax sections of donor eyes were first dewaxed followed by rehydration of sections by sequential immersion for 1 min each in series of alcohols of decreasing concentrations (100%, 90% and 70%) and immersion of sections in distilled water for 3 mins.

In order to semi-quantify the specific immunopositivity of RPE, the melanin pigment needed to be bleached. To effectively bleach the melanin pigment from RPE cells, sections after de-waxing were bleached as previously described (Howard et al., 2010). Briefly, tissue sections were immersed in 0.25% potassium permanganate ($KMnO_4$) for 60 mins followed by immersion in 1% oxalic acid for 5 mins (Figure 2.1). Oxidation by $KMnO_4$ attacks the phenol ring on the melanin pigment which leads to the substitution of manganese dioxide in the tissue, leaving the melanin in the solution. Oxalic acid reduces the manganese dioxide to leave the pigment colourless. Eye

sections were then immersed in distilled water for 3 mins to help wash away excess solution. As the bleaching process can lead to tissue detachment, sections were placed in a humidity chamber at 37^{o}C for 10 mins to help allow tissue to fully re-adhere to slides.

(A)

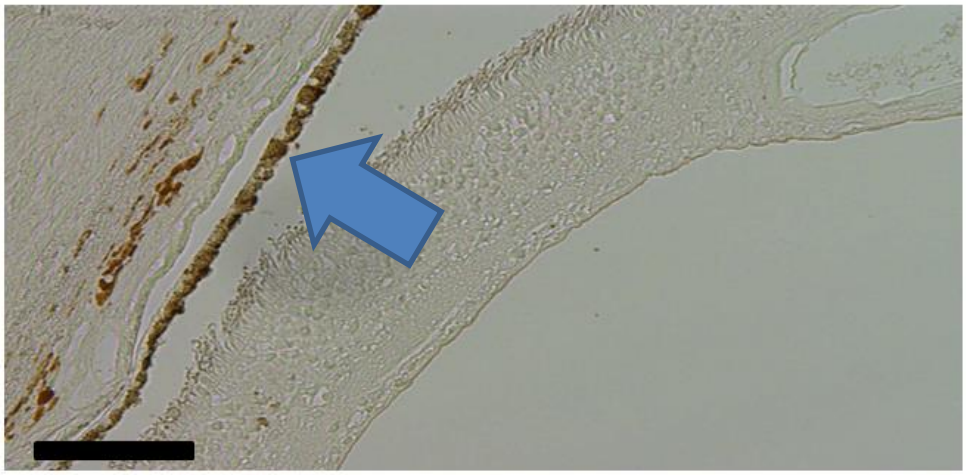

(B)

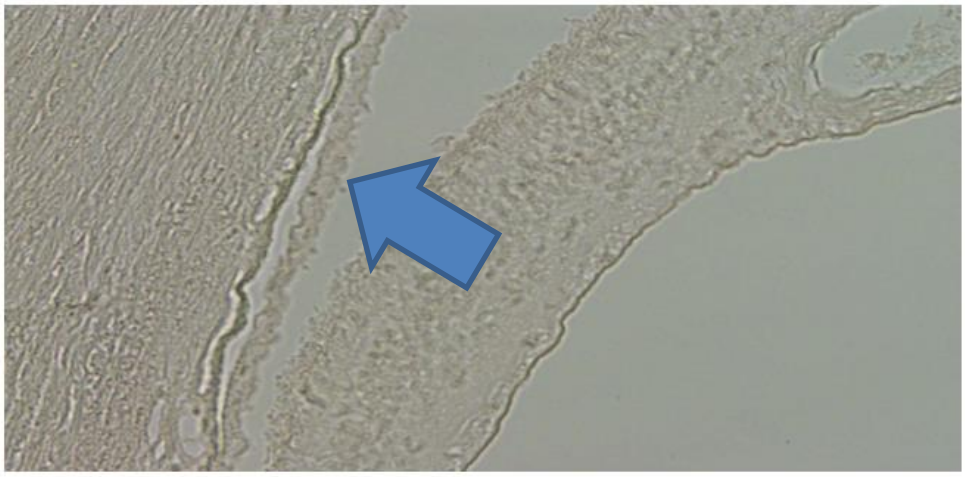

Figure 2.1: Bleaching of melanin pigmentation in RPE cells. (A) Without the bleaching step, eye section showed abundant melanin pigmentation in RPE cells (shown by blue arrow). (B) Bleaching successfully removed melanin pigmentation. Scale bar represents 100µm.

2.4.2- Immunohistochemical detection of cathepsin B, L and S protein with chromogen visualisation

Wax sections of donor eyes were dewaxed, rehydrated and bleached as described above. Following bleaching and removal of slides from the humidity chamber, a hydrophobic boundary was made around the tissue

using silicone after which the slides were immersed in distilled water. The silicone boundary was made to ensure all reagents applied to the tissue remained on the slide. For better penetration of antibody by the tissue, a cell permeabilization step using 0.1% Triton X-100 for 5 mins was carried out, followed by three 5 min washes with 0.1% PBS Tween 20. Triton X-100 is involved in dissolving lipid on cell, nuclear and organelle membranes enabling antibodies to enter these regions and bind antigens. In order to limit the possibility of non-specific background, endogenous peroxidases were blocked by incubation of sections with peroxidase block (0.03% hydrogen peroxide containing sodium azide, DakoCytomation, Ely, UK) for 10 mins. Treatment with $KMnO_4$ is also able to block endogenous peroxidase activity (Alexander et al., 1986). The peroxidase block was followed by three 5 min washes with 0.1% PBS Tween 20. In order to reduce the non-specific binding of the primary antibody to the tissue and minimise background staining, slides were incubated in 20% goat serum in 0.1% PBS-Tween 30 for 40 mins at room temperature. This was followed by one 5 mins wash with 0.1% PBS Tween 20. Tissue sections were then incubated with the primary antibody for the protein of interest (diluted in 5% goat serum in 0.1% PBS Tween 20) at $4^{o}C$ overnight.

After the overnight incubation, unbound antibody was removed by three 5 min washes with 0.1% PBS Tween 20. Peroxidase-labelled secondary goat anti-mouse/anti-rabbit antibody (DakoCytomation, Ely, UK, Envision™ Detection System Kit, goat anti-mouse/goat anti-rabbit) was applied for 40 mins at room temperature after which unbound secondary antibody was removed by three 5 min washes with 0.1% PBS Tween 20.

Reaction product visualisation was achieved by incubation of the sections with 3-amino-9-ethylcarbozole (AEC) + substrate-chromogen (DakoCytomation, Ely, UK, Envision™ Detection System Kit) for 5 mins. This resulted in a red-coloured precipitate being produced at the antigen sites. Termination of the reaction was achieved by immersion of slides in warm distilled water for 3 mins. Time limits had to be adhered at this stage as the reaction products formed the basis of the analysis. The sections were

mounted in Aquatex Mounting Media (Merk-Millipore, Darmstadt, Germany) and secured with a coverslip. Sections were left overnight to dry and were viewed the next day. Negative controls were used in this procedure and included: 1. Isotype control - Substitution of the primary antibody with mouse IgG_1 non-immune immunoglobin used at the same concentration diluted in 5% goat serum. 2. Primary antibody omitted – incubation of sections with antibody diluent 5% goat serum in 0.1% PBS Tween 20 without primary antibody.

2.4.3 - Light microscopy

Sections were viewed and images were captured using a Nikon Optiphot-2 light microscope with an attached Nikon D40X camera colour video camera (Nikon, Surrey, UK). All images captured for the purpose of analysis were taken under standardised microscope conditions. This was done to remove the possibility that the analysis of staining intensity may be affected by microscopy technique. Microscope conditions employed were as follows; light level = 4, field diaphragm = 4, condenser aperture = 0.4 and images captured using the x4 and x40 objective at a shutter speed of $1/15^{th}$ of a second.

2.4.4 - Image analysis for quantification of cathepsin L immunostaining

Images taken by the light microscope at x40 magnification were analysed using ImageJ which is a public domain java-based image processing software (National Institutes of Health Maryland, USA) (Collins, 2007; Schneider et al., 2012). This software generated data that related the intensity of cathepsin L immunostaining of RPE cells in each eye under investigation, allowing the relative intensity of staining to be compared directly between each eye.

For each eye, images were taken of the posterior segment, left periphery and right periphery segments that included the RPE. 3 areas of the RPE in each image were delimited by ‘zooming in’ in the area of interest and using the freehand tool and region of interest (ROI) manager to obtain a measurement of intensity (Figure 2.2). ImageJ software utilised the

computer's grey-scale range, which codes for the intensity of colour on a linear scale from black (value = 0) to white (value = 255) with all values in between representing different shades of grey. The outlined areas of RPE that were measured in each image were inverted so that the grey value for white was now 0 and for black was 255 therefore giving higher numbers for a more intense areas compared to less intense areas. Once the 3 measurements of intensity were recorded for each image the mean grey scale value was calculated. To reduce intra-observer error, 3 different images for each of the anatomical locations (posterior, left peripheral and right peripheral RPE cells) were analysed for each eye in this study. The mean grey-scale value was also calculated for the negative control and was subsequently deducted from each eye mean grey scale value.

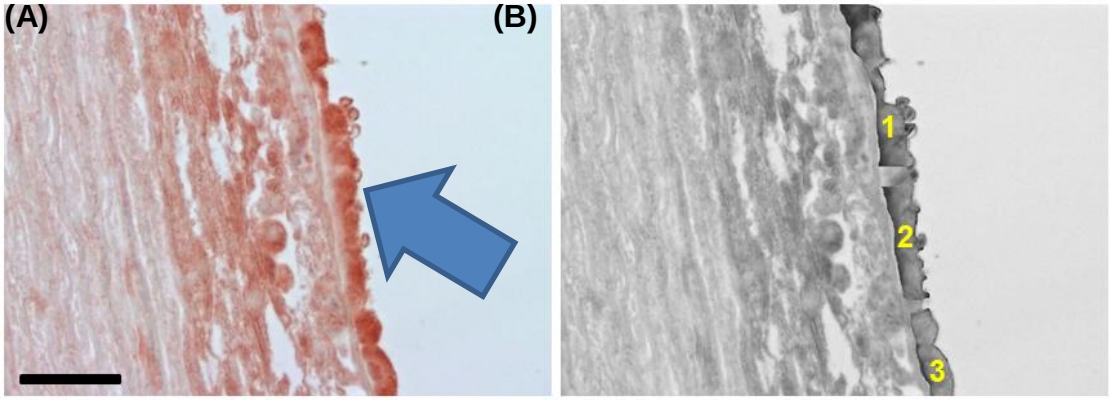

Figure 2.2: RPE area highlighted using ImageJ program for IHC quantification. (A) Image 1 out of 3 for specimen 1 posterior region showing cathepsin L staining in RPE (arrow). (B) Using ImageJ program, 3 areas (designated 1, 2 3 in yellow) of RPE were delimited. Scale bar represents 50µm.

2.5 - CST3-exudative AMD association study

2.5.1 – Association study patient and controls

The study made use of samples from 350 Caucasian exudative AMD patients (126 males and 224 females) (age range 65-96 with mean age of 80.1 years). All participants provided written informed consent that was approved by Leeds (East) Research Ethics Committee. A diagnosis was provided by ophthalmologists based on baseline stereoscopic colour fundus, fluorescein and indocyanine green angiogram images to identify lesion characteristics (McKibbin et al., 2012). Patients included in this study met the following criteria: age 65 years and over, CNV secondary to AMD and involving fovea centre with the CNV occupying more than 50% of total lesion area. Patients were excluded due to their CNV being secondary to pathological myopia, inflammatory disease, angioid streaks or trauma. Population control data was taken from the largest publicly available online database Variant Server, NHBL Go Exome Sequencing Project (ESP), Seattle, WA (URL:http://evs.gs.washington.edu/EVS/) January 2014). This provided genotype information for 3781 Caucasian individuals.

2.5.2 – Genotyping

Primers for the sequence of interest were designed using the Primer3 Detective v4.0 software (http://bioinfo.ut.ee/primer3-0.4.0/primer3/; September 2013) (Koressaar and Remm, 2007; Untergasser et al., 2012).

Primer pairs were designed to be 24-bp long (range 20-28bp) with melting temperatures between 59^{o}C to 65^{o}C and GC% content between 20% and 80%. Primers were checked for their unique hybridisation to desired part of the DNA via UCSC genome BLAT search (https://genome.ucsc.edu/cgi-bin/hgBlat?command=start; September 2013 – January 2014). The UCSC browser was also used to obtain initial information of genes of interest including intron-exon boundaries, genomic sequence, mRNA sequence, protein sequence as well as determining polymorphisms within regions (http://genome.ucsc.edu/; September 2013- January 2014). To identify the optimal and specific PCR conditions, the different combinations of primers

and different annealing temperatures were tested for amplification (Table 2.2).

In this study, the SNP of interest was rs1064039, which is a KspI restriction site found at position +73bp from the transcription start site in the CST3 gene. This SNP is in linkage disequilibrium with two other KspI SNPs rs5030707 and rs73318135. In most cases, primer pairs were designed to enclose the region of the 3 KspI SNPs rs5030707, rs73318135, and rs1064039 of the CST3 gene (Figure 2.3). The only exception was the forward primer CST3AIIF, which when used in amplification reactions, resulted in products where only SNPs rs73318135 and rs1064039 were included. Nevertheless, the main SNP of interest was rs1064039. Therefore the forward primer CST3AIIF was still included in the initial optimisation experiments.

Table 2.2: Different combination of primers and conditions used to amplify genomic DNA sequence of CST3 (F = Forward; R = Reverse).

Primer pairs	Sequence (5'-3')	Product Size (bp)	Annealing Temperature (^{0}C)
CST3AIIF-CST3BIIR	F=GAAGGGATAAACCGCAGTCGC R=TTGCTGGCTTTGTTGTACTCGCC	325	57
CST3LRF-CSTLRR	F=AGAGGAGAAGGAGCCTGAAGAGT R=GGCTCCTGGAAGCTGATCTTAG	1093	57
CS3AIIF-CSTLRR	F=GAAGGGATAAACCGCAGTCGC R=GGCTCCTGGAAGCTGATCTTAG	623	57
CST3LRF-CST3BIIR	F=AGAGGAGAAGGAGCCTGAAGAGT R=TTGCTGGCTTTGTTGTACTCGCC	795	57
CST3LRIIF-CST3LRIIR	F=CAGGAGTGGAGGAGGGAGATG R=CCAGATGAGGGGCTCTGTTTT	1292	60

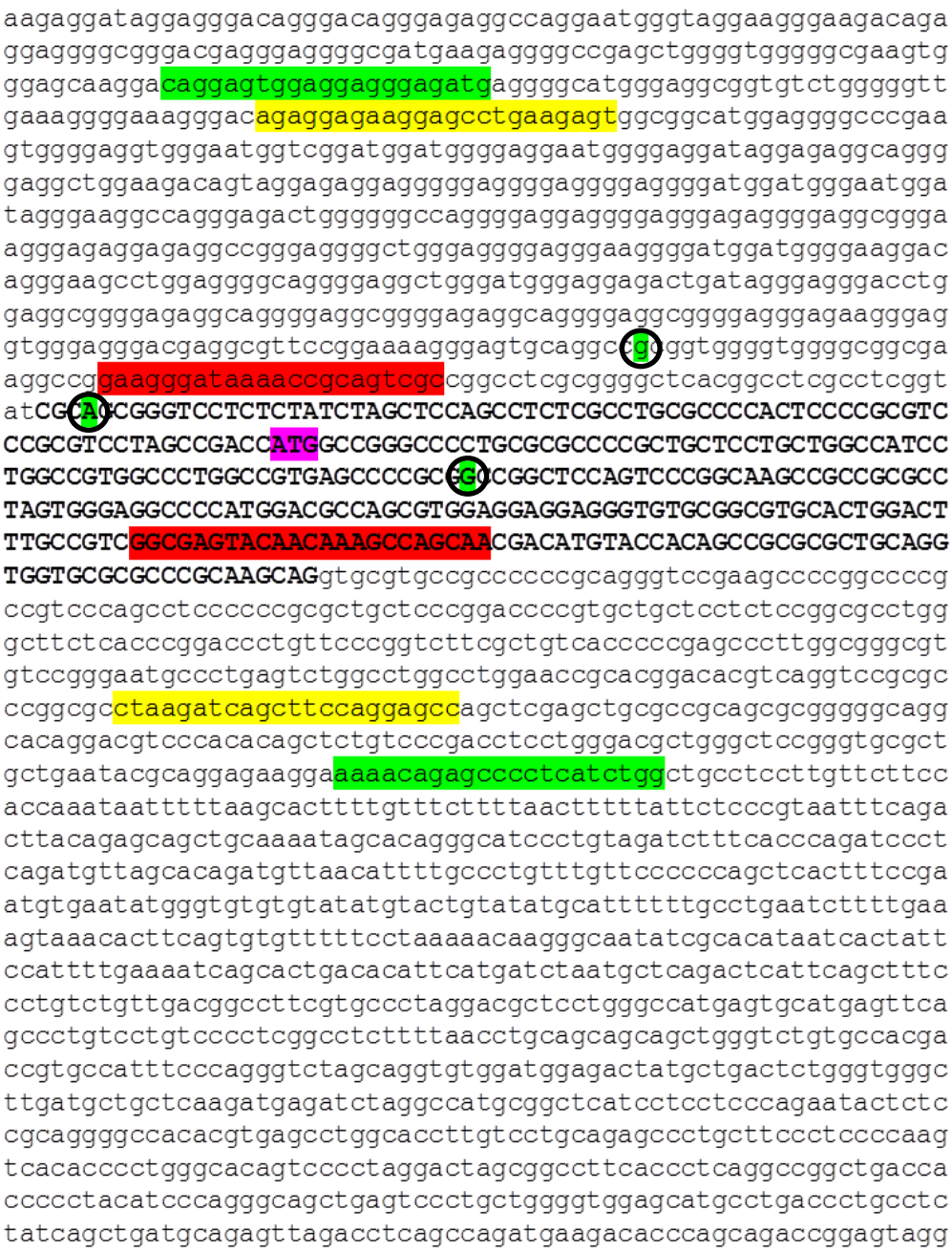

Figure 2.3: CST3 DNA sequence region around Exon 1. In capitals is Exon 1 with the ATG transcription start site highlighted. Circled and highlighted green are the positions of the three KspI SNPs of interest. Sequences heighted in red, yellow and green show where primer pairs CST3AIIF-CSTBIIR, CST3LRF-CST3LRR and CST3LIIF-CST3LIIR align respectively.

2.5.3 – Optimisation of PCR protocol, primer selection and conditions

Initial PCR reactions were performed using HotShot DNA PCR Master Mix (Cleft Life Sciences, UK) (Protocol 1). A 10ul PCR was performed on a set of control DNA used for optimisation, containing 40ng of genomic DNA, 2pM of each forward and reverse primer (Table 2.4), 5µl of HotShot Mastermix (Cleft Life Sciences, UK) and 2.6µl of de-ionised water. Thermo cycling was carried out using the following conditions: An initial denaturation step of 95^{o}C for 12 mins was followed by 40 cycles of 94^{o}C for 20 seconds, 57^{o}C for 20 seconds and 72^{o}C for 60 seconds. A final extension of 75^{o}C for 5 mins completed the reaction before the samples were cooled down to 4^{o}C.

A second PCR protocol (Protocol 2) was also performed in this study using a different set of primers designated CST3LIIF-CST3LIIR. The PCR reaction was as follows: A 10µl PCR was performed, containing 2µl of genomic DNA, 0.2µl of each forward and reverse primer, 5µl of HotShot Mastermix, 2ul Betaine and 0.6µl of de-ionised water. An initial denaturation step of 95^{o}C for 12 mins was followed by 40 cycles of 94^{o}C for 30 seconds, 60^{o}C for 30 seconds and 72^{o}C for 60 seconds. A final extension of 75^{o}C for 5 mins completed the reaction.

2.5.4 - Agarose gel electrophoresis was performed in 1.5% gels

Agarose gels were made using genetic analysis grade agarose (Fisher Scientific, UK) which was initially added to a flask containing 100ml of 1X Tris-borate-EDTA (TBE) electrophoresis buffer. The solution was then mixed and heated in a microwave for 2-3 mins until the agarose was fully dissolved after which the solution was left to cool at room temperature for a few mins. Gel casting tray ends were sealed with tape and appropriate combs were placed within the tray. Before pouring the solution into the tray, 1.3µl of 10mg/ml ethidium bromide was added to the 100ml agarose solution under the fume hood to allow later visualisation of DNA bands. The gel was poured into the tray and allowed to cool for 20-30 mins at room temperature before the sealing tape and combs were removed. The gel was placed into the electrophoresis chamber and covered with 1X TBE buffer. Before loading the samples onto the gel, samples were diluted 1:5 in 0.5X loading buffer.

2µl of an appropriate size standard Easy ladder I (Bioline, UK) was loaded alongside samples on the gel. Electrophoresis was performed at 90V for 30 mins in TBE buffer after which DNA bands were visualised using the ultraviolet light filter on the BioRad Chemic Doc Gel system (Bio-Rad, Hampstead, UK)

2.5.5 - DNA Direct Sanger Sequencing

DNA Sanger Sequencing is a gold standard DNA sequencing method that was developed by Frederick Sanger and colleagues in 1977 (Sanger et al., 1977). Based on PCR methodology, this sequencing technique involves repeated cycles of denaturation, annealing of a primer and extension using a high temperature DNA polymerase enzyme. However, sequencing differs from conventional PCR in that it involves the use of normal deoxynucleotide triphosphates (dNTPs) along with labelled dideoxyribonucleotide triphosphates (ddNTPs) which have a fluorescent dye. These ddNTPs get incorporated into the PCR products and stop the extension of the chain hence given the name chain-terminators. Therefore, a selection of different coloured sized DNA fragments are made ending in a fluorescently labelled nucleotide. These fragments are then separated according to size via gel electrophoresis and analysis of the fragments leads to reading of the original sequencing. In automated systems electrophoresis occurs in a thin capillary tube. In this tube, negatively charged DNA fragments separate out in the gel matrix when an electrical charge is applied and fragments are sorted by size. As the fragments reach the end of the tube, a laser excites the final fluorescent labelled nucleotide which emits light recorded as a coloured peak in the detection system (Figure 2.4). For sequencing reactions in the present study, the long range reverse CST3LRR primer was used to determine the sequences at the three SNPs of interest. To confirm the sequence obtained, a second primer CST3BIIR was used. The data obtained from both primers was used to determine the haplotypes.

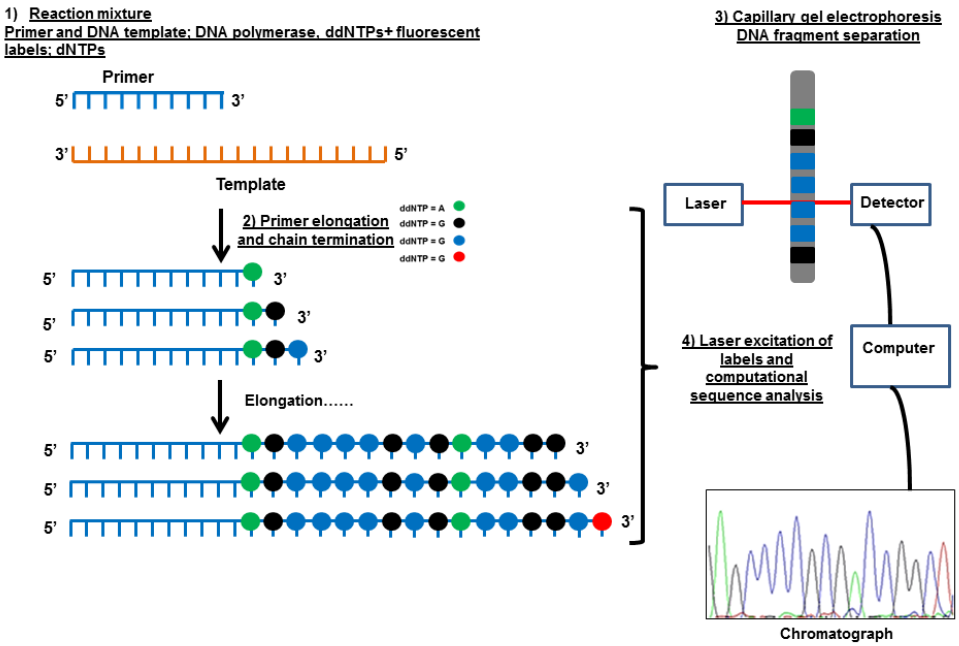

Figure 2.4: Principle of DNA Direct Sanger Sequencing Method. DNA template is mixed with primer, DNA polymerase as well as with dNTPs and chain-terminators ddNTPs+fluorescent label. Due to the presence of ddNTPs, a mixture of different length products are formed ending in fluorescently labelled nucleotide. An automated system is used to carry out the electrophoresis in a thin capillary tube and separate DNA fragments according to size. A laser excites the final fluorescent labelled nucleotide which leads to the detection of coloured peak by the computer system. At the end all the data gathered is put together to give a sequence for the original PCR product.

2.5.5.1 - ExoSap Treatment

Before amplicon sequencing, post-PCR reaction products underwent a clean-up using ExoSAP-IT [Exonuclease I and Shrimp Alkaline Phosphatase (Affymetrix, USA). A 5:2 ratio was used in which 5µl of post-PCR reaction product was added and mixed with 2µl of ExoSAP-IT. The role of ExoSAP-IT was to destroy unincorporated primers and dNTPs. Incubation of the ExoSAP-IT + PCR product mixture was performed at 37^{o}C for 30 mins. After this, a 15 mins incubation step at 80^{o}C was carried out to inactivate the ExoSAP-IT.

Cleaned PCR products were either stored overnight at 4^{o}C or at -20^{o}C for longer term storage until analysed.

2.5.5.2 - Cycle Sequencing Reaction

Cycle sequencing reactions were performed using the BigDye Terminator v3.1 Sequencing Kit (Applied Biosystems, UK). 1µl of cleaned PCR product was mixed with 1µl of BigDye Terminator v3.1 Ready Reaction Mix, 1.5µl of BigDye v3.1 5X Sequencing Buffer and 1µl of primer (1.6pmol/µl). De-ionised water was used to make up the total reaction volume to 10µl. Thermal cycling was carried out under the following conditions: an initial denaturation step of 96^{o}C for 1 min was carried out, followed by 25 cycles of denaturation at 96^{o}C for 10 seconds, annealing at 50^{o}C for 10 seconds and extension at 60^{o}C for 4 mins. At the end of the thermal cycle, the reaction mixture was cooled down to 4^{o}C.

Ethanol precipitation was used to purify sequencing products. Sequencing reaction mixture was transferred to deep well plates. In order to precipitate the mixture, the sequencing products were mixed with 5µl of 125mM EDTA and 60µl of 100% ethanol. The products were then centrifuged at 3200rpm for 30 mins at 22^{o}C. The supernatant was removed carefully and 60µl of 70% ethanol was added to each sample followed by a centrifugation step of 2000rpm for 15 mins at 4^{o}C. Supernatant was removed and the DNA pellet was left to dry for 30 mins at room temperature after which the pellet was resuspended in HiDi formamide (Applied Biosystems, UK).

DNA amplicon precipitates that were resuspended in HiDi formamide were resolved at 60^{o}C on a 36cm array along with POP7 polymer, 3730 sequencing buffer and fragment analysis 36-POP7-1 module using the ABI 3130xl Genetic Analyzer (Applied Biosystems, UK) at the St James Hospital, University of Leeds. Sequencing results were analysed manually using Sequencing Analysis v5.2 (Applied Biosystems, UK). The expected three different genotypes as determined by the nucleotide present at position +73 (SNP rs1064039) in the CST3 gene (Figure 2.5).

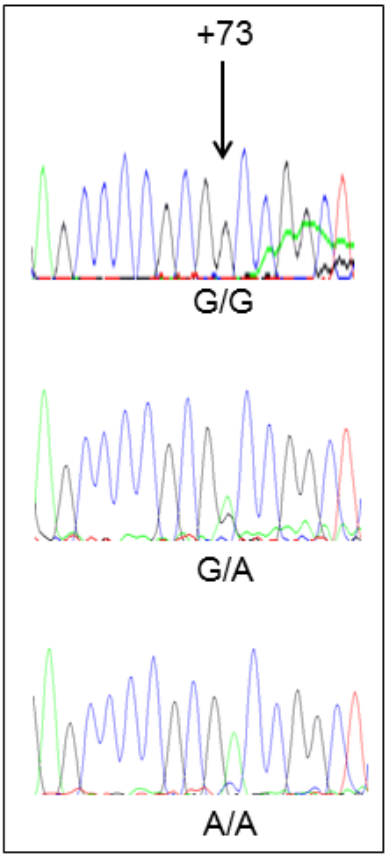

Figure 2.5: Chromatographs showing the three different genotypes expected (homozygous wild type GG, heterozygous GA and homozygous variant AA). Genotypes were determined by detection of a coloured peak at position +73. Black peak represents a G; Green peak represents A; overlap of peaks represents a heterozygous genotype.

2.5.6 - Meta-analysis of exudative AMD data

The data generated in this study was combined with the previous CST3-AMD study carried out in 2002 (Zurdel et al., 2002).

2.5.6.1 – Validation of Zurdel's methodology preceding meta-analysis

15 samples with known genotypes (5 each of GG, GA and AA) were amplified using the primers (024 – 5' – TGGGAGGGACGAGGCGTTCC – 3' and 1026R – 5' – TCCATGGGGCCTCCCACCAG – 3' used in Zurdel et al study (Zurdel et al., 2002). The protocol used for the PCR reaction was as follows: a 10µl PCR was performed, containing 2µl of genomic DNA, 0.2µl of each forward and reverse primer, 5µl of HotShot Mastermix, 2µl Betaine and

0.6µl of de-ionised water. An initial denaturation step of 95^{o}C for 12 mins was followed by 40 cycles of 94^{o}C for 30 seconds, 55^{o}C for 30 seconds and 72^{o}C for 60 seconds. A final extension of 75^{o}C for 5 mins completed the reaction. PCR products generated then underwent agarose gel electrophoresis to determine if bands were present at the expected size of 318bp.

After the PCR reactions, products generated were then digested with the KspI restriction enzyme (Roche, Welwyn, UK). Due to strong linkage disequilibrium between the three KspI SNPs in the CST3 gene, there are two haplotypes known as wild-type and variant B. When wild-type was present, KspI digestion would occur at SNPs number 1 and 3, generating 3 fragments 41, 226 and 51bp in size respectively. For haplotype B, KspI digestion would occur at SNP 2 and therefore 2 fragments of 127 and 191bp would be observed. For heterozygote individuals all 5 fragments would be present. Along with the restriction digest, sequencing was also carried out on the PCR products generated. The primers 024 and 1206R were used in the sequencing reaction.

2.6 - Statistical analysis

Quantitative or semi-quantitative data generated in this investigation was analysed with the appropriate statistical test to determine if results were significant. Excel (Microsoft UK LTD, Reading, UK) and GraphPad Prism 5 (GraphPad Software, Inc, La Jolla, CA, USA) were used to carry out the data analysis using Independent t test and analysis of variance (ANOVA) statistical methods. In addition, Spearman's Rho and Pearson's correlation tests were carried out using an online statistical tool called Social Science Statistics (http://www.socscistatistics.com).

For the genetic study investigating the CST3-AMD association, the odds ratio (OR) was calculated by the Software 'R' (version 3.1.2 R Development Core Team (2008) R: A language and environment for statistical computing, R Foundation for Statistical Computing, Vienna, Austria. ISBN 3-900051-07-0, URL http://www.R-project.org). The OR is a measurement of association between an exposure and an outcome, in this case the exposure being CST3 genotype and outcome being AMD (Szumilas, 2010). Software 'R' was used to perform the 'Z-test', which using the log odd ratio (logOR), measure the genetic effects on the outcome i.e. risk of AMD. Cochrane Review Manager (Review Manager (RevMan) [Computer program]. Version 5.3, Copenhagen: The Nordic Cochrane Centre, The Cochrane Collaboration, 2014) was utilised for the meta-analysis and forest plot generation. An online tool called SNPStats, a simple ready-to use software designed to analyse genetic studies of association, (http://bioinfo.iconcologia.net/SNPstats) was used to provide data for allele and genotype frequencies. SNPStats was also used to test for Hardy-Weinberg equilibrium (HWE). For all the statistical tests, P values ≤0.05 were considered significant unless stated otherwise.

Dr Joe Butler deserves a lot of credit as he carried out a major part of the genetic association analysis. Therefore many thanks to him for his efforts and the guidance he gave in relation to statistical tests.

Chapter 3 - Expression and activity regulation of cathepsins in RPE cells

3.1 – Characterisation of endogenous cathepsins expression and secretion by RPE

The purpose of the first aim of this study was to investigate the protein expression of a group of potent lysosomal proteases, cathepsins B, L and S in RPE cells. In addition, due to the knowledge that cathepsins can exert extracellular function, possible secretion of cathepsins B, L and S from RPE cells was also investigated. Two human cell lines ARPE-19 and D407 were used as RPE models in the experimental procedures (Davis et al., 1995; Dunn et al., 1996) (Figure 3.1).

ARPE-19 cell line is the most widely used well-established human RPE model that exhibits native human RPE characteristics (Dunn et al., 1996). For example, ARPE-19 cells grow in a monolayer with a cobblestone appearance as well as expressing specific RPE markers such as CRALBP and RPE-65 (Dunn et al., 1996). ARPE-19 cells also form polarised monolayers when cultured on a porous support, have normal karyotype and have been used to successfully improve vision by transplantation into subretinal space of animal models of retinal degeneration (Dunn et al., 1996; Lund et al., 2001). On the other hand, although D407 cell line exhibits RPE features such as expression of RPE-specific markers CRABLP and cytokeratins 8 and 18, they also display features not representative of RPE such as not being able to polarise and altered karyotype (Davis et al., 1995; Kuznetsova et al., 2014). In addition, D407 cells do not synthesise pigment and do not polarise (Kuznetsova et al., 2014). D407 cell line was included in this study to further characterise it as an RPE model but it was recognised that these cells might not be the best representative model of RPE function. With these physiological/morphological differences between both RPE cells in mind, it was accepted that results obtained may differ between the cell lines.

To address the first aim of the present study, western blot analysis was used to detect and differentiate between the different forms of cathepsins to provide insight into the processing and proteolytic capability of each RPE cell line tested.

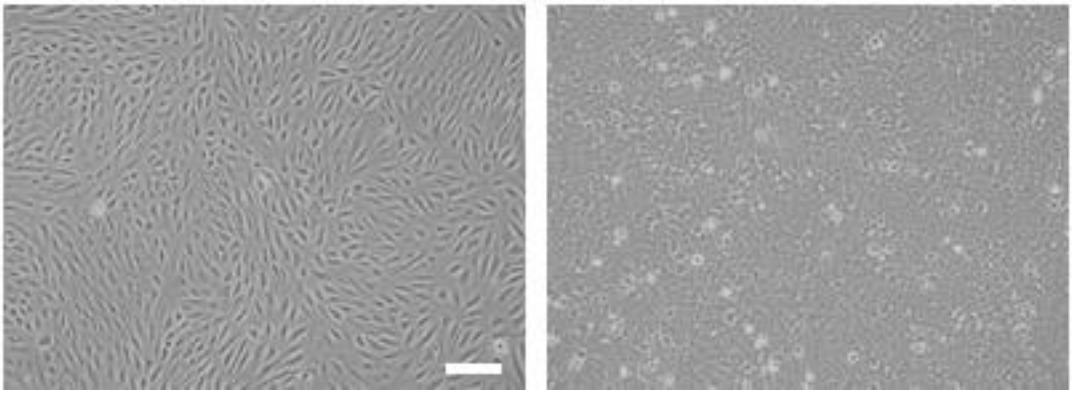

Figure 3.1: ARPE-19 and D407 cell lines grown on plastic. (A) Confluent ARPE-19 cells (B) confluent of D407 cells. Scale bar representative of 100µm.

3.1.1. – Detection of intracellular cathepsins B, L and S protein in RPE cells

Immunoblotting for cathepsin B revealed the detection of specific bands of ~25kDa, ~30kDa, ~37kDa and ~40kDa in RPE cell lines (Figure 3.2). The same bands were also detected in the positive control A549 cell line (Chen et al., 2012b). Cathepsin B is synthesised as an inactive ~44kDa precursor which is processed into a mature single-chain enzyme sizing around ~33kDa. Intralysosomal conversion of the 33kDa form into a two-chain form results in subunits of 27kDa, 24kDa and 5kDa with the 27kDa polypeptide being a glycosylated variant of the carbohydrate-free 24kDa heavy form (Mach et al., 1992). The 40kDa form detected in RPE cells is most likely to correspond to the inactive precursor protein, with the 30kDa form being the single chain form. The 25kDa form that was detected is most likely the heavy chain subunit. The 37kDa band detected may correspond to a pro-cathepsin B species as a similar size protein has been described previously in microglial cells (Ryan et al., 1995).

In ARPE-19, the most abundantly expressed form was the 25kDa form being significantly higher to the 40kDa (~8X higher), 30kDa (~10X higher) and 37kDa (~14X higher) ($p \leq 0.001$, $n = 3$; NB: the 37kDa was not detected in the third blot and therefore average was taken from two independent results for this form). No significant differences were observed between the abundances of other forms of cathepsin B detected.

On the other hand, in D407 cells, the most abundantly expressed cathepsin B form detected was the 40kDa form, followed by the 25kDa, 37kDa and 30kDa forms respectively. Statistical analysis showed that the only significant difference observed was that the 40kDa was significantly more abundant (~3X higher) that the 30kDa ($p \leq 0.05$, $n = 3$).

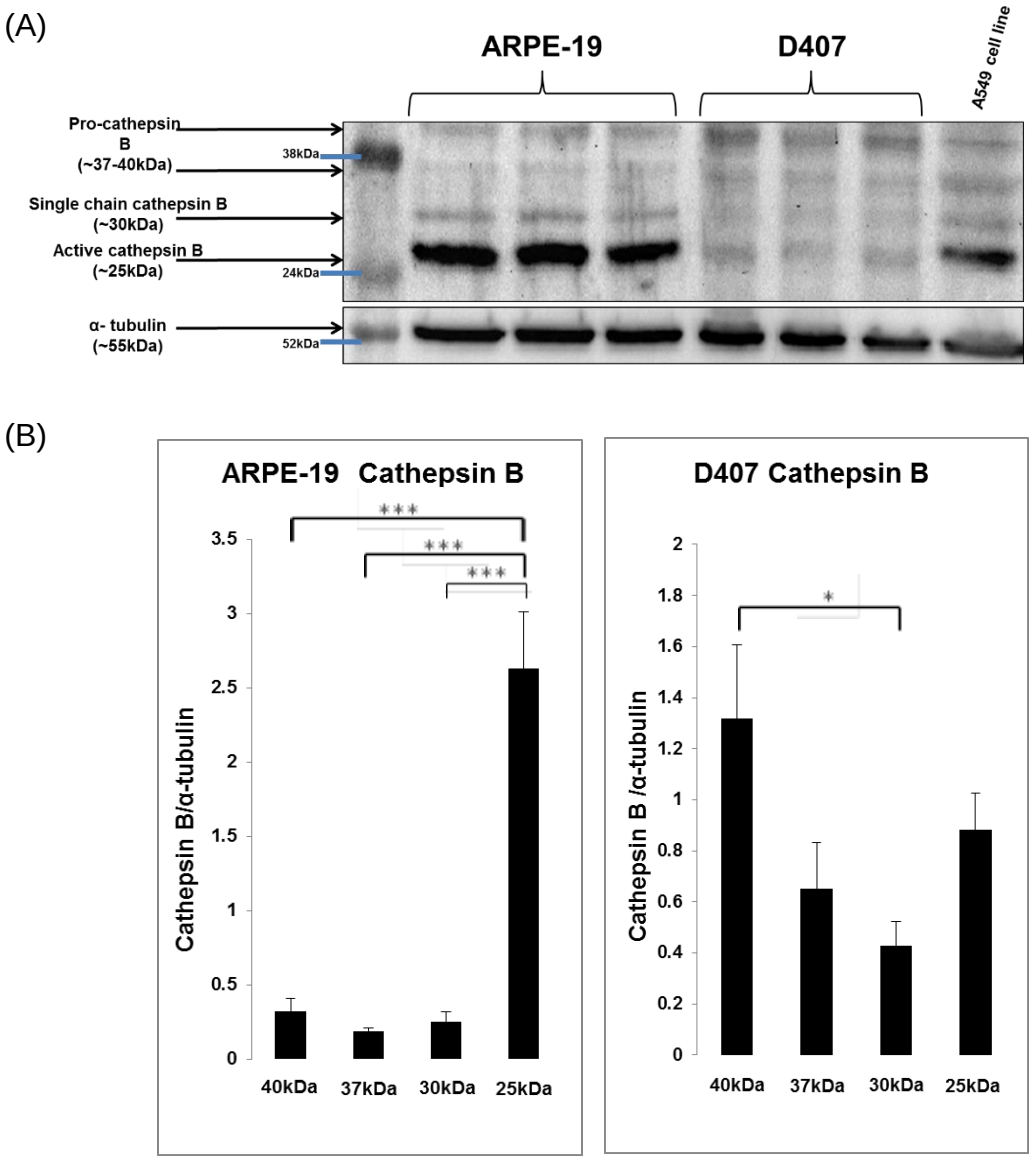

Figure 3.2: Immunodetection of cathepsin B protein forms in ARPE-19 and D407 cells. (A) Immunoblot of cell lysates probed with anti-cathepsin B (Abcam, ab33538, 1:1000) detected active and inactive forms of cathepsin B. α-tubulin (Sigma-Aldrich, T9026, 1:5000) immunoblotting detection was used as a loading control. Samples from 3 independent wells for each cell line tested. (B) Average normalised cathepsin B protein expression (arbitrary units) ± S.E.M. for all samples tested (n=3 with a minimum of 8 technical replicates for each cell line). One way ANOVA followed by Tukey's Post Hoc Test, *= $p \leq 0.05$, ***= $p \leq 0.001$.

Immunoblotting for cathepsin L revealed the presence of active and inactive forms in RPE cells. Specific bands at 26kDa and 36kDa were detected in both RPE cell lines (Figure 3.3). These bands were also detected in the positive control A549 and Hela cell lines (Hsu et al., 2009; Wille et al., 2002) Cathepsin L is synthesised as a precursor protein (~43kDa) that is processed to its fully active form (~25kDa) via an intermediate form (~34kDa) (Reilly et al., 1989). The 36kDa form detected in RPE cells most likely correspond to the intermediate form with the 26kDa form detected corresponding to active cathepsin L.

In ARPE-19, the predominant cathepsin L form was the 26kDa active which was significantly higher than the 36kDa proform (~5.0X higher) ($p \leq 0.01$, $n = 3$). In D407 cells, no significant differences between the 26kDa and 36kDa of cathepsin L was observed ($n = 3$).

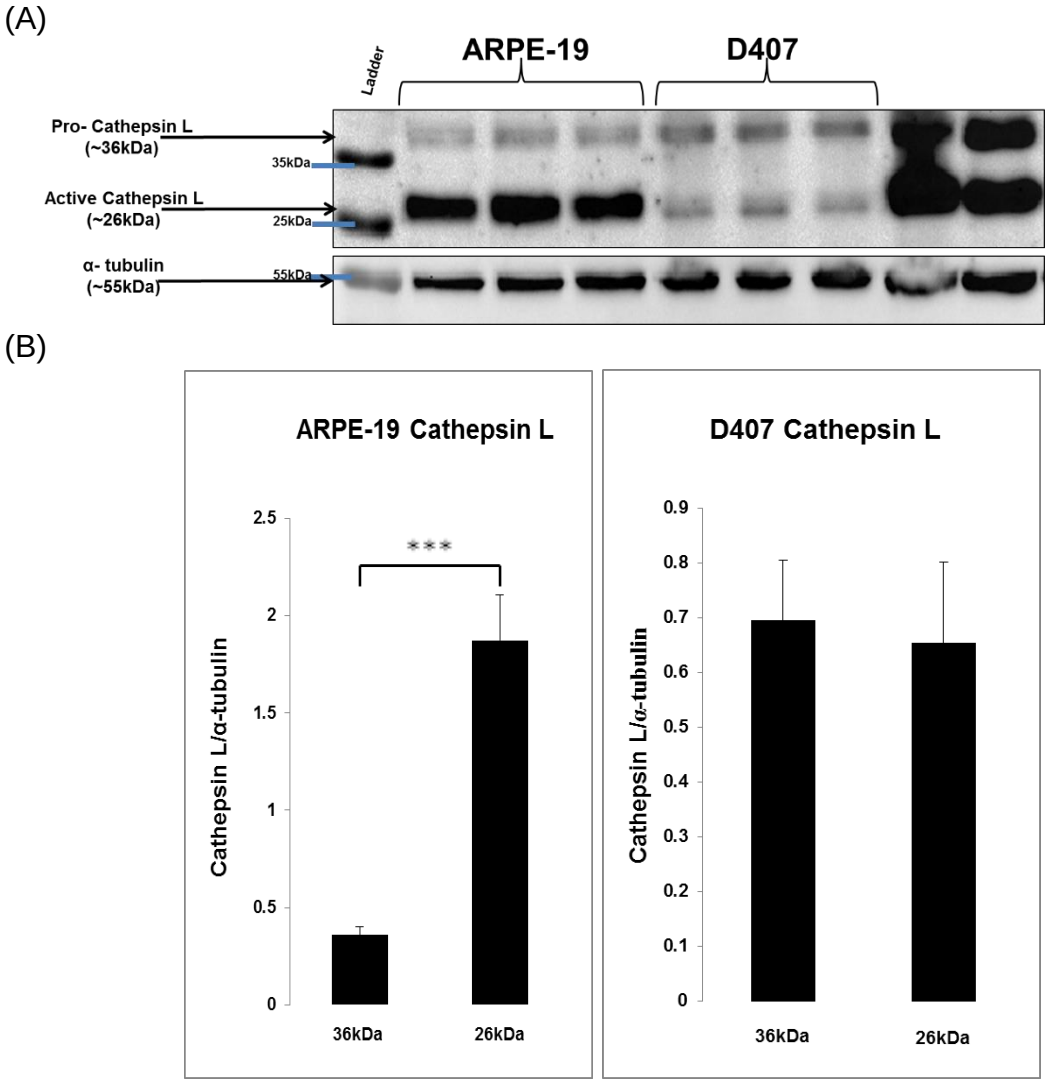

Figure 3.3: Immunodetection of cathepsin L protein forms in ARPE-19 and D407 cells. (A) Immunoblot of cell lysates probed with anti-cathepsin L (Abcam, ab6314, 1:1000) detected active and inactive forms of cathepsin L. α-tubulin (Sigma-Aldrich, T9026, 1:5000) immunoblotting detection was used as a loading control. A549 and Hela cell lysates were used as positive controls. Samples from 3 independent wells for each cell line tested. (B) Average normalised cathepsin L protein expression (arbitrary units) ± S.E.M. for all samples tested (n=3 with a minimum of 9 technical replicates for each cell line). Independent t test, ***=$p \leq 0.001$.

Immunoblotting for cathepsin S revealed that bands at 24kDa, 36kDa and 37kDa were detected in RPE cells (Figure 3.4). The same bands, with an additional band at ~25kDa, were also detected in both positive control A549 and U87MG cell lines (Chen et al., 2012a; van's Gravesande et al., 2002; Zhang et al., 2014). The 36kDa and 37kDa bands are most likely to correspond to pro-forms of cathepsin S (Gillet et al., 2009; Schwarz et al., 2002). The two bands detected at ~24kDa and ~25kDa are likely to be active forms of cathepsin S (Gillet et al., 2009; Wilder et al., 2011).

In ARPE-19 cells, the 24kDa form was present in significantly higher amounts compared to the 36kDa (~7.7X higher) and 37kDa (~3.3X higher) forms ($p \leq 0.001$, $n = 3$). No significant differences were observed between the 36kDa and 37kDa forms of cathepsin S. Similarly in D407 cells, the 24kDa form was also present in significantly higher levels compared to the 36kDa (~6.4X higher) and 37kDa (~45.5X higher) forms ($p \leq 0.05$, $n = 3$). No significant differences were observed between the 36kDa and 37kDa forms in D407 cells.

Taken together, these results indicated that both active and inactive forms of cathepsins B, L and S are present in both RPE cell lines suggesting that both cell lines are capable of synthesising and processing cathepsins. However, cathepsin expression patterns differed in both cell lines with the predominant form being the active form for all cathepsins tested in ARPE-19 cells, whereas in D407 cell line the active forms of cathepsins B and L are similar to or less than the inactive forms detected. This highlights that both cell lines have differences in cathepsin processing events which suggests differences in proteolytic potential/capability of both cell lines.

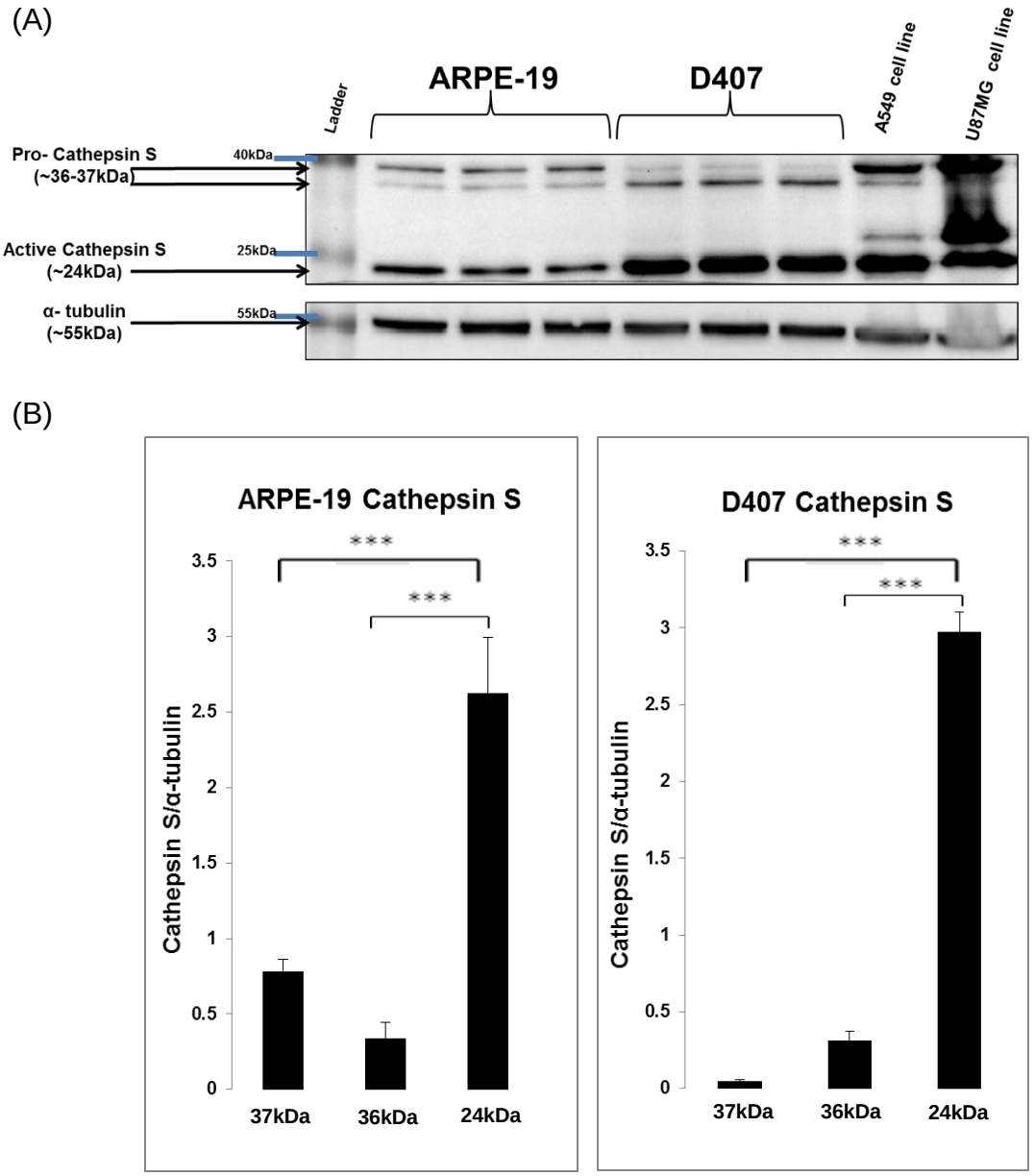

Figure 3.4: Immunodetection of cathepsin S protein forms in ARPE-19 and D407 cells. (A) Immunoblot of cell lysates probed with anti-cathepsin S (ab92780, 1:1000) detected active and inactive forms of cathepsin S. α-tubulin (Sigma-Aldrich, T9026, 1:5000) immunoblotting detection was used as a loading control. A549 and U87MG cell lysates were used as positive controls. Samples from 3 independent wells for each cell line tested. (B) Average normalised cathepsin S protein expression (arbitrary units) ± S.E.M. for all samples tested (n=3 with a minimum of 8 technical replicates for each cell line). One way ANOVA followed by Tukey's Post Hoc Test**,** ***=$p \leq 0.001$.

3.1.2 - Cathepsins B, L and S secretion from RPE cells

Cathepsins have been shown to exert extracellular function (Fonovic and Turk, 2014). In addition, a potent inhibitor of cathepsins, cystatin C, was shown to be secreted from RPE cells (Paraoan et al., 2001). Therefore, the next part of the study investigated cathepsins secretion from RPE cells. Conditioned media (3 days olds leading up to confluent state) was prepared and subjected to western blot analysis for cathepsins B, L and S immunoreactivity. A549 and U87MG cell lysates were used as positive controls.

Two bands at 24kDa and 27kDa, corresponding to two active forms of cathepsin B, were detected in the conditioned media from both RPE cell lines. The difference in sizes between both cathepsin B active forms detected is a potential modification step (Mach et al., 1992) (Figure 3.5).

For cathepsin L detection, bands at around 30kDa and 40kDa were detected in conditioned media from both RPE cell lines (Figure 3.5). Cathepsin L is synthesised as a precursor protein (~43kDa) that is processed to its active form (~25kDa) via an intermediate form (~34kDa) (Reilly et al., 1989). The 40kDa form may correspond to the precursor form of cathepsin L. Evidence shows that a 30kDa single chain active form of cathepsin L exists (Mattock et al., 2010) which may correspond to the 30kDa band detected. Levels of 30kDa form detected were similar to that found in the unconditioned media control for both cell lines suggesting that this protein was not secreted by the cells but likely to come from the media itself. Also, levels of proform cathepsin L in conditioned media from ARPE-19 were similar to that of the unconditioned media, again indicating that the protein was most likely from media. Taken together, this data suggests that only the 40kDa proform was secreted by D407 cells line with potentially no detectable amounts of active form secreted from both RPE cell lines.

For cathepsin S, two bands at 24kDa and 25kDa were detected in media from D407 cell line with only the 25kDa detected in media from ARPE-19 cell line (Figure 3.5). However, the 25kDa form is of similar levels to that of the control media suggesting that protein is most likely from media and not

secreted from the cells. D407 cells also appear to secrete two different proforms (36kDa and 37kDa) of cathepsin S along with the 24kDa active form of cathepsin S.

Results obtained showed that extracellular forms differ from the intracellular detected in both RPE cell lines. For example, two precursor isoforms at ~40kDa and ~37kDa plus a single chain ~30kDa and an active ~25kDa isoform for cathepsin B were detected in RPE cells. The presence of two isoforms at ~24kDa and ~27kDa extracellularly show differences to intracellular isoforms. Differences seen in the intracellular and extracellular isoforms of cathepsins suggests that possible post-translational modifications may help regulate cathepsin localisation.

The presence of cathepsin B, L and S forms in conditioned media from RPE cell lines indicates secretion thus supporting a potential extracellular role. This difference in secretion pattern suggests difference in proteolytic potential between both cell lines. Nevertheless, the secretion of cathepsins from RPE cell lines indicates extracellular functions in the surrounding area i.e. in the IPM and BrM regions.

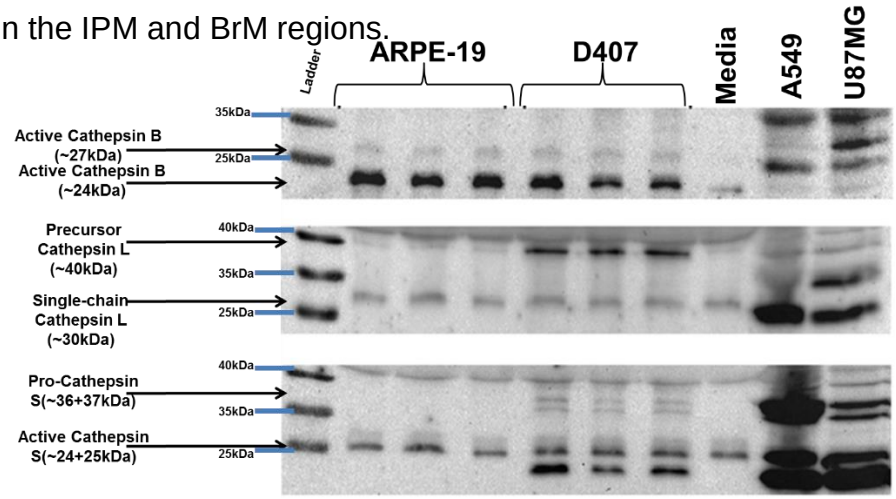

Figure 3.5: Immunodetection of cathepsin B, L and S in conditioned media of RPE cell lines. Conditioned media was probed with anti-cathepsin B (Abcam, ab33538, 1:1000), anti-cathepsin L (Abcam, ab6314, 1:1000) and anti-cathepsin S (Abcam, ab92780, 1:1000). Samples from 3 independent cell cultures for each line were loaded according to equal protein content. Media lane represented unconditioned media whilst A549 and U87MG cell lysates were used as positive controls.

3.1.3 – Immunohistochemistry detection of cathepsins B, L and S protein in human RPE cells.

Before staining the eye sections, it was important to optimise antibody concentrations in order to determine conditions that avoided saturation of the staining. An example for cathepsin L antibody optimisation is shown (Figure 3.6).

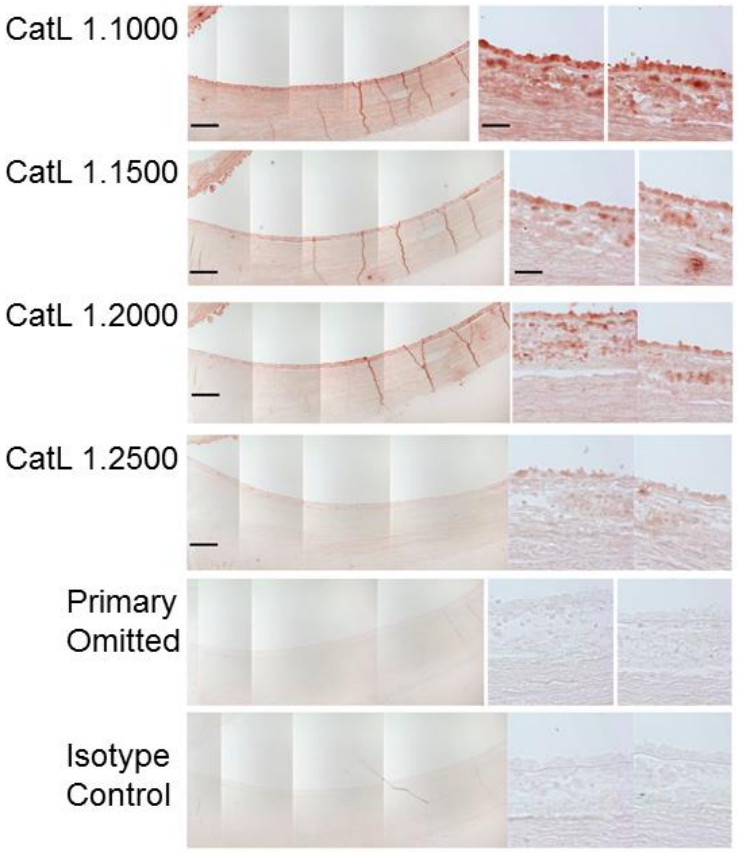

Figure 3.6: Optimisation of cathepsin L immunostaining in RPE cells of human eye sections (specimen EOU217). A range of different anti-cathepsin L antibody (Abcam, ab6314) concentrations were analysed to select the appropriate amount to be used in test experiments. Scale bar for lower magnification images represents 500µm and for higher magnification images represents 50µm respectively.

After determining appropriate antibody concentrations, IHC analysis showed that cathepsins B, L and S immunoreactivity was observed in the choroid and RPE cells in sections of paraffin embedded human eyes (Figure 3.7). Specifically, RPE cells stained strongly in all cases. In addition parts of the choroid also stained positively suggesting the presence of cathepsins in components of the choroid. For cathepsin B and L, the RPE staining was strong relative to the choroid whereas for cathepsin S, the RPE staining was similar to that of the choroid.

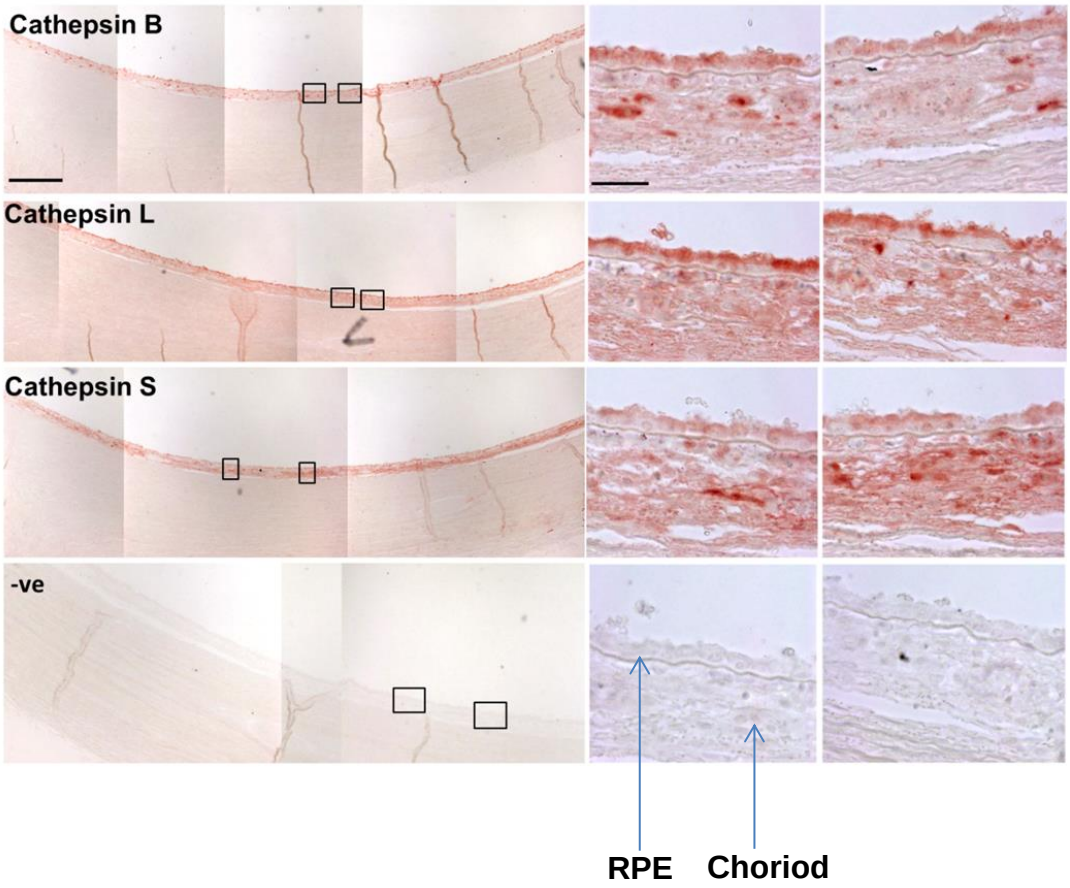

Figure 3.7: Cathepsin B, L and S immunostaining in human RPE cells. Paraffin embedded eye sections (4µm) were stained with cathepsin B (Abcam, ab33538, 1:1000), cathepsin L (Abcam, ab6314, 1:1000) and cathepsin S (Abcam, ab92780, 1:1000) antibodies. Negative control (primary omitted) was included in the experiment. Scale bar for lower magnification images represents 500µm and for higher magnification images represents 50µm respectively.

3.2 – Effects of Advanced Glycation End-Products (AGEs) on cathepsins expression, processing and activity in cultured RPE cells

After confirming the protein expression of cathepsin B, L and S from RPE cells, the next part of the study investigated how exposure of RPE cells to AGEs, a molecular event associated with the process of ageing, affects the expression/processing and activity of these proteases. In order to get a greater understanding of AGEs effects on cathepsins and subsequent lysosomal activity, the aspartic protease cathepsin D was also included for analysis. Cathepsin D has high activity in the RPE and is involved in critical functions of the RPE such as digestion of POS (Regan et al., 1980; Zimmerman et al., 1983) as well as processing interactions with other proteases such as cathepsin L (Laurent-Matha et al., 2006; Wille et al., 2004; Zheng et al., 2008).

3.2.1 – Cell density and morphological differences between control and AGEs exposed RPE cultures

ARPE-19 cells and D407 cell lines were used in a culture that aimed to model BrM ageing (Glenn et al., 2009). Cells were grown on control MG™ to mimic young BrM or grown on glycolaldehyde-treated MG™ (AGEs-modified MG™) which was induced to accumulate AGEs, to mimic aged BrM. The amount of AGE-modification and collagen-cross linking in the AGEs-modified MG™ substrate has previously been described (Honda et al., 2001; Stitt et al., 2004). Measurements of cathepsin expression/processing and activity were taken at 1 week and 2 week time points for ARPE-19 cells. Only 1 week time point was used for D407 as cells displayed increased cell death beyond this point.

ARPE-19 cells seeded upon control MG™ had a higher rate of population control compared to cells seeded upon AGEs-modified MG™ (Figure 3.8). At day 5 post-seeding, ARPE-19 cells had reached a confluent state when grown on control MG™ whereas cells grown on AGEs-modified MG™ were around ~40% confluent (Figure 3.8 B, E). At day 14, ARPE-19 cells grown on both control and AGEs-modified MG™ were confluent and developed a cobblestone appearance (Figure 3.8 C, F). However, when closely

observed, ARPE-19 cells grown on control MG™ were more tightly packed than cells grown on an AGEs-modified MG™ which may contribute to the higher number of cells being present in the control culture compared to the AGEs-modified culture. The observation that there was a greater density of ARPE-19 cells present in the control cultures compared to the AGEs-modified culture is further supported by cell counts that were carried out on cells grown on control MG™ and AGEs-modified MG™ for 1 week and 2 week time points (Table 3.1).

Table 3.1: Cell counts recorded from ARPE-19 cells grown on non-AGEd (NA) and AGEs-modified MG™ (A). 3 technical replicates for each condition.

Culture	Culture name	Cell count at 1 week (cell/ml)	Cell count at 2 week (cells/ml)
Non-AGEd	NA1	$13.75x10^4$	$20.5x10^4$
	NA2	$16x10^4$	$34x10^4$
	NA3	$17x10^4$	$27.5x10^4$
AGEs-modified	A1	$5x10^4$	$19.25x10^4$
	A2	$2.75x10^4$	$17.5x10^4$
	A3	$3.5x10^4$	$17.5x10^4$

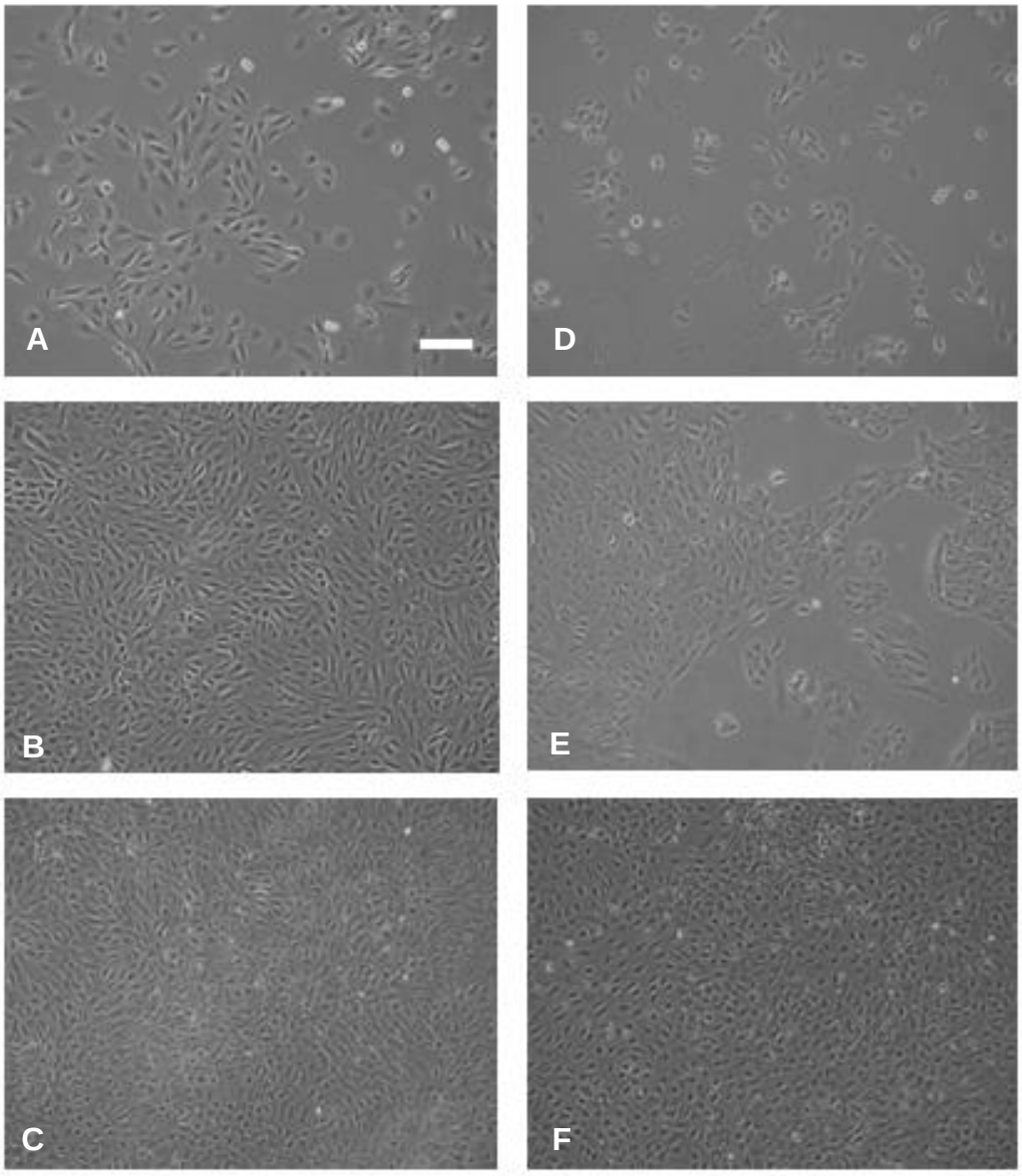

Figure 3.8: ARPE-19 cells grown on control MG™ (A, B and C) or AGEs-modified MG™ (D, E, and F). ARPE-19 cells grown on control MG™ showed a higher cell density compared to cells grown on AGEs-modified MG™. 24 hours post seeding (A, D) no real difference could observed between ARPE-19 cells upon control MG™ or AGEs-modified MG™. By day 5 (B, E) APRE-19 cells grown on control MG™ were more confluent (~90%) compared to cells grown on AGEs-modified MG™ (~40% confluent). By day 14 (C, F) ARPE-19 cells grown on control MG™ or AGEs-modified MG™ seemed similar in confluency but upon closer observation, it can be seen that the control cells are closely packed suggesting a higher number of cells. Scale bar represents 100µm.

Similar to ARPE-19 cell line, D407 cells grown on control MG™ also had a higher rate of population for control cultures compared to cells seeded upon AGEs-modified MG™ (Figure 3.9). As early as 24 hours post seeding, it could be observed that D407 cells grown on control MG™ were more confluent compared to cells grown on AGEs-modified MG™ (Figure 3.9 A, F). By day 6 post-seeding, D407 cells grown on both control MG™ and AGEs-modified MG™ were confluent (Figure 3.9 B, G). At day 7, the confluent state of D407 cells was accompanied by possible increased cell death (Figure 3.9 C, H). This cell death became more pronounced with time as observed at day 8 (Figure 3.9 D, I) and day 12 (Figure 3.9 E, J) post-seeding in both control and treated cultures respectively. Due to this increased cell death, only a 1 week AGEs exposure time point was chosen for D407 cells grown in culture. Although there seemed to be equal confluency reached for cells in both control and treated cultures, cell counts at the 1 week time point showed that the cell number was higher in the control cultures at day 7 compared to cells grown on AGEs-modified MG™ (Table 3.2). Although not as clear as APRE-19 cells, this could be explained by cells being more tightly packed on control MG™ compared to the AGEs-modified MG™ culture.

The observation that the growth of ARPE-19 cells and D407 cells grown on AGEs-modified MG™ lagged behind the growth of cells upon a control matrix suggests that the AGEs impaired cellular replicative capacity. In addition, even in apparent similar confluency observed for cells grown on control MG™ and AGEs-modified MG™ at the experimental time points, cell counts consistently showed less cells present in AGEs-modified MG™ cultures**.** This decrease in cell number may be explained by the observation that cells seem more tightly packed on control MG™ than cells grown on an AGEs-modified MG™ (more apparent for ARPE-19 cell cultures than for D407 cells). In addition, the decrease in cell number could be explained by a greater amount of cell death occurring within the AGEs-modified MG™ culture, as AGEs are known to induce cell death, a response associated with oxidative insult (Wang et al., 2015b).

Table 3.2: Cell counts recorded from D407 cells grown on non-AGEd (NA) and AGEs-modified MG™ (A). 3 technical replicates for each condition.

Culture	Culture name	Cell count at 1 week (cell/ml)
Non-AGEd	NA1	$79.5x10^4$
	NA2	$89.5x10^4$
	NA3	$87.5x10^4$
AGEs-modified	A1	$71x10^4$
	A2	$76.75x10^4$
	A3	$45.5x10^4$

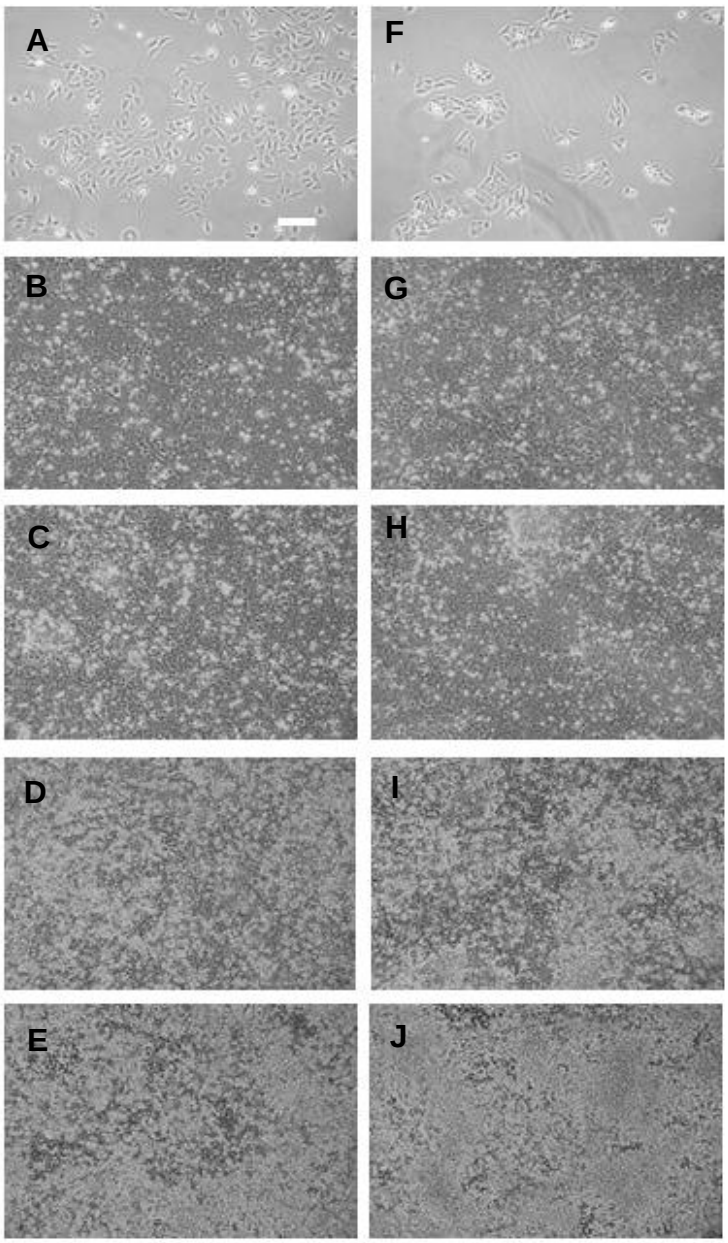

Figure 3.9: D407 cells grown on control MG™ (A-E) or AGEs-modified MG™ (F-J). D407 cells grown on control MG™ showed a higher cell density compared to cells grown on AGEs-modified MG™. 24 hours post seeding (A, F), a higher confluency was observed for D407 cells grown on control MG™ compared to cells grown on AGEs-modified MG™. By day 6 (B, G) D407 cells grown on control MG™ or AGEs-modified MG™ were similar in confluency. By day 7 (C, H) although still confluent, there appeared to be an increased cell death in both control and treated cultures cells. This cell death became more pronounced at day 8 (D, I) and day 12 (E, J) in both control and treated. Scale bar represents 100µm.

3.2.2 – GAPDH was an appropriate loading control in western blotting analysis for AGEs experiments samples

The next aim of this study was to determine whether the commonly used loading controls were affected by the experimental condition after equal amounts of protein were loaded. Initially, α- tubulin was tested for its relevance as an appropriate loading control. Samples prepared from ARPE-19 cultured on control MG™ or AGEs-modified MG™ for 1 week were equally loaded and subjected to western blotting analysis. The result suggested that α- tubulin levels decreased in cells exposed to AGEs (Figure 3.10). This raised the possibility that α- tubulin is affected by the experimental conditions and therefore not used as a loading control for subsequent experiments.

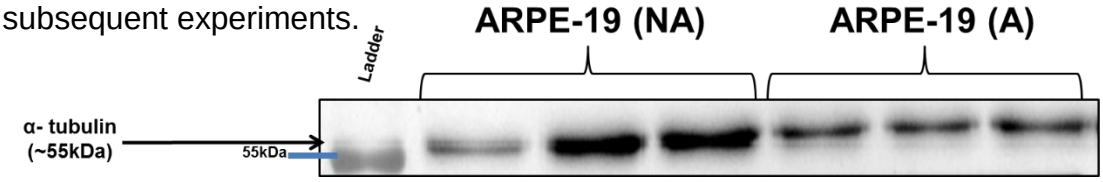

Figure 3.10: Immunodetection of α- tubulin protein expression in ARPE-19 cultured on control MG™ (NA) or AGEs-modified MG™ (A) for 1 week. Immunoblot of cell lysates probed anti- α-tubulin detected a band at 55kDa (Sigma-Aldrich, T9026, 1:5000). Samples of ARPE-19 from 3 separate of NA cells and 3 separate A treated cells are shown (n = 1).

GAPDH was then tested to determine whether AGEs exposure would affect its protein expression. Samples prepared from ARPE-19 and D407 cultured on control MG™ or AGEs-modified MG™ for the respective time points were subjected to western blotting analysis. Ponceau S stain was chosen as a control for normalisation as it can be used to assess equal protein loading as well as a valid alternative loading control in western blotting (Romero-Calvo et al., 2010). Results showed that GAPDH levels were not affected in the experimental conditions and was therefore chosen as an appropriate loading control (n = 3) (Figure 3.11).

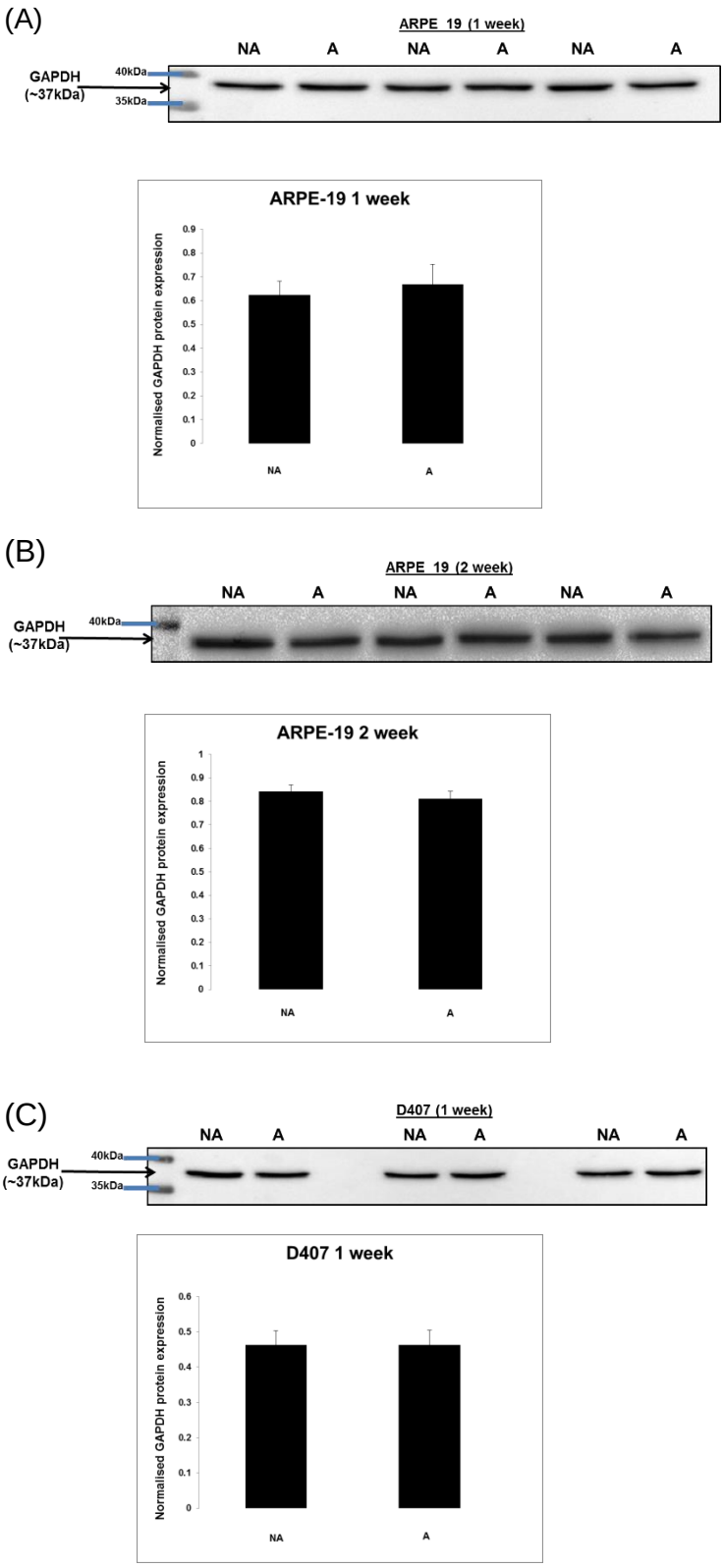

Figure 3.11: Immunodetection of GAPDH protein expression in ARPE-19 and D407 cells cultured on control MG™ (NA) or AGEs-modified MG™ (A) for 1 week/2 week. Immunoblot of cell lysates probed with anti-GAPDH (Abcam, ab8245 1:30000). (A) D407 cells exposure to AGEs for 1 week (B) ARPE-19 cells exposed to AGEs for 1 week (C) ARPE-19 cells exposed to AGEs for 2 weeks. Graphs show average GAPDH protein levels normalised to Ponceau S stain values (arbitrary units) ± S.E.M. for all samples tested (n=3 with a minimum of 8 technical replicates for each condition, Independent t test).

3.2.3 – Active cathepsin L protein level was increased in ARPE-19 cells cultured on AGEs-modified MG™ for 1 week/2 week

After determining GAPDH was a suitable loading control, protein levels/processing of lysosomal proteases cathepsins B, L, D and S were assessed in RPE cells exposed to AGEs for 1 week and 2 weeks. Cell lysates prepared from ARPE-19 cells cultured on AGEs-modified MG™ for 1 week and 2 week time points, underwent western blot analysis for their cathepsin B, D, L and S protein content.

For cathepsin B, bands at ~25kDa, ~30kDa and 40kDa were detected, consistent with the expected band size of cathepsin B active form, single chain and proform respectively at the 1 week time point (Figure 3.12). All forms of cathepsin B detected remained unchanged after AGEs exposure (n = 4 for 25kDa form; n=2 for other forms). At the 2 week time point, only a band of 25kDa corresponding to the active form of cathepsin B was detected (Figures 3.13). No significant differences for cathepsin B was observed between treated and control cells (n = 3).

Cathepsin D is synthesised on the rough endoplasmic reticulum (RER) as a pre-pro enzyme that undergoes proteolytic cleavage to produce a mature form. Initial steps during the processing of cathepsin D is the removal of the signal peptide which yields a 52kDa pro-cathepsin D (Laurent-Matha et al., 2006). Further processing of cathepsin D eventually leads to the formation of two active form fragments, the 30kDa heavy chain and the 15kDa light chain (Erickson et al., 1981). For cells that were cultured for 1 week, bands at 28kDa and 55kDa were detected most likely corresponding to the mature heavy chain active form and a pro-form of cathepsin D respectively. AGEs exposure caused no alterations in protein levels of either form compared to controls (n = 5) (Figure 3.14). Cells cultured for 2 weeks only presented a band corresponding to the active form (28kDa) for cathepsin D (Figure 3.15). Interestingly, active form protein level of cathepsin D (28kDa) significantly increased (~125% increase) after AGEs exposure (n= 4, p=0.005).

For both 1 week and 2 week time points, cathepsin S immunoblotting detected the presence of bands at 37kDa, 36kDa and 24kDa, corresponding

to two proforms and an active form respectively (Figure 3.16 and 3.17). No significant changes were detected for all forms of cathepsin S in cells after 1 week AGEs exposure compared to controls (n=3) (Figure 3.16). However, in cells exposed to AGEs for 2 week, both the total pro (36+37kDa) and active (24kDa) forms of cathepsin S were significantly decreased by ~40% (p=0.04) and 74% (n=3, p=0.004) respectively (Figure 3.17).

Immunoblotting for cathepsin L revealed the presence of a band at 26kDa, corresponding to active form cathepsin L at both 1 and 2 week time points (Figure 3.18 and 3.19 respectively). A significant decrease of 40% in cells exposed to AGEs at 1 week and a 33% decrease in cells after 2 week AGEs exposure for active cathepsin L protein level was observed when compared to control cells respectively (1 week p = 0.02, n =3 **;** 2 week, p = 0.03, n= 4) (Figure 3.18 and 3.19 respectively).

The main findings from the above data are summarised as follows:

- No changes in cathepsin B protein levels were observed in ARPE-19 cells exposed to AGEs compared to control cells.
- Cathepsin D active protein levels significantly increased while cathepsin S protein levels decreased in ARPE-19 cells exposed to AGEs for 2 week compared to control cells.
- A significant decrease of active cathepsin L protein level was observed in ARPE-19 cells exposed to AGEs compared to control cells.

(A)

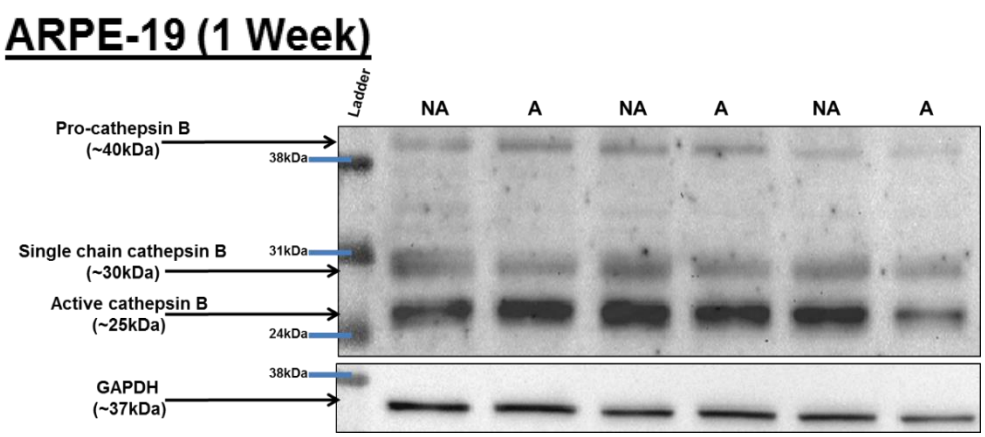

(B)

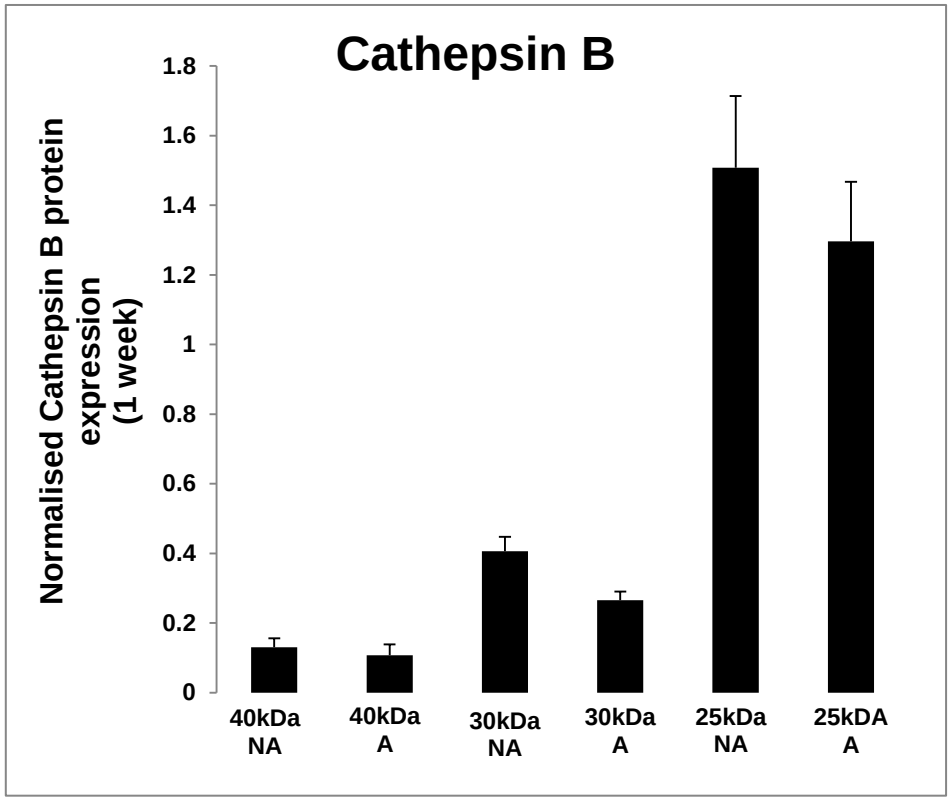

Figure 3.12: Immunodetection of cathepsin B protein forms in ARPE-19 cells cultured on control MG™ or AGEs-modified MG™ for 1 week. (A) Immunoblot of cell lysates probed with anti-cathepsin B (Abcam, ab33538, 1:500) detected active and inactive forms of cathepsin B. GAPDH (Abcam, ab8245, 1:30000) immunoblotting detection was used as a loading control. ARPE-19 cells from 3 separate untreated (NA) and 3 separate AGEs (A) treated wells are shown. (B) Average normalised cathepsin B expression expression (arbitrary units) ± S.E.M. for all samples tested (n=2 with a minimum of 6 technical replicates for 40kDa and 30kDa bands; n=4 with a minimum of 10 technical replicates for 25kDa band).

(A)

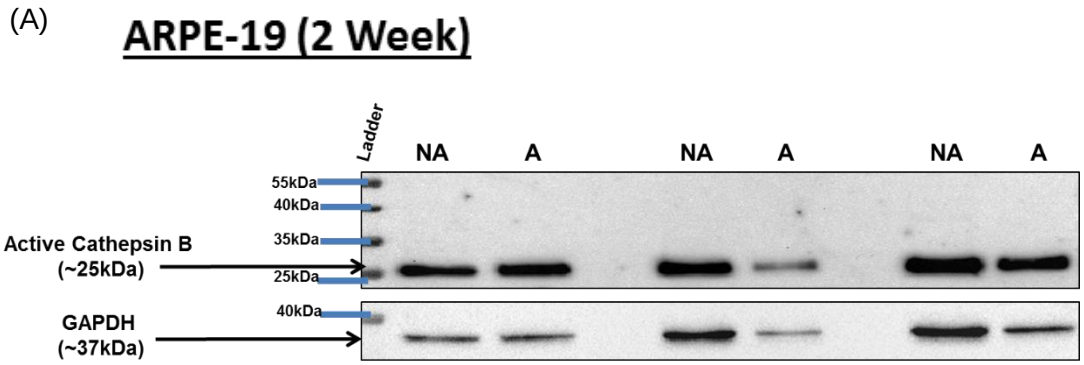

(B)

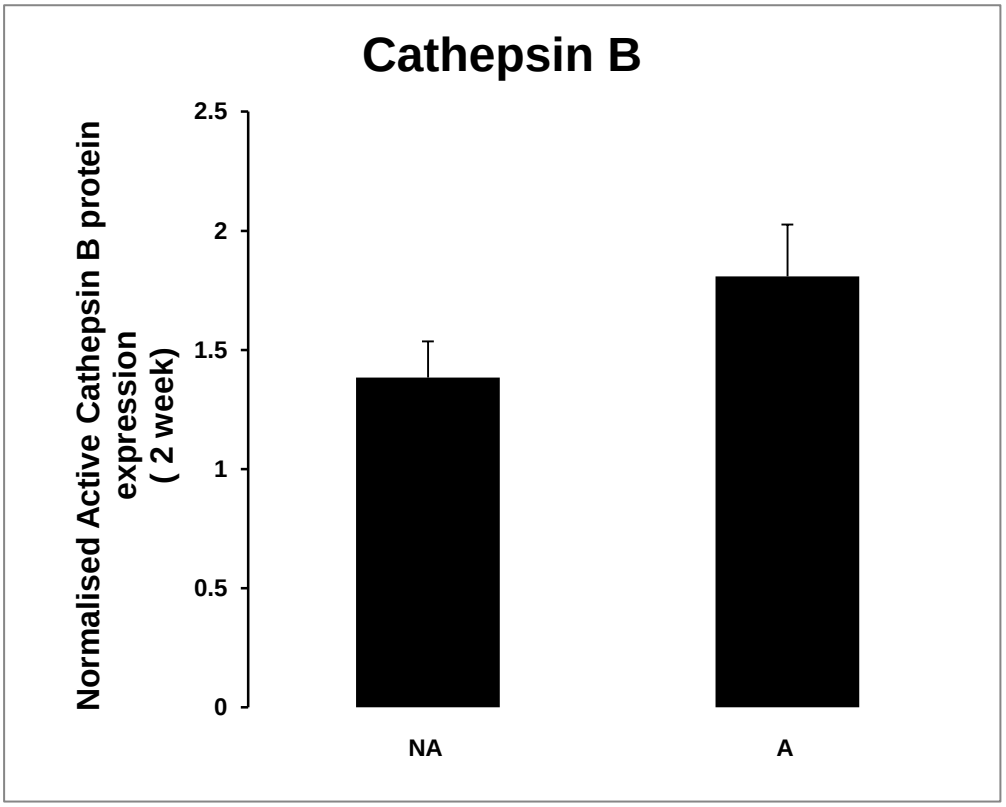

Figure 3.13: Immunodetection of cathepsin B protein forms in ARPE-19 cells cultured on control MG™ or AGEs-modified MG™ for 2 week. (A) Immunoblot of cell lysates probed with anti-cathepsin B (Abcam, ab33538, 1:500) detected an active forms of cathepsin B. GAPDH (Abcam, ab8245, 1:30000) immunoblotting detection was used as a loading control. ARPE-19 cells from 3 separate untreated (NA) and 3 separate AGEs (A) treated wells are shown. (B) Average normalised cathepsin B expression (arbitrary units) ± S.E.M. for all samples tested (n=3 with a minimum of 9 technical replicates for each condition).

(A)

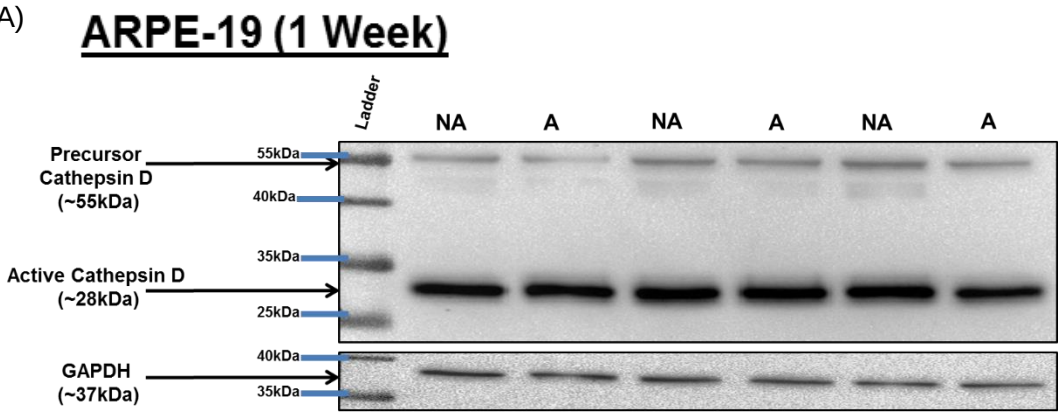

(B)

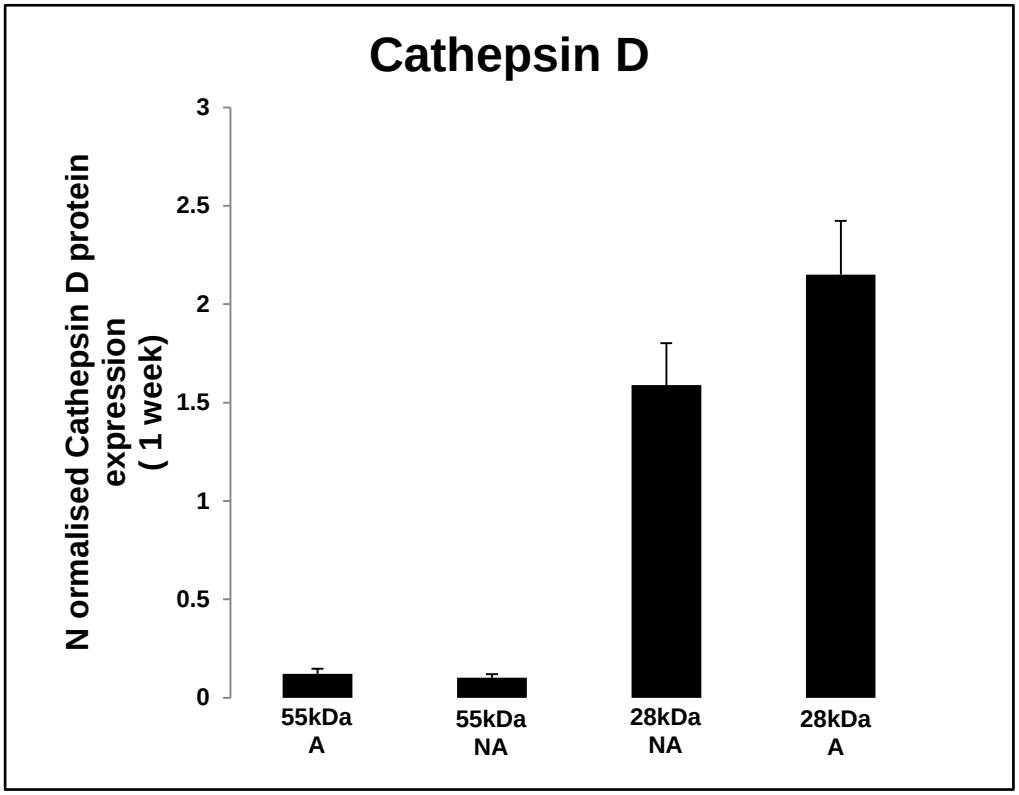

Figure 3.14: Immunodetection of cathepsin D protein forms in ARPE-19 cells cultured on control MG™ or AGEs-modified MG™ for 1 week. (A) Immunoblot of cell lysates probed with anti-cathepsin D (BD Biosciences, 610800, 1:500) detected active and inactive forms of cathepsin D. GAPDH (Abcam, ab8245, 1:30000) immunoblotting detection was used as a loading control. ARPE-19 cells from 3 separate untreated (NA) and 3 separate AGEs (A) treated wells are shown. (B) Average normalised cathepsin D expression (arbitrary units) ± S.E.M. for all samples tested (n=5 with a minimum of 12 technical replicates for each condition).

(A) **ARPE-19 (2 Week)**

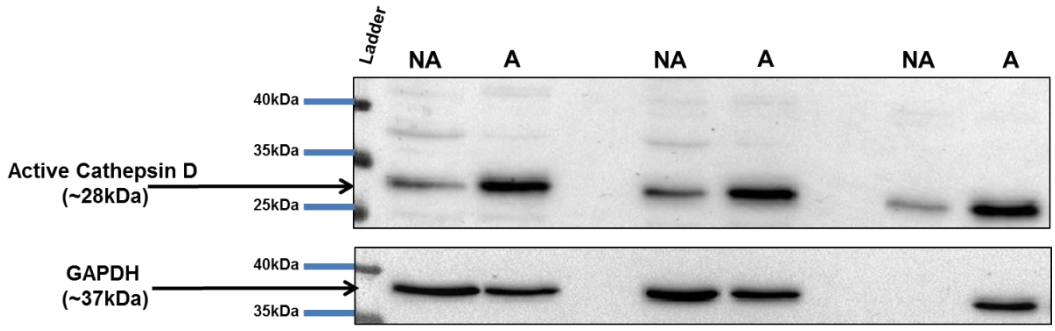

(B)

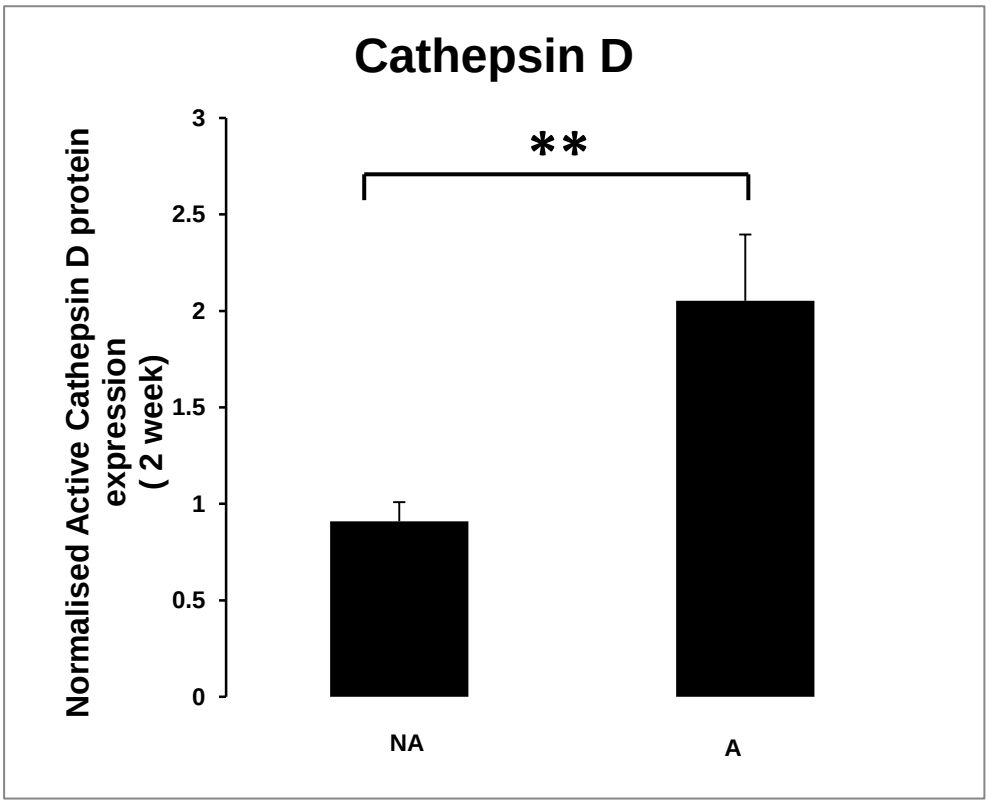

Figure 3.15: Immunodetection of cathepsin D protein forms in ARPE-19 cells cultured on control MG™ or AGEs-modified MG™ for 2 week. (A) Immunoblot of cell lysates probed with anti-cathepsin D (BD Biosciences, 610800, 1:500) detected an active form of cathepsin D. GAPDH (Abcam, ab8245, 1:30000) immunoblotting detection was used as a loading control. ARPE-19 cells from 3 separate untreated (NA) and 3 separate AGEs (A) treated wells are shown. (B) Average normalised cathepsin D expression (arbitrary units) ± S.E.M. for all samples tested (n= 4 with a minimum of 11 technical replicates for each condition). Independent t test, **=$p \leq 0.01$.

(A)

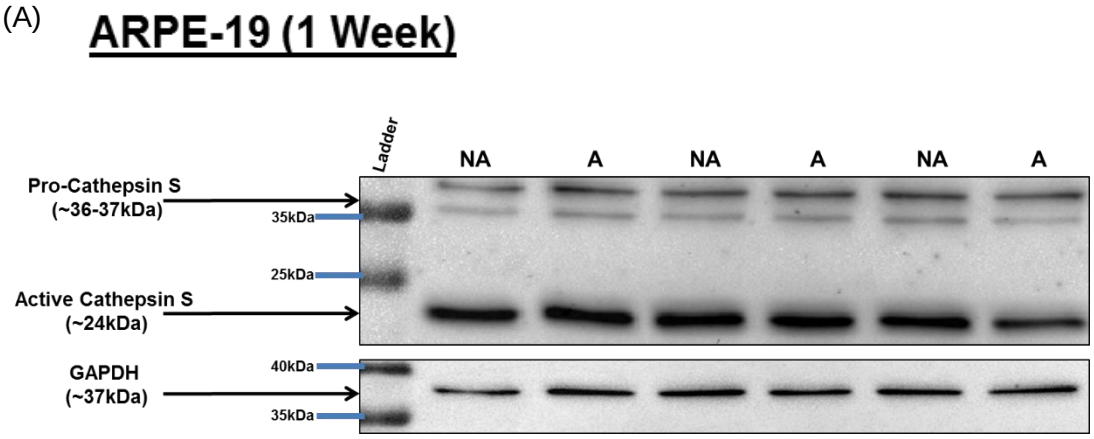

(B)

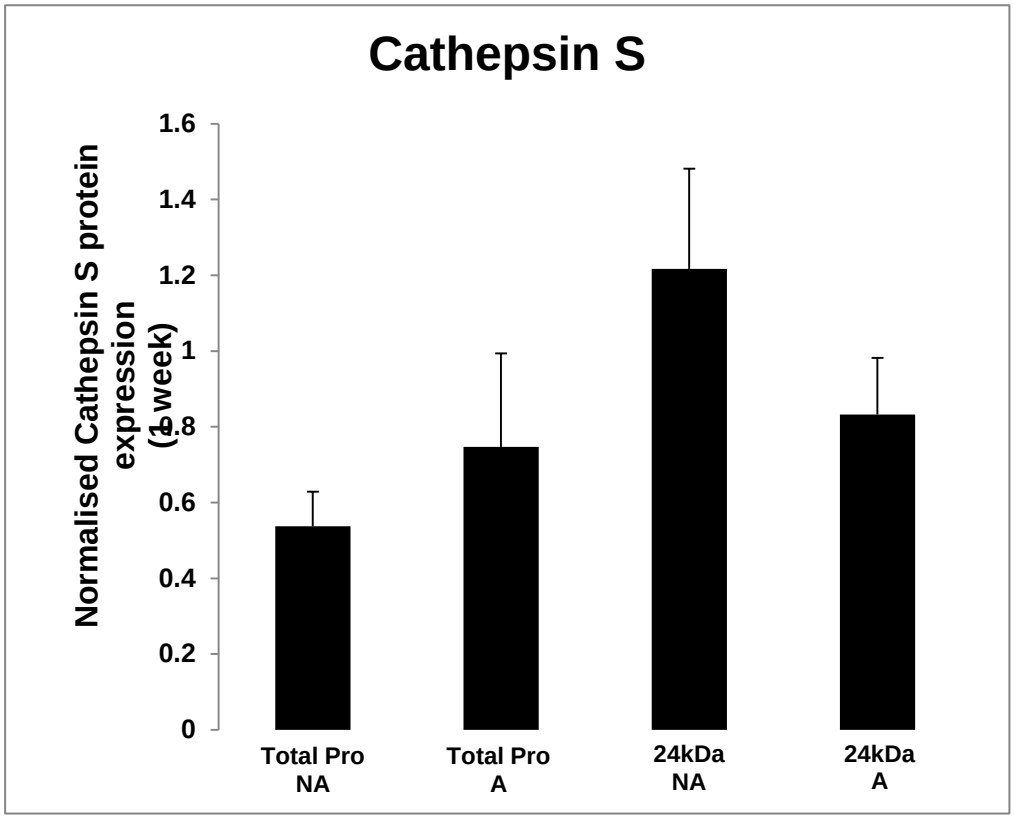

Figure 3.16: Immunodetection of cathepsin S protein forms in ARPE-19 cells cultured on control MG™ or AGEs-modified MG™ for 1 week. (A) Immunoblot of cell lysates probed with anti-cathepsin S (Abcam, ab92780, 1:500) detected active and inactive forms of cathepsin S. GAPDH (Abcam, ab8245, 1:30000) immunoblotting detection was used as a loading control. ARPE-19 cells from 3 separate untreated (NA) and 3 separate AGEs (A) treated wells are shown. (B) Average normalised cathepsin S expression (arbitrary units) ± S.E.M. for all samples tested (n=3 with a minimum of 9 technical replicates for each condition).

(A)

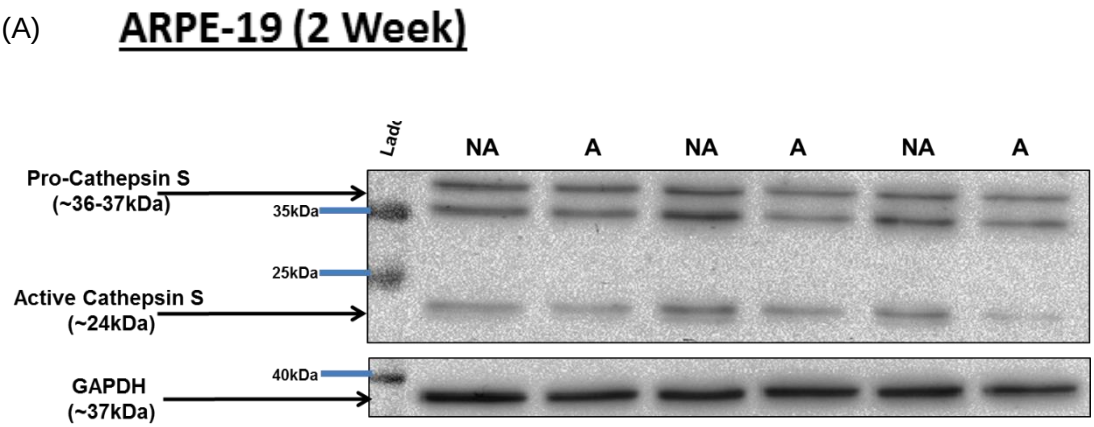

(B)

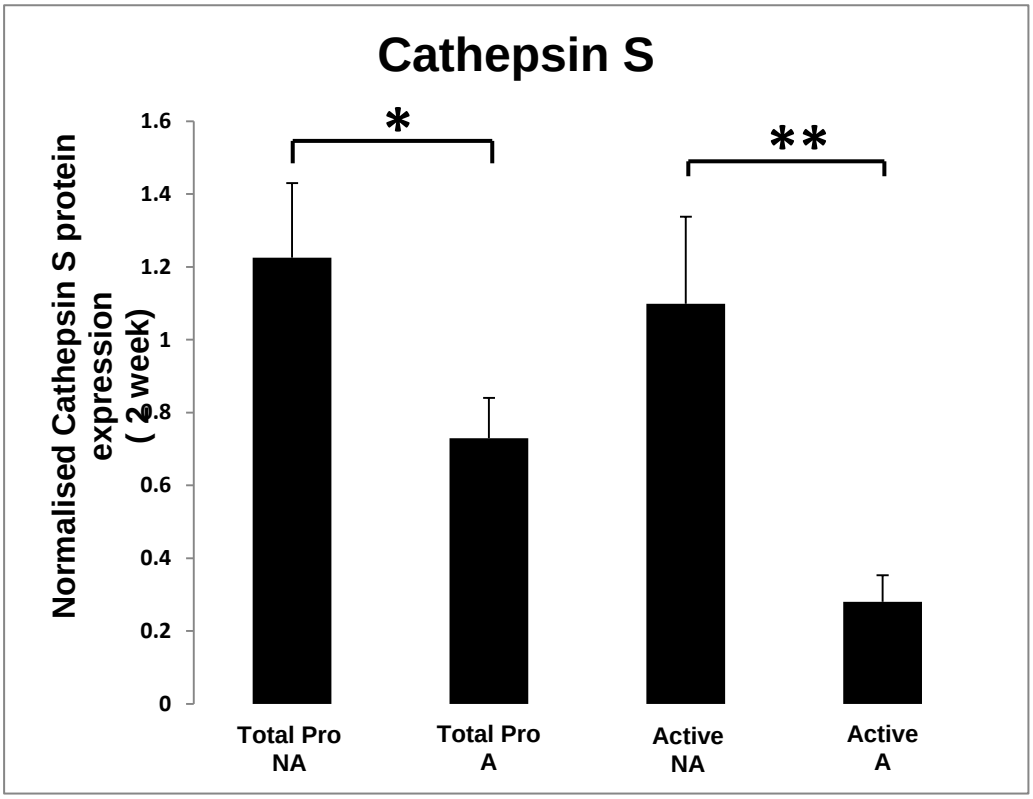

Figure 3.17: Immunodetection of cathepsin S protein forms in ARPE-19 cells cultured on control MG™ or AGEs-modified MG™ for 2 week. (A) Immunoblot of cell lysates probed with anti-cathepsin S (Abcam, ab92780, 1:500) detected active and inactive forms of cathepsin S. GAPDH (Abcam, ab8245, 1:30000) immunoblotting detection was used as a loading control. ARPE-19 cells from 3 separate untreated (NA) and 3 separate AGEs (A) treated wells are shown. (B) Average normalised cathepsin S expression (arbitrary units) ± S.E.M. for all samples tested (n=3 with 9 technical replicates for each condition). Independent t test, *= $p \leq 0.05$, **=$p \leq 0.01$.

(A) **ARPE-19 (1 Week)**

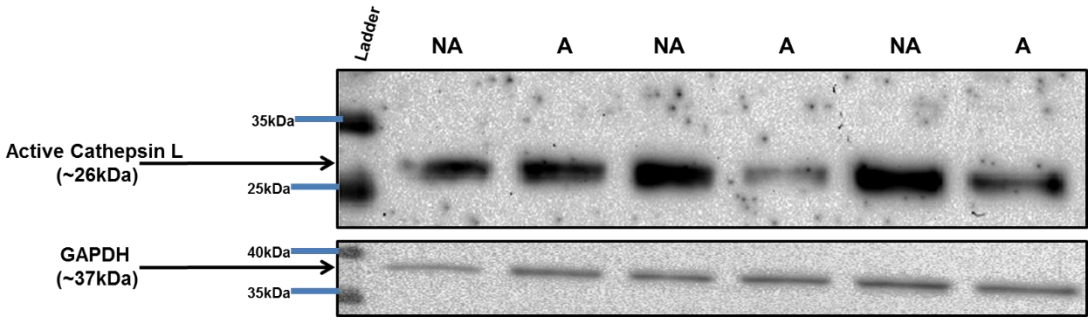

(B)

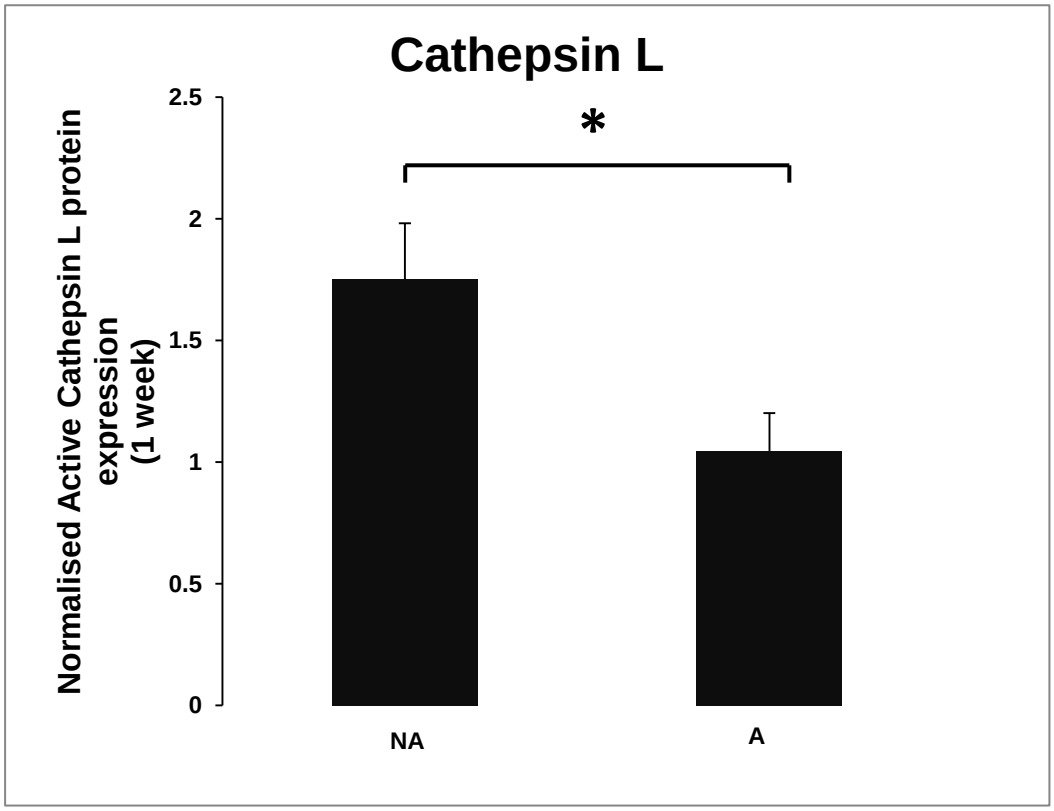

Figure 3.18: Immunodetection of cathepsin L protein forms in ARPE-19 cells cultured on control MG™ or AGEs-modified MG™ for 1 week. (A) Immunoblot of cell lysates probed with anti-cathepsin L (Abcam, ab6314, 1:500) detected an active form of cathepsin L. GAPDH (Abcam, ab8245, 1:30000) immunoblotting detection was used as a loading control. ARPE-19 cells from 3 separate untreated (NA) and 3 separate AGEs (A) treated wells are shown. (B) Average normalised cathepsin L expression (arbitrary units) ± S.E.M. for all samples tested (n=3 with a minimum of 9 technical replicates for each condition). Independent t test, *=p ≤ 0.05.

(A)

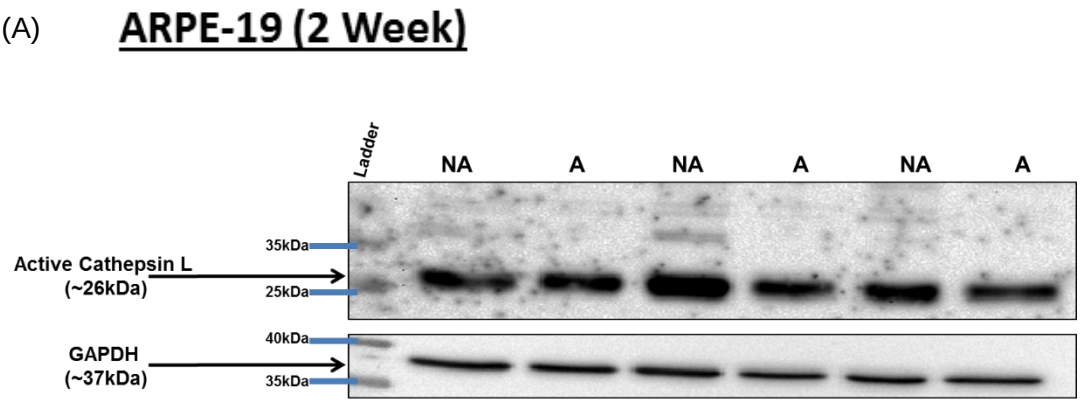

(B)

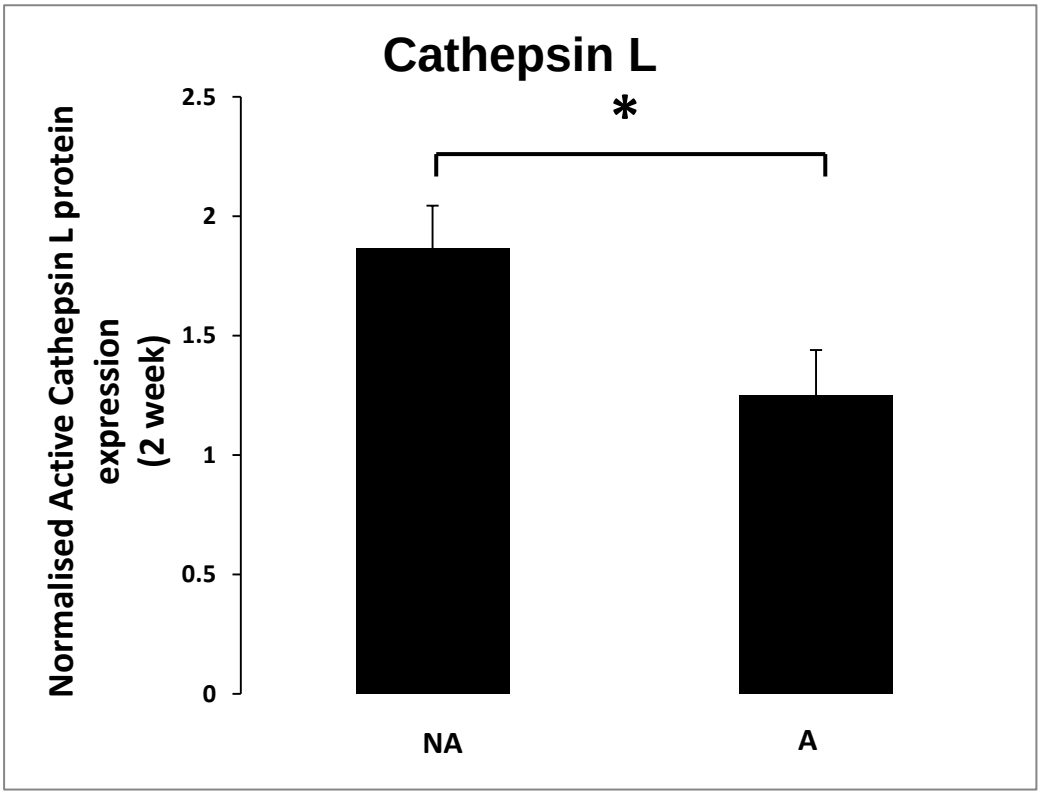

Figure 3.19: Immunodetection of cathepsin L protein forms in ARPE-19 cells cultured on control MG™ or AGEs-modified MG™ for 2 week. (A) Immunoblot of cell lysates probed with anti-cathepsin L (Abcam, ab6314, 1:500) detected an active form of cathepsin L. GAPDH (Abcam, ab8245, 1:30000) immunoblotting detection was used as a loading control. ARPE-19 cells from 3 separate untreated (NA) and 3 separate AGEs (A) treated wells are shown. (B) Average normalised cathepsin L expression (arbitrary units) ± S.E.M. for all samples tested (n=4 with a minimum of 12 technical replicates for each condition). Independent t test, * = p≤ 0.05.

3.2.4 - Active cathepsin L protein level increased in D407 cells cultured on AGEs-modified MG™ for 1 week

Cathepsin B, D, L and S protein content was also assessed in D407 cell line exposed to AGEs-modified MG™ for 1 week. Immunoblotting for cathepsin B revealed detection of bands at ~25kDa, ~30kDa and 37kDa, consistent with the expected band size of the active form, single chain form and a pro-form of cathepsin B respectively (Figure 3.20). Bands were also observed at the ~40kDa mark which may be representative of proforms of cathepsin B. However, these bands were not quantified due to the high background around this area. All quantifiable forms of cathepsin B remained unchanged after 1 week AGEs exposure when compared to control cells (n= 3 for 37kDa and 25kDa; n =2 for 30kDa form).

Similar to ARPE-19 cells, immunoblotting for cathepsin D detected two bands at approximately 55kDa and 28kDa (Figure 3.21). No significant changes were detected for both 55kDa and 28kDa cathepsin D forms in cells exposed to AGEs when compared to control cells (n = 4). An additional band between the 35kDa and 40kDa protein marks was also observed in some samples tested. However, due not being consistently present in samples from the 4 independent experiments, this band was not quantified.

Cathepsin S immunoblotting revealed that both total inactive 36-37kDa forms as well as the 24kDa active forms were detected. No significant changes were detected for all forms of cathepsins S in cells exposed to AGEs when compared to controls cells (n= 3) (Figure 3.22).

Bands of 26kDa and 36kDa were detected for cathepsin L which corresponded to the pro-form and active form respectively. No change was observed for the 36kDa form. Contrary to ARPE-19 cells, a significant increase (259% increase) of active cathepsin L protein level was observed in D407 cells exposed to AGEs compared to control cells (p= 0.04, n= 3) (Figure 3.23).

(A) **D407 (1 Week)**

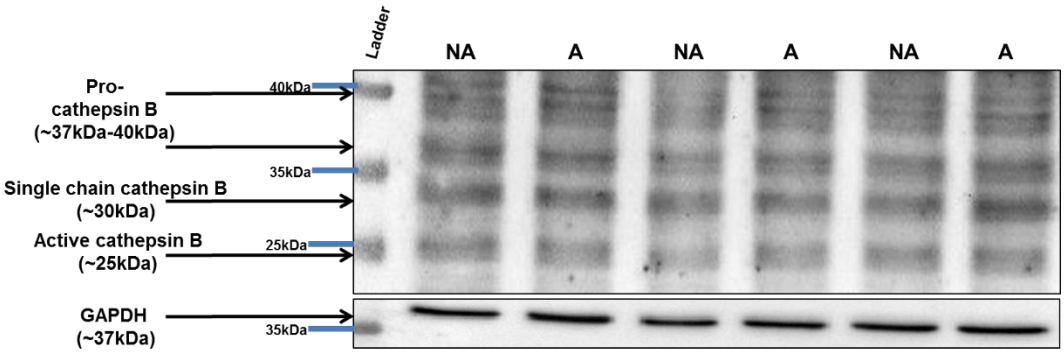

(B)

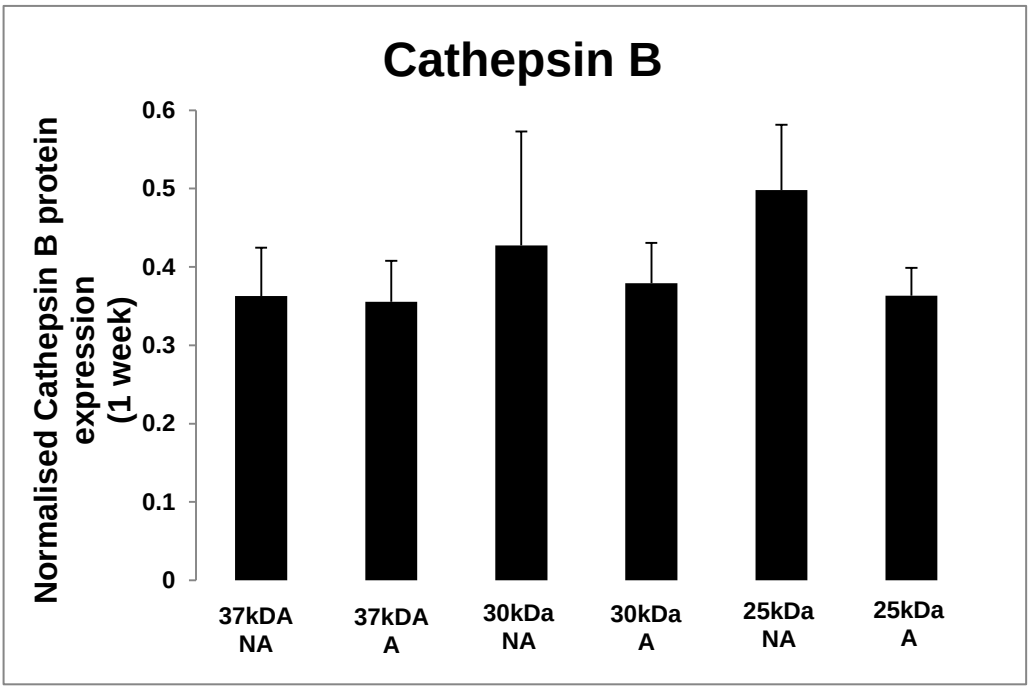

Figure 3.20: Immunodetection of cathepsin B protein forms in D407 cells cultured on control MG™ or AGEs-modified MG™ for 1 week. (A) Immunoblot of cell lysates probed with anti-cathepsin B (Abcam, ab33538, 1:500) detected active and inactive forms of cathepsin B. GAPDH (Abcam, ab8245, 1:30000) immunoblotting detection was used as a loading control. D407 cells from 3 separate untreated (NA) and 3 separate AGEs (A) treated wells are shown. (B) Average cathepsin B expression normalised to GAPDH (arbitrary units) ± S.E.M. for all samples tested (n=3 with a minimum of 8 technical replicates for 37kDa and 25kDa bands; n=2 with a minimum of 5 technical replicates for 30kDa band).

(A)

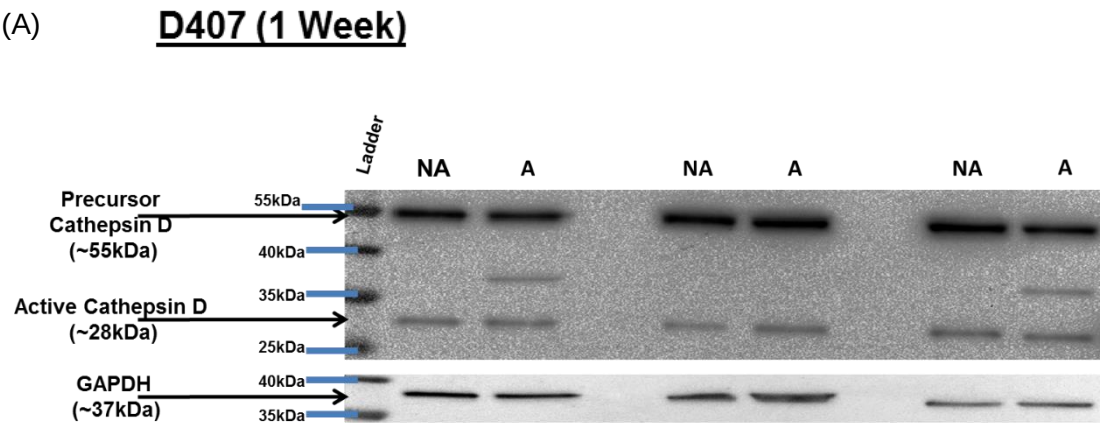

(B)

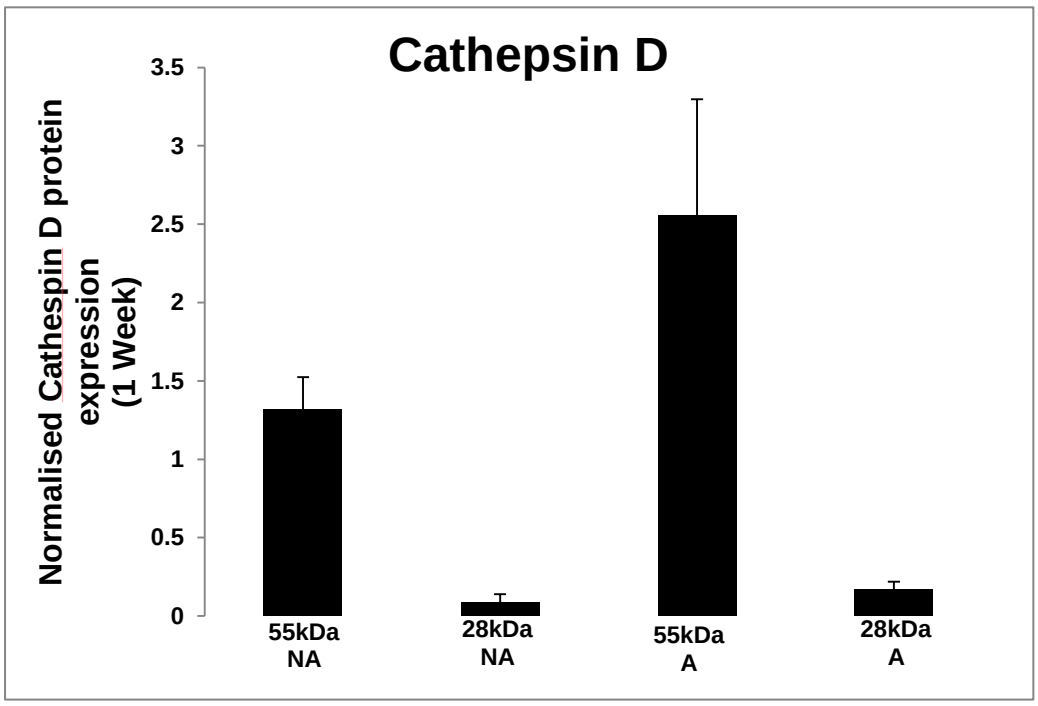

Figure 3.21: Immunodetection of cathepsin D protein forms in D407 cells cultured on control MG™ or AGEs-modified MG™ for 1 week. (A) Immunoblot of cell lysates probed with anti-cathepsin D (BD Biosciences, 610800, 1:500) detected active and inactive forms of cathepsin D. GAPDH (Abcam, ab8245, 1:30000) immunoblotting detection was used as a loading control. D407 cells from 3 separate untreated (NA) and 3 separate AGEs (A) treated wells are shown. (B) Average normalised cathepsin D expression (arbitrary units) ± S.E.M. for all samples tested (n=4 with a minimum of 9 technical replicates for each condition).

(A)

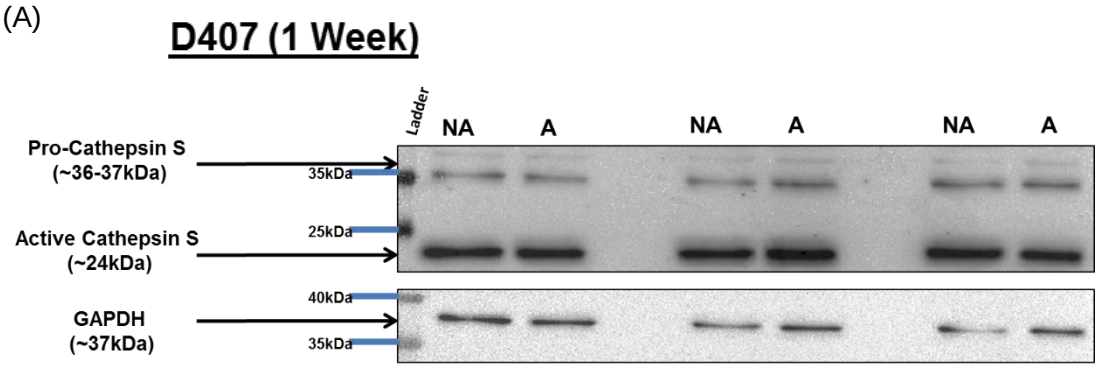

(B)

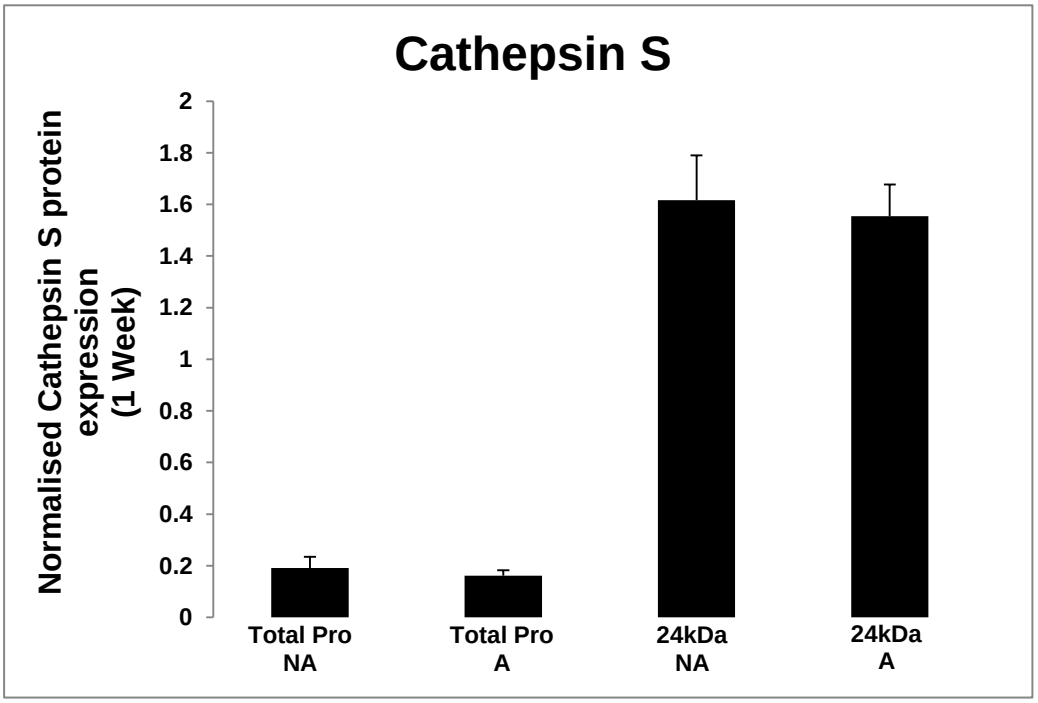

Figure 3.22: Immunodetection of cathepsin S protein forms in D407 cells cultured on control MG™ or AGEs-modified MG™ for 1 week. (A) Immunoblot of cell lysates probed with anti-cathepsin S (Abcam, ab92780, 1:500) detected active and inactive forms of cathepsin S. GAPDH (Abcam, ab8245, 1:30000) immunoblotting detection was used as a loading control. D407 cells from 3 separate untreated (NA) and 3 separate AGEs (A) treated wells are shown. (B) Average normalised cathepsin S expression (arbitrary units) ± S.E.M. for all samples tested (n=3 with a minimum of 9 technical replicates for each condition).

(A)

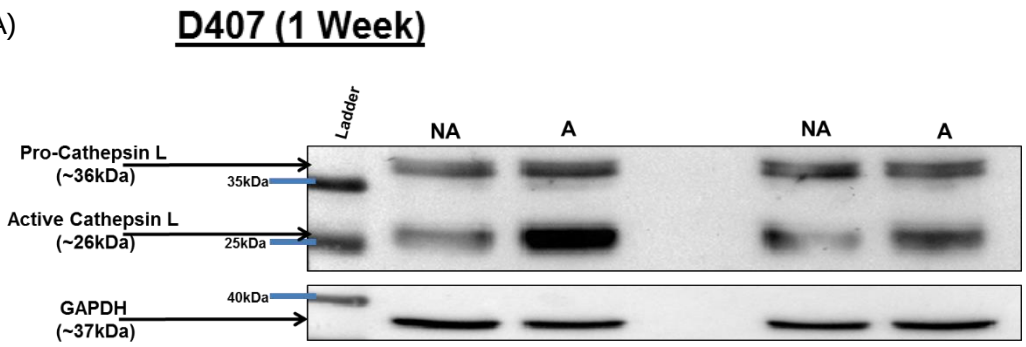

(B)

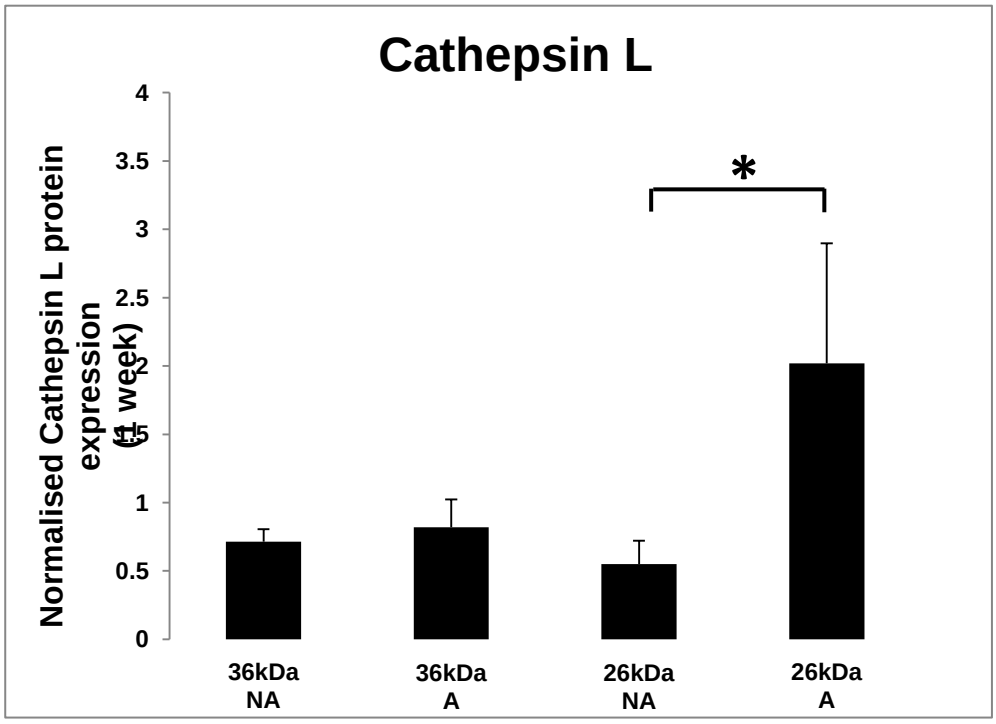

Figure 3.23: Immunodetection of cathepsin L protein forms in D407 cells cultured on control MG™ or AGEs-modified MG™ for 1 week. (A) Immunoblot of cell lysates probed with anti-cathepsin L (Abcam, ab6314, 1.500) detected an active form of cathepsin L. GAPDH (Abcam, ab8245, 1:30000) immunoblotting detection was used as a loading control. D407 cells from 2 separate untreated (NA) and 2 separate AGEs (A) treated wells are shown. (B) Average normalised cathepsin L expression (arbitrary units) ± S.E.M. for all samples tested (n=3 with a minimum of 7 technical replicates for each condition). Independent t test, *=p ≤ 0.05.

3.2.5 – Activity of cathepsins B, D, L and in RPE cells cultured on AGEs-modified MG™ for 1 week/2 week.

Thus far, AGEs exposure caused alteration of cathepsin protein expression/processing in RPE cells. Changes in levels of active forms of cathepsins may affect the activity of cathepsins. Therefore, the next part of the study was to investigate whether cathepsin activity was affected in RPE cells after AGEs exposure at the relevant time points.

N.B. Due to unaltered cathepsin B protein levels under experimental conditions, the activity of this protease was not measured. However, this does not rule out that cathepsin B activity may be affected in RPE cells exposed to AGEs as activity does not solely depend on how much of the active form of protein is available. Activity of cathepsins can be affected by a variety of factors including levels of protein, amount of cathepsin inhibitors present and the environment cathepsins encounter (Guha and Padh, 2008).

3.2.5.1 – Optimisation of appropriate levels of protein required for cathepsin activity kits.

Before determining how activity of cathepsins D, L and S were affected in RPE cells cultured on AGEs-modified MG™, a range of protein concentrations from control ARPE-19 and D407 samples were used to determine amount of protein needed to detect activity in the linear range of each kit. Protein amounts of 30µg, 60µg and 10µg were chosen for use in cathepsin D, L and S kits respectively (Figure 3.24).

3.2.5.2 – Cathepsin L activity levels decreased in ARPE-19 cells cultured on AGEs-modified MG™ for 2 weeks.

ARPE-19 cells that were exposed to AGEs-modified MG™ for 1 week showed no detectable differences of cathepsin activities when compared with control cells (n= 3) (Figure 3.25A). However, ARPE-19 cells exposed to AGEs-modified MG™ for 2 week, produced a significant decrease of 36% in cathepsin L activity when compared to control cells ($p= 0.02$, n= 3). No changes were detected in the activity levels for both cathepsins D and S (n= 3) (Figure 3.25B). D407 cells exposed to AGEs-modified MG™ for 1 week

showed no activity changes in all cathepsins tested when compared to control cells (n=3) (Figure 3.25C).

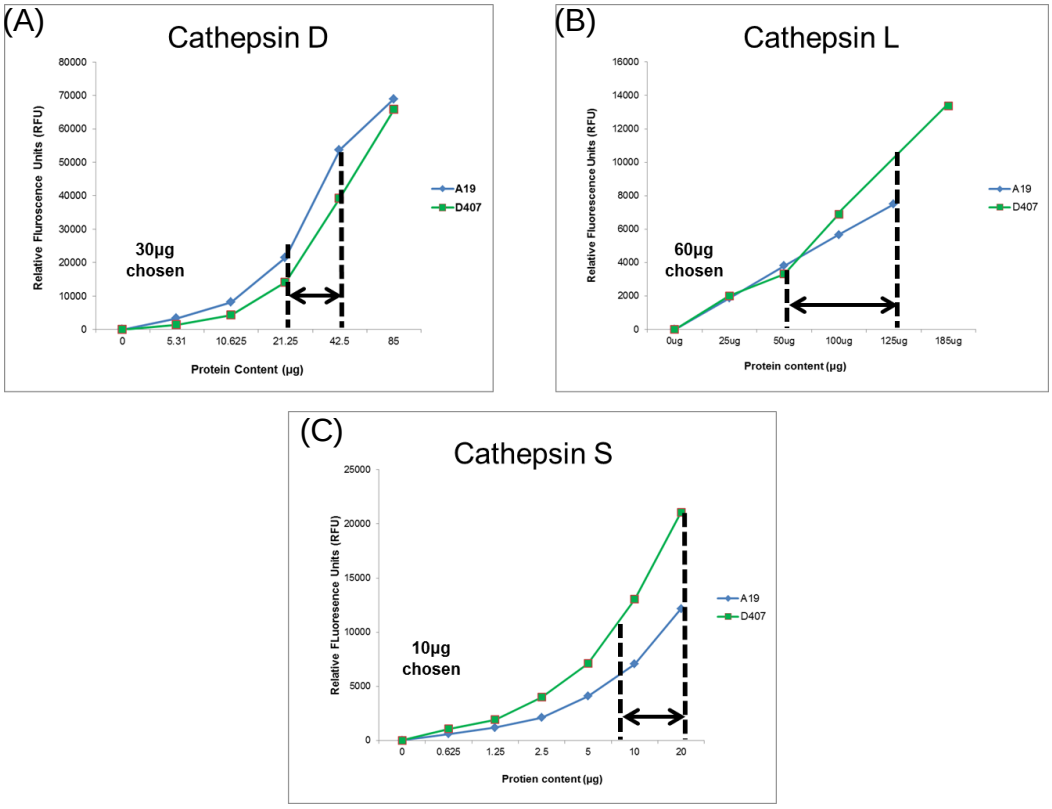

Figure 3.24: Optimisation of appropriate protein concentrations to be used in Cathepsin D, L and S activity assays. Cathepsin activity levels measured in ARPE-19 and D407 cell lysates over a range of different protein amounts to determine the linear range of each kit. Areas that are outlined are regions of linear range from which protein amounts used in experiments were determined. (A) Cathepsin D (B) Cathepsin L (C) Cathepsin S.

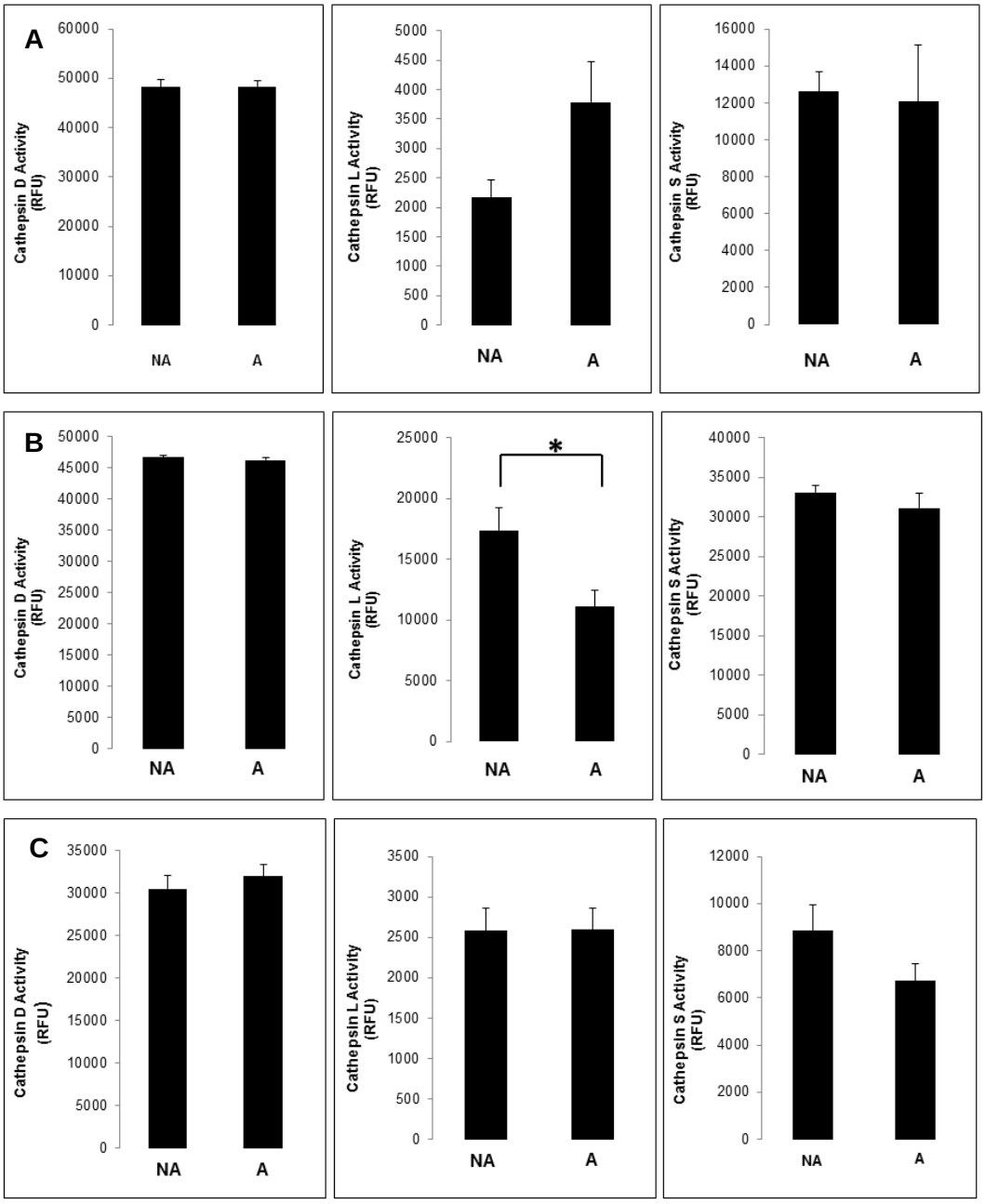

Figure 3.25: Cathepsin D, L and S activity measurement in RPE cells cultured on control MG™ or AGEs-modified MG™ for 1/2 weeks. (A) ARPE-19 cells cultured for 1 week (B) ARPE-19 cells cultured for 2 weeks (C) D407 cells cultured for 1 week. Average values of 6 technical replicates from 3 independent experiments followed by subtraction of value obtained for buffer only samples ± S.E.M. Independent t test, *=$p<0.05$.

3.2.6 – LC3-II protein expression levels were decreased in ARPE-19 cells cultured on AGEs-modified MG™ for 2 week.

Having observed differences at a morphological and expression level between ARPE-19 cells and D407 cells and due to the previous evidence pointing towards D407 being, at least in part, an inappropriate model for functional RPE, it was decided not to proceed with the use of these cells for further functional experiments. In addition, due to the observation that cathepsin L protein and activity levels significantly decreased in ARPE-19 cells exposed to AGEs for 2 weeks, this experimental model was used in the following related experiments.

Being a potent lysosomal protease, a decrease in cathepsin L protein and activity levels may affect the autophagy process (Dennemarker et al., 2010; Sun et al., 2013). The next step of this study focused on whether AGEs exposure affects the autophagy process in ARPE-19 cells. Autophagy alterations observed in ARPE-19 cells exposed to AGEs may, in part, be attributed to alterations in cathepsin L levels.

In order to measure autophagy, the immunoblot analysis of the autophagy marker, microtubule-associated protein light chain (LC3) protein was performed (Mizushima and Yoshimori, 2007). The conversion of LC3-I to LC3-II, due to lipidation, correlates well with the number of autophagosomes present and therefore can be measured in immunoblot analysis to give an indication of whether autophagy is being altered in experimental conditions.

Due to LC3-II being more sensitive for detection by immunoblotting, a comparison between LC3-I and LC3-II and ratio calculations may not be appropriate for monitoring autophagy (Mizushima and Yoshimori, 2007). Rather, the amount of LC3-II is better used as a comparison between the control and test samples. On the immunoblot, LC3-II migrates quicker than LC3-I on the SDS-gel due to lipidation making LC3-II more hydrophobic. Therefore, the lower band at approximately 14kDa is LC3-II with LC3-I detected around the 16kDa mark (Mizushima and Yoshimori, 2007). In this present study, immunoblot analysis detected bands at ~14kDa and ~16kDa in ARPE-19 samples corresponding to both LC3-II and LC3-I respectively

(Figure 3.26). Interestingly, levels of LC3-II were significantly decreased (~74% decrease) in RPE cells exposed to AGEs compared to controls ($p = 0.02$, $n = 2$).

Measurement of LC3-II alone does not measure autophagy flux as a decrease in LC3-II could either mean an increase in autophagy flux due to LC3-II degradation by autophagy or impaired autophagy initiation leading to a lack of autophagosome formation. Nevertheless, as levels of LC3-II do change, the result highlights that AGEs are affecting the autophagy process, which may partly be attributed to the decrease in cathepsin L observed in RPE cells after AGEs exposure.

(A)

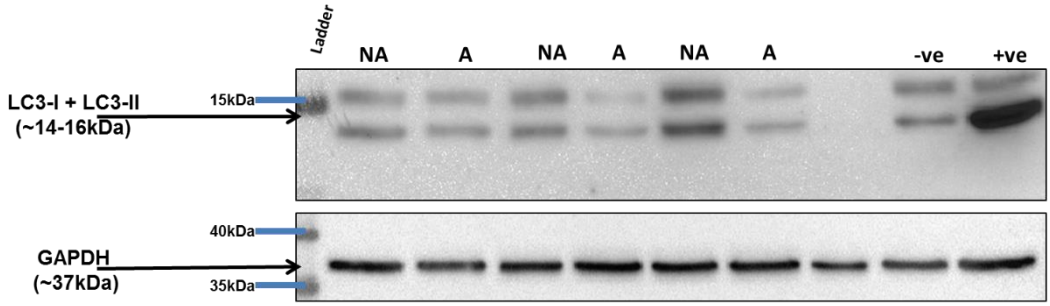

(B)

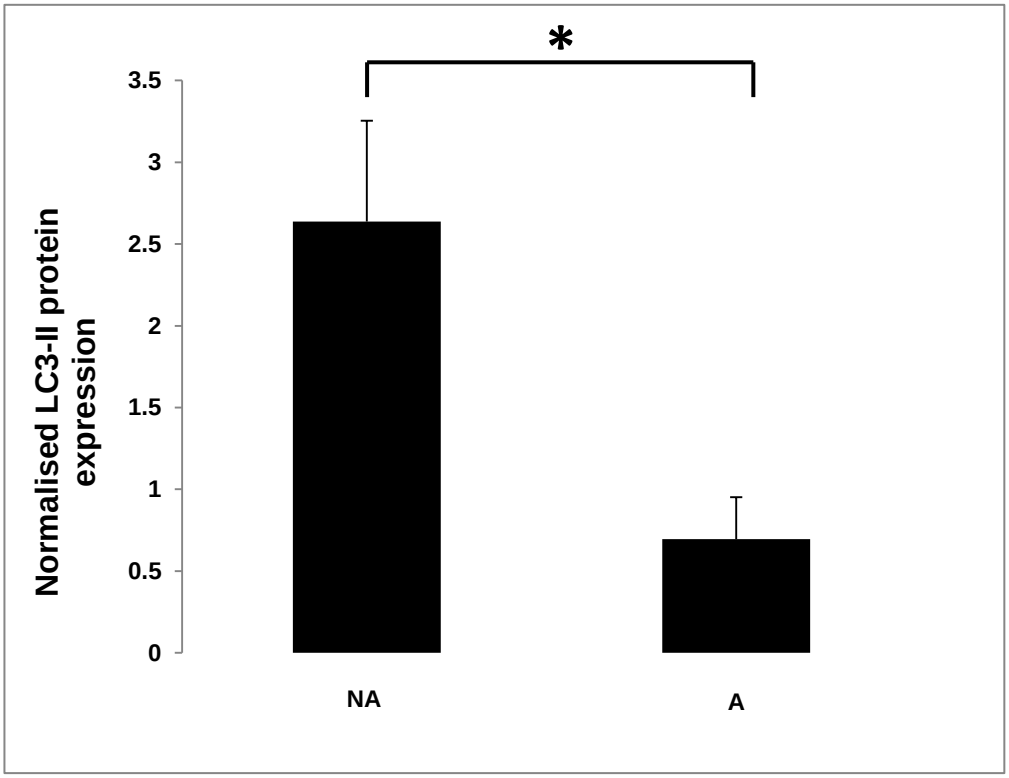

Figure 3.26: Immunodetection of LC3 protein expression in ARPE-19 cells cultured on control MG™ or AGEs-modified MG™ for 2 week. (A) Immunoblot of cell lysates probed with anti-LC3B (D11) (Cell Signalling, 3868, 1:500) detected bands of LC3 proteins. GAPDH (Abcam, ab8245, 1:30000) immunoblotting detection was used as a loading control. ARPE-19 cells from 3 separate untreated (NA) and 3 separate AGEs (A) treated wells are shown. Hela cells were used as controls (-ve = untreated; +ve = Hela + 50μM lysosomal inhibitor chloroquine overnight treatment). (B) Average normalised LC3-II protein expression (arbitrary units) ± S.E.M. for all samples tested (n=2 with a minimum of 6 technical replicates for each condition). Independent t test, *= p≤ 0.05.

3.2.7 – NF-κB p65 and NF-κB Ser536 protein expression levels were decreased in ARPE-19 cells cultured on AGEs-modified MG™ for 2 week.

As cathepsin L contributes to regulation of NF-κB activity, alterations of this enzyme could influence NF-κB activity (Tang et al., 2009; Wang et al., 2013; Xiang et al., 2011). NF-κB p65 is a subunit of the NF-κB complex, which is usually found in the cytoplasm bound to inhibitory proteins, the IκBs i.e. IκB-α (Sakurai et al., 1999). In the process of NF-κB activation, IκB proteins are phosphorylated and targeted for degradation. In addition, NF-κB p65 is phosphorylated on a serine residue at position 536 (Ser536) in the transactivation domain prior to nuclear translocation (Sakurai et al., 1999). Therefore, the next part of the study sought out to investigate the effects of AGEs on protein expression of NF-κB p65 and phosphorylated NF-κB p65 Ser536 along with the NF-κB inhibitor IκB-α in ARPE-19 cells.

Initially, analysis of two independent experiments showed decreased NF-κB p65, NF-κB p65 Ser536 and IκB-α protein levels in APRE-19 cells exposed to AGEs when compared to control cells. Further independent experiments carried out subsequently by another PhD student in the laboratory Nur Musfirah Mahmud showed the same trend in that a decrease in NF-κB p65, NF-κB Ser536 and IκB-α protein levels were observed. Analysis of the collated data showed that the decrease observed for NF-κB p65 (~62% decrease) and NF-κB Ser546 (~47% decrease) were significant ($p = 0.0004$ and $p = 0.03$ respectively, $n = 4$) (Figures 3.27 and 3.28 respectively). This suggests overall decreased NF-κB activity.

For IκB-α immunoblotting, 3 bands of approximately 25kDa, 35kDa and 37kDa were detected (Figure 3.29). In line with the datasheet and the positive controls used (HeLa cell lysates -/+ TNF- α), the band of 37kDa most likely corresponded to IκB-α, with the other two detected bands possible post-translational modifications or non-specific bands. Analysis of the collated data for IκB-α showed protein levels (37kDa) significantly decreased in APRE-19 cells exposed to AGEs compared to control cells (~31% decrease, $p = 0.02$, $n = 3$).

(A)

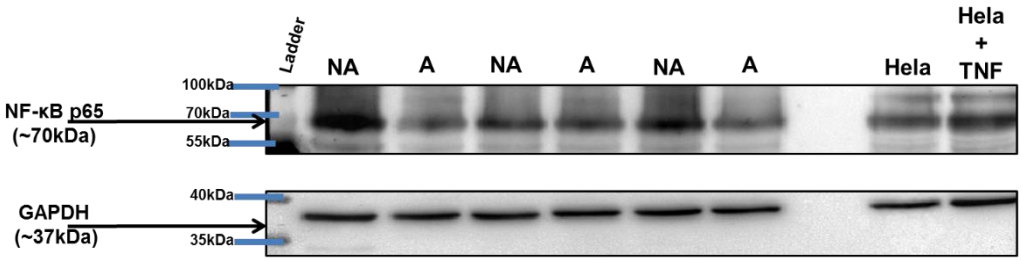

(B)

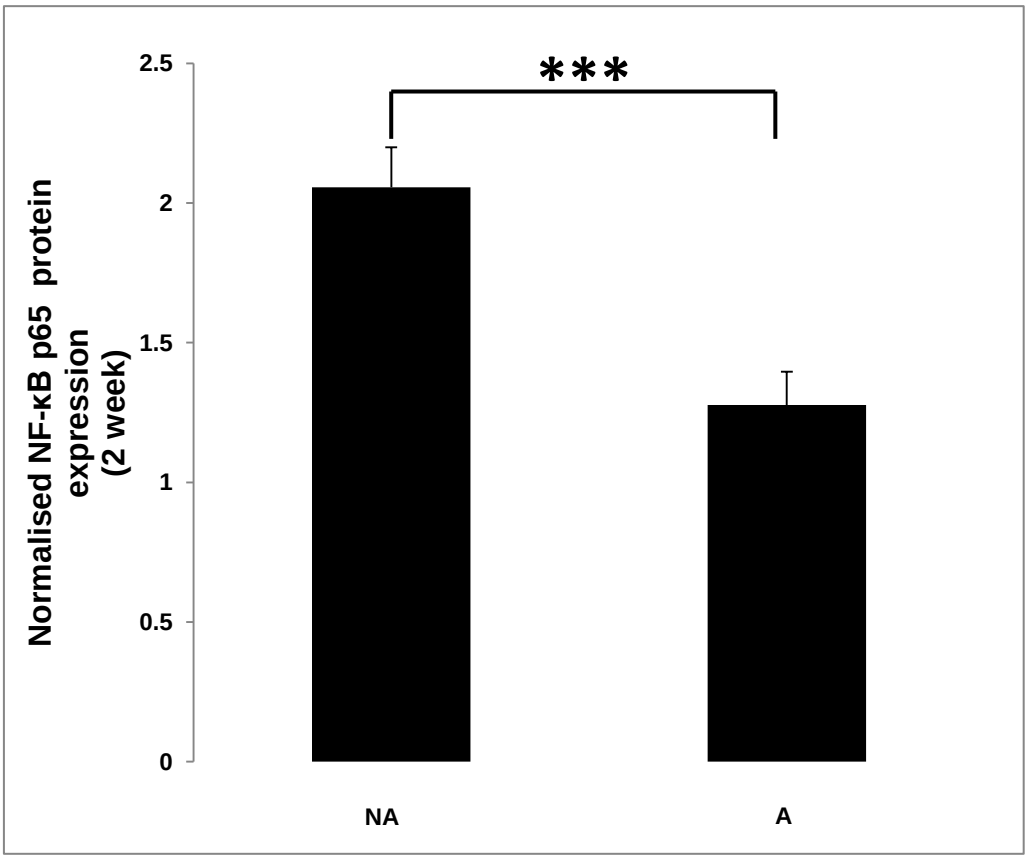

Figure 3.27: Immunodetection of NF-κB p65 protein expression in ARPE-19 cells cultured on control MG™ or AGEs-modified MG™ for 2 week. (A) Immunoblot of cell lysates probed with anti- NF-κB p65 (Abcam, ab16502, 1:500) detected a band of NF-κB p65 protein. GAPDH (Abcam, ab8245, 1:30000) immunoblotting detection was used as a loading control. ARPE-19 cells from 3 separate untreated (NA) and 3 separate AGEs (A) treated wells are shown. Hela cells were used as positive controls. (B) Average normalised NF-κB p65 protein expression (arbitrary units) ± S.E.M. for all samples tested (n=4 with a minimum of 12 technical replicates for each condition). Independent t test, ***= p≤ 0.001.

(A)

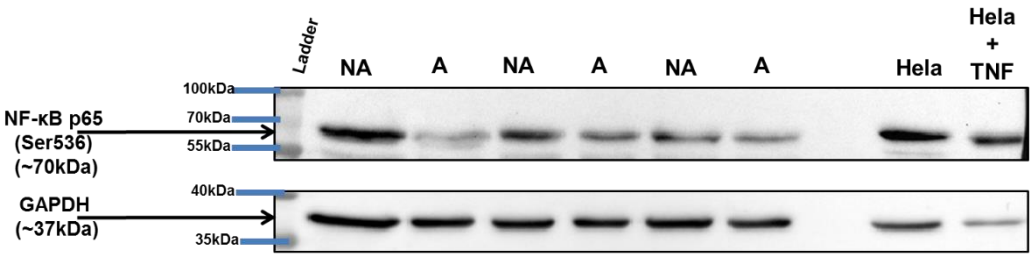

(B)

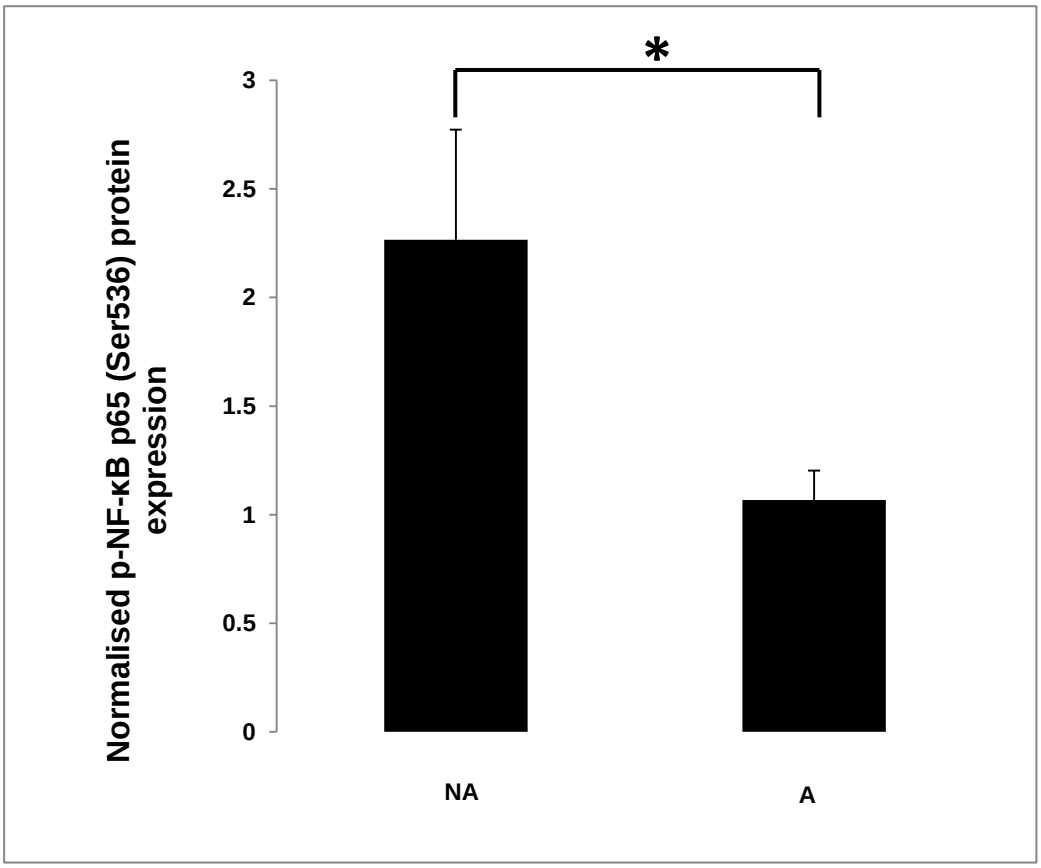

Figure 3.28: Immunodetection of NF-κB p65 (Ser536) protein expression in ARPE-19 cells cultured on control MG™ or AGEs-modified MG™ for 2 week. (A) Immunoblot of cell lysates probed with anti- NF-κB p65 (Cell Signalling, 93H1, 1.500) detected a band of NF-κB p65 (Ser536) protein. GAPDH (Abcam, ab8245, 1: 30000) immunoblotting detection was used as a loading control. ARPE-19 cells from 3 separate untreated (NA) and 3 separate AGEs (A) treated wells are shown. Hela cells were used as positive controls. (B) Average normalised NF-κB p65 (Ser536) expression (arbitrary units) ± S.E.M. for all samples tested (n=4 with a minimum of 12 technical replicates for each condition). Independent t test, *=p <0.05.

(A)

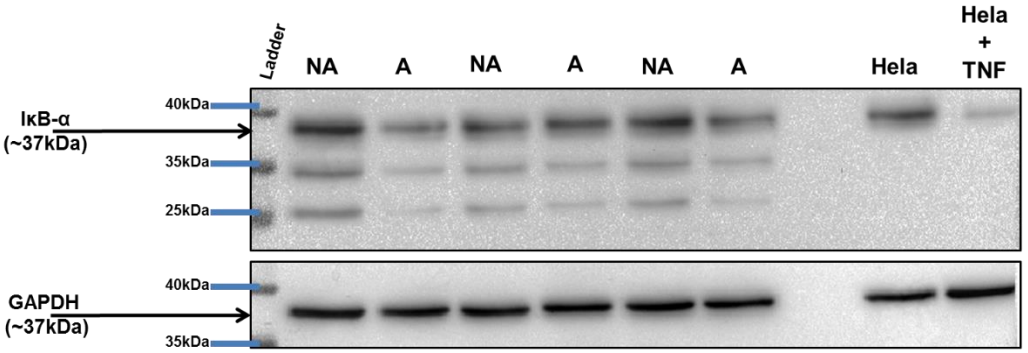

(B)

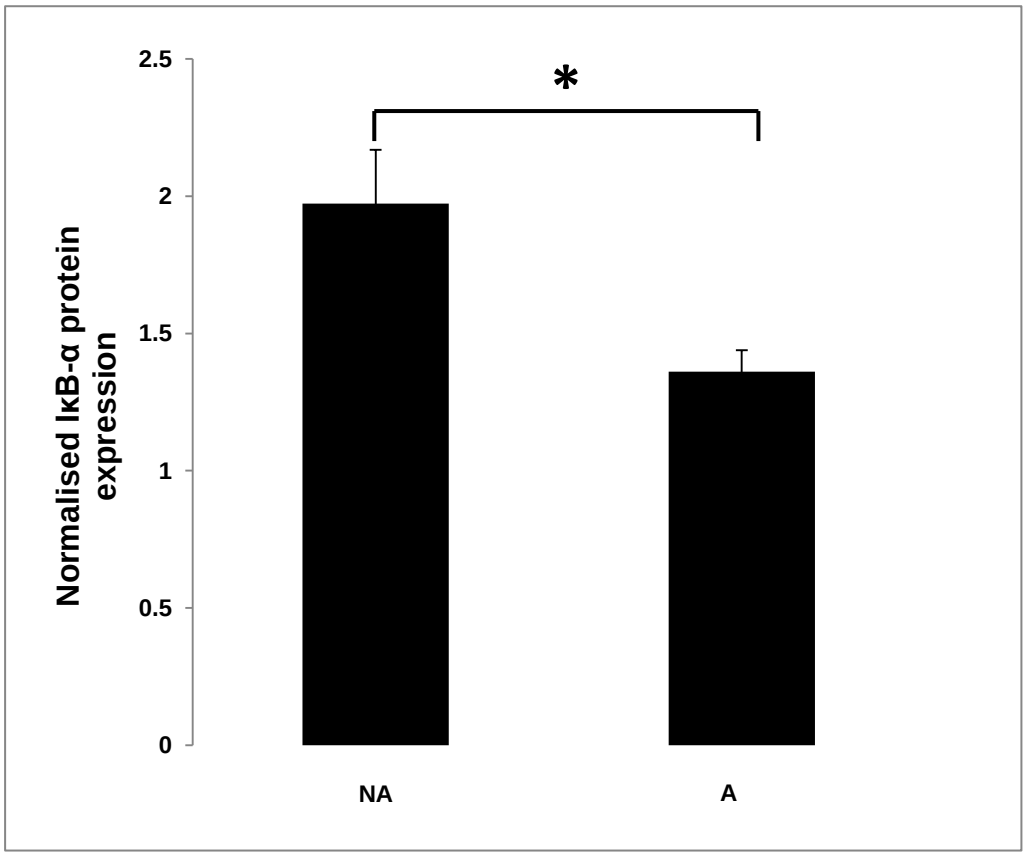

Figure 3.29: Immunodetection of IκB-α protein expression in ARPE-19 cells cultured on control MG™ or AGEs-modified MG™ for 2 week. (A) Immunoblot of cell lysates probed with anti- IκB-α (Abcam, ab32518 [E150], 1:500) detected bands of IκB-α protein. GAPDH (abcam, ab8245, 1:30000) immunoblotting detection was used as a loading control. ARPE-19 cells from 3 separate untreated (NA) and 3 separate AGEs (A) treated wells are shown. Hela cells were used as positive controls. (B) Average normalised IκB-α expression (arbitrary units) ± S.E.M. for all samples tested (n=3 with a minimum of 9 technical replicates for each condition). Independent t test, *=p <0.05.

3.3 – Effects of Hydrogen Peroxide (H_2O_2)-induced stress on cathepsins expression, processing and activity in RPE cells

Oxidative stress and free radical damage to the RPE contributes to AMD pathogenesis (Jarrett and Boulton, 2012). This study was conducted to assess the effects of H_2O_2-induced oxidative stress on cathepsins protein expression/processing and activity in RPE cells.

3.3.1 – Cell Viability Assay determined that H_2O_2 concentrations of 200µM and above caused significant cell death to ARPE-19 cells.

MTT assay was used to measure cell viability of ARPE-19 cells treated with different concentrations of H_2O_2, specifically 0µM, 50µM, 100µM, 200µM, 500µM, for 24 hours. ARPE-19 cells treated with 200µM H_2O_2 or higher showed significant decrease in cell viability (Figure 3.30). Cells treated up to 100µM cell have good structure and maintained integrity whereas in cells treated with concentration of 200µM upwards, a loss of cell integrity and structure was observed. This finding was in line with a previous study in which H_2O_2 concentrations equal to or higher than 200µM were lethal to ARPE-19 cells (Kim et al., 2010). The same study also measured intracellular ROS levels after H_2O_2 treatment of ARPE-19 showing that anything above concentrations of 50µM induced significant increase in ROS levels in ARPE-19 cells compared to control cells (Kim et al., 2010).

Given that ROS accumulation occurs over concentration of 50µm of H_2O_2 (Kim et al., 2010) and concentration of up to 100µm resulted in no significant cell death (Figure 3.30B), the concentration chosen for further experiments was 100µm.

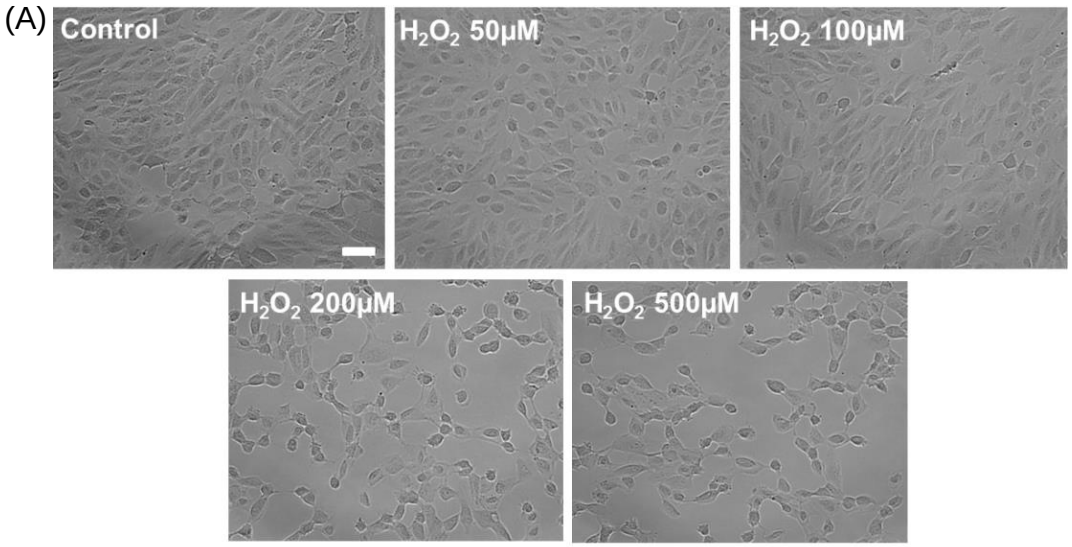

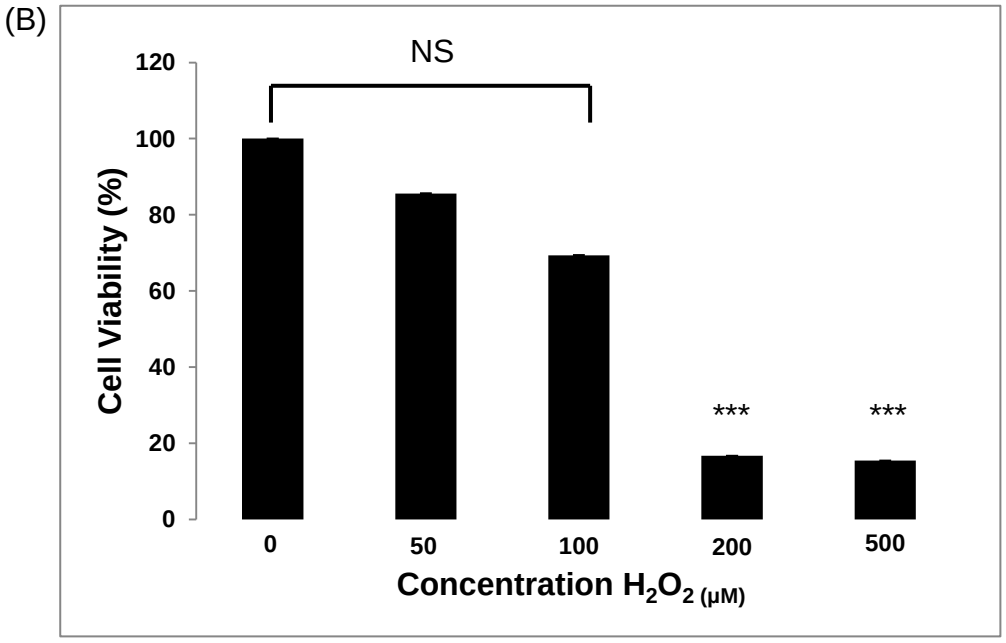

Figure 3.30: APRE-19 cells treated with 0-500µM H2O2 for 24 hours. (A) ARPE-19 cells treated with 0-500µM H_2O_2 treatment for 24h hours (B) Cell viability was measured in ARPE-19 cells treated with different concentrations of H_2O_2 by MTT assay. Each value is representative of the mean ± S.E.M of one independent experiment with a minimum of 4 technical replicates. One way ANOVA followed by Tukey's Post Hoc Test, *= $p < 0.05$, *** = $p < 0.001$. Scale bar represents 50µm.

3.3.2 – No significant changes of cathepsins B, D, L and S protein levels were observed in ARPE-19 cells treated with 100µM H2O2 for 24 hours

Western blotting analysis was carried out to determine how H_2O_2-induced stress affected cathepsins B, D, L and S protein levels. Initially, GAPDH levels were analysed in order to see if GAPDH was susceptible to alterations due to H_2O_2-induced stress. GAPDH levels were normalised against Ponceau S stain densitometric values and the result showed that there were no significant changes in protein levels in stressed samples compared to control (Figure 3.31). Therefore, for all remaining experiments, GAPDH was used as an appropriate loading control.

ARPE-19 treated with H_2O_2 did not cause any significant changes in protein expression for all cathepsins tested. For cathepsin B, two active forms (24kDa and 27kDa) were detected and did not alter under stressed conditions (n= 3) (Figure 3.32). For cathepsin D a band of 28kDa was detected corresponding to the active form and showed no changes under the stressed conditions (n = 3) (Figure 3.33). Cathepsin L active form band was detected (26kDa) and was not altered under stressed conditions (n =3) (Figure 3.34). For cathepsin S, two proform bands (36kDa and 37kDa) as well as an active form band (24kDa) were detected. The total proform and the active form of cathepsin S did not change after cells were stressed (n =3) (Figure 3.35).

(A)

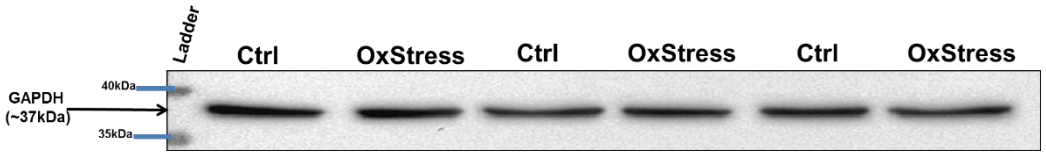

(B)

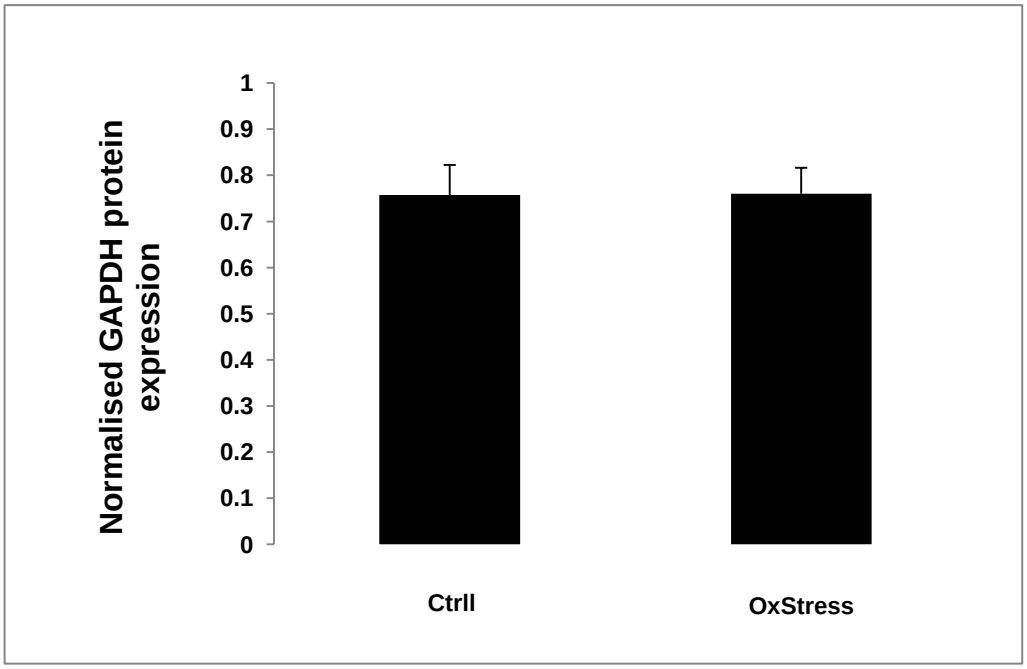

Figure 3.31: Immunodetection of GAPDH protein expression in ARPE-19 cells treated with 100μM H2O2. (A) Immunoblot of cell lysates probed with anti-GAPDH (Abcam, ab8245, 1:30000) detected a band for GAPDH protein. ARPE-19 cells from 3 separate untreated (Ctrl) and 3 separate treated (OxStress) treated wells are shown. Hela cells were used as positive controls. (B) Average normalised GAPDH expression (arbitrary units) ± S.E.M. for all samples tested (n=3 with a minimum of 9 technical replicates for each condition).

(A)

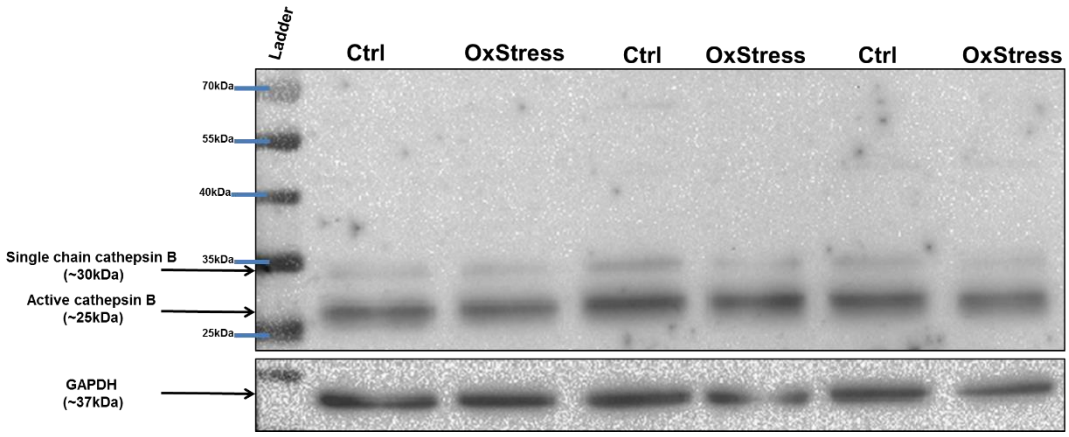

(B)

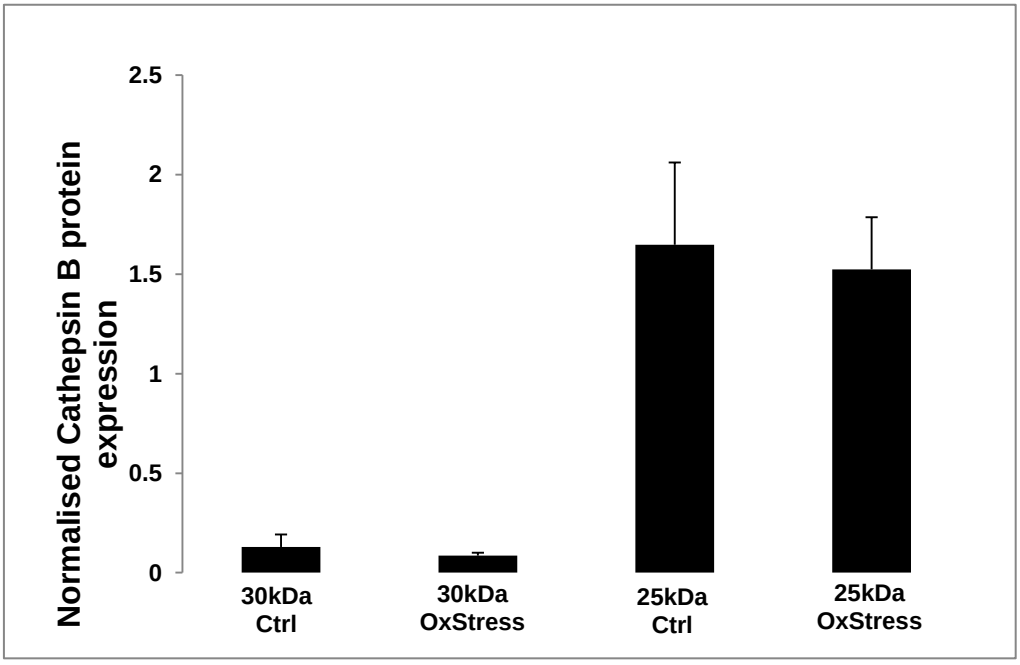

Figure 3.32: Immunodetection of cathepsin B protein expression in ARPE-19 cells treated with 100µM H2O2. (A) Immunoblot of cell lysates probed with anti-cathepsin B (Abcam, ab38558, 1:500) detected different forms of cathepsin B. GAPDH (Abcam, ab8245, 1:30000) immunoblotting detection was used as a loading control. ARPE-19 cells from 3 separate untreated (Ctrl) and 3 separate treated (OxStress) wells are shown. (B) Average normalised cathepsin B expression (arbitrary units) ± S.E.M. for all samples tested (n=2 with a minimum of 6 technical replicates for the 30kDa form; n=3 with a minimum of 9 technical replicates for 25kDa).

(A)

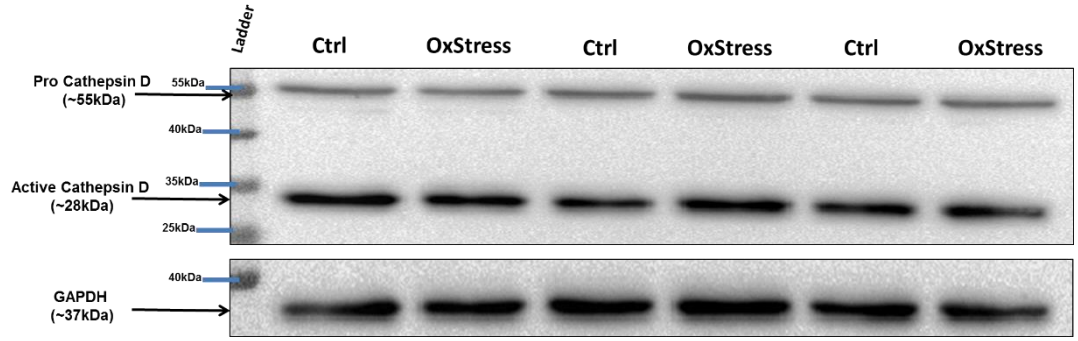

(B)

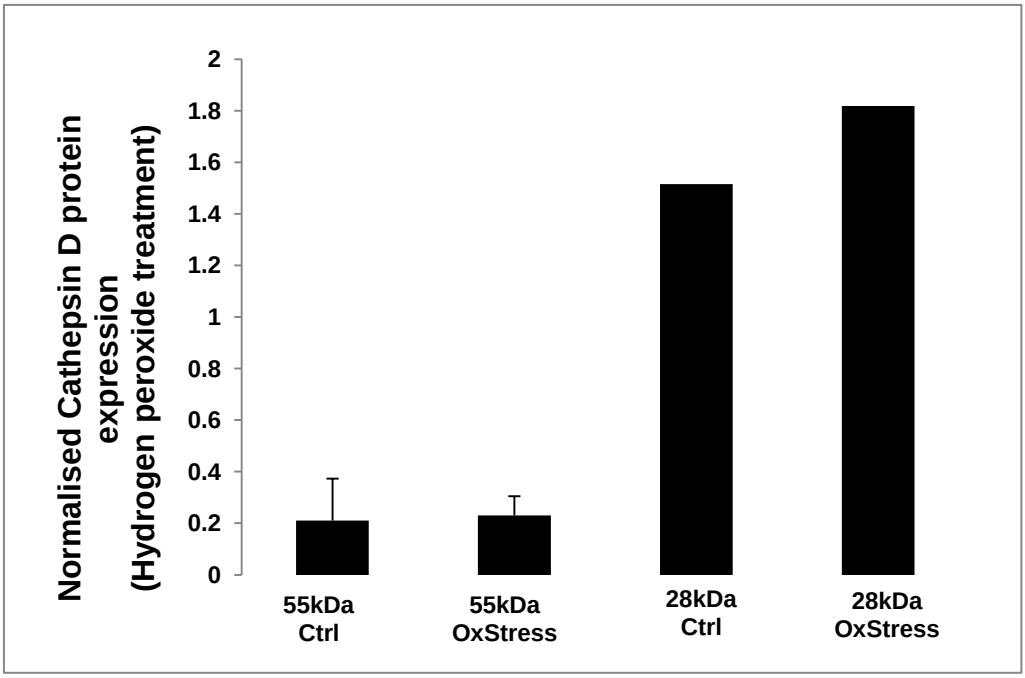

Figure 3.33: Immunodetection of cathepsin D protein expression in ARPE-19 cells treated with 100µM H2O2. (A) Immunoblot of cell lysates probed with anti-cathepsin D (BD Biosciences, 610800, 1:500) detected inactive and active forms of cathepsin D. GAPDH (abcam, ab8245, 1:30000) immunoblotting detection was used as a loading control. ARPE-19 cells from 3 separate untreated (Ctrl) and 3 separate treated (OxStress) wells are shown. (B) Average normalised cathepsin D expression (arbitrary units) ± S.E.M. for all samples tested (n=3 with a minimum of 9 technical replicates for each condition).

(A)

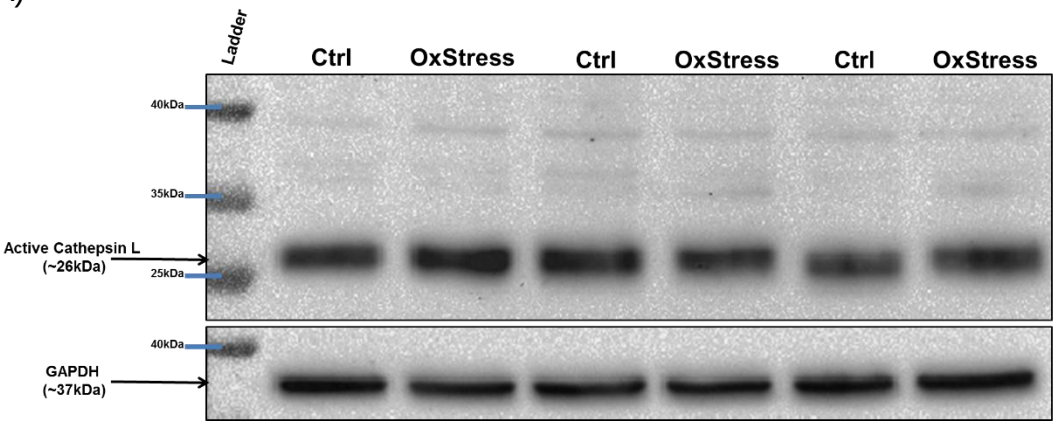

(B)

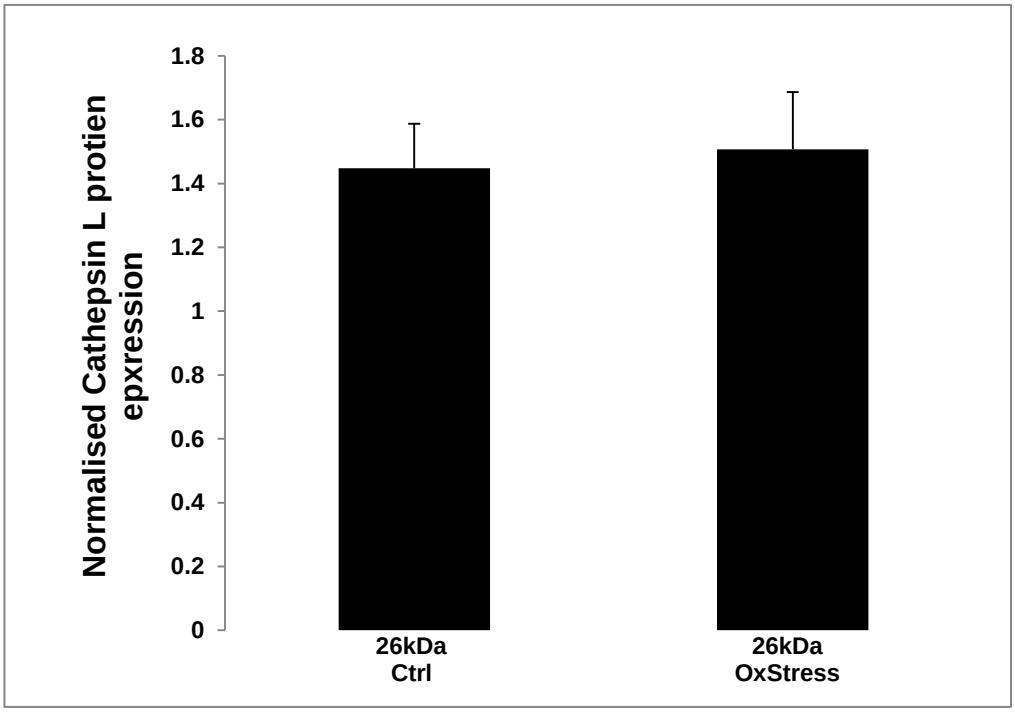

Figure 3.34: Immunodetection of cathepsin L protein expression in ARPE-19 cells treated with 100µM H2O2. (A) Immunoblot of cell lysates probed with anti-cathepsin L (Abcam, ab6314, 1:500) detected an active form of cathepsin L. GAPDH (Abcam, ab8245, 1:30000) immunoblotting detection was used as a loading control. ARPE-19 cells from 3 separate untreated (Ctrl) and 3 separate treated (OxStress) wells are shown. (B) Average normalised cathepsin L expression (arbitrary units) ± S.E.M. for all samples tested (n=3 with a minimum of 9 technical replicates for each condition).

(A)

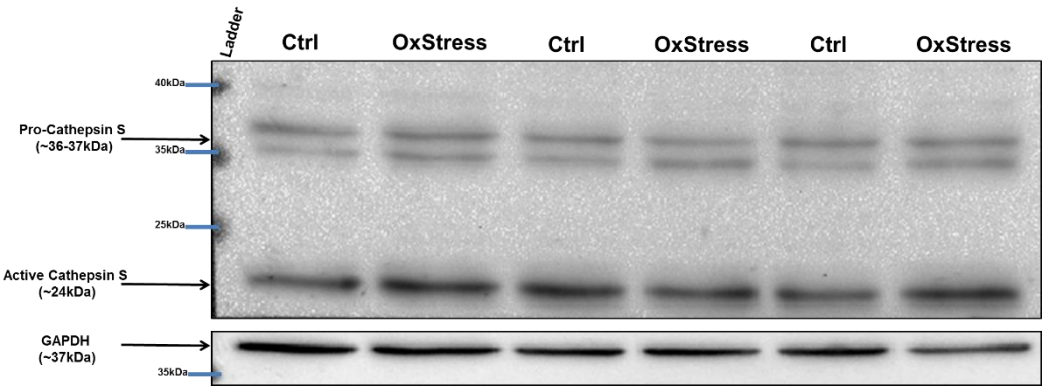

(B)

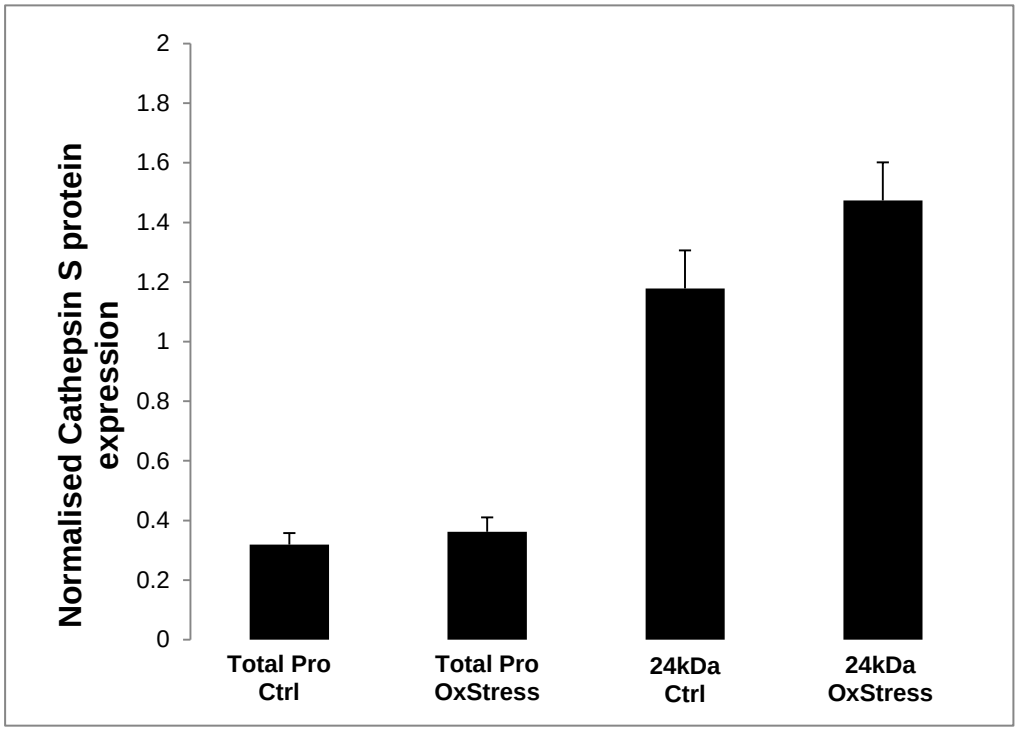

Figure 3.35: Immunodetection of cathepsin S protein expression in ARPE-19 cells treated with 100μM H2O2. (A) Immunoblot of cell lysates probed with anti-cathepsin S (Abcam, ab92780, 1.500) detected inactive and active forms of cathepsin S. GAPDH (Abcam, ab8245, 1:30000) immunoblotting detection was used as a loading control. ARPE-19 cells from 3 separate untreated (Ctrl) and 3 separate treated (OxStress) wells are shown. (B) Average normalised cathepsin S expression (arbitrary units) ± S.E.M. for all samples tested (n=3 with a minimum of 9 technical replicates for each condition).

3.3.3 – No significant changes of cathepsins D, L and S activity levels were observed in ARPE-19 cells treated with 100µM H_2O_2 for 24 hours.

Activity levels of cathepsins D, L and S was measured in APRE-19 cells subjected to H_2O_2 treatment. Results showed that no significant changes were observed in the activity levels of cathepsins D, L and S in ARPE-19 cells treated with 100µM H_2O_2 for 24 hours compared to untreated control cell (Figure 3.36). Therefore, the observed data indicates that all cathepsins tested, at protein and activity levels, were not susceptible to H_2O_2-induced oxidative stress alterations.

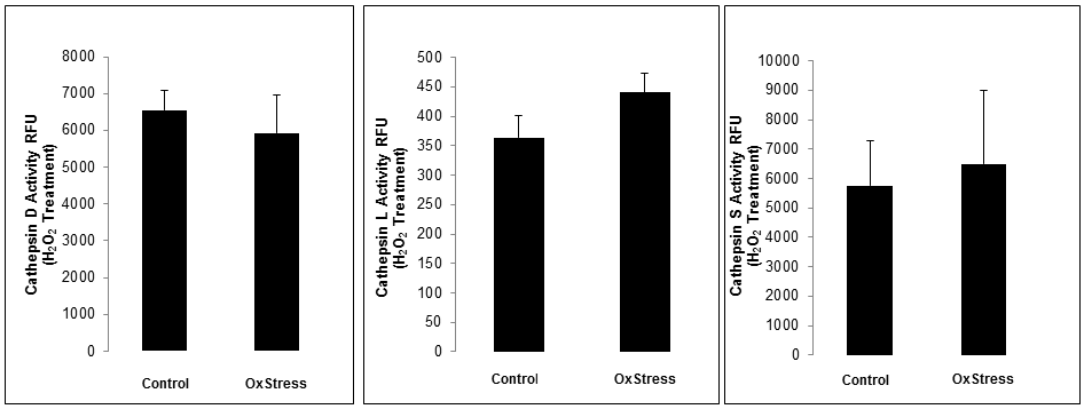

Figure 3.36: Measurement of cathepsin activity in control ARPE-19 cells and ARPE-19 cells treated with 100µM H2O2. From left, the three graphs show cathepsin D, cathepsin L and cathepsin S activity measurement in untreated ARPE-19 cells (control) compared against ARPE-19 cells treated with 100µM H2O2 (OxStress) for 24 hours respectively. Averaged values of 6 technical replicates from 3 independent experiments followed by subtraction of value obtained for buffer only samples.

3.4 – Immunohistochemistry and image analysis of cathepsin L protein in human RPE cells in relation to region and age.

Regional variation and age-related changes of lysosomal enzymes such as cathepsin D has been previously demonstrated in RPE cells (Boulton et al., 1994). Having shown by *in vitro* analysis of RPE cell lines, that age-related stresses i.e. AGEs exposure, resulted in alterations of protein and activity levels of cathepsin L, the next focus of this present study was to investigate whether cathepsin L showed regional and age-related variation in *ex vivo* human RPE cells samples. For this analysis, sections containing RPE derived from human donor eyes from different ages were investigated for cathepsin L immunoreactivity.

3.4.1 – All donor eye sections showed positive cathepsin L immunoreactivity within the posterior and peripheral RPE regions

All eyes used in this study were age-masked to help minimise bias and were identified only upon their specimen number. Eyes that were included in this study has no history of ocular disease, had been retrieved and placed in fixation within 48 hours after death. The relative cathepsin L protein concentration in posterior and peripheral RPE cells of each donor was examined by automated densitometric analysis. ImageJ 1.47v analysis software was used to generate densitometric average grey-scale values of the stained donor eye which were then compared.

A total of 32 eyes were used in this study, of which 14 were aged ≤ 65 years old and 18 were > 65 years old. The age range for the donors was 35-91 years with a median of 56.5 for the ≤ 65 year group and 81 for the > 65 group (Table 3.3 – donor eye information). Immunohistochemistry staining of the 32 eyes was performed over four separate runs (First run: Specimens 1-8; second run: Specimens: 9-16; third run: Specimens 17-27; fourth run: Specimens: 28-32). All 32 samples tested showed the presence of cathepsin L, with varying amount of staining observed. An example of the immunohistochemistry staining of the specimens from the first run is shown below (Figure 3.37).

Table 3.3: Information of donor eyes used in the present study

Reference No for identification in this study	EOU Specimen reference No:	Age of donor (years)
1	EOU217	35
2	EOU104	85
3	EOU131	58
4	EOU134	71
5	EOU139	72
6	EOU179	60
7	EOU211	75
8	EOU213	71
9	EOU221	91
10	EOU234	64
11	EOU248	66
12	EOU253	65
13	EOU256	61
14	EOU288	81
15	EOU293	82
16	EOU406	54
17	EOU505	81
18	EOU509	55
19	EOU568	88
20	EOU570	63
21	EOU573	79
22	EOU575	88
23	EOU577	82
24	EOU580	55
25	EOU711	55
26	EOU758	46
27	EOU767	61
28	EOU225	78
29	EOU299	84
30	EOU129	50
31	EOU048	72
32	EOU083	81

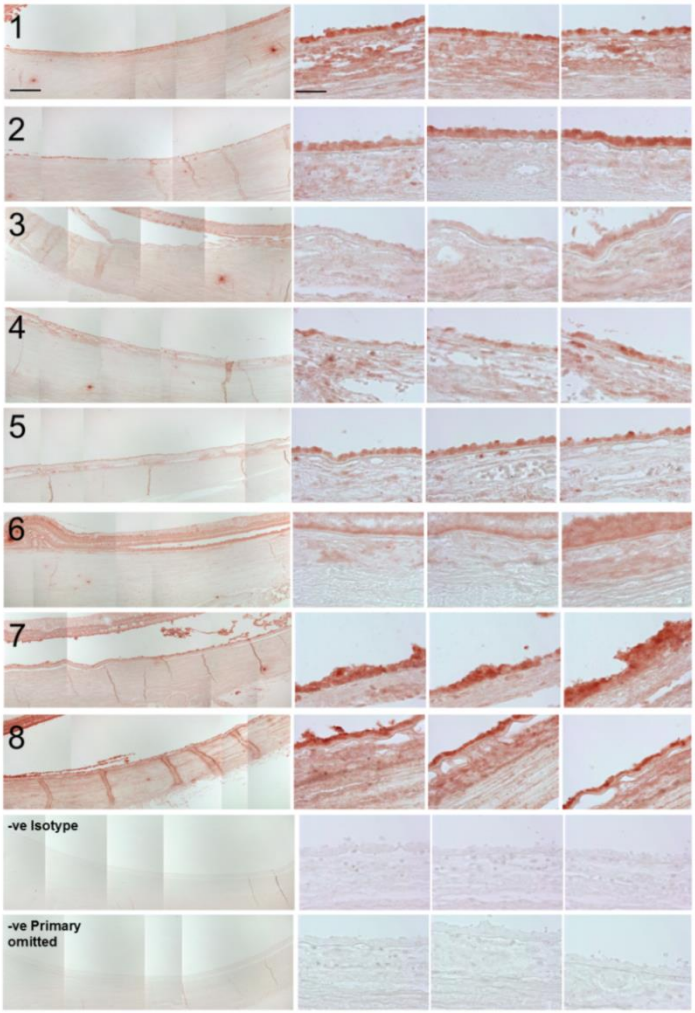

Figure 3.37: Cathepsin L staining for specimen 1-8 in posterior region of RPE from run 1. Paraffin embedded eye sections (4µm) were stained with cathepsin L (Abcam, ab6314, 1:1000) antibody. Negative controls (Isotype and primary antibody omitted) were included in each run. Scale bar for lower magnification images represents 500µm and for higher magnification images represents 50µm respectively.

3.4.2 – Quantitative assessment of cathepsin L protein levels within the posterior and peripheral RPE of donor eyes.

For each eye, 3 images were taken for the posterior region, the left periphery and the right periphery separately. After this, 3 separate areas from each image was analysed hence giving a total of 9 measurements for each region. The overall average grey-scale periphery value was an average of both left and right periphery readings combined. In order to reduce variability

of staining across runs, specimen 1 was included in all runs as an internal control. The average-grey scale value obtained for the posterior region in specimen 1 was normalised to itself to give a reading of 1 and all other readings obtained were expressed relative to this for each individual eye. The average grey-scale value of each region was very similar for each run (Figure 3.38). Therefore, by including an internal control to which all other samples was normalised, it enabled the data generated for the 32 eyes to be brought together for analysis.

(A)

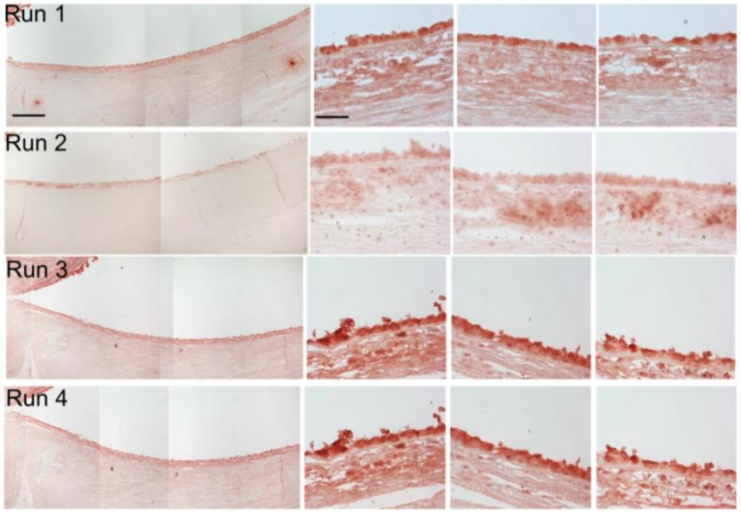

(B)

Run	Specimen	Average Posterior greyscale value	Left Periphery grey-scale value	Right Periphery grey-scale value	Average Periphery grey-scale value
Run 1	EOU217a	1	0.81	0.64	0.73
Run 2	EOU217a	1	0.89	0.69	0.79
Run 3	EOU217a	1	0.78	0.88	0.83
Run 4	EOU217a	1	0.87	0.68	0.77

Figure 3.38: Specimen 1 used in all cathepsin L staining runs as an internal control. (A) Paraffin embedded sections (4µm) were stained with cathepsin L (Abcam, ab6314, 1:1000) antibody. Cathepsin L staining for specimen 1 in posterior region of RPE from each run (B) Table showing normalised average grey-scale values generated from image analysis of donor eye sections immunohistochemically stained for cathepsin L in posterior and peripheral RPE cells. Scale bar for lower magnification images represents 500µm and for higher magnification images represents 50µm respectively.

3.4.3 – Cathepsin L relative protein level were not affected by regional and age-related changes in human RPE cells

Differences between cathepsin L immunostaining within the RPE in relation to the age of the donor and the region of cells were examined. It was observed that the age of the donor appeared to affect the intensity of cathepsin L immunostaining in particular for peripheral RPE cells. A slight decrease of 3.7% (approximately 0.03 normalised grey-scale values) in the peripheral region, as donor age rises from below to above 65 years, was observed. On the other hand it seemed that the posterior RPE cells showed no changes in immunostaining as the age of the donor rises from below to above 65 years of age (Table 3.4).

Table 3.4: Means of overall normalised average grey-scale values for cathepsin L immunostaining in each region of RPE cells in relation to the two different age groups.

	Age-group	
Region of RPE cells	**≤65 years old**	**<65 years old**
Posterior	0.74	0.74
Periphery	0.68	0.65

In addition, the anatomical region of the RPE cells also appeared to effect cathepsin L staining as in both age groups, the posterior RPE cells showed higher staining. To elaborate, for the younger group (≤65 years of age), the posterior showed stronger staining with normalised average grey-scale value approximately 0.06 units higher than in the peripheral region. This difference was slightly greater in the older donors (<65 years of age) where the posterior region had stronger staining, with a normalised average grey-scale value of approximately 0.09 units higher than in the periphery (Table 3.5). To further highlight the differences between the posterior and peripheral cells, the intensity of cathepsin L staining was compared between the two RPE regions (posterior and periphery) for each donor eye. Results showed that for 26 out of the 32 eyes tested, the intensity of cathepsin L staining was

higher in the posterior RPE cells compared to the peripheral RPE cells, with specimens 9, 18, 21, 24, 26 and 31 showing higher intensity for the peripheral RPE cells (Figure 3.39; Table 3.5).

These observations suggested that more cathepsin L protein was present within the posterior RPE cells compared to peripheral RPE cells. In addition, it seemed that peripheral RPE cell cathepsin L levels were more inclined to age-related changes.

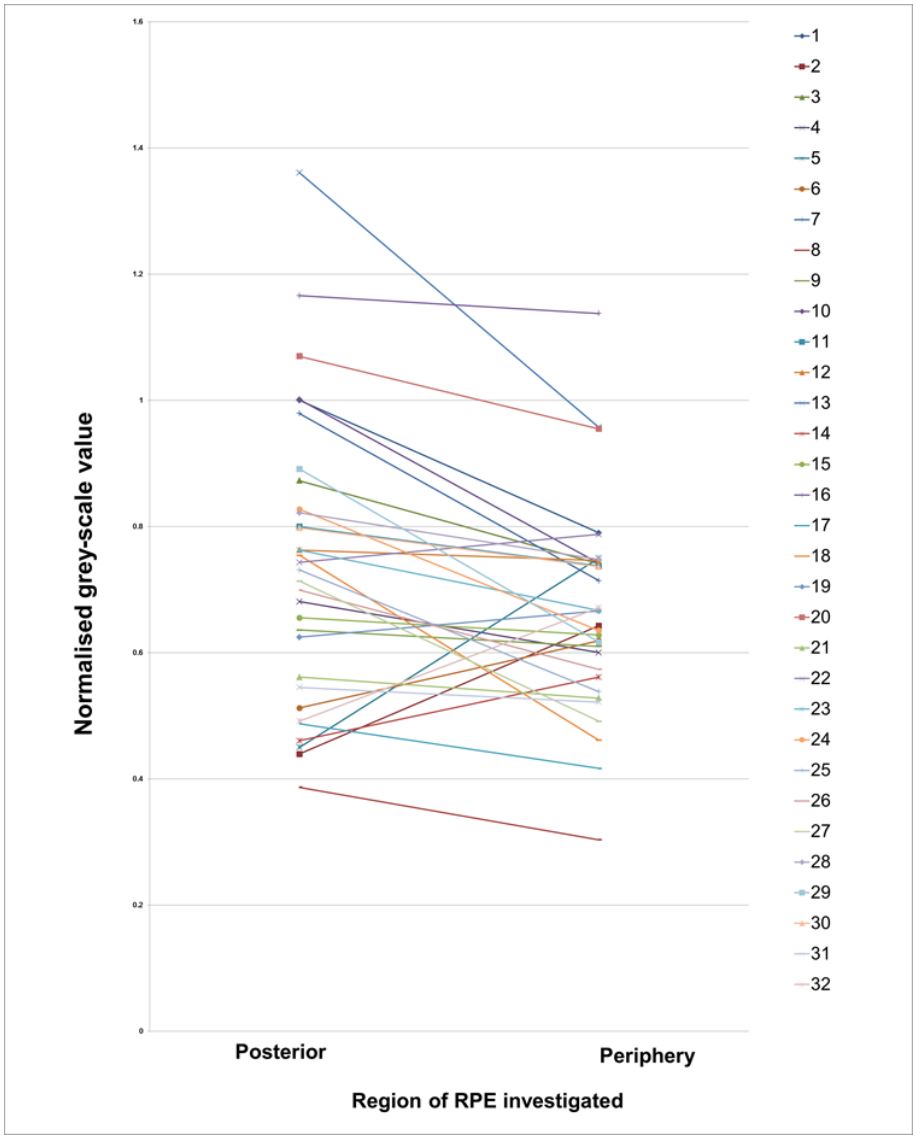

Figure 3.39: Regional differences in cathepsin L staining of RPE cells. Differences in the normalised average-grey scale values of cathepsin L concentration between posterior and peripheral RPE cells for the 32 donor eyes tested. The legend on the right shows the specimen number of each donor.

Table 3.5: Normalised average grey-scale values generated from image analysis for the 32 donor eye sections immunohistochemically stained for cathepsin L in posterior and peripheral RPE cells.

Specimen	Normalised Average grey-scale value (Posterior)	Normalised Average grey-scale value (Periphery)
1	1	0.79
2	0.89	0.62
3	0.39	0.30
4	0.49	0.42
5	0.75	0.46
6	0.64	0.61
7	1.07	0.95
8	1.17	1.14
9	0.49	0.67
10	1.36	0.97
11	0.66	0.63
12	0.46	0.56
13	1.00	0.74
14	0.76	0.67
15	0.70	0.57
16	0.68	0.60
17	0.83	0.64
18	0.45	0.75
19	0.80	0.74
20	0.76	0.75
21	0.74	0.79
22	0.54	0.52
23	0.71	0.49
24	0.51	0.62
25	0.98	0.71
26	0.44	0.64
27	0.80	0.74
28	0.56	0.53
29	0.82	0.75
30	0.87	0.74
31	0.62	0.67
32	0.73	0.54

The trends between cathepsin L staining, region of the donor and age of donor that were observed are displayed below (Figure 3.40). The box plot showed that in younger donors, higher amounts of cathepsin L protein were observed in the peripheral region compared to the older donors. Whereas for

the posterior RPE cells, similar amounts of cathepsin L protein were present for both age groups.

To determine whether the trends observed in relation to region of RPE, age of the donor and the intensity of cathepsin L staining were significant, Two-way Analysis of Variance (ANOVA) statistical method was used.

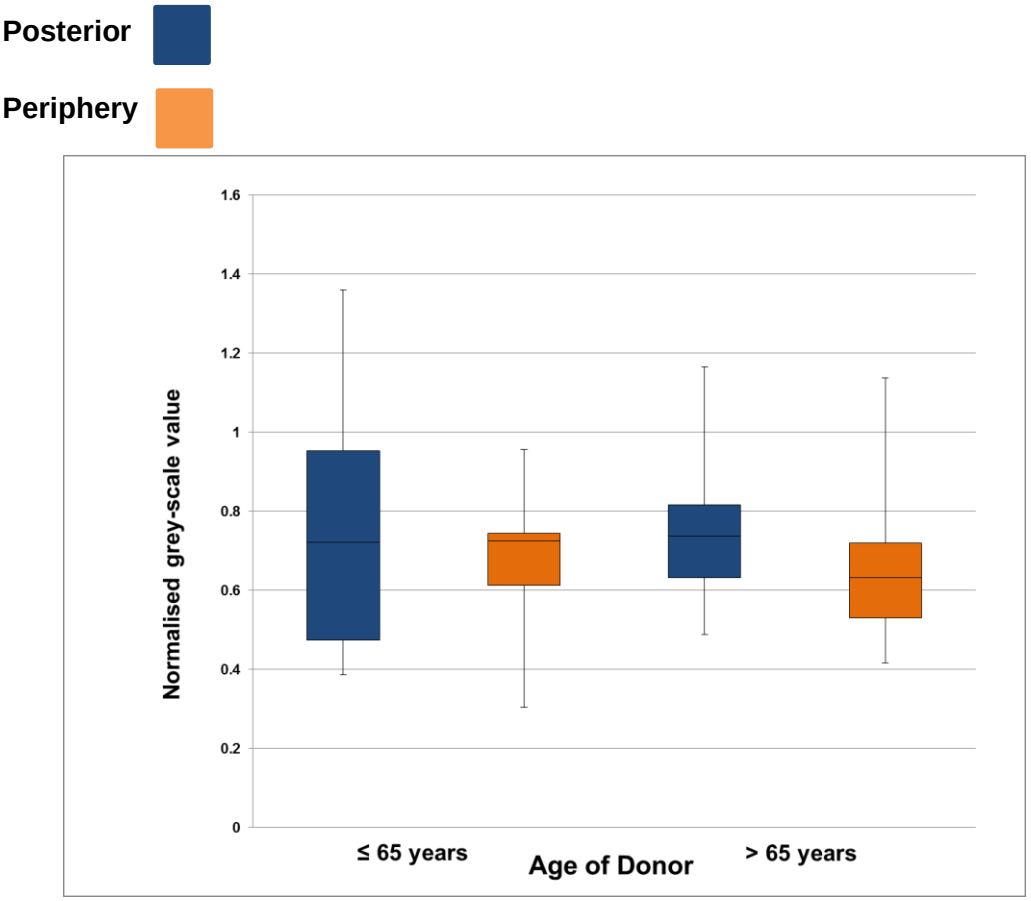

Figure 3.40: Box-plot demonstrating the trends observed in cathepsin L staining intensity in RPE cells. Posterior region (Blue) and peripheral region (orange) of donor eyes were grouped according to age (Younger donors ≤65 years of age, Older donors >65 years of age).

Two-way ANOVA found that the age of the donor had no significant influence on cathepsin L immunostaining ($p = 0.8235$). Also, the region of RPE did not exert any significant influence on the intensity of cathepsin L immunostaining ($p = 0.14$). In addition, no association was seen when looking at the interplay between the region of RPE and age of donor on cathepsin L staining ($p = 0.7849$). Independent t test was also used to further investigate each region separately with the intensity of cathepsin L staining

within each age group. Results showed that the intensity of cathepsin L staining did not significantly alter in RPE cells from posterior and periphery regions, in both younger (p = 0.49) and older donors (p = 0.15)**.** Overall, these findings showed that similar amounts of cathepsin L protein are found throughout the different RPE regions and that age did not alter the amount of cathepsin L present in the eyes tested.

3.4.4 – Cathepsin L relative protein level were not significantly affected by age in posterior and peripheral RPE cells

The relative cathepsin L protein concentration was also plotted against age of donors for both the posterior and periphery regions (Figure 3.41 and Figure 3.42 respectively). A line of best-fit was added to the graphs and a measurement of the coefficient of determination value (R^2). The R^2 is a measurement of how much variability of one factor can be explained by its relationship to another factor.

Analysis of the graphs revealed the existence of a weak negative correlation between cathepsin L levels and increasing age for both the posterior (R^2 = 0.0009) and periphery (R^2 = 0.012) regions of RPE cells. As the R^2 value was greater for the peripheral RPE cells, it showed that the level of cathepsin L protein decreases at a greater extent compared to the posterior. Analysis of the strength of linear association of cathepsin L immunostaining in the RPE cells and the age of donor was carried out using the Pearson's correlation and the Spearman's Rho correlation tests. The Pearson's correlation test assumes that the data has normal distribution, whereas the Spearman's Rho test does not assume normality and instead data is ranked and the strength of linear association is measured. Analysis showed that the negative correlation seen for both posterior and periphery regions were not significant at $p \leq 0.05$ as determined by the Pearson's correlation and Spearman's Rho.

Therefore in conclusion, in the 32 donor eyes analysed, cathepsin L protein levels in the posterior and periphery region showed a weak negative correlation with age. However these correlations were not significantly altered with age in both regions.

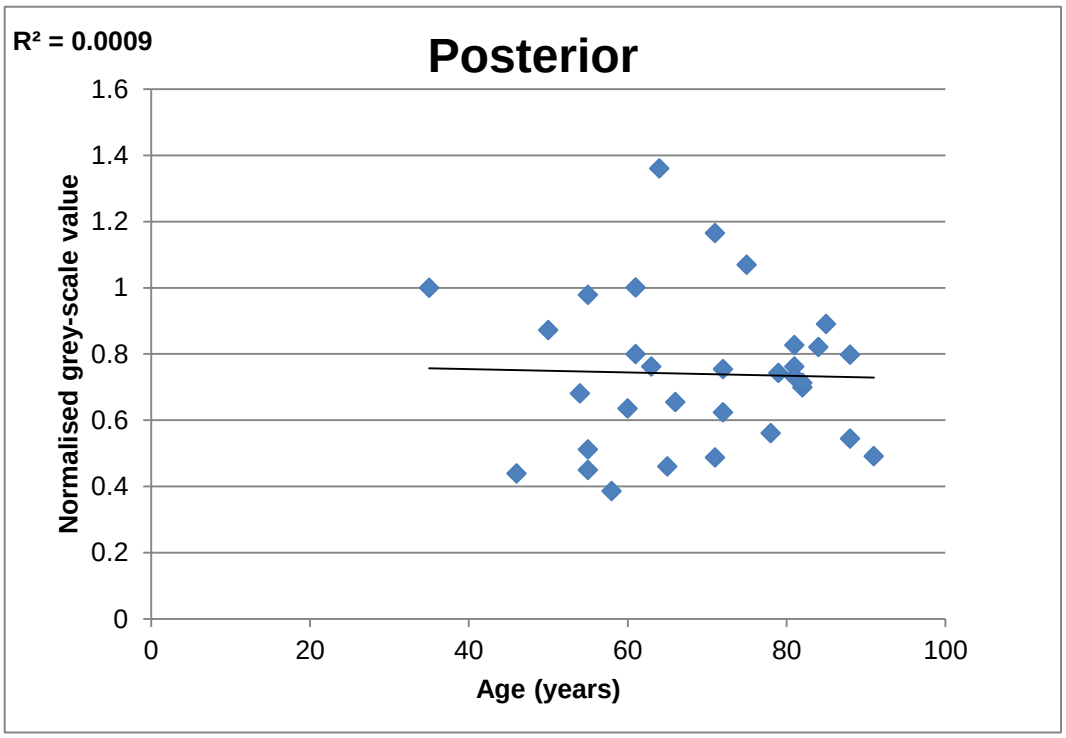

Figure 3.41: Scatter plot of normalised grey-scale values for cathepsin L staining in the posterior RPE against age of donor (n=32).

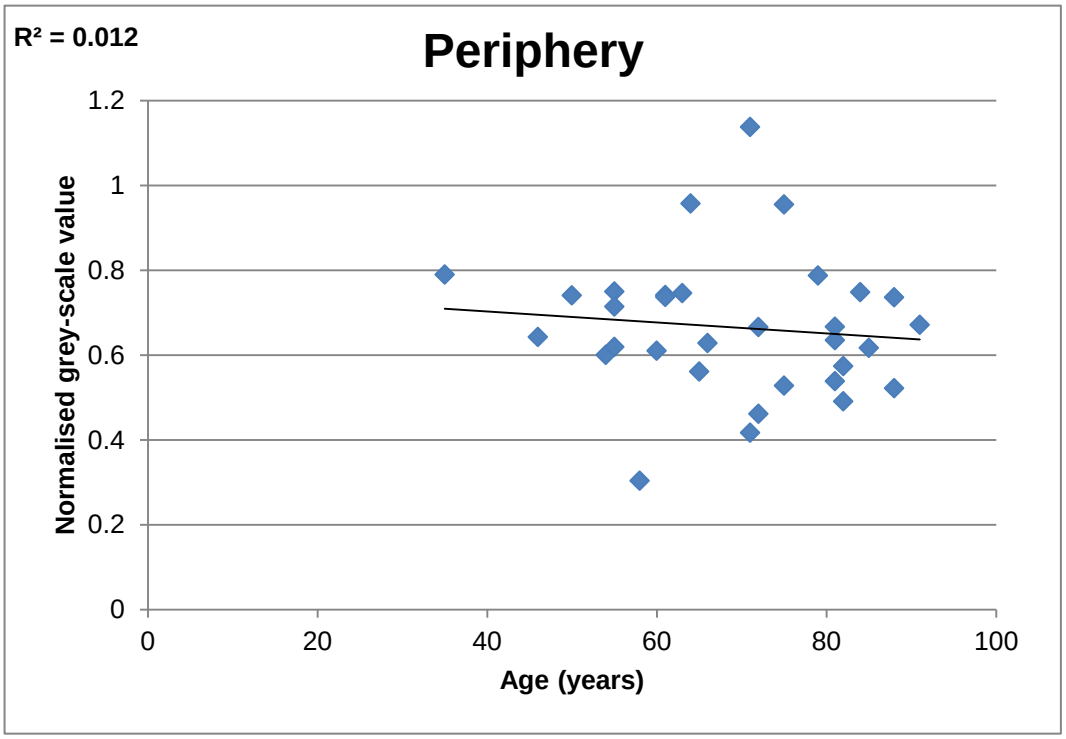

Figure 3.42: Scatter plot of normalised grey-scale values for cathepsin L staining in the periphery RPE against age of donor (n=32).

Chapter 4 - Analysis of the genetic association between the cysteine protease inhibitor CST3 and exudative AMD

4.1 - Investigating the association of CST3 rs1064039 SNP with exudative AMD

As the genetic association for the rs1064039 SNP in the CST3 gene with exudative AMD has only one reported case-control study (Zurdel et al. 2002), the aim of this study was to further investigate the CST3-AMD association. A case-control study was first performed after which the data obtained was combined with the existing AMD study as a meta-analysis to examine the association of CST-AMD.

4.1.1 - Preliminary work for optimisation – Primer pair CST3LRF-CSTLRR was chosen for genotyping with primers CST3LRR and CSTBIIR chosen for sequencing.

PCR protocol 1 (described in section 2.5.3) was used to amplify the CST3 gene in a set of DNA control samples designated F, G, H and I with the different combinations of primers designed (see Table 2.2). The primer pair CST3LRF-CST3LRR produced a clear single band just above the 1000bp mark corresponding to the predicted band size of 1093 bp (Figure 4.1). CST3LRF-CSTBIIR combination also produced bands at predicted band size of 795bp along with non-specific bands at 500bp. The other two combinations CST3AIIF-CST3LRR and CST3AIIF-CST3BIIR showed very weak bands or no bands at all at predicted band sizes. Therefore, the primer pair CST3LRF-CSTLRR was chosen for amplification of test samples.

PCR products generated using primer pair CST3LRF-CST3LRR were then sequenced. In the sequencing reaction only one primer is used. Primers (Table 2.2) were tested to determine the one that gave the cleanest sequence. Sequencing data was best achieved using the two reverse primers CST3LRR and CST3BIIR. The CST3LRR primer was used to determine sequences at SNPs rs5030707, rs73318135 and rs1064039. The second sequencing reaction using CST3BIIR primer confirmed the sequence and together the data obtained was used to determine the correct haplotype. Samples G, H and I were all homozygous wild-type (haplotype A) as determined by the sequencing chromatograph. The chromatograph for

sample F showed that an adenine nucleotide was present at position +73 meaning that this individual was homozygous AA (haplotype B) (Figure 4.2).

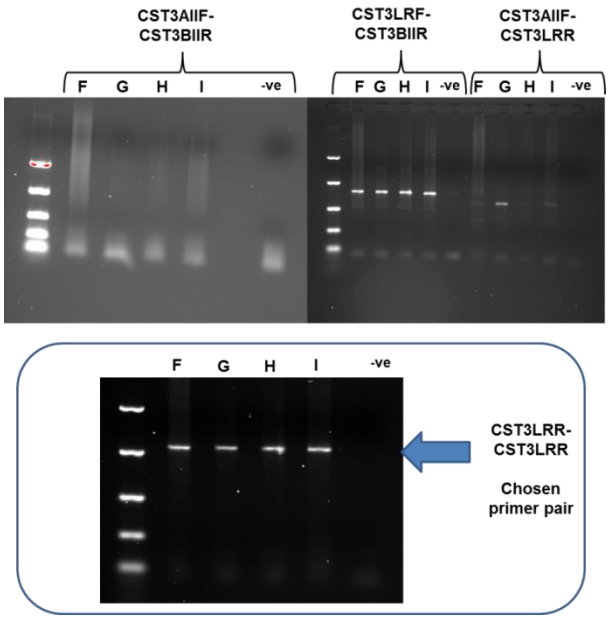

Figure 4.1: PCR amplification products of CST3 gene using 4 different combinations of primer pairs. Primer pairs CS3AIIF-CST3BIIR, CST3LRF-CST3BIIR, CST3AIIF-CST3LRR and CST3LRF-CST3LRR were used to amplify DNA control samples F, G, H and I. Easy Ladder I DNA molecular weight ladder was used as size marker. Circled gel shows that amplification was best obtained with the CSTLRF-CST3LRR primer pair.

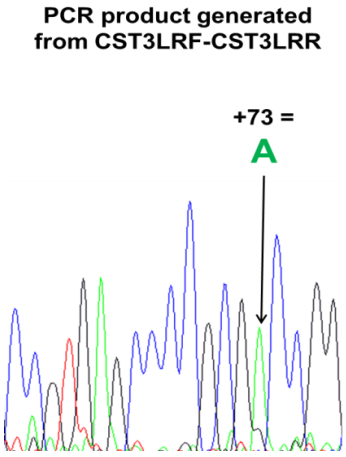

Figure 4.2: Sequencing chromatograph for sample F. At position +73, a single green peak (adenine nucleotide) was observed, therefore making sample F a homozygous AA individual.

4.1.2 – Initial analysis of first 153 samples tested showed a skewing of Hardy Weinberg Equilibrium (HWE) suggesting false results.

From the initial 153 AMD patient samples genotyped and sequenced, data indicated a skewing of the Hardy Weinberg Equilibrium (HWE). This principle states that allele and genotype frequencies in a population will remain constant from one generation to another unless there is some sort of evolutionary influences (Trikalinos et al., 2006). Genotype counts showed that 100 individuals were homozygous for the common homozygous GG genotype whereas 16 and 37 genotypes counts were observed for the heterozygous GA and homozygous variant AA respectively (Table 4.1). Allele frequencies for the common allele 'G' and for the rare allele 'A' were 71% and 29% respectively. Under the HWE principle, expected counts for the GG, GA, and AA genotypes were 76, 64, and 13 respectively. This data, albeit only with a 153 tested samples, suggested that an under representation of heterozygous individuals and an over representation for both homozygous genotypes when compared to HWE was being observed. This raised the possibility that the assay used for genotyping was causing a possible allele drop out that resulted in a deviation of the HWE.

Table 4.1: Genotype counts observed for the first 153 AMD samples tested along with genotype counts expected under the HWE principle.

Genotype	**Expected Genotype Counts**	**Observed**
Common homozygotes	76	100
Heterozygotes	64	16
Rare homozygotes	13	37

4.1.3 – Optimisation of new primer pair CST3LRIIF-CST3LRIIR

To investigate if data obtained for the initial 153 AMD samples was (un)true, a new primer pair was used to re-amplify sample DNA. The PCR products were sequenced and compared with previous sequencing data. The new primer pair was designated CST3LIIF-CST3LIIR and optimised on DNA

samples F, G, H and I using the second PCR protocol (section 2.5.3). A PCR product at the predicted size of 1292bp was seen for all samples tested (Figure 4.3a). PCR products were sequenced using primers CST3LRR and CST3BIIR. Interestingly, the previously detected homozygous AA sample F was now detected as a heterozygous with other samples remaining the same (Figure 4.3b).

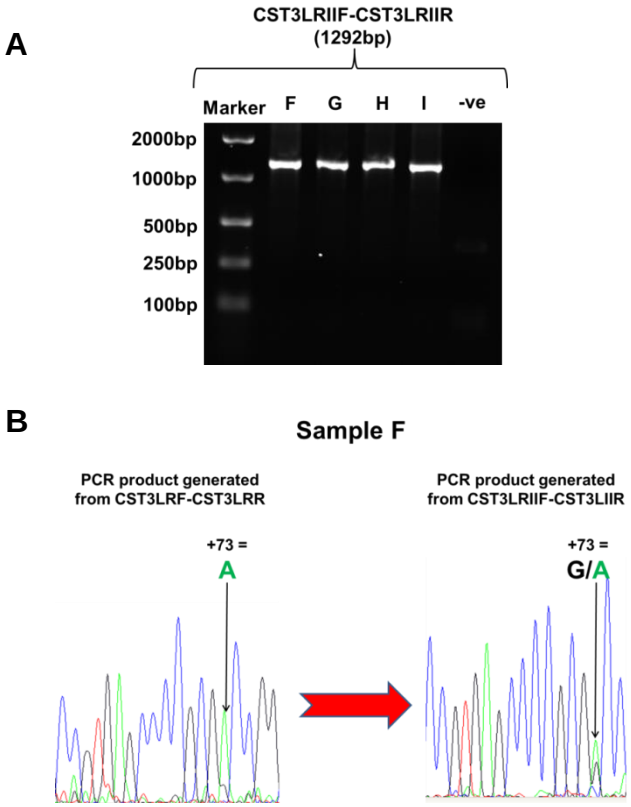

Figure 4.3: Testing of new primer pair CST3LRIIF-CST3LIIR on control DNA samples F, G, H and I. (A) PCR amplification products of CST3 gene using the new primer pair CST3LRIIF-CST3LIIR (B) chromatographs sequencing results showed that sample F, which was previously detected as homozygous AA individual, showed up as heterozygous as represented by the overlapping black (guanine) and green (adenine) peak at position +73, when gDNA was amplified with new primer pair CST3LRIIF-CST3LIIR.

4.1.4 – Sequencing of PCR products re-amplified with new primer CST3LRIIF-CST3LRIIR showed that most previously detected homozygous A/A were indeed heterozygous individuals.

After detecting that sample F was heterozygous, primer pair CST3LIIF-CST3LIIR was used to re-amplify the genomic DNA from the samples that

were detected as homozygote AA from the initial 153 AMD tested samples. Interestingly, sequencing data obtained showed that a majority of the 37 samples previously detected as homozygous AA were indeed heterozygous individuals with only 9 remaining as true AA genotypes (Figure 4.4). To exclude that the over representation of the common genotype homozygous GG was also due to a potential missing allele, 20 samples of homozygous GG were also retested with the new primers. Results showed that all retested samples remained the same when sequenced. Therefore, it was concluded that the assay was now trustworthy with the new primer pair CST3LRIIF-CST3LRIIR and was used to genotype the remaining exudative AMD samples.

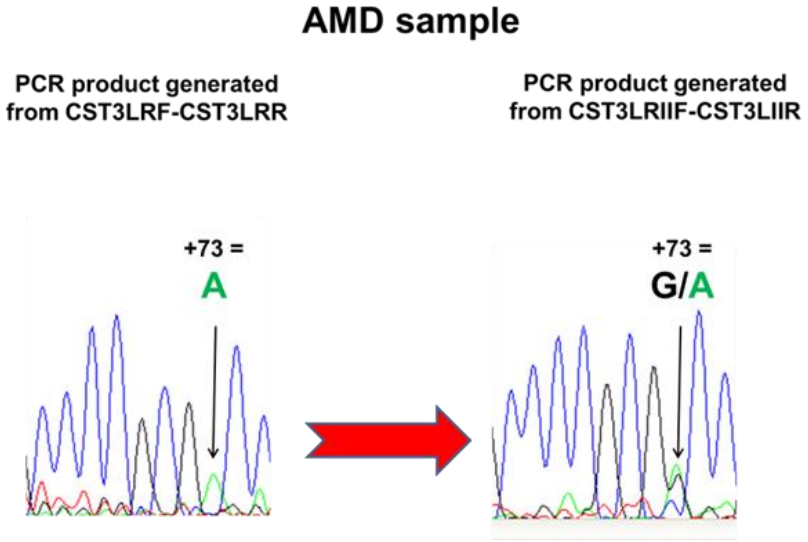

Figure 4.4: An example of sequencing chromatograph for AMD sample PCR product generated by new primer pair CST3LRIIF-CST3LIIR. Sequencing results showed that AMD sample that was previously detected as a homozygous AA individual showed up as a heterozygous when gDNA was amplified with new primer pair CST3LRIIF-CST3LIIR.

4.1.5 – CST3 and AMD association in Caucasian population

A further 197 AMD samples were genotyped using the new primer pair CST3LIIF-CST3LIIR and then sequenced leading a combined data set of 350 Caucasian AMD patient samples. The AMD data gathered was tested against the Exome Sequencing Project control data, the largest publically

available set of population controls (n = 3781). Analysis showed that AA homozygotes were at the greatest risk (OR = 1.56, p = 0.11) compared to the heterozygotes (OR = 1.07, p = 0.18). The GG homozygotes were used as a baseline (Table 4.2). Although not significant, the pattern for genotype risk was similar to those observed by Zurdel et al (Zurdel et al., 2002) (Figure 4.5).

By comparing effect sizes for heterozygotes 'GA' and homozygotes 'AA' against baseline 'GG' for both studies, risk was highest for homozygotes AA but only significant in Zurdel's study (OR: 1.56 for present study and 3.03 for study by Zurdel et al). The risk for heterozygotes was non-significant in both studies and had similar effect (OR: 1.07 and 1.06 respectively) (Figure 4.5). Thus, a recessive model of inheritance best explained the association of CST3 with AMD.

Table 4.2: CST3 genotype distribution (SNP rs1064039) in exudative AMD case and control samples

Genotypes	***CST3* genotype counts (%)**		**OR (95% CI)**
	Case	**Exome Control Database**	
GG	230 (65.7)	2574 (68.1)	1
GA	104 (29.7)	1092 (28.9)	1.07 (0.84 – 1.36)
AA	16 (4.6)	115 (3.0)	1.56 (0.91 – 2.67)

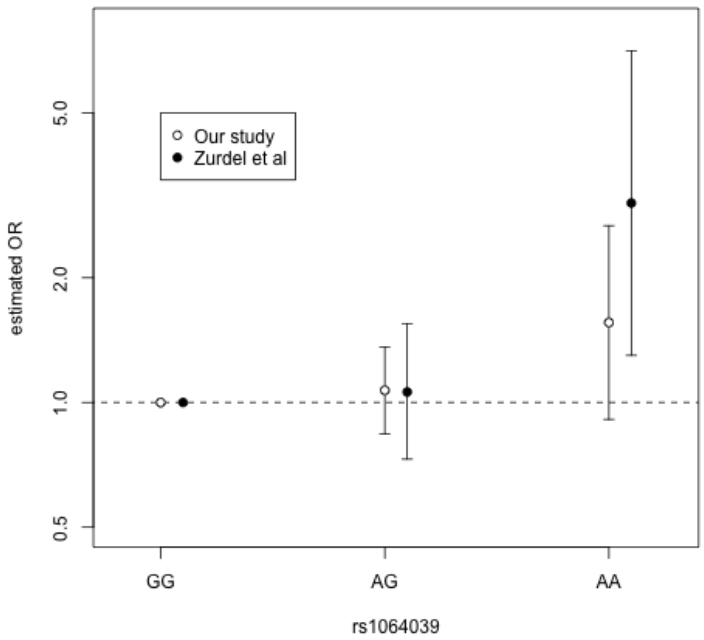

Figure 4.5: CST3 genotype at rs1064039 odds ratios (OR) estimated for AMD by our study and Zurdel et al study. ORs are measured relative to the 'GG' genotype, which is the baseline of 1. Error bars represent 95% CIs.

4.1.6 – Combined analysis of existing CST3-AMD datasets showed a significant association of AA genotype with AMD

After observing similarity in pattern between data from this study and the existing CST3-AMD association by Zurdel et al, a preliminary meta-analysis bringing together the results of the two CST3-AMD association studies was performed.

Before the meta-analysis, it was first tested to see if the association reported in Zurdel's was reproducible to exclude the chance that the data obtained was due to genotype error. 5 samples of each genotype (GG, GA and AA) were taken and amplified using the primers 024 and 1206R from the study by Zurdel et al (Zurdel et al., 2002). The PCR products generated were sequenced using both 024 and 1206R primers, as well as being subjected to restriction digestion using the enzyme KspI (Figure 4.6). The PCR reaction using Zurdel's primers amplified a 318bp fragment for all samples tested as shown by the agarose gel (Figure 4.6a). The restriction digest using the KspI enzyme showed a distinct pattern of bands with expected fragment sizes observed for each genotype (Figure 4.6b). For homozygote AA, two distinct bands at around approximately 127bp/180bp were detected as expected.

However, an extra band above the two expected bands was observed which most likely was due to the presence of non-specific bands from the PCR reaction. For the other two genotypes GG and GA, expected band fragment sizes corresponding to 41/226/51bp and all 5 fragments were seen respectively. Again, additional bands observed were most likely due to non-specific products generated from the initial PCR reaction. From the sequencing data obtained using 024 and 1206R primers for all 15 samples tested, PCR products generated using Zurdel's primers matched the known genotypes (Figure 4.6c). Taking the restriction digest and sequencing data observed, the association reported in the study by Zurdel et al was unlikely due to genotype error and therefore both existing CST3-AMD datasets were next brought together as a meta-analysis.

The goal of the meta-analysis was to estimate the overall combined effect of CST3 genotype on AMD development. Some studies may be more precise than others in that more information is carried. Therefore, more 'weight' is assigned to the studies which carry more information contributing to a weighted effect size. The weight of the studies can be assigned in two ways known as 'fixed' and 'random' effect meta-analysis models (Borenstein et al., 2010).

In a fixed effect model, an assumption is made that only one true effect size is shared by all studies i.e. the combined effect is the estimate of the common effect size in the studies tested. Therefore, weight of all studies is based entirely on the amount of data gathered from a study i.e. a large study would give more weight compared to a smaller study (Borenstein et al., 2010). A random effect a model by contrast takes into consideration that the true effect varies between studies i.e. the effect size being higher or lower from study to study. This results in the combined effect representing a mean effect size of all studies. In this model, each study has different effect sizes and accounts towards the mean effect size that is estimated (Borenstein et al., 2010). In order to decide which meta-analysis model to use, heterogeneity testing between both CST3-AMD data set was carried out. Heterogeneity testing examines the null hypothesis which states that all

studies evaluated are of the same effect (Higgins et al., 2003). The Cohran's Q test is a statistical test used to examine the presence of heterogeneity (Higgins et al., 2003). Q statistic is a measure of deviation of the observed effect sizes from the overall effect size (Higgins et al., 2003).

The Cohran's Q test was used to analyse heterogeneity between the two CST3-AMD association studies. Results supported homogeneity between the CST3-AMD studies as the null hypothesis was not rejected (Q = 1.68, p = 1.19). It should be taken into account that Cohran's Q test has low statistical power when study number is low (Higgins et al., 2003). This can mean that non-significant results do not necessary indicate homogeneity. In order to further test for heterogeneity between the two studies of interest, I^2 test can be used. The I^2 test describes the percentage of variation across studies that occur due to heterogeneity instead of chance (Higgins et al., 2003). I^2 values calculated are between 0% and 100% with numbers closer to 0 suggesting no heterogeneity and larger numbers showing an increased heterogeneity. However, there are no set values of when heterogeneity becomes significant. It is proposed that low heterogeneity is <25%, moderate being between 25-75% and high being >75% (Higgins et al., 2003). Further statistical analysis by Dr Joe Butler showed an I^2 of 40% for the two CST3-AMD studies tested suggesting a moderate heterogeneity. Taking together, the Cohran's Q value along with the I^2 value not in high criteria, results are indicative of homogeneity between the studies. Therefore a fixed-effects meta-analysis was chosen.

Bringing both studies together the total number of samples were 4815 (517 exudative AMD patients and 4298 controls). The genotype 'GG' was set as baseline and when analysis of 'AA' vs 'GG' was carried out, a significant effect with exudative AMD was observed (OR AA = 1.89, p = 0.005) (Figure 4.7a). No significant effect was reported when comparing 'AG' vs 'GG' genotypes (OR AG = 1.06, p = 0.55) (Figure 4.7b). Thus, results showed that when both CST3-AMD studies are combined, a significant association of the CST3 genotype AA with AMD was observed.

(A)

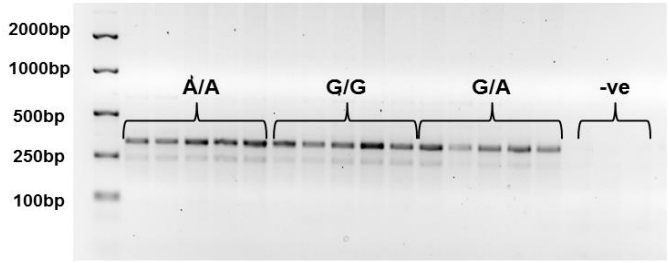

(B)

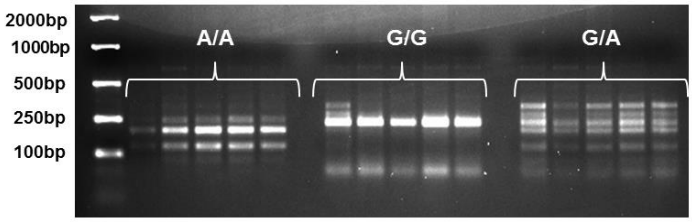

(C)

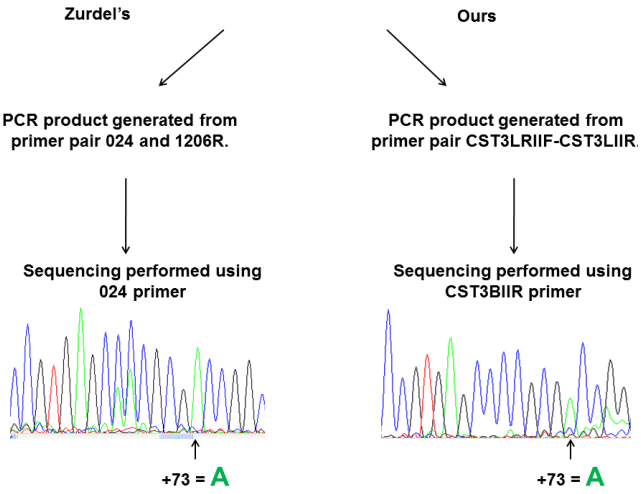

Figure 4.6: Validation of primers 024 and 1206R. (A) PCR amplification products using Zurdel's primers from genomic DNA from 15 individuals of known CST3 genotypes (B) Restriction digest using the KspI enzyme showed a distinct pattern of bands with the expected fragment sizes observed for each genotype (C) Sequencing of PCR products generated from two different set of primers tested on the same gDNA. First product (left) was generated using Zurdel primers (024 and 1206R) and sequenced using the 024 primer. The second product (right) was generated using primers CST3RIIF and CST3LIIR and sequenced using CST3BIIR.

(A)

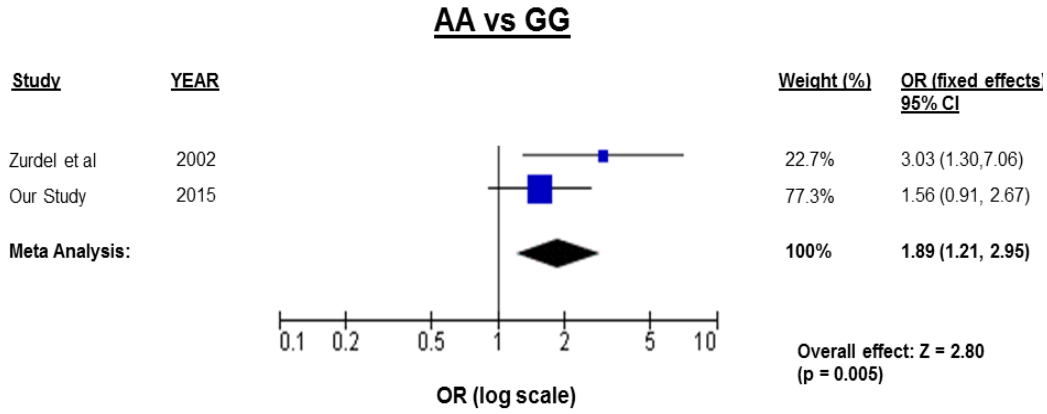

(B)

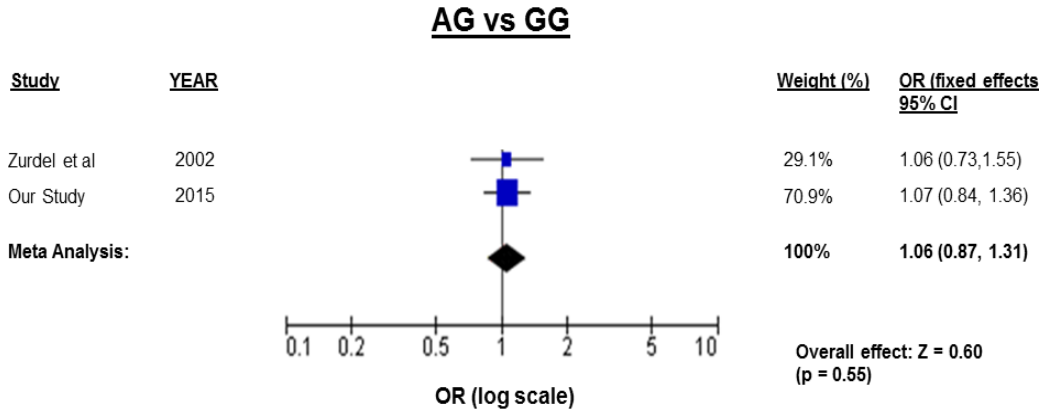

Figure 4.7: Forest plots for the fixed effects meta-analysis model of CST3 rs1064039 with exudative AMD in the Caucasian population. Size of the squares represents the weight of the study and horizontal bars represent 95% CI of the OR. (A) 'AA' genotype vs 'GG' genotype (B) 'AG' genotype vs 'GG' genotype.

Chapter 5 - Discussion

5.1 – Summary of results

In this study the presence of cathepsins B, L and S protein in two human RPE cell lines (ARPE-19 and D407) was observed. Immunohistochemical analysis also showed the presence of cathepsins B, and L and S in *ex vivo* human RPE/choroid. In addition, cathepsins B, L and S proteins were detected in conditioned media from RPE cells, indicative of their secretion.

A major finding within this present study was that the expression/activity of cathepsins was altered after exposure to AGEs. Results demonstrated that cathepsins D, L and S protein levels were altered in RPE cells grown on AGEs-modified MG™. In addition, analysis of cathepsins activity levels showed that cathepsin L activity decreased in RPE cells grown on AGEs-modified MG™. RPE cells were also exposed to H_2O_2 to induce oxidative stress and cathepsin expression/processing and activity levels were analysed. Cathepsins protein and activity levels were not altered in RPE cells exposed to H_2O_2.

Immunohistochemical analysis investigating the relationship between cathepsin L protein expression and age in *ex vivo* human RPE from 32 eyes showed that a weak negative correlation existed in both posterior and peripheral regions. However these correlations were not significant.

The final aspect of this present study analysed the genetic association of a cathepsin inhibitor, cystatin C (CST3 gene) with exudative AMD. The case-control genetic association of the CST3 SNP rs1064039 with exudative AMD showed a similar pattern to the previous reported study in that the homozygote variant B genotype (AA) was of the greatest risk (Zurdel et al., 2002). However this result was not significant due to the power of study alone. A preliminary meta-analysis to bring the data from the two existing CST3-AMD association studies together was performed and demonstrated the existence of a significant overall recessive effect of the homozygote variant B with exudative AMD.

5.2 – Expression and secretion of cathepsins B, L and S in human RPE cells

The lysosomal system is important in the removal of cellular debris (Ciechanover, 2005; Hershko and Ciechanover, 1998). In RPE cells, the lysosomes handle proteins destined for degradation from endocytic, phagocytic and autophagy processes (Lakkaraju, 2012; Strauss, 2005; Wang et al., 2009b). Impaired lysosomal degradative capacity of the RPE is assumed to play a role in RPE dysfunction and AMD pathogenesis (Finnemann et al., 2002; Holz et al., 1999; Kaemmerer et al., 2007; Shamsi and Boulton, 2001). Maintenance of the lysosomes along with their respective functional enzymes is vital to help prevent the accumulation of damaged proteins in RPE (Kaarniranta et al., 2013; Ryhanen et al., 2009). Lysosomal function is governed by a major class of proteases, the cathepsins including the cysteine proteases cathepsin B, L and S (Appelqvist et al., 2013b; Rossi et al., 2004). Cathepsins are synthesised as pre-pro enzymes that undergo proteolytic processing through the ER/Golgi network where eventually, the enzymes are delivered and processed into their active proteases in the acidic environment of the late endosomes/lysosomes (Coutinho et al., 2012; Guha and Padh, 2008; Repnik et al., 2013). Although lysosomal in nature and involved in intracellular proteolysis, cathepsins also exert extracellular function, where they are involved in ECM degradation (Fonovic and Turk, 2014). The first aim of the study was to characterise the intracellular cathepsins B, L and S protein expression from two RPE cell lines, ARPE-19 and D407 as well as in *ex vivo* human RPE cell samples. Additionally, the knowledge that cathepsins can exert extracellular function also encouraged investigation of RPE cathepsin secretion. This could potentially shed light on turnover of the surrounding RPE ECM such as IPM and BrM.

Inactive and active forms of cathepsin B, L and S were expressed in RPE cells. However, the cathepsin protein expression profile differed in both cell lines with ARPE-19 cell lines expressing predominantly active forms for all cathepsins tested. D407 cells on the other hand expressed similar levels of inactive and active forms for both cathepsin B and L which may highlight

differences in proteolytic capacity between both cell lines. Differences in both tested RPE cell lines have been observed previously in which the expression of efflux proteins was measured (Mannermaa et al., 2009). Results showed that a similar efflux profile was observed in ARPE-19 with the two primary RPE cell cultures whereas D407 cell line differed (Mannermaa et al., 2009). As ARPE-19 had a similar protein pattern to primary RPE cells, it suggested that they are more physiologically similar native RPE cells found *in vivo*. However, in order to make a similar conclusion in this study, analysis of cathepsin expression in primary RPE cells would be needed. Nevertheless, as both RPE cell lines showed detection of both inactive and active forms of cathepsins taken together with the knowledge that both cell lines are capable of digesting POS (Finnemann et al., 2002; Glenn et al., 2009) made these cell lines suitable for the study of lysosomal function. In addition, the presence of cathepsin B, L and S was confirmed in *ex vivo* human RPE/choroid samples.

The presence of cathepsins such as B, L and S in RPE cells has been previously demonstrated. For example, cathepsin B expression has been detected in rat, bovine and rabbit RPE cells (Bernstein et al., 1989; Frohlich and Klessen, 2001; Wasselius et al., 2003). Cathepsin S mRNA and protein detection has also been demonstrated in rat RPE cells (Sugano et al., 2003). In a study that surveyed the expression of cysteine protease cathepsins in mouse, cathepsin B was the major cysteine protease in RPE and choroid followed by cathepsin L and cathepsin S respectively (Alizadeh et al., 2006). In addition, the expression and activity of cathepsins such as B, L and S has also been shown in human RPE cells (Krohne et al., 2010a; Rakoczy et al., 1998; Rakoczy et al., 1994) Therefore, the findings in present study were in line with previous studies and provide further evidence for cathepsins expression in RPE cells.

The major function of cathepsins such as B, L and S is that they are intracellular proteases involved in non-specific protein degradation in the acidic environment of the endosome/lysosome compartment (Turk et al., 2012). In relation to the RPE, cathepsins are likely to be critical regulators of

important lysosomal functions such as POS degradation. POS degradation occurs in RPE cells following phagocytosis where material is delivered to lysosomal enzymes after fusion of phagosome with lysosome (Strauss, 2005). Disposal of degraded material occurs by transport to blood as well as recycling material back to photoreceptors (Strauss, 2005). In order to prevent the accumulation of toxic POS material within the post-mitotic RPE, lysosomes and their enzymes such as cathepsins need to be efficient in POS degradation. RPE cells from rats treated with a broad spectrum cysteine protease inhibitor showed an accumulation of lipofuscin-like inclusions that appeared to be derived from POS, hence highlighting a role of cysteine proteases such as cathepsins B, L and S in POS degradation (Katz and Shanker, 1989). Moreover, in a later study, the use of antisense oligonucleotide technology directed towards cathepsin S led to an increase in accumulation of fluorescent debris in POS-challenged RPE cells compared to controls demonstrating a specific role for cathepsin S in POS degradation (Rakoczy et al., 1994). Cysteine proteases such as cathepsin L and cathepsin S may also affect levels of other proteases known to have important roles in POS degradation such as cathepsin D, a highly expressed protein within the RPE (Regan et al., 1980; Zimmerman et al., 1983). Inhibition of cathepsin S reduced cathepsin D synthesis in RPE cells (Rakoczy et al., 1998). In addition, cells expressing low amounts of cathepsin L showed an increase in active cathepsin D protein and activity (Wille et al., 2004). Therefore taken together, it is possible that cysteine proteases such as cathepsin B, L and S may be involved directly and/or indirectly through interactions with other proteases in POS degradation.

In addition to the process of POS, degradation of autophagy material takes place within the lysosomal compartment. Autophagy is a cellular clearing process whereby cytoplasmic cargo is encapsulated in a double-membrane bound autophagosome, which fuses with the lysosomes where degradation occurs (Yorimitsu and Klionsky, 2005). Constitutive autophagy occurs under normal conditions in cellular repair to help remove damaged organelles and protein aggregates. Under conditions such as oxidative stress, autophagy increases as an effort to remove oxidatively proteins and damaged

organelles such as mitochondria (McCray and Taylor, 2008). As the RPE cells are prone to oxidative damage, autophagy is an important process in helping maintain cellular homeostasis. Indeed, the presence of autophagy markers such Atg5 and LC3-II in RPE cells demonstrates that autophagy occurs in RPE cells (Wang et al., 2009b). Moreover, RPE cells treated with a chemical compound rotenone, known to induce ROS production and subsequent mitochondrial DNA damage, led to increased autophagy markers which indicated increased autophagy in an attempt to remove damaged organelles (Wang et al., 2009b). As the lysosome is the terminal step in the autophagy process, lysosomal enzymes such as the cathepsins are key regulators of autophagy. Indeed, reduced levels cathepsin B, D, L and S have all shown to lead to impairment of the autophagy process (Dennemarker et al., 2010; Pan et al., 2012; Tatti et al., 2012). Although the individual roles of cathepsins in autophagy have not be studied to date in RPE cells, the evidence that autophagy occurs taken together with the presence of cathepsins means it is reasonable to conclude that cathepsins such as B, D, L and S are important regulators of autophagy within RPE cells.

This study confirmed the presence of cathepsins within the RPE cells and cathepsins are most likely important regulators of processes such as POS degradation and autophagy. Although both POS degradation and autophagy are discussed separately, both these processes are inter-linked in that the lysosome compartment is the terminal degradative step. Moreover, a role of a noncanonical autophagy pathway has been demonstrated in helping facilitate phagosome formation and POS degradation highlighting association between both processes (Kim et al., 2013). In order for these important functions to be carried out efficiently a high level of cathepsin activity is required. Any alterations of the cathepsin enzymes could adversely affect both POS degradation and autophagy leading to accumulation of toxic material and subsequent RPE dysfunction.

As well as characterising intracellular cathepsins within RPE cells, a novel finding in this study was the secretion of cathepsins B, L and S from RPE

cells in culture. The secretion of cathepsins is intriguing as this could highlight previously unknown extracellular functions in relation to RPE cells such as involvement in ECM turnover. Interestingly, although cathepsins are normally targeted and localised in the lysosomes, their secretion has been previously demonstrated in other cells under physiological and pathological conditions. The secretion of cathepsins from other cellular systems may provide insight into how cathepsins are secreted from RPE cells as well as what extracellular roles cathepsins could exert.

Cathepsins can be secreted in normal physiological processes such as wound healing and bone remodelling. Cathepsin B secretion was shown to be important for the regeneration of scratch-wounded normal epidermal keratinocytes (Buth et al., 2007). The dependence on extracellular proteolytic activity of cathepsin B for the migration of keratinocytes into the wound area was demonstrated by non-cell permeant cathepsin B inhibition leading to impaired monolayer regeneration (Buth et al., 2007). In pathological conditions such as cancers, up-regulation, altered localisation of cathepsins such as cell surface association and increased secretion has been observed. It is suggested that increased secretion of cathepsins helps facilitate cancer cell metastasis through involvement in ECM degradation (Briozzo et al., 1988; Mohamed and Sloane, 2006). For example, cathepsin D secreted by breast cancer cells facilitated ECM breakdown *in vitro* (Briozzo et al., 1988). In addition, cathepsin B secretion has been observed in colorectal cancer cell lines and contributed to cell invasiveness (Bian et al., 2015). Thus, evidence supports that cathepsins can be secreted from cells and most likely involved in ECM remodelling. The presence of extracellular cathepsins also highlights the presence of transport mechanisms within cells that target cathepsins for secretion. Although, knowledge on these mechanisms is limited and not well understood, possible explanations on how cathepsins are secreted do exist and may provide insight into how cathepsins secretion occurs from RPE cells.

It is known that lysosomal proteases can be constitutively secreted to a certain extent as some fail to bind the M6P receptor in the TGN and

therefore released from the cell (Braulke and Bonifacino, 2009). In addition, a larger amount of cathepsins could be secreted as a consequence of increased production of lysosomal proteases causing saturation of the M6P pathway. For example, in human breast carcinoma cells, increased expression of cathepsin D was shown to saturate the M6P pathway which caused increased secretion of pro-cathepsin D (Mathieu et al., 1991). Another possible explanation of how cathepsins are secreted into the extracellular environment is through lysosomal exocytosis (Rodriguez et al., 1997). Lysosomal exocytosis is a physiological process involved in key mechanisms such plasma membrane repair (Andrews, 2000, 2005). During this process the lysosome fuses with the plasma membrane to seal the damaged hole which causes the release of their contents into the extracellular environment. Indeed, it has been shown in keratinocytes that plasma membrane damage induced by UV irradiation resulted in the extracellular release of cathepsin D (Appelqvist et al., 2013a). In regards to the post-mitotic RPE cells, the plasma membrane would potentially be constantly repaired throughout life as RPE cells encounter many stresses and stimuli which may damage their plasma membrane such as high light levels and oxidative stress. Thus, it is conceivable that lysosomal exocytosis by RPE cells may be a potential route for lysosomal enzymes to make their way outside the cell.

Once outside, cathepsins need to remain active as generally cathepsins undergo inactivation in an irreversible manner at neutral pH (Turk et al., 1993). However, whilst inactivation does occur given the appropriate time, cathepsins could remain active for a short period which may allow sufficient time for substrate cleavage. Another explanation of how cathepsins can remain active outside the lysosome is due to the acidification of the environment that they encounter i.e. the cytosol, pericellular/extracellular environment. Low pH values are observed at sites of inflammation such as arthritis or tumours helping to stabilise cathepsin activity (Konttinen et al., 2002; Rozhin et al., 1994). A pericellular acidic pH resulted in malignant cells increasing secretion of cathepsin B into an environment where it can remain active (Rozhin et al., 1994). Interestingly, chronic inflammatory processes at

the RPE-BrM interface are associated with development of AMD (Augustin and Kirchhof, 2009; Hageman et al., 2001). This inflamed environment could provide an ideal low pH environment for secreted cathepsins to remain active. Cathepsins can also remain active in neutral pH and above by binding to their substrate. For example, cathepsin B was protected from alkaline pH-induced inactivation by binding to heparin (Almeida et al., 2001). In addition, the rate of inactivation of cathepsin L at neutral pH decreased in the presence of substrate suggesting that substrate protected the enzyme from inactivation (Turk et al., 1993). Therefore, the above findings show that cathepsins, given the right conditions, can remain active outside the lysosomes and be involved in possible local proteolysis.

In this study, active form of cathepsin B and S along with pro-cathepsin L are secreted from RPE cells. The presence of active forms of cathepsins B and S suggests that they are potentially able to be act on potential substrates given the right environment i.e. acidic pH. However, secreted pro-cathepsin L may need to be processed into its active form before it can act on substrates. Interestingly, the stable inactive form of cathepsin L may be activated if it encounters an environment which has an acidic pH (Heidtmann et al., 1993). In addition, pro-cathepsin can be activated by heparan sulphate and degrade ECM components such as laminin (Ishidoh and Kominami, 1995). Moreover, other ECM components such as fibronectin were shown to be digested by unprocessed pro-cathepsin L (Ishidoh and Kominami, 1995).

The secretion of cathepsins from RPE cells in culture is interesting as cathepsins can be involved in ECM remodelling (Fonovic and Turk, 2014). Cathepsin B and L were shown to degrade ECM components such as collagen type IV, fibronectin and laminin (Buck et al., 1992; Guinec et al., 1993). In addition, other components of ECM including the proteoglycan nidogen have also been shown to cathepsin cleavage target, in particular for cathepsin S (Sage et al., 2012). Interestingly, in a mouse model of CNV, nidogens, in particular nidogen-1, were shown to have anti-angiogenic effects (Semkova et al., 2014). Taken together with the knowledge that cathepsin S is able to breakdown nidogens, this data may support a possible

role of secreted cathepsin S in CNV. Interestingly, these cathepsin substrates such as nidogens along with collagen type IV and laminin are shown to be present within the BrM (Kunze et al., 2010; Marshall et al., 1992). Therefore, the secretion of cathepsins from the RPE cells raises the possibility of similar extracellular roles and makes it conceivable that uncontrolled activity of cathepsins could be involved in turnover/breakdown of important ECM found around RPE such as the BrM and contribute to hallmarks of AMD such as CNV.

The idea of possible extracellular cathepsin function is further supported by the knowledge that the potent cathepsin inhibitor, cystatin C is predominantly basally secreted from the RPE towards the BrM, therefore raising the possibility that interplay between inhibitor and targets may play a role in modulating BrM matrix turnover (Paraoan et al., 2001). An age-related decrease of wild-type cystatin C secretion was observed from RPE cells (Kay et al., 2014). In addition variant B cystatin C, which is genetically associated with exudative AMD, shows impaired cystatin C secretion from RPE cells (Paraoan et al., 2004). Cystatin C biology within RPE cells points towards the age-related development of uncontrolled extracellular balance between cathepsins and their inhibitor leading to potential destructive consequences.

5.3 – Effects of AGEs exposure on protein expression and activity of cathepsins B, D, L and S in RPE cells.

The RPE is susceptible to oxidative stress due to high metabolic activity as well as being exposed to high oxygen and light levels (Winkler et al., 1999). Oxidative insult leads to protein misfolding which ultimately could cause RPE dysfunction, if they are not efficiently removed (Beatty et al., 2000; Grune et al., 2004; Kopito, 2000). Contributors to an oxidative environment are AGEs, which have been shown to increase ROS production in cells (Basta et al., 2005; Thallas-Bonke et al., 2008).

A progressive rise in AGEs has been observed on the BrM with age (Glenn et al., 2009; Handa et al., 1999). As a direct relationship between the RPE and BrM exists, AGEs deposition on the BrM may be partially attributed to

RPE dysfunction and subsequent atrophy and photoreceptor degeneration. The formation of AGEs involves reactive α-oxaloaldehydes such as glycolaldehyde (Baynes, 2001). Glycolaldehyde-derived AGEs have been observed in human BrM (Glenn et al., 2012; Glenn et al., 2009). In this present study glycolaldehyde was used to induce AGEs formation on the basement membrane matrix. The use of glycolaldehyde to induce AGEs formation on matrix *in vitro* has been shown elsewhere (Glenn et al., 2012; Glenn et al., 2009; Stitt et al., 2004). In addition, the degree of AGE-adducts formation and cross-linking that occurs on matrix due to reaction with glycolaldehyde has previously been demonstrated (Glenn et al., 2012; Glenn et al., 2009; Stitt et al., 2004). Therefore, the use of glycolaldehyde as an AGEs-inducing substance was a relevant physiological choice.

ARPE-19 and D407 cell lines were grown on AGEs-modified MG^{TM}. ARPE-19 cells were kept in culture for up to 2 weeks, when a confluent monolayer was observed for both control and treated cultures. D407 cells formed a confluent monolayer by 1 week in culture for both control and treated conditions. However, the monolayer was not stable, as 1 week onwards an apparent increase in cell death in both control and treated cultures was observed. Therefore, only a 1 week AGEs exposure time point was used for the D407 cell line. Taking into account the D407 cell line behaviour along with the better characterisation of ARPE-19 cell line, it is conceivable that the data obtained using the latter cell line was more physiologically relevant.

In this study, ARPE-19 cells exposed to AGEs had altered cathepsin levels, in particular cathepsin L, which exhibited decreased protein and activity levels. Being a potent lysosomal protease, the implications of decreased cathepsin L activity could have severe impact on crucial lysosomal functions such as autophagy. Since post-mitotic RPE cells are prone to oxidative damage, removal of oxidatively-damaged molecules by the process of autophagy is of critical importance in cellular homeostasis. Interestingly, a deficiency of cathepsin L leads to impairment of the autophagy pathway, specifically in the turnover of the autophagosome (Dennemarker et al., 2010; Sun et al., 2013).

In the study by Dennemarker et al., a cathepsin L knock-out mouse model was crossed with a GFP-LC3 mouse model in order to assess the role of cathepsin L in autophagy (Dennemarker et al., 2010). In GFP-LC3/cathepsin L -/- cells, an increase in number and size of GFP-LC3 positive vesicles was observed compared to control cells, suggesting a potential accumulation of autophagosomes in cathepsin L deficient cells (Dennemarker et al., 2010). As no defect was observed in the initiation of autophagy process in cathepsin L deficient cells, the accumulation of GFP-LC3 vesicles was said to be due to impaired turnover of autophagosomes, hence highlighting the importance of cathepsin L in autophagy.

To further support the role of cathepsin L in autophagy, Sun et al observed increased accumulation of autophagosomes in cathepsin L -/- mice neonatal cardiomyocytes under hypertrophic stimuli (Sun et al., 2013). This observation was based on augmented LC3-II protein levels detected by immunoblot analysis and accompanied by increased accumulation of LC3-positive autophagosome vesicles on immunofluorescence images (Sun et al., 2013). This accumulation of autophagosomes was due to defective lysosomal clearance caused by the lack of cathepsin L (Sun et al., 2013). The *in vitro* findings were corroborated by *in vivo* results (Sun et al., 2013). In cathepsin L -/- mice, a pronounced cardiac hypertrophy was observed compared to control mice under hypertrophic stimuli (Sun et al., 2013). The cathepsin L -/- hypertrophic mice showed higher amounts of protein aggregates which was said to be due to impaired autophagy-lysosomal response (Sun et al., 2013). These observations showed that cathepsin L is an important lysosomal protease as a deficiency in cells leads to impaired autophagy flux. Thus, a decline in cathepsin L in RPE cells caused by AGEs exposure may impair the autophagy-lysosomal clearance system contributing to the accumulation of cellular debris and subsequently lead to age-related dysfunction of RPE cells and AMD development.

Impaired autophagy in RPE cells has been proposed to play a role in the accumulation of debris such as lipofuscin. Although lipofuscin accumulation is thought to primarily originate from incomplete POS degradation, impaired

removal of autophagy material i.e. damaged organelles can also contribute to lipofuscin accumulation (Boulton et al., 1989; Burke and Skumatz, 1998; Feeneyburns and Eldred, 1983; Katz, 1989; Krohne et al., 2010b). In support of a role of autophagy in lipofuscin generation, cultured RPE cells showed an accumulation of autofluorescent granules with lipofuscin properties in absence of photoreceptor challenge (Burke and Skumatz, 1998; Krohne et al., 2010b). Furthermore, lysosomal inhibition by ammonium chloride reduced autophagy and led to increased lipofuscinogenesis induction in the absence of POS feeding of RPE (Krohne et al., 2010b). These observations therefore showed that impaired autophagy in RPE cells may contribute to lipofuscinogenesis.

As well as contributing to lipofuscin accumulation, impaired autophagy may contribute to the accumulation of drusen. In an *in vitro* model of aged RPE, where mitochondrial damage was induced, increased autophagy markers and exosome markers were observed (Wang et al., 2009b). This indicated that the autophagy response and the release of exosomes were both increased. Interestingly, these observations were accompanied by decreased lysosomal activity (Wang et al., 2009b). Furthermore, analysis of drusen from AMD eyes showed the presence of autophagy and exosomes markers suggesting that intracellular proteins somehow make their way outside the cell (Wang et al., 2009b). It was speculated that, in aged RPE, impaired autophagy flux due to decreased lysosomal activity leads to increased exocytotic activity. Increased exocytotic activity leads to the release of damaged intracellular macromolecules via exosomes which in turn contribute building material for drusen. As cathepsin L is a potent lysosomal protease, the decreased levels of this enzyme in RPE cells after AGEs exposure may impair autophagy and therefore initiate subsequent events that contribute to drusen formation.

In addition to AGEs inducing cathepsin alterations, which may have knock-on effects on autophagy at the lysosomal stage, AGEs can also induce the autophagy response as observed in vascular smooth muscle cells and cardiomyocytes (Hou et al., 2014; Hu et al., 2012). Increased

autophagosome isoform LC3-II protein and increased autophagy vacuoles, observed via electron microscopy, in cells exposed to AGEs suggest that AGEs are involved in autophagy induction (Hou et al., 2014; Hu et al., 2012). In order to get a better understanding of how AGEs affect autophagy in RPE cells, protein levels of LC3-II were measured. LC3-II, a key marker of autophagy, correlates closely with the number of autophagosomes and therefore gives an indication of autophagosome formation (Mizushima and Yoshimori, 2007).

Results showed that LC3-II protein levels decreased after AGEs exposure in RPE cells. As LC3-II is incorporated into the maturing autophagosomes the observed protein decrease suggested impaired autophagy induction. However, when autophagosomes fuse with lysosomes to form the autophagolysosome, cargo material along with LC3-II is degraded by lysosomal enzymes (Mizushima and Yoshimori, 2007). Thus, the result obtained could either be indicative of decreased autophagy induction or increased autophagy-lysosomal degradation. Taking into account that decreased cathepsin L levels could result in decreased lysosomal function in RPE cells after AGEs exposure, it is more likely that the decreased LC3-II levels are due to impaired autophagy induction. Further work is needed to fully elucidate the role of AGEs in relation to autophagy flux in RPE cells. As LC3-II levels were susceptible to AGEs-induced alterations, this highlights that AGEs are affecting the autophagy process. Taken together, a decrease in LC3-II protein and cathepsin L protein and activity levels in RPE cells after AGEs exposure suggests that AGEs affect the autophagy pathway at multiple stages i.e. initial and end-stages of autophagy. Dysregulation of autophagy would lead to impaired clearance of damaged material and potentially contribute to accumulation of cellular debris such as lipofuscin and drusen.

Another important lysosomal function which may be affected by alterations in cathepsin levels is POS degradation. Within the lysosome many enzymes such as cathepsin D and the cysteine proteases, cathepsin B, L and S have been shown to be involved in carrying out POS degradation (Ivy et al., 1989;

Katz and Shanker, 1989; Rakoczy et al., 1994; Regan et al., 1980). Thus, alterations of lysosomal enzymes such as cathepsin L will subsequently affect the efficiency of lysosomal activity and related processes like POS. Interestingly, RPE cells exposed to AGEs had compromised POS degradative function which was accompanied by lipofuscin formation (Glenn et al., 2009). It was suggested that decreased POS degradation and increased lipofuscin formation was partially attributed to decreased cathepsin D activity in RPE cells exposed to AGEs, although further work was warranted to confirm this link (Glenn et al., 2009). In the present study, along with the decrease in cathepsin L protein and activity, a decrease in cathepsin S protein levels was also observed in RPE cells exposed to AGEs for 2 weeks. In addition, an increase in cathepsin D protein level was also detected. However, no activity changes were observed for cathepsin S and D. As cathepsin activity may be influenced by interactions with endogenous inhibitors, it is possible that alterations of inhibitor levels also occur due to AGEs which may balance protein levels. Thus, this may provide a possible explanation of why activity levels of cathepsins do not always correlate with protein changes. Nevertheless, alterations of cathepsins, in particular decreased cathepsin L protein and activity, may compromise lysosomal function and contribute to the lipofuscin accumulation that has previously observed in POS-challenged RPE cells exposed to AGEs (Glenn et al., 2009).

In the study by Glenn et al, ARPE-19 cells were exposed to AGEs-modified substrate for a 4 week time period which differed from the present study where cells were exposed for 2 week period (Glenn et al., 2009). This may explain why results were also different in both studies, as is the case for cathepsin D. In the study by Glenn et al cathepsin D activity measurement was significantly supressed by AGEs at the 2 week mark and remained suppressed for 4 weeks (Glenn et al., 2009). However, in the present study an increase in protein cathepsin D was detected with no activity changes observed in RPE cells after 2 week AGEs exposure. Differences in cathepsin D levels between both studies may represent different cellular responses to AGEs due to the time points. In the 2 week time point increased cathepsin D

protein level may be a response by RPE cells in an attempt to reduce the toxic effects of AGEs, a role described for cathepsin D (Grimm et al., 2010; Grimm et al., 2012). However, over a longer period of time, RPE cells eventually succumb to the accumulation of effects of AGEs, which then lead to decreased cathepsin D levels subsequently effecting lysosomal function and the build-up of toxic debris (Glenn et al., 2009). In addition, differences observed in both studies may be explained by the way the *in vitro* experiments were set up subsequently effecting how the cells respond to AGEs exposure.

In the 4 week AGEs exposure study, ARPE-19 cells were initially seeded on AGEs-substrate and only after reaching confluency were maintained for 1 month after which time stable, polarised monolayers were formed (Glenn et al., 2009). Although this experimental model was trying to replicate physiological relevance, the fact that RPE cells can deposit their own ECM (Afshari et al., 2010; Aisenbrey et al., 2006) could diminish the accumulative effects of AGEs in culture. In the present study, the exposure time point began from the day that ARPE-19 cells were seeded on the AGEs-substrate up until when confluency was observed. Time points chosen in this study attempted to make a compromise between cells becoming confluent without potential modulation of AGEs exposure in culture by deposition of their own matrix. Therefore, the model used in this study may represent a more acute response to AGEs compared to the model used by Glenn et al (Glenn et al., 2009). Although it is debatable to which model is more physiological relevant, both the present study and the one by Glenn et al showed that cathepsins are susceptible to AGEs induced changes in RPE cells. These alterations will subsequently affect RPE lysosomal function.

Interestingly, lysosomal dysfunction may impair the removal of AGEs. As AGEs cause cellular dysfunction and lethal effects such as ROS production, their removal is of particular importance. The proteosomal system was shown not to be involved in the degradation of AGEs (Grimm et al., 2010). However, cathepsins, in particular cathepsin D and L, were required for reducing AGEs-induced cellular cytotoxicity suggesting that the lysosome

was required for AGEs degradation (Grimm et al., 2010; Grimm et al., 2012). To further support a role for cathepsins in AGEs degradation, a massive increase of ROS was observed in AGEs treated cells that were deficient in cathepsin D or L as well as decreased cell viability (Grimm et al., 2012). Taking in account the ability of RPE cells to endocytose AGEs and the important roles cathepsin D and L have in the degradation of AGEs, alterations of these key lysosomal proteases may lead to impaired removal of AGEs (Grimm et al., 2010; Grimm et al., 2012; Li et al., 2007).

Decreased cathepsin L protein and activity in RPE cells may compromise the removal and degradation of AGEs. On the other hand, increased cathepsin D protein levels observed in RPE cells after AGEs exposure may represent a mechanism where cells are trying to compensate for decreases in other lysosomal proteases. However, as activity levels of cathepsin D remain unchanged, overall decreased lysosomal activity would occur due to altered cathepsin L levels. Impaired removal of AGEs due to decreased lysosomal activity would allow AGEs to exhibit multiple adverse effects on a RPE cells such as increasing ROS production and subsequent increased oxidative-damaged molecules (Wang et al., 2015a; Wang et al., 2015b). The decrease in cathepsin L would also affect lysosomal processes such as autophagy that aid in the removal of AGEs-induced damaged molecules causing debris accumulation and subsequent cellular dysfunction. In order to get a better understanding of how cathepsin alterations affect the removal of AGEs in the system deployed in this present study, further work investigating the efficiently of AGEs removal by RPE cells in which knockdown and/or overpression of cathepsins such as D and L would be needed.

In addition to the core lysosomal functions, cathepsin L has also been shown to be involved in the regulation of the transcription factor NF-κB (Tang et al., 2009; Wang et al., 2013; Xiang et al., 2011). Although the precise mechanism of how cathepsin L regulates NF-κB activity is not clear, it has been suggested that the enzyme may act on NF-κB inhibitory molecules such as IκB-α (Tang et al., 2009). As NF-κB protein resides in the cytosol, there is a notion that cathepsin L finds its way outside the lysosome where it

is then able to control NF-κB activity. This is supported by the study in which neouroblastoma cells treated with the neurotoxin 6-ODHA showed increased cathepsin L detection throughout the cytosol which was accompanied by increased NF-κB activation (Xiang et al., 2011). The regulation of NF-κB is important as it is a transcription factor that participates in the expression of many genes involved in processes such as apoptosis and inflammation (Hiscott et al., 1993; Qin et al., 1999; Suk et al., 2001). Interestingly, both apoptosis and inflammation are implicated in AMD pathogenesis (Augustin and Kirchhof, 2009; Dunaief et al., 2002). Therefore, gaining a better understanding of the molecular mechanism underlying how these processes are controlled could provide insight into RPE dysfunction and AMD developmental.

Cathepsin L has been shown to have a dual role in NF-κB regulation as it is involved in activation and suppression of NF-κB. In regards to cathepsin L leading to NF-κB activation, an *in vitro* cellular Parkinson's disease (PD) model in which neouroblastoma cells were treated with a neurotoxin 6-hydroxydopamine (6-ODHA), exhibited increased active cathepsin L protein levels (Xiang et al., 2011). Increased cathepsin L levels was accompanied by increased nuclear NF-κB p65 levels, increased IκB degradation, as well increased p53 and activated caspase-3 protein levels leading to subsequent cytotoxicity (Xiang et al., 2011). Cathepsin L inhibition was shown to partially reverse all 6-ODHA-induced alterations which subsequently increased cell viability. The observation that NF-κB activity was influenced by levels of cathepsin L highlighted a role of cathepsin L in NF-κB regulation (Xiang et al., 2011).

Supporting a role of cathepsin L in NF-κB activation, a second study in which rats were treated with the neurotoxin glutamate receptor agonist NMDA called quinolinic acid (QA), displayed increased cathepsin L protein and activity levels as well as increased striatal neuronal loss (Wang et al., 2013). Once more, cathepsin L increase was accompanied by an increase in nuclear NF-κB p65 levels and increased IκB degradation in QA treated cells (Wang et al., 2013). The QA-induced changes were all strongly suppressed

by cathepsin L inhibition again highlighting the involvement of cathepsin L in NF-κB regulation (Wang et al., 2013). Taken together, both the studies show that cathepsin L is needed for NF-κB activation as inhibition of cathepsin L lead to subsequent NF-κB decreased activity which seemed to be neuroprotective.

Contrary to the idea that cathepsin L is needed for NF-κB activation, cathepsin L expression has also been shown to block NF-κB activation (Tang et al., 2009). Cathepsin L deficient mice develop heart disease resembling features of human dilated cardiomyopathy (Stypmann et al., 2002). In a study that aimed to clarify the role of cathepsin L in heart disease, induced cardiac hypertrophy in mice was reduced in cathepsin L overexpressing mice compared to wild-type mice (Tang et al., 2009). In addition, *in vitro* experiments on cultured cardiomyocytes showed that cathepsin L overexpression diminished cardiac hypertrophy and attenuated NF-κB activation and inflammatory responses (Tang et al., 2009). This study therefore showed that cathepsin L is needed to block NF-κB activation which in turn protected cells from related processes such as inflammation. The decrease in cathepsin L protein and activity level observed in RPE cells after AGEs exposure taken together with the knowledge that cathepsin L is involved in NF-κB activity regulation means it is possible that the cathepsin L decrease may contribute to activation or blockage of NF-κB activity. This could have possible implications for NF-κB induced processes such as apoptosis and inflammation, processes that are associated with RPE dysfunction and AMD development.

The next step of this study was to investigate the effects of AGEs on NF-κB control in RPE cells, in which cathepsin L could be involved. NF-κB transcription factors consist of proteins such as p65, p50 and p52 that come together to form hetero or homo-dimers (Hu et al., 2004). NF-κB p65 protein has the strongest transactivation domain with the best characterised NF-κB pathway known to apply to dimers where p65 is present such as p65-p50 and p65-p52 (Hu et al., 2004). NF-κB is confined to the cytoplasm and held there through inhibitory proteins such as IκB-α (Hu et al., 2004). In order to

allow the liberation of NF-κB so that it can translocate to the nucleus, IκB-α is phosphorylated and sent for degradation (Hu et al., 2004). Although IκB-α degradation is crucial for NF-κB nuclear translocation, it is not sufficient for activation as additional post-translation modification such as phosphorylation of residues within NF-κB are critical for transactivation and target gene expression (Hu et al., 2004). Among the phosphorylation residues, serine 536 (Ser536) is required for activation of p65 (Hu et al., 2004). Therefore, measurement of protein levels of NF-κB p65, IκB-α and the phosphorylated form (Ser536) of NF-κB p65 protein expression in RPE cells exposed to AGEs were compared against control cells.

It was hypothesised that AGEs exposure would lead to NF-κB activation as AGEs and activation of their receptors such as RAGE cause activation of NF-κB (Bierhaus et al., 1997; Huttunen et al., 1999). Surprisingly, results obtained showed that protein levels of NF-κB p65 as well as phosphorylated Ser536 p65 levels decreased in RPE cells after AGEs exposure indicating decreased NF-κB activity. Being a transcriptional factor, NF-κB p65 is known to regulate the expression of pro-apoptotic genes such as p53 (Wu and Lozano, 1994). In the apoptotic pathway, p53 is known to be a tumour suppressor and induces cell death (Amaral et al., 2010). In the RPE cell culture system deployed in this present study, decreased NF-κB activity, which may in part be due to decreased cathepsin L levels, follow studies in which cathepsin L inhibition contributed to decreased NF-κB activation and was protective for cells against apoptosis (Wang et al., 2013; Xiang et al., 2011). Thus, decreased NF-κB activation in this present study may be a response in which apoptotic signals are reduced in order to help RPE cells remain viable in adverse conditions i.e. AGEs exposure.

Interestingly, in this present study, cells grown on AGEs-modified substrate lagged behind in their growth compared to control cells. This suggests that AGEs are having an impact on normal cell growth dynamics leading to impairment of cellular replicative capacity. The role of AGEs impacting growth of cells has previously been described in which retinal pericytes grown on an AGEs-modified substrate showed decreased replicative ability

(Stitt et al., 2004). Decreased replicative ability of cells grown on AGEs-modified substrate could explain why decreased cell numbers were observed for treated cells. In addition, the decreased cell number observed for cells grown on AGEs-modified may also in part be due to cellular apoptosis as AGEs are known to induce apoptosis, a response that is associated with increased oxidative insult (Scivittaro et al., 2000; Wang et al., 2015b). However, apoptosis may contribute to the reduced cell numbers observed, cells that survive on the AGEs-modified substrate implement mechanisms that enable them to remain viable. Given the role cathepsin L has in the regulation of NF-κB along with the knowledge that NF-κB has apoptotic functions, it is possible that RPE cells are responding to their adverse environment i.e. AGEs exposure by implementing a survival mechanism involving decreased cathepsin L, NF-κB signalling and related processes such as apoptosis.

In studies that support a role for decreased cathepsin L and NF-κB as a protective mechanism for cells, it should be noted that cathepsin L and NF-κB levels were increased in cells after respective treatments (Wang et al., 2013; Xiang et al., 2011). The increased cathepsin L and NF-κB levels were accompanied by augmented cell death. Only, when cathepsin L was inhibited, in an attempt to restore basal levels, a protective effect was observed (Wang et al., 2013; Xiang et al., 2011). In the present study, AGEs treatment caused levels of cathepsin L and NF-κB to drop below basal levels which ultimately will result in adverse effects. Decreased cathepsin L, as discussed earlier, may impair important lysosomal processes such as autophagy and POS degradation, making cells susceptible to debris accumulation and subsequent dysfunction. Due to its complex nature, decreased NF-κB activity would also lead to adverse cellular effects.

In addition to the pro-apoptotic roles, NF-κB also has anti-apoptotic activity. The anti-apoptotic molecules Bcl-2 and Bcl-X have been shown to be regulated by NF-κB (Tamatani et al., 2000). Levels of Bcl-2 and Bcl-X were increased in cultured neurons exposed to hypoxia/reoxygenation. Inhibition of NF-κB activity via adenoviral-meditated transduction of IκB-α expression

abolished increased Bcl-2 and Bcl-x and significantly increased neuronal cell death (Tamatani et al., 2000). Interestingly, AGEs exposure increased RPE cell death (Wang et al., 2015b). This cell death was accompanied by high levels of caspases-9 activation as well as reductions in Bcl-2 levels. As Bcl-2 levels are regulated by NF-κB activity, it is possible that AGEs cause cell death by influencing NF-κB levels. The reduction of NF-κB levels in RPE cells exposed to AGEs in the present study may lead to decreased expression of anti-apoptotic molecules i.e. Bcl-2 and push RPE cells towards death.

Down-regulation of NF-κB levels can also influence the adhesion of cells to ECM. In a study where colonic cells were made highly tumorigenic, via oncogene transfection, NF-κB activity decreased which was also accompanied by reduced adhesion of cells to ECM substrate (Cadoret et al., 1997). Reduced adhesion to ECM was partially corrected when NF-κB activity was stimulated in tumorigenic cells. This indicated that NF-κB activity was partly responsible for the reduced adhesive properties observed in the cells (Cadoret et al., 1997). Interestingly, AGEs have been shown to reduce adhesive capacity of cells to matrix proteins (Haucke et al., 2014). It is possible that AGEs affect adhesion of cells to matrix via regulation of NF-κB levels. In the present study, reduced NF-κB levels, indicative of decreased activity, observed in RPE cells after AGEs exposure may cause a reduction of cells to the matrix. In relation to RPE interaction with BrM, failure of cellular adhesion to BrM has been shown to contribute to CNV development (Shirinifard et al., 2012). Therefore, decreased NF-κB activity in RPE cells after AGEs exposure which causes reduced adhesion of cells to ECM such as BrM, may contribute to development of CNV, a characteristic feature of AMD.

Another important process that would be affected by changes in NF-κB activity is inflammation. In regards to inflammation, NF-κB is a transcriptional factor that regulates the expression of important pro-inflammatory cytokines genes IL-1β and IL-18 (Hiscott et al., 1993; Suk et al., 2001). Both IL-1β and IL-18 are synthesised as precursor which require proteolytic maturation via

the action of caspase-1, which itself must be first activated by multiprotein complexes known as inflammasomes (Mariathasan and Monack, 2007). In theory, as NF-κB activation is a prerequisite for inflammasome action i.e. by up-regulating gene expression for pro-inflammatory cytokines genes such as IL-1β and IL-18, decreased NF-κB activity as suggested by the results obtained in the present study, may indicate that RPE cells are protecting themselves from inflammatory damage after AGEs exposure in culture.

Contradictory to this idea that AGEs exposure leads to a decreased inflammatory response, it was recently demonstrated that AGEs treatment promoted the expression of pro-inflammatory cytokines such as IL-1β in RPE cells (Zhang et al., 2015). The production of AGEs-induced pro-inflammatory cytokines in RPE cells was shown to be mediated by the high mobility group box 1 (HGMB1) protein (Zhang et al., 2015). HGMB1 is a nuclear protein that acts as a transcription factor like protein by regulating gene expression (Stros et al., 2002). In addition, HGMB1 is also secreted by macrophages and can act as a mediator of inflammation (Yang et al., 2010). Interestingly, HGMB1 caused nuclear translocation and activation the NF-κB signalling pathway which led to the up-regulation of pro-inflammatory cytokines in human umbilical vein endothelial cells (Luan et al., 2010). As HGMB1 was increased in RPE cells after AGEs exposure and caused nuclear translocation of NF-κB, it is possible in the present study that after AGEs treatment, although less NF-κB protein is present compared to control cells, NF-κB is more active due to the presence of HGMB1. This increase in NF-κB activity could then potentially lead to up-regulation of pro-inflammatory cytokine gene expression as well as apoptotic gene expression. The regulatory control of NF-κB via HGMB1 also highlights the dynamic and complex nature of NF-κB signalling and shows that by assessing protein levels of NF-κB p65 and phosphorylated Ser536, as done in this present study, NF-κB activity may not be entirely reflected.

In further support of the dynamic and complex nature of NF-κB activity, other site specific post-translational modifications of NF-κB p65 residues, in addition to Ser536, such as Ser276 phosphorylation also increase the

transactivation of NF-κB p65 and mediate selective gene expression such as for IL-8 (Nowak et al., 2008). Phosphorylation of Ser276 is known to occur coincidently with IκB-degradation. Interestingly, in this study IκB-α protein levels were decreased in RPE cells after AGEs exposure. This decrease in IκB-α protein levels may be indicative of decreased synthesis as its gene transcription it negatively controlled by activated NF-κB or due to increased degradation (Oeckinghaus and Ghosh, 2009). Nevertheless, a decrease in IκB-α may allow the residual amount NF-κB p65 to move more freely into the nucleus as well as being more exposed to post-translational modifications. It is possible that although decreased amounts of NF-κB p65 are observed in RPE cells after AGEs exposure, NF-κB p65, if not already more active through other post-translational modification such as phosphorylation of Ser276, may be more susceptible activation due to less IκB-α present. Further investigation of NF-κB p65 cellular localisation as well as the phosphorylation of other residues will give a more robust interpretation of activity. In addition, expression of NF-κB inducible genes such as those involved in apoptosis and inflammation in RPE cells after AGEs exposure will also provide information of NF-κB activity regulation in RPE cells.

As well as possible involvement in regulating NF-κB activity, which in turn effects the gene expression of apoptotic and inflammation related genes, cathepsins have been shown to be involved in these processes via more direct routes after moving from the lysosome into the cytosol. A prerequisite for the movement of cathepsins from the lysosome into the cytosol is for LMP to occur. Important agents that are known to cause LMP are ROS, which are elevated in oxidative stress conditions (Zdolsek et al., 1993). Interestingly, AGEs are able to increase ROS and elicit oxidative stress (Scivittaro et al., 2000; Wang et al., 2015b). Therefore, it is conceivable that due to AGEs-induced oxidative stress, destabilisation of lysosomes occurs and leads to the release cathepsins into the cytosol. Once in the cytosol, cathepsins have been shown to be involved in the cleavage of important molecules that can cause apoptosis and inflammasome activation.

Cathepsins, such as B, L and S can cleave Bid into the potent pro-apoptotic tBiD (Cirman et al., 2004). In addition anti-apoptotic Bcl-2 proteins such as Bcl-2 and Bcl-X_L have been shown to be cathepsin substrates demonstrating the involvement of cathepsins in the apoptotic pathway (Droga-Mazovec et al., 2008). In addition to apoptosis, cathepsins have been shown to be involved in inflammasome activation. In RPE cells, the NLRP3 inflammasome has been shown to be expressed and furthermore is activated when lysosomal destabilisation is induced (Tseng et al., 2013). Interestingly, Inhibition of cathepsin B and L caused attenuation of lysosomal damage induced inflammasome activation (Tseng et al., 2013). This suggests that cathepsins B/L are able to cause NLRP3 activation leading to inflammasome activation and subsequent inflammation. Further work investigating whether lysosomal destabilisation occurs in the experimental model of this study is necessary in order to see whether cathepsins play a more direct role in apoptosis and inflammation in RPE cells exposed to AGEs.

Thus far, the results discussed are from those obtained in ARPE-19 cells exposed to AGEs. For the D407 cell model of AGE exposure for 1 week, an increase in cathepsin L protein level was detected with no significant change seen in activity. This result was contradictory to that obtained for ARPE-19 cells, which suggests opposite implications for how lysosomal function is affected in response to AGEs. Although no increase in cathepsin L activity was detected in D407 cells exposed to AGEs, the increase in cathepsin L protein levels may represent an initial stage before a rise in activity is detected if cells are given sufficient time. This idea is supported by findings in ARPE-19 cells where decreased cathepsin L protein levels was first detected after 1 week exposure but activity changes were not observed until 2 week AGEs exposure. In this model, growing D407 cells on AGEs substrate for 2 week was not feasible and therefore data was not obtained. It is also possible that regulatory mechanisms such as the presence of cathepsin inhibitors may be altered after AGEs exposure which caused cathepsins regulation to be altered in control and treated cells. In the case of D407 cells, it may well be that cathepsin L protein increase is accompanied

by an increase in inhibitor levels which counteracts activity and leads to detection of similar activity in both control and treated cells. Further work investigating regulatory mechanism such as measurement of endogenous inhibitors in the present model would help shed light on why changes in cathepsin protein levels do not coincide with the expected changes in activity. Nevertheless, as there is an increase in cathepsin L protein levels in D407 cells exposed to AGEs, there may be opposite implications to that described for ARPE-19 cells.

As discussed previously, cathepsin L is an important executor of the autophagy process (Dennemarker et al., 2010). AGEs induce the production of ROS which is likely to increase the amount of oxidatively damaged molecules (Wang et al., 2015a; Wang et al., 2015b). Therefore, an up-regulation of cathepsin L protein levels could be indicative of cells increasing the autophagy process in response to help remove damaged molecules. Also, as cathepsin L is important for the removal and degradation of AGEs, an increase in cathepsin L protein levels could be a mechanism by which cells are trying to remove the AGEs and their subsequent toxic effects (Grimm et al., 2012). Cathepsin L protein level increase could also have implications for NF-κB regulation. It is possible that alterations in cathepsin L levels could contribute to cell survival and inflammatory responses as well as cell adhesion to matrix via NF-κB control, similar to the idea presented for APRE-19 cells beforehand. However, as the activity of NF-κB was not assessed, no conclusions can be made on how cathepsin L affects NF-κB activity in in D407 cells exposed to AGEs. Further work investigating processes such as autophagy, AGEs clearance and NF-κB activation in D407 cells exposed to AGEs would be needed to establish whether a possible link with increased cathepsin L in D407 cells exposed to AGEs exists.

Throughout this study, differences were observed between both RPE cell lines tested. However, it is the belief of this study that the results obtained for ARPE-19 cells may be more physiological relevant compared to D407 cells. To further support this, the IHC analysis of cathepsin L immunoreactivity in

RPE cells from human donors of different ages showed that a negative correlation existed for both peripheral and posterior RPE regions. This negative correlation was not significant which may in part be explained by the limitation of a lack of young eye donors used in the study. However, a negative trend suggests that cathepsin L protein levels decrease with age and this trend corroborates with cathepsin L results seen in ARPE-19 cells exposed to AGEs. To further investigate which RPE cell line is more representative of RPE cells *in vivo*, the use of primary human RPE cells in experiments would be needed to fully support the data gathered in this study.

In conclusion, evidence is provided that cathepsins are susceptible to age-related changes in RPE cells, in particular cathepsin L. The changes in cathepsin L in RPE cells after AGEs exposure encourages further investigation into how important processes such as POS degradation and autophagy as well as regulation of NF-κB activation are affected. This would then shed light onto possible mechanisms in how accumulation of debris occurs and how RPE cells elicit apoptotic and inflammatory signals ultimately leading to cellular dysfunction and progressive to diseases such as AMD.

5.4 – Effects of H_2O_2 exposure on RPE cathepsins B, D, L and S protein expression and activity

In addition to AGEs, H_2O_2 a non-radical ROS can cause oxidative insult to cells (Beatty et al., 2000). A major source of production of ROS such as H_2O_2 occurs during mitochondrial respiratory chain (Hroudova and Fisar, 2013). In RPE cells, phagocytosis of POS also induces production of H_2O_2 (Miceli et al., 1994). In order to protect themselves from oxidative insult, RPE cells contain endogenous antioxidant systems that help counteract ROS induced damage. For example, RPE cells are known to have catalase activity, an enzyme known to neutralise the oxidative effects of H_2O_2 (Miceli et al., 1994). Interestingly, catalase activity was shown to decrease with age in both peripheral and macula RPE (Liles et al., 1991). Also a decrease in catalase activity was observed in the RPE of macula isolated from AMD

donors (Frank et al., 1999). Therefore, a constant production of ROS such as H_2O_2 from cellular metabolism and POS phagocytosis will ultimately overcome the defensive capabilities of the cell that decrease with age subsequently inducing oxidative stress and cellular damage.

The treatment of RPE cells with H_2O_2 to investigate oxidative stress-induced cellular changes is an established *in vitro* model (Ballinger et al., 1999; Kim et al., 2010). H_2O_2 treatment of RPE cells increased intracellular ROS production, induced mitochondrial DNA damage and effected the expression of RPE markers such as RPE-65 and CRALP65, demonstrating the cellular damaging effects of H_2O_2 (Ballinger et al., 1999; Kim et al., 2010). In addition, H_2O_2 has been shown to induce alterations to lysosomal proteases. H_2O_2 caused impairment of the processing of cysteine proteases such as cathepsin K as well as inactivation in a time and concentration manner (Godat et al., 2008). Also, the aspartic protease cathepsin D has been shown to be susceptible to H_2O_2 induced alterations (Lee et al., 2007). Taken together, H_2O_2 contributes to the accumulation of oxidatively damaged molecules i.e. causing mitochondrial DNA damage as well as affecting the activity of key lysosomal proteases which in turn can affect the clearance of damaged material. Therefore, it was investigated whether oxidative stress induced by H_2O_2 was able to induce changes in cathepsins in RPE cells that in turn may affect key lysosomal clearance mechanisms such as autophagy.

The concentration of H_2O_2 (100μM) used in the present study to treat ARPE-19 cells with has been previously shown to be sub-lethal and increased ROS levels within the cell (Kim et al., 2010). The same H_2O_2 *in vitro* model was implemented in this study to assess the effects of H_2O_2 induced oxidative stress on RPE cells, with particular focus on cathepsins protein and activity levels. Interestingly, under sub-lethal oxidative stress conditions, H_2O_2 did not display adverse effects on cathepsin protein and activity levels. Given that the active sites for proteases such as the cysteine cathepsins are highly sensitive to oxidative reagents such as H_2O_2, the results obtained in this study suggested that potent antioxidant systems may be in place protecting

cathepsins from being inactivated. This is supported by the knowledge that cathepsin activity may in part be protected from H_2O_2 induced-inactivation due to the presence of catalase (Herve-Grepinet et al., 2008). H_2O_2 did not display inactivation effects on secreted cathepsins from the monocyte-macrophage THP-1 cell line, showing that cathepsins are somehow able to resist being oxidised and inactivated (Herve-Grepinet et al., 2008). Interestingly, the use of extracellular catalase inhibitors led to decreased cathepsin activity therefore showing the involvement of catalase in preserving cathepsin activities (Herve-Grepinet et al., 2008).

In regards to the present study, it is possible that upon the addition of H_2O_2, catalase activity increased which in turn neutralised H_2O_2 and protected cathepsins from inactivation. In further support of this idea, increased catalase mRNA and activity levels were observed in RPE cells treated with exogenous H_2O_2 (Tate et al., 1995). Further work in which measurement of catalase activity in the present study is analysed would provide insight into how cathepsins may be protected from H_2O_2-induced inactivation. Furthermore, the inhibition of catalase activity in addition to exogenous H_2O_2 treatment would be necessary to see if cathepsins escape inactivation due to catalase. The inhibition of catalase would also be more representative of the ageing RPE as catalase activity decreases with age (Liles et al., 1991).

As previously eluded to, the concentration of H_2O_2 (100μM) used for treating RPE cells causes increased ROS levels (Kim et al., 2010). Catalase neutralises H_2O_2 by converting it to water and therefore in theory reducing ROS levels (Thannickal and Fanburg, 2000). However, as ROS levels are known to be increased in RPE cells for the H_2O_2 concentration used in the present study, it suggests that some H_2O_2 escapes neutralisation from catalase. If this is the case, it is conceivable that other cellular mechanisms in addition to catalase may be in place in protecting cathepsins against the ROS increase after H_2O_2 treatment. The identification of these mechanisms helping to protect cathepsin activity would shed light on how cathepsins can retain activity in oxidising environments.

Although no changes in the protein expression and activity of cathepsins were observed in this study, an increase in ROS levels could cause LMP (Zdolsek et al., 1993). LMP can cause release of cathepsins into the cytosol, where cathepsins may contribute to processes such as inflammasome activation and apoptosis, both of which are implicated in AMD development (Lin et al., 2010; Repnik et al., 2012; Tseng et al., 2013). Therefore, further work investigating whether LMP occurs after H_2O_2 treatment may provide additional information on how the H_2O_2 may affect cathepsins localisation.

In conclusion, the results observed showed that cathepsins are protected from H_2O_2 inactivation in the *in vitro* RPE oxidative stress model used. This protection may in part be due to catalase activity or other defensive mechanisms within the cell allowing cathepsins to retain their activity. However, further work is necessary to establish a role for catalase in protecting cathepsins from oxidative stress-induced alterations within the RPE cells. In addition, although H_2O_2 may not directly affect cathepsin protein or activity, it may alter cathepsin localisation via LMP. This may then allow cathepsins to be involved in functions such as apoptosis and inflammation.

5.5 –Cathepsin L IHC human RPE analysis

Regional variation of proteins between peripheral and macular regions of the RPE cells such as Na/K adenosine triphosphatase (ATPase) pump, insulin-like growth factor binding protein 2, heme oxygenase-1, catalase as well as the lysosomal enzymes cathepsin D and acid phosphatase has previously been demonstrated (Boulton et al., 1994; Burke et al., 1991; Miyamura et al., 2001; Miyamura et al., 2004). These regional variations of proteins highlight differences in functional demand of RPE cells in specific regions. A higher mean ratio of photoreceptor cells per RPE cell was found in the macula region in comparison to perimacular and peripheral regions (Dorey et al., 1989). This suggests that the phagocytic load on an individual RPE cell was highest in the macula and may also explain why higher amounts of cathepsin D were also observed in this region (Boulton et al., 1994). In addition to regional variations, lysosomal enzymes such as cathepsin D,

were also shown to be susceptible to age-related changes (Boulton et al., 1994). Given that cathepsin L was susceptible to age-related stresses i.e. AGEs in RPE cells *in vitro* in this present study, it was investigated whether this lysosomal enzyme was susceptible to regional and age-related changes in *ex vivo* human RPE cells.

Human donor eyes were grouped into young (≤65 years of age) and old (>65 years of age) and a comparison was made in regards to effects of age and region of RPE cells on cathepsin L immunostaining. The prevalence of the occurrence of AMD increases from 2.4% in people aged between 21 and 34 years to 9.8% in individuals 65 and over (Klein et al., 2010). Therefore, the age of 65 years was used as a cut-off point to group individuals into a young and old. Although not significant, results showed that for both age groups, a trend exhibiting higher cathepsin L immunostaining in the posterior compared to the periphery was observed. This was further highlighted by 26 eyes (out of 32) showing stronger cathepsin L immunostaining in the posterior RPE cells compared to the peripheral RPE cells. This suggested that more cathepsin L was present within the posterior RPE cells, possibly reflecting increased lysosomal activity within this region. An important function of the RPE cells is the phagocytosis and degradation of POS within the lysosomal apparatus (Strauss, 2005). The trend of higher amount of cathepsin L in the posterior region compared to the periphery region may therefore be reflective of higher lysosomal activity due to higher phagocytic load within this region. As briefly mentioned before, the activity of the lysosomal enzyme cathepsin D was shown to be higher in RPE cells isolated from the macula region when compared to peripheral RPE cells, supporting the idea that lysosomal activity was higher in the posterior (Boulton et al., 1994).

In regards to age and its effects on cathepsin L immunostaining, results showed that there was no significant association. However certain trends were observed which may shed light on how RPE dysfunction occurs with age. In both peripheral and posterior regions a negative correlation of cathepsin L protein level in RPE with age was observed. This possible

decrease in cathepsin L protein levels within the RPE could have adverse effects on lysosomal functions such as POS degradation. It has been shown in an ageing *in vitro* RPE model, that POS degradation was less efficient compared to control cells (Yu et al., 2014). Being a potent lysosomal protease, a potential decrease in cathepsin L levels could contribute to the age-related impairment of POS degradation.

The negative correlation of cathepsin L protein level in the RPE with age is greater in the peripheral region suggesting that the age-related cathepsin L decline occurs more slowly in the posterior. This suggests that cathepsin L levels in the posterior try to persevere at similar levels to that seen in the younger RPE cells. As the posterior RPE cells, in particular those found in the macula, have high metabolic demand and activity, it may be that the posterior RPE cells try to maintain levels of cathepsin L in order to counteract the harsh environment such as ROS production. As cathepsin L are important regulators of lysosomal processes such as autophagy, the enzyme may be crucial in helping clear oxidatively damaged molecules. Ultimately decreased amounts of cathepsin L would lead to accumulation of debris and cause RPE dysfunction.

Although these correlations of cathepsin L protein levels with age did not reach significance for both posterior and peripheral regions, it cannot be ruled out that cathepsin L protein processing/activity alterations do occur within the ageing RPE. In the IHC analysis, total cathepsin L protein expression levels (inactive and active forms of cathepsin L) were immunostained. This type of staining negates that fact that post-translational processing events in which more or less active form is made can occur and affect cathepsin L activity with age. It may well be that total amounts of cathepsin L are not altered with age but rather the processing is what is affected. The idea that total protein levels may not change with age but activity of cathepsin L may alter with age is potentially supported by the *in vitro* work in this study in which RPE cells were exposed to AGEs, a phenomenon of the ageing process. Results showed that protein active form and activity of cathepsin L decreased in ARPE-19 cells exposed to AGEs.

To address whether this age-related change in cathepsin L was attributed to decreased mRNA production, Dr Paul Kay (personal communicator) showed that levels of mRNA remained the same for both control and AGEs-treated RPE cells. This suggested that the changes in cathepsin L protein forms were possible post-translational processing events rather than expression levels. Therefore, by carrying out differential IHC assessment of inactive and active forms of cathepsin L in human RPE cells, a better understanding on the possible age-related changes of cathepsin L would be obtained.

In conclusion, the trends observed in regards to cathepsin L immunostaining suggest that regional differences of cathepsin L protein levels do exist and that cathepsin L is prone to possible age-related changes. This could have implications of processes such as POS degradation and autophagy subsequently leading RPE dysfunction. Although results were not significant, the observed trends encourages further work in which a larger cohort of eyes including younger donors is used with the additional measurements of cathepsin L inactive/active forms and activity. This would then shed light on whether cathepsin L is susceptible to regional and age-related changes and allow conclusions to be made on the physiologically relevant consequences.

5.6 – Association of variant B CST3 with exudative AMD

Evidence was provided which strengthens the hypothesis that a polymorphism in the CST3 gene (rs1064039) is associated with susceptibility to exudative AMD. In particular, results showed that the variant B CST3 allele A, acting in a recessive manner, increases the risk of exudative AMD development. Initially, case-control analysis showed that the AA genotype was of the greatest risk although not significant. Further investigation showed that a similarity in genotype pattern with the only previously reported CST3-AMD association study by Zurdel et al for AA was observed. Both studies showed that the same recessive trend for variant B led to an elevated risk for exudative AMD (Zurdel et al., 2002). Data from the two CST3-AMD studies taken together as a meta-analysis found a significant association of AA genotype ($p = 0.0005$). Interestingly, the same CST3 SNP, rs1064039, has been associated in a recessive manner with AD (Hua et al.,

2012). It should be pointed out that AMD is a complex disease which itself does not manifest or follow Mendelian pattern of inheritance i.e. the disease is not autosomal dominant or recessive. For a complex disease such as AMD, many genetic variations may contribute to disease development and each of these variations may show a dominant, recessive or additive pattern when analysed separately. In this study, data showed two variant B CST3 allele A together are needed for an increase in risk for AMD development and therefore it is said that this allele in particular behaves in a 'recessive' manner.

Of interest, the protein product of the CST3 gene, cystatin C, is one of the most abundantly expressed and secreted proteins from the RPE (Kay et al., 2014; Paraoan et al., 2000). In the RPE, cystatin C is shown to be secreted predominantly basolaterally towards the BrM and choriocapillaries (Paraoan et al., 2001). Mechanistically, the variant form of cystatin C impairs processing and is a driver of reduced secretion leading to reduced extracellular levels. Transfection with a construct encoding a different amino acid (Ser) at the penultimate position of the signal peptide of cystatin C leads to an intermediate secretion level between the wild-type (alanine) and the variant (threonine) cystatin C (Ratnayaka et al., 2007). In addition, an age-related decrease of wild-type cystatin C mRNA and protein expression levels as well as secretion has been observed in RPE cells (Kay et al., 2014). This decrease of cystatin C with age in theory could be further augmented in a variant B expression situation, hence explaining the increased risk posed by the risk allele. Moreover, a recent GWAS detected an association between a SNP (rs6048952) downstream of CST3 and cystatin C plasma levels (Akerblom et al., 2014). The variant that was associated with decreased cystatin C plasma levels is in linkage disequilibrium with the AMD risk allele rs1064039 A (Butler et al., 2015). This observation that was noticed by Dr Joe Butler further supports the existence of a mechanistic link between genotype and disease phenotype.

As a protease inhibitor, cystatin C is conceivably involved in proteolytic regulation at its sites of action i.e. at the BrM via interactions with its

molecular targets such as cathepsins. As previously mentioned, cathepsins, although lysosomal in nature, have been shown to exert extracellular effects such as being involved in degradation of ECM (Fonovic and Turk, 2014). Also, this present study provided evidence for the secretion of cathepsins from RPE cells. Taken together with the knowledge that cysteine proteases such as cathepsins B, L and S are inhibited by cystatin C, a reduced secretion would lead to proteolytic imbalance contributing to AMD-associated changes of the BrM such as disruption in stability and function of the BrM.

In addition, cystatin C has been shown to interact with a member of the complement cascade, C4, indicating that cystatin C plays a regulatory role in activation of complement system (Ghiso et al., 1990). Reduced amounts of cystatin C may lead to increased complement activation, a process linked with pathogenesis of AMD (Schramm et al., 2014; Sparrow et al., 2012). Further support to the idea of cystatin C in complement regulation is provided through its interaction with amyloid-β. Amyloid-β is found in drusen and is known to be an activator of the complement system by inhibiting complement factor I (Wang et al., 2008). Complement factor I is an inhibitor of complement activation and therefore when blocked by amyloid-β, low grade chronic inflammation occurs in subretinal tissues (Wang et al., 2008). Interestingly, Cystatin C was shown to inhibit cerebral amyloid-β deposition in a mouse model of AD highlighting a role for cystatin C in targeting amyloid (Mi et al., 2007). In a mouse model of AMD, anti-amyloid therapy protected against RPE damage and vision loss (Ding et al., 2011). In relation to the RPE, cystatin C may target amyloid-β and aid in cell protection i.e. by reducing complement activation. Thus, reduced amounts of cystatin C seen with age as well as in the CST3 variant B scenario could affect molecular events such as amyloid-β deposition and complement activation/inflammation, contributing to RPE dysfunction and AMD development.

Although GWASs of AMD have not reported an association with CST3 it does not dismiss it as a risk variant for AMD (Arakawa et al., 2011; Chen et

al., 2010; Cipriani et al., 2012; Fritsche et al., 2013). This is shown by the fact that the CST3-AD association, validated by a meta-analysis (Hua et al., 2012), has also failed to report association in GWASs (Harold et al., 2009; Hollingworth et al., 2011). Thus, it is implied that all GWASs for AD failed to detect an association for CST3 because of being underpowered, not because an association did not exist. A failure of why a GWAS fails to detect recessive effects is due to a common practice of GWASs to examine additive models only (Lettre et al., 2007). This type of GWAS model only has one degree of freedom and assumes a uniform linear increase in risk for each copy of allele. This means that an additive model has good power to detect both additive and dominant effects but may be underpowered to detect recessive effects (Lettre et al., 2007). The use of an inappropriate model may explain how GWAS studies become underpowered and miss recessive effects. This may also provide an explanation on the current missing heritability for common diseases. For AMD, it is predicted that up to 65% of total genetic contribution has been explained by the loci identified so far (Fritsche et al., 2013). Some of the missing heritability seen is said to be due to common variants with weak effects known as the infinitesimal model (Gibson, 2011). Taking this infinitesimal model, it may be that some of these common variants with weak effect may be common variants with a recessive effect. Using an additive GWAS model may result in common recessive variants exerting a weak effect. Therefore, through the use of an appropriate test, the effect may be stronger. With this knowledge, analysis of existing GWAS datasets to specifically look at recessive effects could be informative.

In conclusion, the data presented here showed that CST3 is associated with AMD pathogenesis, in particular homozygous individuals for the variant B allele ‘A’ being at an increased risk. A recessive effect implies that a single wild-type copy is expected to maintain proteolytic homeostasis and compensate for a variant allele. Absence of both wild-type alleles would potentially lead to a proteolytic imbalance. The CST3-AMD association that is observed in the data presented encourages investigating into the biology of cystatin at a functional level and the cellular pathways it is involved to provide insight into RPE dysfunction and AMD development and potentially

help identify molecular targets for treatment and prevention. Additionally, due to the recessive nature of inheritance, replacement therapy i.e. administrating the functional protein or more recently gene therapy is a possible treatment avenue (Escobar, 2013; Gaudet et al., 2013).

5.7 – Limitations of experiments

5.7.1 – Limitations of RPE cell cultures used to determine intracellular and extracellular cathepsins protein levels

The ARPE-19 cell line has been developed and characterised as a human cell line with some functional and structural properties representative of RPE cells *in vivo* thus making it a relatively widely used model for the study of RPE function (Dunn et al., 1996). In the first aim of the research project, ARPE-19 cell line was employed in a cell culture model to investigate the intracellular and extracellular protein levels of cathepsins B, L and S. Although a relevant RPE model, a limitation of the ARPE-19 cell culture model used in this study was that cells were not grown long enough for them to develop typical RPE properties which may undermine the physiological relevance of this study.

As it was observed, ARPE-19 cells cultured for 7-10 days, although confluent, did not form a 'cobblestone-like' monolayer and demonstrated a more fibroblastic-like phenotype. This may highlight cells that had not fully differentiated into a proper epithelial monolayer in the given time. This idea that ARPE-19 cells were not fully differentiated in the 7-10 days culture is supported by the observation by Dunn et al that ARPE-19 cells, once confluent, require 3-4 weeks to develop most properties of normal RPE such as 'cobblestone appearance' with pigmentation as well as barrier function (Dunn et al., 1996). In order to be reflective of the RPE cells *in vivo,* long-term culture of ARPE-19 cells i.e. 3-4 weeks after confluency would have been a more appropriate model for RPE study instead of the one used in this study. A proper established ARPE-19 cell line culture determined by morphology as well as tight barrier function via measurement of trans-epithelial resistance (TER) would have enabled a more physiologically relevant approach at assessing cathepsins in cells.

5.7.2 – Limitations of RPE cell cultures on AGEs-modified MG™

The *in vitro* model used in which RPE cells are cultured on AGEs-modified MG™ substrate does not fully mirror the development of age-related changes of RPE that occur *in vivo*. RPE cells *in vivo* do not grow and form a monolayer on an aged-BrM, but instead form a monolayer on a 'young' BrM. In reality, both RPE and the BrM overtime experience cumulative age-related changes and damage. The RPE cells *in vivo* therefore undergo a slow progression of insult, which the RPE cells will try to protect against by regulating defensive cellular responses. It is therefore likely that RPE cells that are seeded directly onto substrates containing aggregates of AGEs like in the *in vitro* model used in this study may differ in cellular responses that occur *in vivo*.

A factor that may affect the physiological relevance of the *in vitro* study was that possible pre-confluent cultures were assessed for their protein and activity levels of cathepsins, in particular for cells grown on AGEs-modified MG™. As it was noticed, cells grown on AGEs-modified MG™ did not reach confluence at the same rate as cells grown on control substrate. It is known that AGE-modification of a subcellular substrate can affect the replicative capacity of cells during short term cell culture and this seemed to be reproduced in this study (Stitt et al., 2004). This differs from what occurs *in vivo* where RPE cells are already an established monolayer upon the BrM and therefore are at their optimal functional capacity. In order to mimic the *in vivo* situation, RPE cells that are fully confluent would be more appropriate to use for assessment. Therefore, if this experiment was repeated, cells would be seeded at a higher density and the relevant time points for assessment after seeding would be when a monolayer is established in order to make it more physiologically relevant. Testing for monolayer establishment would include measurement of TER and examining whether a polarised phenotype of RPE cells could be achieved.

Another limitation of the experimental set-up used in this present study is that the influence of AGEs on cells may be diminished over time. AGEs formation is an irreversible step and their bioavailability depends on the half-

life of the protein it modifies. For example, collagens are known to be long-lived with reported half-lives of around 15 years to over 100 years which makes them susceptible to accumulation of AGEs formation (Verzijl et al., 2000). Taking into account that collagens are long-lived, it is reasonable to conclude that AGEs-induced formation of the MG™ substrate, in particular of collagen components would still exist at the respective time points used in this present study for cell culture. However, the fact that RPE cells can deposit their own ECM as well as being able to endocytose AGEs means that the effect of AGEs on cells may be a route for modulation of AGEs present on the MG™ over time (Afshari et al., 2010; Aisenbrey et al., 2006; Li et al., 2007). In order to confirm that AGEs are still present on the glycolaldehyde treated MG™ at one week and two week cell culture models, measurement of AGEs would be needed. A way of estimating the amount of AGEs on the matrix could be achieved by using ammonium hydroxide to remove cells from the matrix after which the matrix could be analysed for fluorescence using the AGEs-specific indicator spectrum of 370nm excitation/440nm emission (Honda et al., 2001). This measurement would have also allowed for a more suitable time point for cells in regards to studying the effects of AGEs as it would determine the time at which AGEs are no longer effective or present on the MG™.

5.7.3 - Limitations of regional variation and age-related IHC analysis of cathepsin L staining in human RPE cells

During the study in which cathepsin L protein levels were investigated for immunohistochemical analysis, RPE cells were grouped as peripheral or posterior. The RPE cells classified within the posterior analysis were defined as ‘opposite the cornea’. This definition means that RPE cells isolated for analysis may or may not have been from the macula region, the area affected in eye diseases such as AMD. RPE cells underlying the macula region were not specifically isolated for analysis as for some eyes it was a difficult region to precisely identify. To increase the chances that the macula region may be included in the analysis, three separate ‘posterior’ areas were analysed for each eye specimen and an average result was calculated. However, as RPE cells are known to be adapted to the region they are found

in, the cells found in the ‘posterior’ region may differ to cells that are truly from the macula. It is possible that results may be different if RPE cells exclusively from the macula were isolated and used for analysis.

There is also difficultly in performing age-dependant studies in regards to maintaining control between external variables between biological samples. Each eye donor has a unique history i.e. illness, treatments, smoking and quality of diet as well as different causes of death i.e. younger donors die due to more traumatic related experiences whereas older donors succumb to chronic illnesses, and this results in viability between donors. It is very difficult to establish whether these factors affect the expression and turnover of proteins such as cathepsin L.

To make this study statistically stronger, a possible expansion to include a greater number of younger donors would be required. A limitation in availability of younger donor tissue for analysis meant that the ‘younger’ donor group included a greater number of donors that are in the upper limit of the group. An increase in younger donors would potentially increase the negative correlation (although not significant) that was observed for both cathepsin L posterior and peripheral RPE cells staining in relation to age. However, as young donor eyes are in high research demand, the availability and attainment of these eyes was very difficult.

Another potential limitation of the experimental setup was the choice of concentration used for the anti-cathepsin L antibody. Although strong staining was observed when using 1/1000 diluted antibody, higher dilutions such as 1/1500 and 1/2000 could have been used instead for the IHC experiment (Figure 3.6). The choice of antibody concentration is critical in order to establish differences between different human donor RPE cells and thus using the 1/1000, which gave a strong stain, may have masked subtle differences between different donors.

A better technique that would help enable an ideal concentration of antibody to be chosen for the IHC experiment would be through the use of fluorescence-based IHC approach compared to the traditional chromogenic

approach. The fluorescence IHC approach is more advantageous compared to the chromogenic detection system as it has an ability to generate high-resolution images which enable protein localisation studies as well as having a capacity to a generate more quantitative signals compared to the semi-quantitative nature of chromogenic IHC analysis. In addition, due to a myriad of fluorophore colours available, multiple antigens can be stained simultaneously which makes this approach ideal for co-localisation studies. Taking into account that cathepsin L is a lysosomal protease, using an antibody concentration where colocalisation of cathepsin L with a lysosomal marker such as LAMP-1 is observed would determine the appropriate concentration to use for IHC experiment.

5.7.4 - Limitations of genetic association study investigating CST3 gene with exudative AMD

In the genetic study investigating the association of CST3 gene with exudative AMD, the CST3 genotype information used for controls was taken from the largest publicly available online database Variant Server, NHBL Go Exome Sequencing Project. As individuals within this control group were not tested for AMD, there is a possibility that the control group may contain individuals with AMD as well as individuals that could manifest AMD later on in life. In addition, confounding factors such as age and gender are not controlled for in this population control therefore not allowing the analysis of their effect on the results of this study. To increase the statistical power of this study the use of an age-matched AMD free control group could be used. Although the use of an age-matched AMD free control group was considered before carrying out the case-control study, getting a cohort proved difficult.

5.8 – Future directions

A possible use of human donor peripheral and posterior RPE cells harvested and cultured to further characterise age-related changes of cathepsin mRNA, protein and activity levels in RPE cells, via quantitative PCR, Western blotting and activity assays would help strengthen/complement/support the data obtained in RPE cell lines used in this study. Primary human RPE cells, although limited in lifespan, retain

many characteristics of cells *in vivo* and therefore the data gathered would be more physiologically relevant than that found in cell lines, where over time due to continuous propagation can lose *in vivo* characteristics. The use of primary human cells would also allow conclusions to be made on the physiological relevance of the RPE cell lines used in this study. In addition, research into other culture models that are a potential tool for studying RPE function has highlighted the use of human induced pluripotent stem cells (hiPSC)-derived RPE cultures (Singh et al., 2013). These hiPSC-derived RPE cells display many *in vivo* RPE features such as functional tight junctions, POS phagocytosis and degradation as well as polarisation. Furthermore, these cells also express characteristic RPE markers such as BEST1 and RPE65. However, similar to primary human RPE cells, the hiPSC-derived RPE cells have a limited lifespan as over passage 4 they lose their RPE characteristics (Singh et al., 2013). As discussed previously, the results obtained for cathepsin L protein levels in ARPE-19 and D407 cell lines after AGE exposure were contradictory. This begs the question of which result is more relevant and the use of primary RPE cells as well as the potential use of hiPSC-derived RPE cells may help address this issue. Although confident in the results obtained for ARPE-19 cell line, the use of other RPE cultures would further strengthen this study.

A novel finding in this study was the potential secretion of cathepsins B, L and S from RPE cell lines. To help further characterise the secretion of cathepsins from RPE cells, the use of primary cell conditioned media would be more physiologically relevant and would potentially strengthen the data observed in this study. In addition further secretion detection methods could be used such as enzyme linked immunosorbent assay (ELISA) as well as the use of cathepsin activity assays on conditioned media to confirm the presence of extracellular cathepsins. Taken together, with the knowledge that the potent cathepsin inhibitor, cystatin C is predominantly basally secreted towards the BrM, it raises the possibility that interplay between inhibitor and targets may play a role in modulating BrM matrix turnover (Paraoan et al., 2001). In order to determine whether cathepsins are secreted apically or basally, experiments analysing polarised secretion in

RPE cells through the use of an *in vitro* transwell insert cell culture system as described previously could be performed (Kay et al., 2014). Analysis of conditioned media from upper (apical) and lower chamber (basal) would provide information on the direction that cathepsins are secreted. Also investigation of cathepsins secretion pattern from conditioned media of RPE cells exposed to AGEs would help in gaining a better understanding on how the ageing process may affect proteolytic balance in the extracellular environment.

A major finding from the AGEs exposure study was that cathepsin L protein and activity levels were decreased compared to controls. Cathepsin L is an important lysosomal protease and therefore alterations of its levels will affect lysosomal processes such as POS degradation and autophagy. It would be interesting to see how these processes are affected in RPE cells exposed to AGEs and how cathepsin L could contribute to any alterations observed. In this study immunoblot analysis of LC3-II levels showed a decrease in RPE cells exposed to AGEs. As autophagy is a dynamic process, the decrease in LC3 protein levels could mean the following: increased autophagy response causing increased turnover of LC3 or autophagy suppression leading to decreased autophagosome formation. Thus, the measurement of LC3 levels via immunoblot is not sufficient to measure autophagy flux and should be complemented with other assays to make a strong interpretation of autophagy changes (Zhang et al., 2013). An example of a more accurate measure of autophagy flux would be by blocking the autophagosome-lysosome fusion step using bafilomycin A1 (Mizushima and Yoshimori, 2007). The use of bafilomycin A1 prevents autophagosomal cargo degradation, which would provide answers to whether decreased LC3-II levels observed is due to increased turnover. Autophagy flux is more accurately measured by looking at differences in LC3 levels in the presence or absence of lysosomal inhibitors such as bafilomycin A1 (Mizushima and Yoshimori, 2007). Once established how autophagy is affected by AGEs exposure in RPE cells, it would be interesting to determine how cathepsin L contributes to any changes observed. The measurement of autophagy flux in cells after the inhibition of cathepsin L in cells via chemical or interfering

RNA would provide possible links on how cathepsin L is involved in any autophagy changes observed in AGEs exposed cells. It should be acknowledged that AGEs may produce non-cathepsin L related autophagy changes.

Another lysosomal function of relevant interest is POS degradation. RPE cells exposed to AGEs, when challenged with POS, show an accumulation of autofluorescent lipofuscin-like material (Glenn et al., 2009). As POS degradation occurs in the lysosome and cathepsin L is a lysosomal protease, it is reasonable to propose that a decrease in cathepsin L may contribute to the accumulation of autofluorescent material observed. As compromised lysosomal activity contributes to lipofuscin accumulation, the measurement of lipofuscin accumulation in POS-challenged RPE cells exposed to AGEs would determine if an impairment of lysosomal function, which may be in part to altered cathepsin L levels, has occurred in the models used in the present study. Lipofuscin, being autofluorescent, can be observed in cells as previously described through fluorescent microscopy using a fluorescein filter set (excitation 480/40nm and emission 535/50nm) as well as flow cytometric quantification through the use of a FITC channel (excitation 488nm, detection filter wavelength 535/30nm) (Brandstetter et al., 2015). In addition, studying the effect of cathepsin L inhibition in POS-challenged RPE cells and measuring lipofuscin accumulation in RPE would give a more direct link with cathepsin L involvement and also provide insight into molecular events that contribute to debris accumulation in RPE cells with age.

As well as key lysosomal functions that may be affected by alterations in cathepsin L levels in RPE cells exposed to AGEs, other important roles of this enzyme have been established such as involvement in NF-κB regulation (Tang et al., 2009; Wang et al., 2013; Xiang et al., 2011). In the results obtained, protein levels of NF-κB p65 and NF-κB phosphorylated p65 decreased in RPE cells exposed to AGEs indicating decreased activity. The contribution of cathepsin L to AGEs-induced changes of NF-κB levels should be evaluated via experiments where cathepsin L is inhibited to determine

any possible links with NF-κB in the RPE-AGEs cell culture system. This would then allow insight into molecular pathways that may be affected and contribute to AGEs-induced RPE changes.

The changes of NF-κB levels observed in this study also open up avenues for investigation of processes such as apoptosis and inflammation. Experiments investigating apoptosis-related components in RPE cells would shed light on how AGEs effect and influence apoptosis. Examining protein expression levels of p53 along with other pro-apoptotic molecules such as Bax and activated caspases 3 would allow sufficient analysis on AGEs influence on apoptotic process in RPE cells. In addition, further experiments addressing the effects of AGEs on inflammasome induction in RPEs would be needed to determine whether inflammation is occurring or not. Secretion of IL-1β and IL-18 is indicative of inflammasome activation. Therefore, analysis of these proteins from RPE cells exposed to AGEs could be performed. In addition mRNA and protein measurement for intracellular levels of the pro-forms of IL-1β and IL-18 along with caspases-1 protein and activity measurement would allow a thorough interpretation to be made on how AGEs influence inflammasome activation. Both apoptosis and inflammation pathways are very complex and the involvement of NF-κB in regulating certain arms of these processes i.e. p53 regulation, IL-1β and IL-18 regulation is recognised. Taken together along with the idea that cathepsin L may contribute to NF-κB regulation, alterations of cathepsin L, in part, may affect multiple aspects of RPE cell function, which may contribute to AMD pathogenesis.

In regards to the genetic association study between CST3 gene and AMD, further validation through the use of replication cohort and possibly a more suitable control i.e. age matched and AMD free could be done. In addition, as both dry and wet AMD share many characteristics between them such drusen formation, it may be worth investigating the association of the CST3 gene with the dry form of AMD. Also worth investigating would be genetic association studies of other known risk factors of AMD such as CFH and ARMS2 loci alongside CST3 gene together and their risk on AMD

susceptibility. Currently within the laboratory, characterising the biological function of cystatin C in RPE along with the implications of variant cystatin C on RPE functions is being investigated. One direction that is currently being addressed is trying to generate an RPE cell line that constitutively expresses the variant B form of cystatin C only. A RPE cell line that only expresses the variant B form of cystatin C would be a more physiological relevant model that mimics the AMD genetic risk scenario. This model would then be utilised to study the biological effects of variant B cystatin C form on RPE function.

5.9 – Final conclusions

Intracellular detection of cathepsins such as B, L and S within RPE cells highlights involvement of cathepsin in important lysosomal functions such as POS digestion and autophagy. An important finding in the present study was that cathepsins were susceptible to change in RPE cells exposed to the common pathological change associated with ageing, specifically the accumulation of AGEs. Importantly, a decrease of cathepsin L active form and activity levels in cultured RPE cells (ARPE-19 cell lines) exposed to AGEs-modified MG™ was observed. Being a lysosomal effector, a decrease in cathepsin L levels will affect processes such as POS digestion and autophagy, vital processes in the post-mitotic RPE cells. Impairment of these processes would contribute to the accumulation of cellular debris such as lipofuscin which will subsequently lead to RPE dysfunction. The *in vitro* decrease in cathepsin L observed due to the age-related stress of AGEs exposure corroborated with the IHC cathepsin L RPE staining data in which a trend (although not significant) of decreased cathepsin L protein levels for both posterior and peripheral RPE cells with age was observed.

As AGEs are known to induce oxidative insult, which could result in cellular apoptosis, an idea was presented that alterations of cathepsin L levels within RPE cells may play a role in helping cells to survive as a response to AGEs accumulation. Due to the fact that cathepsin L has been shown to regulate the activity of an important transcription factor NF-κB, a decrease in cathepsin L could affect important NF-κB related processes such as apoptosis and inflammation. In this present study, RPE cells cultured upon

AGEs-modified MG™ showed reduced amounts of NF-κB p65 and Ser536 phosphorylated form compared to control cells, indicative of decreased activity. As NF-κB is transcription factor for the gene expression of genes such as p53, a decrease in its activity, which could in part be due to decreased cathepsin L levels, may be a possible mechanism by which RPE cells are remaining alive upon AGEs exposure. However, as NF-κB is also known to be involved in regulating anti-apoptotic genes such as Bcl-2 and Bcl-x, a decrease in its activity may in fact push a cell towards apoptosis (Tamatani et al., 2000). Decreased NF-κB activity also affects the adhesion of cells to matrix which could have implications for RPE interaction with BrM and processes such as CNV (Shirinifard et al., 2012). Further work investigating how changes in NF-κB affect related processes such apoptosis, inflammation as well as adhesion is needed. This would then shed light on how AGEs contribute to RPE dysfunction with age and in diseases such as AMD.

Another important finding in this study was that cystatin C gene was associated with exudative AMD. In particular, the variant B allele was shown to act in a recessive manner in its association with exudative AMD. Wild-type cystatin C is produced by RPE cells and is secreted basolaterally towards the BrM, indicating potential roles in control of proteolysis events in this region. The biological implications of the presence of a variant cystatin C form within RPE cells has so far shown that there is intracellular retention and reduced secretion towards its sites of action. Given that this present study has also shown that the molecular targets of cystatin C, cathepsins, are secreted from RPE cells, it raises the possibility that an imbalance between cystatin C and its molecular targets in its sites of actions could exist i.e. at the BrM region. Reduced secretion of cystatin C may allow uncontrolled cathepsin activity leading to destructive consequences i.e. BrM breakdown as well as involvement in angiogenesis, processes implicated in AMD development.

References

Abrahamson, M. (1996). Molecular basis for amyloidosis related to hereditary brain hemorrhage. Scand J Clin Lab Invest Suppl 226, 47-56.

Abrahamson, M., Grubb, A., Olafsson, I., and Lundwall, A. (1987). Molecular cloning and sequence analysis of cDNA coding for the precursor of the human cysteine proteinase inhibitor cystatin C. FEBS Lett 216, 229-233.

Abrahamson, M., Islam, M.Q., Szpirer, J., Szpirer, C., and Levan, G. (1989). The human cystatin C gene (CST3), mutated in hereditary cystatin C amyloid angiopathy, is located on chromosome 20. Hum Genet 82, 223-226.

Afshari, F.T., Kwok, J.C., Andrews, M.R., Blits, B., Martin, K.R., Faissner, A., Ffrench-Constant, C., and Fawcett, J.W. (2010). Integrin activation or alpha 9 expression allows retinal pigmented epithelial cell adhesion on Bruch's membrane in wet age-related macular degeneration. Brain 133, 448-464.

Aisenbrey, S., Zhang, M., Bacher, D., Yee, J., Brunken, W.J., and Hunter, D.D. (2006). Retinal pigment epithelial cells synthesize laminins, including laminin 5, and adhere to them through alpha3- and alpha6-containing integrins. Invest Ophthalmol Vis Sci 47, 5537-5544.

Akerblom, A., Eriksson, N., Wallentin, L., Siegbahn, A., Barratt, B.J., Becker, R.C., Budaj, A., Himmelmann, A., Husted, S., Storey, R.F., et al. (2014). Polymorphism of the cystatin C gene in patients with acute coronary syndromes: Results from the PLATelet inhibition and patient Outcomes study. American heart journal 168, 96-102 e102.

Alder, V.A., and Cringle, S.J. (1985). The effect of the retinal circulation on vitreal oxygen tension. Curr Eye Res 4, 121-129.

Alexander, R.A., Hiscott, P.S., Hart, R.L., and Grierson, I. (1986). Effect of melanin bleaching on immunoperoxidase, with reference to ocular tissues and lesions. Medical laboratory sciences 43, 121-127.

Alizadeh, P., Smit-McBride, Z., Oltjen, S.L., and Hjelmeland, L.M. (2006). Regulation of cysteine cathepsin expression by oxidative stress in the retinal pigment epithelium/choroid of the mouse. Exp Eye Res 83, 679-687.

Allikmets, R., and Consortium, I.A.S. (2000). Further evidence for an association of ABCR alleles with age-related macular degeneration. Am J Hum Genet 67, 487-491.

Allikmets, R., Shroyer, N.F., Singh, N., Seddon, J.M., Lewis, R.A., Bernstein, P.S., Peiffer, A., Zabriskie, N.A., Li, Y., Hutchinson, A., et al. (1997). Mutation of the Stargardt disease gene (ABCR) in age-related macular degeneration. Science 277, 1805-1807.

Almeida, P.C., Nantes, I.L., Chagas, J.R., Rizzi, C.C., Faljoni-Alario, A., Carmona, E., Juliano, L., Nader, H.B., and Tersariol, I.L. (2001). Cathepsin B activity regulation. Heparin-like glycosaminogylcans protect human cathepsin B from alkaline pH-induced inactivation. J Biol Chem 276, 944-951.

Amaral, J.D., Xavier, J.M., Steer, C.J., and Rodrigues, C.M. (2010). The role of p53 in apoptosis. Discov Med 9, 145-152.

Anderson, D.H., Talaga, K.C., Rivest, A.J., Barron, E., Hageman, G.S., and Johnson, L.V. (2004). Characterization of beta amyloid assemblies in drusen: the deposits associated with aging and age-related macular degeneration. Exp Eye Res 78, 243-256.

Andrews, N.W. (2000). Regulated secretion of conventional lysosomes. Trends Cell Biol 10, 316-321.

Andrews, N.W. (2005). Membrane repair and immunological danger. EMBO Rep 6, 826-830.

Appelqvist, H., Waster, P., Eriksson, I., Rosdahl, I., and Ollinger, K. (2013a). Lysosomal exocytosis and caspase-8-mediated apoptosis in UVA-irradiated keratinocytes. J Cell Sci 126, 5578-5584.

Appelqvist, H., Waster, P., Kagedal, K., and Ollinger, K. (2013b). The lysosome: from waste bag to potential therapeutic target. J Mol Cell Biol 5, 214-226.

Arakawa, S., Takahashi, A., Ashikawa, K., Hosono, N., Aoi, T., Yasuda, M., Oshima, Y., Yoshida, S., Enaida, H., Tsuchihashi, T., et al. (2011). Genome-wide association study identifies two susceptibility loci for exudative age-related macular degeneration in the Japanese population. Nat Genet 43, 1001-1004.

Augustin, A.J., and Kirchhof, J. (2009). Inflammation and the pathogenesis of age-related macular degeneration. Expert Opin Ther Targets 13, 641-651.
Baehr, W., Wu, S.M., Bird, A.C., and Palczewski, K. (2003). The retinoid cycle and retina disease. Vision Res 43, 2957-2958.
Baici, A., Lang, A., Horler, D., Kissling, R., and Merlin, C. (1995). Cathepsin B in osteoarthritis: cytochemical and histochemical analysis of human femoral head cartilage. Ann Rheum Dis 54, 289-297.
Balbin, M., and Abrahamson, M. (1991). SstII polymorphic sites in the promoter region of the human cystatin C gene. Hum Genet 87, 751-752.
Balbin, M., Grubb, A., and Abrahamson, M. (1993). An Ala/Thr variation in the coding region of the human cystatin C gene (CST3) detected as a SstII polymorphism. Hum Genet 92, 206-207.
Ballinger, S.W., Van Houten, B., Jin, G.F., Conklin, C.A., and Godley, B.F. (1999). Hydrogen peroxide causes significant mitochondrial DNA damage in human RPE cells. Exp Eye Res 68, 765-772.
Ban, Y., and Rizzolo, L.J. (2000). Differential regulation of tight junction permeability during development of the retinal pigment epithelium. American journal of physiology Cell physiology 279, C744-750.
Barrett, A.J. (1986). The cystatins: a diverse superfamily of cysteine peptidase inhibitors. Biomed Biochim Acta 45, 1363-1374.
Barrett, A.J. (1987). The Cystatins - a New Class of Peptidase Inhibitors. Trends Biochem Sci 12, 193-196.
Barrett, A.J., Davies, M.E., and Grubb, A. (1984). The place of human gamma-trace (cystatin C) amongst the cysteine proteinase inhibitors. Biochem Biophys Res Commun 120, 631-636.
Barrett, A.J., Rawlings, N.D., and Woessner, J.F. (2004). Handbook of proteolytic enzymes, 2nd edn (Amsterdam ; Boston: Elsvier Academic Press).
Basta, G., Lazzerini, G., Del Turco, S., Ratto, G.M., Schmidt, A.M., and De Caterina, R. (2005). At least 2 distinct pathways generating reactive oxygen species mediate vascular cell adhesion molecule-1 induction by advanced glycation end products. Arterioscl Throm Vas 25, 1401-1407.

Baynes, J.W. (2001). The role of AGEs in aging: causation or correlation. Exp Gerontol 36, 1527-1537.

Bazan, N.G., Gordon, W.C., and Rodriguez de Turco, E.B. (1992). Docosahexaenoic acid uptake and metabolism in photoreceptors: retinal conservation by an efficient retinal pigment epithelial cell-mediated recycling process. Adv Exp Med Biol 318, 295-306.

Beatty, S., Koh, H., Phil, M., Henson, D., and Boulton, M. (2000). The role of oxidative stress in the pathogenesis of age-related macular degeneration. Surv Ophthalmol 45, 115-134.

Becerra, S.P., Fariss, R.N., Wu, Y.Q., Montuenga, L.M., Wong, P., and Pfeffer, B.A. (2004). Pigment epithelium-derived factor in the monkey retinal pigment epithelium and interphotoreceptor matrix: apical secretion and distribution. Exp Eye Res 78, 223-234.

Benussi, L., Ghidoni, R., Steinhoff, T., Alberici, A., Villa, A., Mazzoli, F., Nicosia, F., Barbiero, L., Broglio, L., Feudatari, E., et al. (2003). Alzheimer disease-associated cystatin C variant undergoes impaired secretion. Neurobiology of disease 13, 15-21.

Bernstein, H.G., Reichenbach, A., Kirschke, H., and Wiederanders, B. (1989). Cell Type-Specific Distribution of Cathepsin-B and Cathepsin-D Immunoreactivity within the Rabbit Retina. Neurosci Lett 98, 135-138.

Bhutto, I., and Lutty, G. (2012). Understanding age-related macular degeneration (AMD): relationships between the photoreceptor/retinal pigment epithelium/Bruch's membrane/choriocapillaris complex. Mol Aspects Med 33, 295-317.

Bian, B., Mongrain, S., Cagnol, S., Langlois, M.J., Boulanger, J., Bernatchez, G., Carrier, J.C., Boudreau, F., and Rivard, N. (2015). Cathepsin B promotes colorectal tumorigenesis, cell invasion, and metastasis. Mol Carcinog.

Bierhaus, A., Chevion, S., Chevion, M., Hofmann, M., Quehenberger, P., Illmer, T., Luther, T., Berentshtein, E., Tritschler, H., Muller, M., et al. (1997). Advanced glycation end product-induced activation of NF-kappaB is suppressed by alpha-lipoic acid in cultured endothelial cells. Diabetes 46, 1481-1490.

Bjork, I., Brieditis, I., Raub-Segall, E., Pol, E., Hakansson, K., and Abrahamson, M. (1996). The importance of the second hairpin loop of cystatin C for proteinase binding. Characterization of the interaction of Trp-106 variants of the inhibitor with cysteine proteinases. Biochemistry 35, 10720-10726.

Blomgran, R., Zheng, L., and Stendahl, O. (2007). Cathepsin-cleaved Bid promotes apoptosis in human neutrophils via oxidative stress-induced lysosomal membrane permeabilization. J Leukoc Biol 81, 1213-1223.

Bobek, L.A., and Levine, M.J. (1992). Cystatins--inhibitors of cysteine proteinases. Critical reviews in oral biology and medicine : an official publication of the American Association of Oral Biologists 3, 307-332.

Bok, D. (1993). The retinal pigment epithelium: a versatile partner in vision. Journal of cell science Supplement 17, 189-195.

Bok, D., and Hall, M.O. (1971). The role of the pigment epithelium in the etiology of inherited retinal dystrophy in the rat. J Cell Biol 49, 664-682.

Booij, J.C., Baas, D.C., Beisekeeva, J., Gorgels, T.G., and Bergen, A.A. (2010). The dynamic nature of Bruch's membrane. Prog Retin Eye Res 29, 1-18.

Borenstein, M., Hedges, L.V., Higgins, J.P., and Rothstein, H.R. (2010). A basic introduction to fixed-effect and random-effects models for meta-analysis. Res Synth Methods 1, 97-111.

Boulton, M., and Dayhaw-Barker, P. (2001). The role of the retinal pigment epithelium: topographical variation and ageing changes. Eye 15, 384-389.

Boulton, M., Mckechnie, N.M., Breda, J., Bayly, M., and Marshall, J. (1989). The Formation of Auto-Fluorescent Granules in Cultured Human Rpe. Invest Ophth Vis Sci 30, 82-89.

Boulton, M., Moriarty, P., Jarvis-Evans, J., and Marcyniuk, B. (1994). Regional variation and age-related changes of lysosomal enzymes in the human retinal pigment epithelium. Br J Ophthalmol 78, 125-129.

Boya, P., Gonzalez-Polo, R.A., Poncet, D., Andreau, K., Vieira, H.L.A., Roumier, T., Perfettini, J.L., and Kroemer, G. (2003). Mitochondrial membrane permeabilization is a critical step of lysosome-initiated apoptosis induced by hydroxychloroquine. Oncogene 22, 3927-3936.

Brandstetter, C., Mohr, L.K., Latz, E., Holz, F.G., and Krohne, T.U. (2015). Light induces NLRP3 inflammasome activation in retinal pigment epithelial cells via lipofuscin-mediated photooxidative damage. J Mol Med (Berl) 93, 905-916.

Braulke, T., and Bonifacino, J.S. (2009). Sorting of lysosomal proteins. Biochim Biophys Acta 1793, 605-614.

Bressler, N.M., Bressler, S.B., Congdon, N.G., Ferris, F.L., 3rd, Friedman, D.S., Klein, R., Lindblad, A.S., Milton, R.C., Seddon, J.M., and Age-Related Eye Disease Study Research, G. (2003). Potential public health impact of Age-Related Eye Disease Study results: AREDS report no. 11. Arch Ophthalmol 121, 1621-1624.

Bressler, N.M., Bressler, S.B., and Fine, S.L. (1988). Age-related macular degeneration. Surv Ophthalmol 32, 375-413.

Briozzo, P., Morisset, M., Capony, F., Rougeot, C., and Rochefort, H. (1988). In vitro degradation of extracellular matrix with Mr 52,000 cathepsin D secreted by breast cancer cells. Cancer Res 48, 3688-3692.

Bron, A.J., Tripathi, R.C., Tripathi, B.J., and Wolff, E. (1997). Wolff's anatomy of the eye and orbit, 8th edn (London ; New York: Chapman & Hall Medical).

Buck, M.R., Karustis, D.G., Day, N.A., Honn, K.V., and Sloane, B.F. (1992). Degradation of extracellular-matrix proteins by human cathepsin B from normal and tumour tissues. The Biochemical journal 282 (Pt 1), 273-278.

Burke, J.M., and Hjelmeland, L.M. (2005). Mosaicism of the retinal pigment epithelium: seeing the small picture. Molecular interventions 5, 241-249.

Burke, J.M., Mckay, B.S., and Jaffe, G.J. (1991). Retinal-Pigment Epithelial-Cells of the Posterior Pole Have Fewer Na/K Adenosine-Triphosphatase Pumps Than Peripheral Cells. Invest Ophth Vis Sci 32, 2042-2046.

Burke, J.M., and Skumatz, C.M. (1998). Autofluorescent inclusions in long-term postconfluent cultures of retinal pigment epithelium. Invest Ophthalmol Vis Sci 39, 1478-1486.

Burns, M.S., and Hartz, M.J. (1992). The retinal pigment epithelium induces fenestration of endothelial cells in vivo. Curr Eye Res 11, 863-873.

Buschini, E., Piras, A., Nuzzi, R., and Vercelli, A. (2011). Age related macular degeneration and drusen: neuroinflammation in the retina. Prog Neurobiol 95, 14-25.

Buth, H., Buttigieg, P.L., Ostafe, R., Rehders, M., Dannenmann, S.R., Schaschke, N., Stark, H.J., Boukamp, P., and Brix, K. (2007). Cathepsin B is essential for regeneration of scratch-wounded normal human epidermal keratinocytes. Eur J Cell Biol 86, 747-761.

Butler, J.M., Sharif, U., Ali, M., McKibbin, M., Thompson, J.P., Gale, R., Yang, Y.C., Inglehearn, C., and Paraoan, L. (2015). A missense variant in CST3 exerts a recessive effect on susceptibility to age-related macular degeneration resembling its association with Alzheimer's disease. Hum Genet 134, 705-715.

Cadoret, A., Bertrand, F., BaronDelage, S., Levy, P., Courtois, G., Gespach, C., Capeau, J., and Cherqui, G. (1997). Down-regulation of NF-kappa B activity and NF-kappa B p65 subunit expression by ras and polyoma middle T oncogenes in human colonic Caco-2 cells. Oncogene 14, 1589-1600.

Caglic, D., Pungercar, J.R., Pejler, G., Turk, V., and Turk, B. (2007). Glycosaminoglycans facilitate procathepsin B activation through disruption of propeptide-mature enzyme interactions. J Biol Chem 282, 33076-33085.

Cai, X., and McGinnis, J.F. (2012). Oxidative stress: the achilles' heel of neurodegenerative diseases of the retina. Front Biosci (Landmark Ed) 17, 1976-1995.

Cayouette, M., Smith, S.B., Becerra, S.P., and Gravel, C. (1999). Pigment epithelium-derived factor delays the death of photoreceptors in mouse models of inherited retinal degenerations. Neurobiology of disease 6, 523-532.

Chen, K.L., Chang, W.S., Cheung, C.H., Lin, C.C., Huang, C.C., Yang, Y.N., Kuo, C.P., Kuo, C.C., Chang, Y.H., Liu, K.J., et al. (2012a). Targeting cathepsin S induces tumor cell autophagy via the EGFR-ERK signaling pathway. Cancer Lett 317, 89-98.

Chen, L., Miyamura, N., Ninomiya, Y., and Handa, J.T. (2003). Distribution of the collagen IV isoforms in human Bruch's membrane. Br J Ophthalmol 87, 212-215.

Chen, Q.Y., Shi, J.G., Yao, Q.H., Jiao, D.M., Wang, Y.Y., Hu, H.Z., Wu, Y.Q., Song, J., Yan, J., and Wu, L.J. (2012b). Lysosomal membrane permeabilization is involved in curcumin-induced apoptosis of A549 lung carcinoma cells. Molecular and Cellular Biochemistry 359, 389-398.

Chen, W., Stambolian, D., Edwards, A.O., Branham, K.E., Othman, M., Jakobsdottir, J., Tosakulwong, N., Pericak-Vance, M.A., Campochiaro, P.A., Klein, M.L., et al. (2010). Genetic variants near TIMP3 and high-density lipoprotein-associated loci influence susceptibility to age-related macular degeneration. Proc Natl Acad Sci U S A 107, 7401-7406.

Cheng, R., Lin, B., and Ortwerth, B.J. (2002). Rate of formation of AGEs during ascorbate glycation and during aging in human lens tissue. Biochim Biophys Acta 1587, 65-74.

Chong, E.W., Kreis, A.J., Wong, T.Y., Simpson, J.A., and Guymer, R.H. (2008). Alcohol consumption and the risk of age-related macular degeneration: a systematic review and meta-analysis. Am J Ophthalmol 145, 707-715.

Ciechanover, A. (2005). Proteolysis: from the lysosome to ubiquitin and the proteasome. Nat Rev Mol Cell Biol 6, 79-87.

Cipriani, V., Leung, H.T., Plagnol, V., Bunce, C., Khan, J.C., Shahid, H., Moore, A.T., Harding, S.P., Bishop, P.N., Hayward, C., et al. (2012). Genome-wide association study of age-related macular degeneration identifies associated variants in the TNXB-FKBPL-NOTCH4 region of chromosome 6p21.3. Hum Mol Genet 21, 4138-4150.

Cirman, T., Oresic, K., Mazovec, G.D., Turk, V., Reed, J.C., Myers, R.M., Salvesen, G.S., and Turk, B. (2004). Selective disruption of lysosomes in HeLa cells triggers apoptosis mediated by cleavage of Bid by multiple papain-like lysosomal cathepsins. J Biol Chem 279, 3578-3587.

Collins, T.J. (2007). ImageJ for microscopy. BioTechniques 43, 25-30.

Conus, S., and Simon, H.U. (2008). Cathepsins: key modulators of cell death and inflammatory responses. Biochem Pharmacol 76, 1374-1382.

Costa, V., and Moradas-Ferreira, P. (2001). Oxidative stress and signal transduction in Saccharomyces cerevisiae: insights into ageing, apoptosis and diseases. Mol Aspects Med 22, 217-246.

Coutinho, M.F., Prata, M.J., and Alves, S. (2012). Mannose-6-phosphate pathway: a review on its role in lysosomal function and dysfunction. Mol Genet Metab 105, 542-550.

Crane, I.J., and Liversidge, J. (2008). Mechanisms of leukocyte migration across the blood-retina barrier. Semin Immunopathol 30, 165-177.

Cruickshanks, K.J., Klein, R., Klein, B.E., and Nondahl, D.M. (2001). Sunlight and the 5-year incidence of early age-related maculopathy: the beaver dam eye study. Arch Ophthalmol 119, 246-250.

Cui, H., Kong, Y., and Zhang, H. (2012). Oxidative stress, mitochondrial dysfunction, and aging. J Signal Transduct 2012, 646354.

Curcio, C.A., and Millican, C.L. (1999). Basal linear deposit and large drusen are specific for early age-related maculopathy. Arch Ophthalmol 117, 329-339.

Curcio, C.A., Sloan, K.R., Kalina, R.E., and Hendrickson, A.E. (1990). Human photoreceptor topography. J Comp Neurol 292, 497-523.

Davis, A.A., Bernstein, P.S., Bok, D., Turner, J., Nachtigal, M., and Hunt, R.C. (1995). A human retinal pigment epithelial cell line that retains epithelial characteristics after prolonged culture. Invest Ophthalmol Vis Sci 36, 955-964.

Dawson, D.W., Volpert, O.V., Gillis, P., Crawford, S.E., Xu, H., Benedict, W., and Bouck, N.P. (1999). Pigment epithelium-derived factor: a potent inhibitor of angiogenesis. Science 285, 245-248.

de Jong, P.T. (2006). Age-related macular degeneration. N Engl J Med 355, 1474-1485.

Del Priore, L.V., Geng, L., Tezel, T.H., and Kaplan, H.J. (2002). Extracellular matrix ligands promote RPE attachment to inner Bruch's membrane. Curr Eye Res 25, 79-89.

Del Priore, L.V., and Tezel, T.H. (1998). Reattachment rate of human retinal pigment epithelium to layers of human Bruch's membrane. Arch Ophthalmol 116, 335-341.

Dennemarker, J., Lohmuller, T., Muller, S., Aguilar, S.V., Tobin, D.J., Peters, C., and Reinheckel, T. (2010). Impaired turnover of autophagolysosomes in cathepsin L deficiency. Biological Chemistry 391, 913-922.

Ding, J.D., Johnson, L.V., Herrmann, R., Farsiu, S., Smith, S.G., Groelle, M., Mace, B.E., Sullivan, P., Jamison, J.A., Kelly, U., et al. (2011). Anti-amyloid therapy protects against retinal pigmented epithelium damage and vision loss in a model of age-related macular degeneration. Proc Natl Acad Sci U S A 108, E279-287.

Dominguez, L., Sosa-Peinado, A., and Hansberg, W. (2010). Catalase evolved to concentrate H2O2 at its active site. Archives of Biochemistry and Biophysics 500, 82-91.

Donoso, L.A., Kim, D., Frost, A., Callahan, A., and Hageman, G. (2006). The role of inflammation in the pathogenesis of age-related macular degeneration. Surv Ophthalmol 51, 137-152.

Dorey, C.K., Wu, G., Ebenstein, D., Garsd, A., and Weiter, J.J. (1989). Cell loss in the aging retina. Relationship to lipofuscin accumulation and macular degeneration. Invest Ophthalmol Vis Sci 30, 1691-1699.

Driessen, C.A., Janssen, B.P., Winkens, H.J., van Vugt, A.H., de Leeuw, T.L., and Janssen, J.J. (1995). Cloning and expression of a cDNA encoding bovine retinal pigment epithelial 11-cis retinol dehydrogenase. Invest Ophthalmol Vis Sci 36, 1988-1996.

Droga-Mazovec, G., Bojic, L., Petelin, A., Ivanova, S., Romih, R., Repnik, U., Salvesen, G.S., Stoka, V., Turk, V., and Turk, B. (2008). Cysteine cathepsins trigger caspase-dependent cell death through cleavage of bid and antiapoptotic Bcl-2 homologues. J Biol Chem 283, 19140-19150.

Duewell, P., Kono, H., Rayner, K.J., Sirois, C.M., Vladimer, G., Bauernfeind, F.G., Abela, G.S., Franchi, L., Nunez, G., Schnurr, M., et al. (2010). NLRP3 inflammasomes are required for atherogenesis and activated by cholesterol crystals. Nature 464, 1357-1361.

Dunaief, J.L., Dentchev, T., Ying, G.S., and Milam, A.H. (2002). The role of apoptosis in age-related macular degeneration. Arch Ophthalmol 120, 1435-1442.

Dunn, K.C., Aotaki-Keen, A.E., Putkey, F.R., and Hjelmeland, L.M. (1996). ARPE-19, a human retinal pigment epithelial cell line with differentiated properties. Exp Eye Res 62, 155-169.

Edwards, A.O., Ritter, R., 3rd, Abel, K.J., Manning, A., Panhuysen, C., and Farrer, L.A. (2005). Complement factor H polymorphism and age-related macular degeneration. Science 308, 421-424.

Eldred, G.E., and Lasky, M.R. (1993). Retinal age pigments generated by self-assembling lysosomotropic detergents. Nature 361, 724-726.

Erickson, A.H., Conner, G.E., and Blobel, G. (1981). Biosynthesis of a lysosomal enzyme. Partial structure of two transient and functionally distinct NH2-terminal sequences in cathepsin D. J Biol Chem 256, 11224-11231.

Escobar, M.A. (2013). Advances in the treatment of inherited coagulation disorders. Haemophilia : the official journal of the World Federation of Hemophilia 19, 648-659.

Eskelinen, E.L., Tanaka, Y., and Saftig, P. (2003). At the acidic edge: emerging functions for lysosomal membrane proteins. Trends Cell Biol 13, 137-145.

Esterbauer, H., Schaur, R.J., and Zollner, H. (1991). Chemistry and biochemistry of 4-hydroxynonenal, malonaldehyde and related aldehydes. Free Radic Biol Med 11, 81-128.

Everts, V., Hou, W.S., Rialland, X., Tigchelaar, W., Saftig, P., Bromme, D., Gelb, B.D., and Beertsen, W. (2003). Cathepsin K deficiency in pycnodysostosis results in accumulation of non-digested phagocytosed collagen in fibroblasts. Calcif Tissue Int 73, 380-386.

Everts, V., Korper, W., Niehof, A., Jansen, I., and Beertsen, W. (1995). Type-Vi Collagen Is Phagocytosed by Fibroblasts and Digested in the Lysosomal Apparatus - Involvement of Collagenase, Serine Proteinases and Lysosomal-Enzymes. Matrix Biol 14, 665-676.

Fang, I.M., Yang, C.H., Yang, C.M., and Chen, M.S. (2009). Overexpression of integrin alpha6 and beta4 enhances adhesion and proliferation of human retinal pigment epithelial cells on layers of porcine Bruch's membrane. Exp Eye Res 88, 12-21.

Feeney-Burns, L., Hilderbrand, E.S., and Eldridge, S. (1984). Aging human RPE: morphometric analysis of macular, equatorial, and peripheral cells. Invest Ophthalmol Vis Sci 25, 195-200.

Feeney, L. (1978). Lipofuscin and melanin of human retinal pigment epithelium. Fluorescence, enzyme cytochemical, and ultrastructural studies. Invest Ophthalmol Vis Sci 17, 583-600.

Feeneyburns, L., and Eldred, G.E. (1983). The Fate of the Phagosome - Conversion to Age Pigment and Impact in Human Retinal-Pigment Epithelium. T Ophthal Soc Uk 103, 416-421.

Felbor, U., Dreier, L., Bryant, R.A., Ploegh, H.L., Olsen, B.R., and Mothes, W. (2000). Secreted cathepsin L generates endostatin from collagen XVIII. The EMBO journal 19, 1187-1194.

Felbor, U., Kessler, B., Mothes, W., Goebel, H.H., Ploegh, H.L., Bronson, R.T., and Olsen, B.R. (2002). Neuronal loss and brain atrophy in mice lacking cathepsins B and L. Proc Natl Acad Sci U S A 99, 7883-7888.

Ferreras, M., Felbor, U., Lenhard, T., Olsen, B.R., and Delaisse, J. (2000). Generation and degradation of human endostatin proteins by various proteinases. FEBS letters 486, 247-251.

Festa, A., Schmolzer, B., Schernthaner, G., and Menzel, E.J. (1998). Differential expression of receptors for advanced glycation end products on monocytes in patients with IDDM. Diabetologia 41, 674-680.

Finckh, U., von der Kammer, H., Velden, J., Michel, T., Andresen, B., Deng, A., Zhang, J., Muller-Thomsen, T., Zuchowski, K., Menzer, G., et al. (2000). Genetic association of a cystatin C gene polymorphism with late-onset Alzheimer disease. Arch Neurol 57, 1579-1583.

Finnemann, S.C. (2003). Focal adhesion kinase signaling promotes phagocytosis of integrin-bound photoreceptors. EMBO J 22, 4143-4154.

Finnemann, S.C., Bonilha, V.L., Marmorstein, A.D., and Rodriguez-Boulan, E. (1997). Phagocytosis of rod outer segments by retinal pigment epithelial cells requires alpha(v)beta5 integrin for binding but not for internalization. Proc Natl Acad Sci U S A 94, 12932-12937.

Finnemann, S.C., Leung, L.W., and Rodriguez-Boulan, E. (2002). The lipofuscin component A2E selectively inhibits phagolysosomal degradation of photoreceptor phospholipid by the retinal pigment epithelium. P Natl Acad Sci USA 99, 3842-3847.

Fisher, S.A., Abecasis, G.R., Yashar, B.M., Zareparsi, S., Swaroop, A., Iyengar, S.K., Klein, B.E., Klein, R., Lee, K.E., Majewski, J., et al. (2005). Meta-analysis of genome scans of age-related macular degeneration. Hum Mol Genet 14, 2257-2264.

Fonovic, M., and Turk, B. (2014). Cysteine cathepsins and extracellular matrix degradation. Biochim Biophys Acta 1840, 2560-2570.

Frank, R.N., Amin, R.H., and Puklin, J.E. (1999). Antioxidant enzymes in the macular retinal pigment epithelium of eyes with neovascular age-related macular degeneration. Am J Ophthalmol 127, 694-709.

Franze, K., Grosche, J., Skatchkov, S.N., Schinkinger, S., Foja, C., Schlid, D., Uckermann, O., Travis, K., Reichenbach, A., and Guck, J. (2007). Muller cells are living optical fibers in the vertebrate retina. P Natl Acad Sci USA 104, 8287-8292.

Fritsche, L.G., Chen, W., Schu, M., Yaspan, B.L., Yu, Y., Thorleifsson, G., Zack, D.J., Arakawa, S., Cipriani, V., Ripke, S., et al. (2013). Seven new loci associated with age-related macular degeneration. Nat Genet 45, 433-439, 439e431-432.

Fritsche, L.G., Freitag-Wolf, S., Bettecken, T., Meitinger, T., Keilhauer, C.N., Krawczak, M., and Weber, B.H. (2009). Age-related macular degeneration and functional promoter and coding variants of the apolipoprotein E gene. Human mutation 30, 1048-1053.

Frohlich, E., and Klessen, C. (2001). Enzymatic heterogeneity of bovine retinal pigment epithelial cells in vivo and in vitro. Graefes Arch Clin Exp Ophthalmol 239, 25-34.

Fukai, N., Eklund, L., Marneros, A.G., Oh, S.P., Keene, D.R., Tamarkin, L., Niemela, M., Ilves, M., Li, E., Pihlajaniemi, T., et al. (2002). Lack of collagen XVIII/endostatin results in eye abnormalities. The EMBO journal 21, 1535-1544.

Fusek, M., and Vetvicka, V. (2005). Dual role of cathepsin D: ligand and protease. Biomed Pap Med Fac Univ Palacky Olomouc Czech Repub 149, 43-50.

Garg, T.K., and Chang, J.Y. (2004). 15-deoxy-delta 12, 14-Prostaglandin J2 prevents reactive oxygen species generation and mitochondrial membrane depolarization induced by oxidative stress. BMC Pharmacol 4, 6.

Gaudet, D., Methot, J., Dery, S., Brisson, D., Essiembre, C., Tremblay, G., Tremblay, K., de Wal, J., Twisk, J., van den Bulk, N., et al. (2013). Efficacy and long-term safety of alipogene tiparvovec (AAV1-LPLS447X) gene therapy for lipoprotein lipase deficiency: an open-label trial. Gene therapy 20, 361-369.

Gehrs, K.M., Anderson, D.H., Johnson, L.V., and Hageman, G.S. (2006). Age-related macular degeneration--emerging pathogenetic and therapeutic concepts. Annals of medicine 38, 450-471.

Gelb, B.D., Shi, G.P., Chapman, H.A., and Desnick, R.J. (1996). Pycnodysostosis, a lysosomal disease caused by cathepsin K deficiency. Science 273, 1236-1238.

Ghiso, J., Saball, E., Leoni, J., Rostagno, A., and Frangione, B. (1990). Binding of cystatin C to C4: the importance of sense-antisense peptides in their interaction. Proc Natl Acad Sci U S A 87, 1288-1291.

Giard, D.J., Aaronson, S.A., Todaro, G.J., Arnstein, P., Kersey, J.H., Dosik, H., and Parks, W.P. (1973). In vitro cultivation of human tumors: establishment of cell lines derived from a series of solid tumors. Journal of the National Cancer Institute 51, 1417-1423.

Gibson, G. (2011). Rare and common variants: twenty arguments. Nat Rev Genet 13, 135-145.

Gillet, L., Roger, S., Besson, P., Lecaille, F., Gore, J., Bougnoux, P., Lalmanach, G., and Le Guennec, J.Y. (2009). Voltage-gated Sodium Channel Activity Promotes Cysteine Cathepsin-dependent Invasiveness and Colony Growth of Human Cancer Cells. J Biol Chem 284, 8680-8691.

Glenn, J.V., Mahaffy, H., Dasari, S., Oliver, M., Chen, M., Boulton, M.E., Xu, H., Curry, W.J., and Stitt, A.W. (2012). Proteomic profiling of human retinal pigment epithelium exposed to an advanced glycation-modified substrate. Graefes Arch Clin Exp Ophthalmol 250, 349-359.

Glenn, J.V., Mahaffy, H., Wu, K., Smith, G., Nagai, R., Simpson, D.A., Boulton, M.E., and Stitt, A.W. (2009). Advanced glycation end product (AGE)

accumulation on Bruch's membrane: links to age-related RPE dysfunction. Invest Ophthalmol Vis Sci 50, 441-451.

Glomb, M.A., and Monnier, V.M. (1995). Mechanism of protein modification by glyoxal and glycolaldehyde, reactive intermediates of the Maillard reaction. J Biol Chem 270, 10017-10026.

Godat, E., Herve-Grvepinet, V., Veillard, F., Lecaille, F., Belghazi, M., Bromme, D., and Lalmanach, G. (2008). Regulation of cathepsin K activity by hydrogen peroxide. Biol Chem 389, 1123-1126.

Goldberg, A.L., and Dice, J.F. (1974). Intracellular protein degradation in mammalian and bacterial cells. Annu Rev Biochem 43, 835-869.

Gong, J., Sagiv, O., Cai, H., Tsang, S.H., and Del Priore, L.V. (2008). Effects of extracellular matrix and neighboring cells on induction of human embryonic stem cells into retinal or retinal pigment epithelial progenitors. Experimental Eye Research 86, 957-965.

Gonzalez, M.R., Bischofberger, M., Pernot, L., van der Goot, F.G., and Freche, B. (2008). Bacterial pore-forming toxins: the (w)hole story? Cell Mol Life Sci 65, 493-507.

Gordois, A., Cutler, H., Pezzullo, L., Gordon, K., Cruess, A., Winyard, S., Hamilton, W., and Chua, K. (2012). An estimation of the worldwide economic and health burden of visual impairment. Global public health 7, 465-481.

Gottlieb, R.A., Giesing, H.A., Zhu, J.Y., Engler, R.L., and Babior, B.M. (1995). Cell acidification in apoptosis: granulocyte colony-stimulating factor delays programmed cell death in neutrophils by up-regulating the vacuolar H(+)-ATPase. Proc Natl Acad Sci U S A 92, 5965-5968.

Grimm, S., Ernst, L., Grotzinger, N., Hohn, A., Breusing, N., Reinheckel, T., and Grune, T. (2010). Cathepsin D is one of the major enzymes involved in intracellular degradation of AGE-modified proteins. Free Radical Res 44, 1013-1026.

Grimm, S., Horlacher, M., Catalgol, B., Hoehn, A., Reinheckel, T., and Grune, T. (2012). Cathepsins D and L reduce the toxicity of advanced glycation end products. Free Radic Biol Med 52, 1011-1023.

Grindle, C.F., and Marshall, J. (1978). Ageing changes in Bruch's membrane and their functional implications. Trans Ophthalmol Soc U K 98, 172-175.

Grizzard, S.W., Arnett, D., and Haag, S.L. (2003). Twin study of age-related macular degeneration. Ophthalmic Epidemiol 10, 315-322.

Grune, T., Jung, T., Merker, K., and Davies, K.J. (2004). Decreased proteolysis caused by protein aggregates, inclusion bodies, plaques, lipofuscin, ceroid, and 'aggresomes' during oxidative stress, aging, and disease. Int J Biochem Cell Biol 36, 2519-2530.

Guha, S., and Padh, H. (2008). Cathepsins: fundamental effectors of endolysosomal proteolysis. Indian J Biochem Biophys 45, 75-90.

Guinec, N., Dalet-Fumeron, V., and Pagano, M. (1993). "In vitro" study of basement membrane degradation by the cysteine proteinases, cathepsins B, B-like and L. Digestion of collagen IV, laminin, fibronectin, and release of gelatinase activities from basement membrane fibronectin. Biol Chem Hoppe Seyler 374, 1135-1146.

Hageman, G.S., Anderson, D.H., Johnson, L.V., Hancox, L.S., Taiber, A.J., Hardisty, L.I., Hageman, J.L., Stockman, H.A., Borchardt, J.D., Gehrs, K.M., et al. (2005). A common haplotype in the complement regulatory gene factor H (HF1/CFH) predisposes individuals to age-related macular degeneration. Proc Natl Acad Sci U S A 102, 7227-7232.

Hageman, G.S., Luthert, P.J., Chong, N.H.V., Johnson, L.V., Anderson, D.H., and Mullins, R.F. (2001). An integrated hypothesis that considers drusen as biomarkers of immune-mediated processes at the RPE-Bruch's membrane interface in aging and age-related macular degeneration. Progress in Retinal and Eye Research 20, 705-732.

Haines, J.L., Hauser, M.A., Schmidt, S., Scott, W.K., Olson, L.M., Gallins, P., Spencer, K.L., Kwan, S.Y., Noureddine, M., Gilbert, J.R., et al. (2005). Complement factor H variant increases the risk of age-related macular degeneration. Science 308, 419-421.

Hall, A., Dalboge, H., Grubb, A., and Abrahamson, M. (1993). Importance of the evolutionarily conserved glycine residue in the N-terminal region of human cystatin C (Gly-11) for cysteine endopeptidase inhibition. Biochem J 291 (Pt 1), 123-129.

Hamann, S. (2002). Molecular mechanisms of water transport in the eye. International review of cytology 215, 395-431.

Hammond, C.J., Webster, A.R., Snieder, H., Bird, A.C., Gilbert, C.E., and Spector, T.D. (2002). Genetic influence on early age-related maculopathy: a twin study. Ophthalmology 109, 730-736.

Handa, J.T., Verzijl, N., Matsunaga, H., Aotaki-Keen, A., Lutty, G.A., te Koppele, J.M., Miyata, T., and Hjelmeland, L.M. (1999). Increase in the advanced glycation end product pentosidine in Bruch's membrane with age. Invest Ophthalmol Vis Sci 40, 775-779.

Harold, D., Abraham, R., Hollingworth, P., Sims, R., Gerrish, A., Hamshere, M.L., Pahwa, J.S., Moskvina, V., Dowzell, K., Williams, A., et al. (2009). Genome-wide association study identifies variants at CLU and PICALM associated with Alzheimer's disease. Nat Genet 41, 1088-1093.

Haucke, E., Navarrete-Santos, A., Simm, A., Silber, R.E., and Hofmann, B. (2014). Glycation of extracellular matrix proteins impairs migration of immune cells. Wound Repair Regen 22, 239-245.

He, Q., You, H., Li, X.M., Liu, T.H., Wang, P., and Wang, B.E. (2012). HMGB1 promotes the synthesis of pro-IL-1beta and pro-IL-18 by activation of p38 MAPK and NF-kappaB through receptors for advanced glycation end-products in macrophages. Asian Pac J Cancer Prev 13, 1365-1370.

Hedstrom, L. (2002). Serine protease mechanism and specificity. Chem Rev 102, 4501-4524.

Heidtmann, H.H., Salge, U., Havemann, K., Kirschke, H., and Wiederanders, B. (1993). Secretion of a latent, acid activatable cathepsin L precursor by human non-small cell lung cancer cell lines. Oncol Res 5, 441-451.

Hershko, A., and Ciechanover, A. (1998). The ubiquitin system. Annu Rev Biochem 67, 425-479.

Herve-Grepinet, V., Veillard, F., Godat, E., Heuze-Vourc'h, N., Lecaille, F., and Lalmanach, G. (2008). Extracellular catalase activity protects cysteine cathepsins from inactivation by hydrogen peroxide. FEBS Lett 582, 1307-1312.

Hewitt, A.T., Nakazawa, K., and Newsome, D.A. (1989). Analysis of newly synthesized Bruch's membrane proteoglycans. Invest Ophthalmol Vis Sci 30, 478-486.

Hewitt, A.T., and Newsome, D.A. (1985). Altered synthesis of Bruch's membrane proteoglycans associated with dominant retinitis pigmentosa. Curr Eye Res 4, 169-174.

Higgins, J.P., Thompson, S.G., Deeks, J.J., and Altman, D.G. (2003). Measuring inconsistency in meta-analyses. BMJ 327, 557-560.

Hiscott, J., Marois, J., Garoufalis, J., D'Addario, M., Roulston, A., Kwan, I., Pepin, N., Lacoste, J., Nguyen, H., Bensi, G., et al. (1993). Characterization of a functional NF-kappa B site in the human interleukin 1 beta promoter: evidence for a positive autoregulatory loop. Mol Cell Biol 13, 6231-6240.

Hoffmann, S., Friedrichs, U., Eichler, W., Rosenthal, A., and Wiedemann, P. (2002). Advanced glycation end products induce choroidal endothelial cell proliferation, matrix metalloproteinase-2 and VEGF upregulation in vitro. Graefes Arch Clin Exp Ophthalmol 240, 996-1002.

Hofmann, K.P. (1999). Signalling states of photoactivated rhodopsin. Novartis Foundation symposium 224, 158-175; discussion 175-180.

Hogan, M.J. (1961). Ultrastructure of the choroid. Its role in the pathogenesis of chorioretinal disease. Trans Pac Coast Otoophthalmol Soc Annu Meet 42, 61-87.

Hogan, M.J., Alvarado, J.A., and Weddell, J.E. (1971). Histology of the human eye; an atlas and textbook (Philadelphia,: Saunders).

Hohn, A., Jung, T., Grimm, S., and Grune, T. (2010). Lipofuscin-bound iron is a major intracellular source of oxidants: role in senescent cells. Free Radic Biol Med 48, 1100-1108.

Hollingworth, P., Harold, D., Sims, R., Gerrish, A., Lambert, J.C., Carrasquillo, M.M., Abraham, R., Hamshere, M.L., Pahwa, J.S., Moskvina, V., et al. (2011). Common variants at ABCA7, MS4A6A/MS4A4E, EPHA1, CD33 and CD2AP are associated with Alzheimer's disease. Nat Genet 43, 429-435.

Hollyfield, J.G. (1999). Hyaluronan and the functional organization of the interphotoreceptor matrix. Invest Ophthalmol Vis Sci 40, 2767-2769.

Holopainen, J.M., Angelova, M.I., and Kinnunen, P.K. (2000). Vectorial budding of vesicles by asymmetrical enzymatic formation of ceramide in giant liposomes. Biophys J 78, 830-838.

Holz, F.G., Schutt, F., Kopitz, J., Eldred, G.E., Kruse, F.E., Volcker, H.E., and Cantz, M. (1999). Inhibition of lysosomal degradative functions in RPE cells by a retinoid component of lipofuscin. Invest Ophthalmol Vis Sci 40, 737-743.

Honda, S., Farboud, B., Hjelmeland, L.M., and Handa, J.T. (2001). Induction of an aging mRNA retinal pigment epithelial cell phenotype by matrix-containing advanced glycation end products in vitro. Invest Ophthalmol Vis Sci 42, 2419-2425.

Hook, V.Y., Kindy, M., and Hook, G. (2008). Inhibitors of cathepsin B improve memory and reduce beta-amyloid in transgenic Alzheimer disease mice expressing the wild-type, but not the Swedish mutant, beta-secretase site of the amyloid precursor protein. J Biol Chem 283, 7745-7753.

Hornung, V., Bauernfeind, F., Halle, A., Samstad, E.O., Kono, H., Rock, K.L., Fitzgerald, K.A., and Latz, E. (2008). Silica crystals and aluminum salts activate the NALP3 inflammasome through phagosomal destabilization. Nat Immunol 9, 847-856.

Hou, X., Hu, Z., Xu, H., Xu, J., Zhang, S., Zhong, Y., He, X., and Wang, N. (2014). Advanced glycation endproducts trigger autophagy in cadiomyocyte via RAGE/PI3K/AKT/mTOR pathway. Cardiovasc Diabetol 13, 78.

Howard, C., Garcia-Finana, M., Yan, Q., and Hiscott, P. (2010). Human retinal pigment epithelial SPARC expression and age: an immunohistochemical study. Histology and histopathology 25, 1163-1169.

Howes, K.A., Liu, Y., Dunaief, J.L., Milam, A., Frederick, J.M., Marks, A., and Baehr, W. (2004). Receptor for advanced glycation end products and age-related macular degeneration. Invest Ophthalmol Vis Sci 45, 3713-3720.

Hroudova, J., and Fisar, Z. (2013). Control mechanisms in mitochondrial oxidative phosphorylation. Neural Regen Res 8, 363-375.

Hsu, K.F., Wu, C.L., Huang, S.C., Wu, C.M., Hsiao, J.R., Yo, Y.T., Chen, Y.H., Shiau, A.L., and Chou, C.Y. (2009). Cathepsin L mediates resveratrol-induced autophagy and apoptotic cell death in cervical cancer cells. Autophagy 5, 451-460.

Hu, J., Nakano, H., Sakurai, H., and Colburn, N.H. (2004). Insufficient p65 phosphorylation at S536 specifically contributes to the lack of NF-kappa B

activation and transformation in resistant JB6 cells. Carcinogenesis 25, 1991-2003.

Hu, P., Lai, D., Lu, P., Gao, J., and He, H. (2012). ERK and Akt signaling pathways are involved in advanced glycation end product-induced autophagy in rat vascular smooth muscle cells. Int J Mol Med 29, 613-618.

Hua, Y., Zhao, H., Lu, X., Kong, Y., and Jin, H. (2012). Meta-analysis of the cystatin C(CST3) gene G73A polymorphism and susceptibility to Alzheimer's disease. Int J Neurosci 122, 431-438.

Hughes, C.S., Postovit, L.M., and Lajoie, G.A. (2010). Matrigel: a complex protein mixture required for optimal growth of cell culture. Proteomics 10, 1886-1890.

Huttunen, H.J., Fages, C., and Rauvala, H. (1999). Receptor for advanced glycation end products (RAGE)-mediated neurite outgrowth and activation of NF-kappaB require the cytoplasmic domain of the receptor but different downstream signaling pathways. J Biol Chem 274, 19919-19924.

Ida, H., Boylan, S.A., Weigel, A.L., Smit-McBride, Z., Chao, A., Gao, J., Buchoff, P., Wistow, G., and Hjelmeland, L.M. (2004). EST analysis of mouse retina and RPE/choroid cDNA libraries. Mol Vis 10, 439-444.

Inatani, M., and Tanihara, H. (2002). Proteoglycans in retina. Prog Retin Eye Res 21, 429-447.

Iriyama, A., Fujiki, R., Inoue, Y., Takahashi, H., Tamaki, Y., Takezawa, S., Takeyama, K., Jang, W.D., Kato, S., and Yanagi, Y. (2008). A2E, a pigment of the lipofuscin of retinal pigment epithelial cells, is an endogenous ligand for retinoic acid receptor. Journal of Biological Chemistry 283, 11947-11953.

Ishibashi, T., Murata, T., Hangai, M., Nagai, R., Horiuchi, S., Lopez, P.F., Hinton, D.R., and Ryan, S.J. (1998). Advanced glycation end products in age-related macular degeneration. Arch Ophthalmol 116, 1629-1632.

Ishidoh, K., and Kominami, E. (1995). Procathepsin L degrades extracellular matrix proteins in the presence of glycosaminoglycans in vitro. Biochem Biophys Res Commun 217, 624-631.

Ivy, G.O., Kanai, S., Ohta, M., Smith, G., Sato, Y., Kobayashi, M., and Kitani, K. (1989). Lipofuscin-like substances accumulate rapidly in brain, retina and

internal organs with cysteine protease inhibition. Adv Exp Med Biol 266, 31-45; discussion 45-37.

Jager, R.D., Mieler, W.F., and Miller, J.W. (2008). Age-related macular degeneration. N Engl J Med 358, 2606-2617.

Jaiswal, J.K., Andrews, N.W., and Simon, S.M. (2002). Membrane proximal lysosomes are the major vesicles responsible for calcium-dependent exocytosis in nonsecretory cells. J Cell Biol 159, 625-635.

Jakobsdottir, J., Conley, Y.P., Weeks, D.E., Mah, T.S., Ferrell, R.E., and Gorin, M.B. (2005). Susceptibility genes for age-related maculopathy on chromosome 10q26. Am J Hum Genet 77, 389-407.

Janowski, R., Kozak, M., Jankowska, E., Grzonka, Z., Grubb, A., Abrahamson, M., and Jaskolski, M. (2001). Human cystatin C, an amyloidogenic protein, dimerizes through three-dimensional domain swapping. Nat Struct Biol 8, 316-320.

Jarrett, S.G., and Boulton, M.E. (2012). Consequences of oxidative stress in age-related macular degeneration. Mol Aspects Med 33, 399-417.

Jurkovic, S., Osredkar, J., and Marc, J. (2008). Molecular impact of glutathione peroxidases in antioxidant processes. Biochem Medica 18, 162-174.

Kaarniranta, K., Salminen, A., Haapasalo, A., Soininen, H., and Hiltunen, M. (2011). Age-related macular degeneration (AMD): Alzheimer's disease in the eye? J Alzheimers Dis 24, 615-631.

Kaarniranta, K., Sinha, D., Blasiak, J., Kauppinen, A., Vereb, Z., Salminen, A., Boulton, M.E., and Petrovski, G. (2013). Autophagy and heterophagy dysregulation leads to retinal pigment epithelium dysfunction and development of age-related macular degeneration. Autophagy 9, 973-984.

Kaemmerer, E., Schutt, F., Krohne, T.U., Holz, F.G., and Kopitz, J. (2007). Effects of lipid peroxidation-related protein modifications on RPE lysosomal functions and POS phagocytosis. Invest Ophthalmol Vis Sci 48, 1342-1347.

Kaeser, S.A., Herzig, M.C., Coomaraswamy, J., Kilger, E., Selenica, M.L., Winkler, D.T., Staufenbiel, M., Levy, E., Grubb, A., and Jucker, M. (2007). Cystatin C modulates cerebral beta-amyloidosis. Nat Genet 39, 1437-1439.

Kandarakis, S.A., Piperi, C., Topouzis, F., and Papavassiliou, A.G. (2014). Emerging role of advanced glycation-end products (AGEs) in the pathobiology of eye diseases. Prog Retin Eye Res 42, 85-102.

Karunadharma, P.P., Nordgaard, C.L., Olsen, T.W., and Ferrington, D.A. (2010). Mitochondrial DNA Damage as a Potential Mechanism for Age-Related Macular Degeneration. Invest Ophth Vis Sci 51, 5470-5479.

Karwatowski, W.S., Jeffries, T.E., Duance, V.C., Albon, J., Bailey, A.J., and Easty, D.L. (1995). Preparation of Bruch's membrane and analysis of the age-related changes in the structural collagens. Br J Ophthalmol 79, 944-952.

Katz, M.L. (1989). Incomplete Proteolysis May Contribute to Lipofuscin Accumulation in the Retinal-Pigment Epithelium. Lipofuscin and Ceroid Pigments 266, 109-118.

Katz, M.L., and Robison, W.G., Jr. (1984). Age-related changes in the retinal pigment epithelium of pigmented rats. Exp Eye Res 38, 137-151.

Katz, M.L., and Shanker, M.J. (1989). Development of lipofuscin-like fluorescence in the retinal pigment epithelium in response to protease inhibitor treatment. Mech Ageing Dev 49, 23-40.

Kaushik, S., and Cuervo, A.M. (2012). Chaperone-mediated autophagy: a unique way to enter the lysosome world. Trends Cell Biol 22, 407-417.

Kay, P., Yang, Y.C., Hiscott, P., Gray, D., Maminishkis, A., and Paraoan, L. (2014). Age-related changes of cystatin C expression and polarized secretion by retinal pigment epithelium: potential age-related macular degeneration links. Invest Ophthalmol Vis Sci 55, 926-934.

Kay, P., Yang, Y.C., and Paraoan, L. (2013). Directional protein secretion by the retinal pigment epithelium: roles in retinal health and the development of age-related macular degeneration. Journal of cellular and molecular medicine 17, 833-843.

Kedzierski, R.M., and Yanagisawa, M. (2001). Endothelin system: the double-edged sword in health and disease. Annu Rev Pharmacol Toxicol 41, 851-876.

Kennedy, C.J., Rakoczy, P.E., and Constable, I.J. (1995). Lipofuscin of the retinal pigment epithelium: a review. Eye (Lond) 9 (Pt 6), 763-771.

Keppler, D., Walter, R., Perez, C., and Sierra, F. (2000). Increased expression of mature cathepsin B in aging rat liver. Cell Tissue Res 302, 181-188.

Kim, I., Rodriguez-Enriquez, S., and Lemasters, J.J. (2007). Selective degradation of mitochondria by mitophagy. Arch Biochem Biophys 462, 245-253.

Kim, J.H., Kim, J.H., Jun, H.O., Yu, Y.S., Min, B.H., Park, K.H., and Kim, K.W. (2010). Protective effect of clusterin from oxidative stress-induced apoptosis in human retinal pigment epithelial cells. Invest Ophthalmol Vis Sci 51, 561-566.

Kim, J.Y., Zhao, H., Martinez, J., Doggett, T.A., Kolesnikov, A.V., Tang, P.H., Ablonczy, Z., Chan, C.C., Zhou, Z., Green, D.R., et al. (2013). Noncanonical autophagy promotes the visual cycle. Cell 154, 365-376.

Kimura, K., Isashiki, Y., Sonoda, S., Kakiuchi-Matsumoto, T., and Ohba, N. (2000). Genetic association of manganese superoxide dismutase with exudative age-related macular degeneration. Am J Ophthalmol 130, 769-773.

Klaver, C.C., Kliffen, M., van Duijn, C.M., Hofman, A., Cruts, M., Grobbee, D.E., van Broeckhoven, C., and de Jong, P.T. (1998a). Genetic association of apolipoprotein E with age-related macular degeneration. Am J Hum Genet 63, 200-206.

Klaver, C.C., Wolfs, R.C., Assink, J.J., van Duijn, C.M., Hofman, A., and de Jong, P.T. (1998b). Genetic risk of age-related maculopathy. Population-based familial aggregation study. Arch Ophthalmol 116, 1646-1651.

Klein, D., Bussow, H., Fewou, S.N., and Gieselmann, V. (2005a). Exocytosis of storage material in a lysosomal disorder. Biochem Biophys Res Commun 327, 663-667.

Klein, M.L., Mauldin, W.M., and Stoumbos, V.D. (1994). Heredity and age-related macular degeneration. Observations in monozygotic twins. Arch Ophthalmol 112, 932-937.

Klein, R., Cruickshanks, K.J., Nash, S.D., Krantz, E.M., Nieto, F.J., Huang, G.H., Pankow, J.S., and Klein, B.E. (2010). The prevalence of age-related

macular degeneration and associated risk factors. Arch Ophthalmol 128, 750-758.

Klein, R., Klein, B.E., Knudtson, M.D., Meuer, S.M., Swift, M., and Gangnon, R.E. (2007). Fifteen-year cumulative incidence of age-related macular degeneration: the Beaver Dam Eye Study. Ophthalmology 114, 253-262.

Klein, R.J., Zeiss, C., Chew, E.Y., Tsai, J.Y., Sackler, R.S., Haynes, C., Henning, A.K., SanGiovanni, J.P., Mane, S.M., Mayne, S.T., et al. (2005b). Complement factor H polymorphism in age-related macular degeneration. Science 308, 385-389.

Kolli, N., and Garman, S.C. (2014). Proteolytic activation of human cathepsin A. J Biol Chem 289, 11592-11600.

Konari, K., Sawada, N., Zhong, Y., Isomura, H., Nakagawa, T., and Mori, M. (1995). Development of the Blood-Retinal Barrier in-Vitro - Formation of Tight Junctions as Revealed by Occludin and Zo-1 Correlates with the Barrier Function of Chick Retinal-Pigment Epithelial-Cells. Experimental Eye Research 61, 99-108.

Konttinen, Y.T., Mandelin, J., Li, T.F., Salo, J., Lassus, J., Liljestrom, M., Hukkanen, M., Takagi, M., Virtanen, I., and Santavirta, S. (2002). Acidic cysteine endoproteinase cathepsin K in the degeneration of the superficial articular hyaline cartilage in osteoarthritis. Arthritis Rheum 46, 953-960.

Kopito, R.R. (2000). Aggresomes, inclusion bodies and protein aggregation. Trends Cell Biol 10, 524-530.

Koressaar, T., and Remm, M. (2007). Enhancements and modifications of primer design program Primer3. Bioinformatics 23, 1289-1291.

Kroger, R.H., and Biehlmaier, O. (2009). Space-saving advantage of an inverted retina. Vision Res 49, 2318-2321.

Krohne, T.U., Kaemmerer, E., Holz, F.G., and Kopitz, J. (2010a). Lipid peroxidation products reduce lysosomal protease activities in human retinal pigment epithelial cells via two different mechanisms of action. Exp Eye Res 90, 261-266.

Krohne, T.U., Stratmann, N.K., Kopitz, J., and Holz, F.G. (2010b). Effects of lipid peroxidation products on lipofuscinogenesis and autophagy in human retinal pigment epithelial cells. Exp Eye Res 90, 465-471.

Kumar, P.A., Kumar, M.S., and Reddy, G.B. (2007). Effect of glycation on alpha-crystallin structure and chaperone-like function. The Biochemical journal 408, 251-258.

Kunze, A., Abari, E., Semkova, I., Paulsson, M., and Hartmann, U. (2010). Deposition of nidogens and other basement membrane proteins in the young and aging mouse retina. Ophthalmic Res 43, 108-112.

Kurji, K.H., Cui, J.Z., Lin, T., Harriman, D., Prasad, S.S., Kojic, L., and Matsubara, J.A. (2010). Microarray analysis identifies changes in inflammatory gene expression in response to amyloid-beta stimulation of cultured human retinal pigment epithelial cells. Invest Ophthalmol Vis Sci 51, 1151-1163.

Kuznetsova, A.V., Kurinov, A.M., and Aleksandrova, M.A. (2014). Cell models to study regulation of cell transformation in pathologies of retinal pigment epithelium. J Ophthalmol 2014, 801787.

Kwak, N., Okamoto, N., Wood, J.M., and Campochiaro, P.A. (2000). VEGF is major stimulator in model of choroidal neovascularization. Invest Ophth Vis Sci 41, 3158-3164.

Lakkaraju, A. (2012). Endo-lysosome function in the retinal pigment epithelium in health and disease. Adv Exp Med Biol 723, 723-729.

Lander, H.M., Tauras, J.M., Ogiste, J.S., Hori, O., Moss, R.A., and Schmidt, A.M. (1997). Activation of the receptor for advanced glycation end products triggers a p21(ras)-dependent mitogen-activated protein kinase pathway regulated by oxidant stress. J Biol Chem 272, 17810-17814.

Laurent-Matha, V., Derocq, D., Prebois, C., Katunuma, N., and Liaudet-Coopman, E. (2006). Processing of human cathepsin D is independent of its catalytic function and auto-activation: involvement of cathepsins L and B. Journal of biochemistry 139, 363-371.

Lee, D.C., Mason, C.W., Goodman, C.B., Holder, M.S., Kirksey, O.W., Womble, T.A., Severs, W.B., and Palm, D.E. (2007). Hydrogen peroxide induces lysosomal protease alterations in PC12 cells. Neurochem Res 32, 1499-1510.

Lettre, G., Lange, C., and Hirschhorn, J.N. (2007). Genetic model testing and statistical power in population-based association studies of quantitative traits. Genet Epidemiol 31, 358-362.

Li, R., McCourt, P., Liu, X., Smedsrød, B., and Sørensen, K. (2007). Endocytosis of Advanced Glycation End Products in Bovine Retinal Pigment Epithelial Cells. Invest Ophth Vis Sci 48, 2206-2206.

Li, W.W., Li, J., and Bao, J.K. (2012). Microautophagy: lesser-known self-eating. Cell Mol Life Sci 69, 1125-1136.

Li, Y.M., Mitsuhashi, T., Wojciechowicz, D., Shimizu, N., Li, J., Stitt, A., He, C., Banerjee, D., and Vlassara, H. (1996). Molecular identity and cellular distribution of advanced glycation endproduct receptors: relationship of p60 to OST-48 and p90 to 80K-H membrane proteins. Proc Natl Acad Sci U S A 93, 11047-11052.

Liles, M.R., Newsome, D.A., and Oliver, P.D. (1991). Antioxidant enzymes in the aging human retinal pigment epithelium. Arch Ophthalmol 109, 1285-1288.

Lin, Y., Epstein, D.L., and Liton, P.B. (2010). Intralysosomal iron induces lysosomal membrane permeabilization and cathepsin D-mediated cell death in trabecular meshwork cells exposed to oxidative stress. Invest Ophthalmol Vis Sci 51, 6483-6495.

Liu, J., Itagaki, Y., Ben-Shabat, S., Nakanishi, K., and Sparrow, J.R. (2000). The biosynthesis of A2E, a fluorophore of aging retina, involves the formation of the precursor, A2-PE, in the photoreceptor outer segment membrane. J Biol Chem 275, 29354-29360.

Liu, R.T., Gao, J., Cao, S., Sandhu, N., Cui, J.Z., Chou, C.L., Fang, E., and Matsubara, J.A. (2013). Inflammatory mediators induced by amyloid-beta in the retina and RPE in vivo: implications for inflammasome activation in age-related macular degeneration. Invest Ophthalmol Vis Sci 54, 2225-2237.

Luan, Z.G., Zhang, H., Yang, P.T., Ma, X.C., Zhang, C., and Guo, R.X. (2010). HMGB1 activates nuclear factor-kappaB signaling by RAGE and increases the production of TNF-alpha in human umbilical vein endothelial cells. Immunobiology 215, 956-962.

Lubke, T., Lobel, P., and Sleat, D.E. (2009). Proteomics of the lysosome. Biochim Biophys Acta 1793, 625-635.

Lund, R.D., Adamson, P., Sauve, Y., Keegan, D.J., Girman, S.V., Wang, S., Winton, H., Kanuga, N., Kwan, A.S., Beauchene, L., et al. (2001). Subretinal transplantation of genetically modified human cell lines attenuates loss of visual function in dystrophic rats. Proc Natl Acad Sci U S A 98, 9942-9947.

Ma, M., Guo, X., Chang, Y., Li, C., Meng, X., Li, S., Du, Z.X., Wang, H.Q., and Sun, Y. (2015). Advanced glycation end products promote proliferation and suppress autophagy via reduction of Cathepsin D in rat vascular smooth muscle cells. Mol Cell Biochem 403, 73-83.

Ma, W., Lee, S.E., Guo, J., Qu, W., Hudson, B.I., Schmidt, A.M., and Barile, G.R. (2007). RAGE ligand upregulation of VEGF secretion in ARPE-19 cells. Invest Ophthalmol Vis Sci 48, 1355-1361.

Mach, L., Stuwe, K., Hagen, A., Ballaun, C., and Glossl, J. (1992). Proteolytic processing and glycosylation of cathepsin B. The role of the primary structure of the latent precursor and of the carbohydrate moiety for cell-type-specific molecular forms of the enzyme. Biochem J 282 (Pt 2), 577-582.

Maminishkis, A., Chen, S., Jalickee, S., Banzon, T., Shi, G., Wang, F.E., Ehalt, T., Hammer, J.A., and Miller, S.S. (2006). Confluent monolayers of cultured human fetal retinal pigment epithelium exhibit morphology and physiology of native tissue. Invest Ophthalmol Vis Sci 47, 3612-3624.

Mandelin, J., Hukkanen, M., Li, T.F., Korhonen, M., Liljestrom, M., Sillat, T., Hanemaaijer, R., Salo, J., Santavirta, S., and Konttinen, Y.T. (2006). Human osteoblasts produce cathepsin K. Bone 38, 769-777.

Mannermaa, E., Vellonen, K.S., Ryhanen, T., Kokkonen, K., Ranta, V.P., Kaarniranta, K., and Urtti, A. (2009). Efflux protein expression in human retinal pigment epithelium cell lines. Pharm Res 26, 1785-1791.

Mariathasan, S., and Monack, D.M. (2007). Inflammasome adaptors and sensors: intracellular regulators of infection and inflammation. Nat Rev Immunol 7, 31-40.

Marshall, G.E., Konstas, A.G., Reid, G.G., Edwards, J.G., and Lee, W.R. (1992). Type IV collagen and laminin in Bruch's membrane and basal linear deposit in the human macula. Br J Ophthalmol 76, 607-614.

Marshall, G.E., Konstas, A.G., Reid, G.G., Edwards, J.G., and Lee, W.R. (1994). Collagens in the aged human macula. Graefes Arch Clin Exp Ophthalmol 232, 133-140.

Martinez, I., Chakrabarti, S., Hellevik, T., Morehead, J., Fowler, K., and Andrews, N.W. (2000). Synaptotagmin VII regulates Ca(2+)-dependent exocytosis of lysosomes in fibroblasts. J Cell Biol 148, 1141-1149.

Mathieu, M., Vignon, F., Capony, F., and Rochefort, H. (1991). Estradiol down-regulates the mannose-6-phosphate/insulin-like growth factor-II receptor gene and induces cathepsin-D in breast cancer cells: a receptor saturation mechanism to increase the secretion of lysosomal proenzymes. Mol Endocrinol 5, 815-822.

Matsumura, M., Ogino, N., Shirakawa, H., Yamakawa, R., and Tsukahara, I. (1985). Exocytosis by retinal pigment epithelial cells. Ophthalmic Res 17, 148-153.

Mattock, K.L., Gough, P.J., Humphries, J., Burnand, K., Patel, L., Suckling, K.E., Cuello, F., Watts, C., Gautel, M., Avkiran, M., et al. (2010). Legumain and cathepsin-L expression in human unstable carotid plaque. Atherosclerosis 208, 83-89.

McCord, J.M., and Fridovich, I. (1988). Superoxide dismutase: the first twenty years (1968-1988). Free Radic Biol Med 5, 363-369.

McCray, B.A., and Taylor, J.P. (2008). The role of autophagy in age-related neurodegeneration. Neurosignals 16, 75-84.

McFarlane, S., Glenn, J.V., Lichanska, A.M., Simpson, D.A., and Stitt, A.W. (2005). Characterisation of the advanced glycation endproduct receptor complex in the retinal pigment epithelium. Br J Ophthalmol 89, 107-112.

McKibbin, M., Ali, M., Bansal, S., Baxter, P.D., West, K., Williams, G., Cassidy, F., and Inglehearn, C.F. (2012). CFH, VEGF and HTRA1 promoter genotype may influence the response to intravitreal ranibizumab therapy for neovascular age-related macular degeneration. Br J Ophthalmol 96, 208-212.

McNeil, P.L. (2002). Repairing a torn cell surface: make way, lysosomes to the rescue. J Cell Sci 115, 873-879.

McNeil, P.L., and Khakee, R. (1992). Disruptions of muscle fiber plasma membranes. Role in exercise-induced damage. Am J Pathol 140, 1097-1109.

Meyers, S.M. (1994). A twin study on age-related macular degeneration. Trans Am Ophthalmol Soc 92, 775-843.

Mi, W., Pawlik, M., Sastre, M., Jung, S.S., Radvinsky, D.S., Klein, A.M., Sommer, J., Schmidt, S.D., Nixon, R.A., Mathews, P.M., et al. (2007). Cystatin C inhibits amyloid-beta deposition in Alzheimer's disease mouse models. Nat Genet 39, 1440-1442.

Miceli, M.V., Liles, M.R., and Newsome, D.A. (1994). Evaluation of oxidative processes in human pigment epithelial cells associated with retinal outer segment phagocytosis. Experimental cell research 214, 242-249.

Miller, J.W. (2010). Treatment of age-related macular degeneration: beyond VEGF. Jpn J Ophthalmol 54, 523-528.

Miller, S., and Steinberg, R.H. (1976). Transport of taurine, L-methionine and 3-o-methyl-D-glucose across frog retinal pigment epithelium. Exp Eye Res 23, 177-189.

Miller, S.S., and Steinberg, R.H. (1977a). Active transport of ions across frog retinal pigment epithelium. Exp Eye Res 25, 235-248.

Miller, S.S., and Steinberg, R.H. (1977b). Passive ionic properties of frog retinal pigment epithelium. The Journal of membrane biology 36, 337-372.

Mindell, J.A. (2012). Lysosomal acidification mechanisms. Annu Rev Physiol 74, 69-86.

Miosge, N., Sasaki, T., and Timpl, R. (1999). Angiogenesis inhibitor endostatin is a distinct component of elastic fibers in vessel walls. Faseb J 13, 1743-1750.

Mishima, H., and Hasebe, H. (1978). Some Observations in Fine-Structure of Age-Changes of Mouse Retinal-Pigment Epithelium. A Graef Arch Klin Ex 209, 1-9.

Mishima, H., and Kondo, K. (1981). Ultrastructure of age changes in the basal infoldings of aged mouse retinal pigment epithelium. Exp Eye Res 33, 75-84.

Miyamura, N., Mishima, K., Honda, S., Aotaki-Keen, A.E., Morse, L.S., Handa, J.T., and Hjelmeland, L.M. (2001). Age and topographic variation of insulin-like growth factor-binding protein 2 in the human rpe. Invest Ophthalmol Vis Sci 42, 1626-1630.

Miyamura, N., Ogawa, T., Boylan, S., Morse, L.S., Handa, J.T., and Hjelmeland, L.M. (2004). Topographic and age-dependent expression of heme oxygenase-1 and catalase in the human retinal pigment epithelium. Invest Ophthalmol Vis Sci 45, 1562-1565.

Miyata, T., Wada, Y., Cai, Z., Iida, Y., Horie, K., Yasuda, Y., Maeda, K., Kurokawa, K., and van Ypersele de Strihou, C. (1997). Implication of an increased oxidative stress in the formation of advanced glycation end products in patients with end-stage renal failure. Kidney Int 51, 1170-1181.

Mizushima, N., and Komatsu, M. (2011). Autophagy: renovation of cells and tissues. Cell 147, 728-741.

Mizushima, N., and Yoshimori, T. (2007). How to interpret LC3 immunoblotting. Autophagy 3, 542-545.

Mohamed, M.M., and Sloane, B.F. (2006). Cysteine cathepsins: multifunctional enzymes in cancer. Nat Rev Cancer 6, 764-775.

Moiseyev, G., Nikolaeva, O., Chen, Y., Farjo, K., Takahashi, Y., and Ma, J.X. (2010). Inhibition of the visual cycle by A2E through direct interaction with RPE65 and implications in Stargardt disease. P Natl Acad Sci USA 107, 17551-17556.

Monnier, V.M., Sell, D.R., Nagaraj, R.H., Miyata, S., Grandhee, S., Odetti, P., and Ibrahim, S.A. (1992). Maillard reaction-mediated molecular damage to extracellular matrix and other tissue proteins in diabetes, aging, and uremia. Diabetes 41 Suppl 2, 36-41.

Moore, D.J., and Clover, G.M. (2001). The effect of age on the macromolecular permeability of human Bruch's membrane. Invest Ophthalmol Vis Sci 42, 2970-2975.

Mullins, R.F., Russell, S.R., Anderson, D.H., and Hageman, G.S. (2000). Drusen associated with aging and age-related macular degeneration contain proteins common to extracellular deposits associated with atherosclerosis, elastosis, amyloidosis, and dense deposit disease. Faseb J 14, 835-846.

Munk, M., Kiss, C., Sulzbacher, F., Eisenkolbl, S., Sacu, S., Kalcher, K., Jampol, L., and Schmidt-Erfurth, U. (2012). Short-term progression of wet AMD and correlation with 1-year treatment results. Acta Ophthalmol 90, e420-427.

Murphy, M.P. (2009). How mitochondria produce reactive oxygen species. The Biochemical journal 417, 1-13.

Nagaraj, R.H., Linetsky, M., and Stitt, A.W. (2012). The pathogenic role of Maillard reaction in the aging eye. Amino Acids 42, 1205-1220.

Nakanishi, H., Tominaga, K., Amano, T., Hirotsu, I., Inoue, T., and Yamamoto, K. (1994). Age-related changes in activities and localizations of cathepsins D, E, B, and L in the rat brain tissues. Exp Neurol 126, 119-128.

Narayan, S., Brun, A.M., and Yorio, T. (2004). Endothelin-1 distribution and basolateral secretion in the retinal pigment epithelium. Exp Eye Res 79, 11-19.

Newsome, D.A., Miceli, M.V., Liles, M.R., Tate, D.J., and Oliver, P.D. (1994). Antioxidants in the Retinal-Pigment Epithelium. Progress in Retinal and Eye Research 13, 101-123.

Ng, K.P., Gugiu, B., Renganathan, K., Davies, M.W., Gu, X., Crabb, J.S., Kim, S.R., Rozanowska, M.B., Bonilha, V.L., Rayborn, M.E., et al. (2008). Retinal pigment epithelium lipofuscin proteomics. Molecular & cellular proteomics : MCP 7, 1397-1405.

Nowak, D.E., Tian, B., Jamaluddin, M., Boldogh, I., Vergara, L.A., Choudhary, S., and Brasier, A.R. (2008). RelA Ser276 phosphorylation is required for activation of a subset of NF-kappaB-dependent genes by recruiting cyclin-dependent kinase 9/cyclin T1 complexes. Mol Cell Biol 28, 3623-3638.

Nowak, J.Z. (2006). Age-related macular degeneration (AMD): pathogenesis and therapy. Pharmacological reports : PR 58, 353-363.

Nycander, M., Estrada, S., Mort, J.S., Abrahamson, M., and Bjork, I. (1998). Two-step mechanism of inhibition of cathepsin B by cystatin C due to displacement of the proteinase occluding loop. FEBS letters 422, 61-64.

Ochieng, J., and Chaudhuri, G. (2010). Cystatin superfamily. J Health Care Poor Underserved 21, 51-70.

Oeckinghaus, A., and Ghosh, S. (2009). The NF-kappaB family of transcription factors and its regulation. Cold Spring Harb Perspect Biol 1, a000034.

Okada, T., Ernst, O.P., Palczewski, K., and Hofmann, K.P. (2001). Activation of rhodopsin: new insights from structural and biochemical studies. Trends Biochem Sci 26, 318-324.

Okamoto, T., Tanaka, S., Stan, A.C., Koike, T., Kase, M., Makita, Z., Sawa, H., and Nagashima, K. (2002). Advanced glycation end products induce angiogenesis in vivo. Microvascular research 63, 186-195.

Padgett, L.C., Lui, G.M., Werb, Z., and LaVail, M.M. (1997). Matrix metalloproteinase-2 and tissue inhibitor of metalloproteinase-1 in the retinal pigment epithelium and interphotoreceptor matrix: vectorial secretion and regulation. Exp Eye Res 64, 927-938.

Palsdottir, A., Abrahamson, M., Thorsteinsson, L., Arnason, A., Olafsson, I., Grubb, A., and Jensson, O. (1988). Mutation in cystatin C gene causes hereditary brain haemorrhage. Lancet 2, 603-604.

Pan, L., Li, Y., Jia, L., Qin, Y., Qi, G., Cheng, J., Qi, Y., Li, H., and Du, J. (2012). Cathepsin S deficiency results in abnormal accumulation of autophagosomes in macrophages and enhances Ang II-induced cardiac inflammation. PLoS One 7, e35315.

Panda-Jonas, S., Jonas, J.B., and Jakobczyk-Zmija, M. (1996). Retinal pigment epithelial cell count, distribution, and correlations in normal human eyes. Am J Ophthalmol 121, 181-189.

Paraoan, L., Grierson, I., and Maden, B.E. (2000). Analysis of expressed sequence tags of retinal pigment epithelium: cystatin C is an abundant transcript. Int J Biochem Cell Biol 32, 417-426.

Paraoan, L., Hiscott, P., Gosden, C., and Grierson, I. (2010). Cystatin C in macular and neuronal degenerations: implications for mechanism(s) of age-related macular degeneration. Vision Res 50, 737-742.

Paraoan, L., Ratnayaka, A., Spiller, D.G., Hiscott, P., White, M.R., and Grierson, I. (2004). Unexpected intracellular localization of the AMD-associated cystatin C variant. Traffic 5, 884-895.

Paraoan, L., White, M.R., Spiller, D.G., Grierson, I., and Maden, B.E. (2001). Precursor cystatin C in cultured retinal pigment epithelium cells: evidence for processing through the secretory pathway. Mol Membr Biol 18, 229-236.

Patton, W.P., Routledge, M.N., Jones, G.D., Lewis, S.E., Archer, D.B., Davies, R.J., and Chakravarthy, U. (2002). Retinal pigment epithelial cell DNA is damaged by exposure to benzo[a]pyrene, a constituent of cigarette smoke. Exp Eye Res 74, 513-522.

Pauleikhoff, D., Harper, C.A., Marshall, J., and Bird, A.C. (1990). Aging changes in Bruch's membrane. A histochemical and morphologic study. Ophthalmology 97, 171-178.

Pauleikhoff, D., Zuels, S., Sheraidah, G.S., Marshall, J., Wessing, A., and Bird, A.C. (1992). Correlation between Biochemical-Composition and Fluorescein Binding of Deposits in Bruchs Membrane. Ophthalmology 99, 1548-1553.

Pepper, M.S. (2001). Extracellular proteolysis and angiogenesis. Thrombosis and haemostasis 86, 346-355.

Peters, S., Reinthal, E., Blitgen-Heinecke, P., Bartz-Schmidt, K.U., and Schraermeyer, U. (2006). Inhibition of lysosomal degradation in retinal pigment epithelium cells induces exocytosis of phagocytic residual material at the basolateral plasma membrane. Ophthalmic Res 38, 83-88.

Plafker, S.M., O'Mealey, G.B., and Szweda, L.I. (2012). Mechanisms for countering oxidative stress and damage in retinal pigment epithelium. Int Rev Cell Mol Biol 298, 135-177.

Ponten, J., and Macintyre, E.H. (1968). Long term culture of normal and neoplastic human glia. Acta pathologica et microbiologica Scandinavica 74, 465-486.

Potts, W., Bowyer, J., Jones, H., Tucker, D., Freemont, A.J., Millest, A., Martin, C., Vernon, W., Neerunjun, D., Slynn, G., et al. (2004). Cathepsin L-deficient mice exhibit abnormal skin and bone development and show increased resistance to osteoporosis following ovariectomy. Int J Exp Pathol 85, 85-96.

Puppo, A., and Halliwell, B. (1988). Formation of Hydroxyl Radicals in Biological-Systems - Does Myoglobin Stimulate Hydroxyl Radical Formation from Hydrogen-Peroxide. Free Radical Res Com 4, 415-422.

Purves, D. (2012). Neuroscience, 5th edn (Sunderland, Mass.: Sinauer Associates).

Qin, Z.H., Chen, R.W., Wang, Y., Nakai, M., Chuang, D.M., and Chase, T.N. (1999). Nuclear factor kappaB nuclear translocation upregulates c-Myc and p53 expression during NMDA receptor-mediated apoptosis in rat striatum. J Neurosci 19, 4023-4033.

Querques, G., Massamba, N., Srour, M., Boulanger, E., Georges, A., and Souied, E.H. (2014). Impact of reticular pseudodrusen on macular function. Retina 34, 321-329.

Rajamaki, K., Lappalainen, J., Oorni, K., Valimaki, E., Matikainen, S., Kovanen, P.T., and Eklund, K.K. (2010). Cholesterol crystals activate the NLRP3 inflammasome in human macrophages: a novel link between cholesterol metabolism and inflammation. PLoS One 5, e11765.

Rakoczy, P.E., Lai, C.M., Baines, M., Di Grandi, S., Fitton, J.H., and Constable, I.J. (1997). Modulation of cathepsin D activity in retinal pigment epithelial cells. Biochem J 324 (Pt 3), 935-940.

Rakoczy, P.E., Lai, M.C., Baines, M.G., Spilsbury, K., and Constable, I.J. (1998). Expression of cathepsin S antisense transcripts by adenovirus in retinal pigment epithelial cells. Invest Ophth Vis Sci 39, 2095-2104.

Rakoczy, P.E., Mann, K., Cavaney, D.M., Robertson, T., Papadimitreou, J., and Constable, I.J. (1994). Detection and possible functions of a cysteine protease involved in digestion of rod outer segments by retinal pigment epithelial cells. Invest Ophthalmol Vis Sci 35, 4100-4108.

Ramrattan, R.S., van der Schaft, T.L., Mooy, C.M., de Bruijn, W.C., Mulder, P.G., and de Jong, P.T. (1994). Morphometric analysis of Bruch's

membrane, the choriocapillaris, and the choroid in aging. Invest Ophthalmol Vis Sci 35, 2857-2864.

Raposo, G., and Stoorvogel, W. (2013). Extracellular vesicles: exosomes, microvesicles, and friends. J Cell Biol 200, 373-383.

Ratnayaka, A., Paraoan, L., Spiller, D.G., Hiscott, P., Nelson, G., White, M.R., and Grierson, I. (2007). A dual Golgi- and mitochondria-localised Ala25Ser precursor cystatin C: an additional tool for characterising intracellular mis-localisation leading to increased AMD susceptibility. Experimental eye research 84, 1135-1139.

Reddy, A., Caler, E., and Andrews, N.W. (2001). Plasma membrane repair is mediated by Ca2+-regulated exocytosis of lysosomes. Mol Biol Cell 12, 266a-266a.

Redmond, T.M., Yu, S., Lee, E., Bok, D., Hamasaki, D., Chen, N., Goletz, P., Ma, J.X., Crouch, R.K., and Pfeifer, K. (1998). Rpe65 is necessary for production of 11-cis-vitamin A in the retinal visual cycle. Nature Genetics 20, 344-351.

Regan, C.M., de Grip, W.J., Daemen, F.J., and Bonting, S.L. (1980). Degradation of rhodopsin by a lysosomal fraction of retinal pigment epithelium: biochemical aspects of the visual process. XLI. Exp Eye Res 30, 183-191.

Reilly, J.J., Jr., Mason, R.W., Chen, P., Joseph, L.J., Sukhatme, V.P., Yee, R., and Chapman, H.A., Jr. (1989). Synthesis and processing of cathepsin L, an elastase, by human alveolar macrophages. Biochem J 257, 493-498.

Ren, R.X.F., Sakai, N., and Nakanishi, K. (1997). Total synthesis of the ocular age pigment A2-E: A convergent pathway. J Am Chem Soc 119, 3619-3620.

Renart, J., Reiser, J., and Stark, G.R. (1979). Transfer of proteins from gels to diazobenzyloxymethyl-paper and detection with antisera: a method for studying antibody specificity and antigen structure. Proc Natl Acad Sci U S A 76, 3116-3120.

Repnik, U., Cesen, M.H., and Turk, B. (2013). The endolysosomal system in cell death and survival. Cold Spring Harb Perspect Biol 5, a008755.

Repnik, U., Stoka, V., Turk, V., and Turk, B. (2012). Lysosomes and lysosomal cathepsins in cell death. Biochim Biophys Acta 1824, 22-33.

Richter, C. (1992). Reactive oxygen and DNA damage in mitochondria. Mutat Res 275, 249-255.

Ridge, K.D., Abdulaev, N.G., Sousa, M., and Palczewski, K. (2003). Phototransduction: crystal clear. Trends Biochem Sci 28, 479-487.

Riss, T.L., Moravec, R.A., Niles, A.L., Benink, H.A., Worzella, T.J., Minor, L., Storts, D., and Reid, Y. (2004). Cell Viability Assays. In Assay Guidance Manual, G.S. Sittampalam, N.P. Coussens, H. Nelson, M. Arkin, D. Auld, C. Austin, B. Bejcek, M. Glicksman, J. Inglese, V. Lemmon, et al., eds. (Bethesda (MD)).

Rivera, A., Fisher, S.A., Fritsche, L.G., Keilhauer, C.N., Lichtner, P., Meitinger, T., and Weber, B.H.F. (2005). Hypothetical LOC387715 is a second major susceptibility gene for age-related macular degeneration, contributing independently of complement factor H to disease risk. Human Molecular Genetics 14, 3227-3236.

Roberts, J.M., and Forrester, J.V. (1990). Factors affecting the migration and growth of endothelial cells from microvessels of bovine retina. Exp Eye Res 50, 165-172.

Rodriguez, A., Webster, P., Ortego, J., and Andrews, N.W. (1997). Lysosomes behave as Ca2+-regulated exocytic vesicles in fibroblasts and epithelial cells. J Cell Biol 137, 93-104.

Rodziewicz-Motowidlo, S., Iwaszkiewicz, J., Sosnowska, R., Czaplewska, P., Sobolewski, E., Szymanska, A., Stachowiak, K., and Liwo, A. (2009). The role of the Val57 amino-acid residue in the hinge loop of the human cystatin C. Conformational studies of the beta2-L1-beta3 segments of wild-type human cystatin C and its mutants. Biopolymers 91, 373-383.

Rohlich, P. (1970). The interphotoreceptor matrix: electron microscopic and histochemical observations on the vertebrate retina. Exp Eye Res 10, 80-86.

Romero-Calvo, I., Ocon, B., Martinez-Moya, P., Suarez, M.D., Zarzuelo, A., Martinez-Augustin, O., and de Medina, F.S. (2010). Reversible Ponceau staining as a loading control alternative to actin in Western blots. Analytical biochemistry 401, 318-320.

Rossi, A., Deveraux, Q., Turk, B., and Sali, A. (2004). Comprehensive search for cysteine cathepsins in the human genome. Biol Chem 385, 363-372.

Roth, W., Deussing, J., Botchkarev, V.A., Pauly-Evers, M., Saftig, P., Hafner, A., Schmidt, P., Schmahl, W., Scherer, J., Anton-Lamprecht, I., et al. (2000). Cathepsin L deficiency as molecular defect of furless: hyperproliferation of keratinocytes and pertubation of hair follicle cycling. Faseb J 14, 2075-2086.

Rozanowska, M., Jarvis-Evans, J., Korytowski, W., Boulton, M.E., Burke, J.M., and Sarna, T. (1995). Blue light-induced reactivity of retinal age pigment. In vitro generation of oxygen-reactive species. J Biol Chem 270, 18825-18830.

Rozanowska, M., Sarna, T., Land, E.J., and Truscott, T.G. (1999). Free radical scavenging properties of melanin interaction of eu- and pheo-melanin models with reducing and oxidising radicals. Free Radic Biol Med 26, 518-525.

Rozanowska, M., Wessels, J., Boulton, M., Burke, J.M., Rodgers, M.A., Truscott, T.G., and Sarna, T. (1998). Blue light-induced singlet oxygen generation by retinal lipofuscin in non-polar media. Free Radic Biol Med 24, 1107-1112.

Rozhin, J., Sameni, M., Ziegler, G., and Sloane, B.F. (1994). Pericellular pH affects distribution and secretion of cathepsin B in malignant cells. Cancer Res 54, 6517-6525.

Rubio-Perez, J.M., and Morillas-Ruiz, J.M. (2012). A review: inflammatory process in Alzheimer's disease, role of cytokines. ScientificWorldJournal 2012, 756357.

Ryan, R.E., Sloane, B.F., Sameni, M., and Wood, P.L. (1995). Microglial cathepsin B: an immunological examination of cellular and secreted species. J Neurochem 65, 1035-1045.

Ryhanen, T., Hyttinen, J.M.T., Kopitz, J., Rilla, K., Kuusisto, E., Mannermaa, E., Viiri, J., Holmberg, C.I., Immonen, I., Meri, S., et al. (2009). Crosstalk between Hsp70 molecular chaperone, lysosomes and proteasomes in autophagy-mediated proteolysis in human retinal pigment epithelial cells. Journal of cellular and molecular medicine 13, 3616-3631.

Saari, J.C., and Bredberg, D.L. (1989). Lecithin:retinol acyltransferase in retinal pigment epithelial microsomes. J Biol Chem 264, 8636-8640.

Saari, J.C., Bredberg, L., and Garwin, G.G. (1982). Identification of the endogenous retinoids associated with three cellular retinoid-binding proteins from bovine retina and retinal pigment epithelium. J Biol Chem 257, 13329-13333.

Saftig, P., Hunziker, E., Wehmeyer, O., Jones, S., Boyde, A., Rommerskirch, W., Moritz, J.D., Schu, P., and von Figura, K. (1998). Impaired osteoclastic bone resorption leads to osteopetrosis in cathepsin-K-deficient mice. Proc Natl Acad Sci U S A 95, 13453-13458.

Saftig, P., and Klumperman, J. (2009). Lysosome biogenesis and lysosomal membrane proteins: trafficking meets function. Nat Rev Mol Cell Biol 10, 623-635.

Saftig, P., Schroder, B., and Blanz, J. (2010). Lysosomal membrane proteins: life between acid and neutral conditions. Biochem Soc T 38, 1420-1423.

Sage, J., Leblanc-Noblesse, E., Nizard, C., Sasaki, T., Schnebert, S., Perrier, E., Kurfurst, R., Bromme, D., Lalmanach, G., and Lecaille, F. (2012). Cleavage of nidogen-1 by cathepsin S impairs its binding to basement membrane partners. PLoS One 7, e43494.

Sajithlal, G.B., Chithra, P., and Chandrakasan, G. (1998). Advanced glycation end products induce crosslinking of collagen in vitro. Biochim Biophys Acta 1407, 215-224.

Sakai, N., Decatur, J., Nakanishi, K., and Eldred, G.E. (1996). Ocular age pigment "A2-E": An unprecedented pyridinium bisretinoid. J Am Chem Soc 118, 1559-1560.

Sakurai, H., Chiba, H., Miyoshi, H., Sugita, T., and Toriumi, W. (1999). I kappa B kinases phosphorylate NF-kappa B p65 subunit on serine 536 in the transactivation domain. Journal of Biological Chemistry 274, 30353-30356.

Sanger, F., Nicklen, S., and Coulson, A.R. (1977). DNA sequencing with chain-terminating inhibitors. Proc Natl Acad Sci U S A 74, 5463-5467.

Sano, H., Nagai, R., Matsumoto, K., and Horiuchi, S. (1999). Receptors for proteins modified by advanced glycation endproducts (AGE)--their functional role in atherosclerosis. Mech Ageing Dev 107, 333-346.

Sarks, S., Cherepanoff, S., Killingsworth, M., and Sarks, J. (2007). Relationship of Basal laminar deposit and membranous debris to the clinical presentation of early age-related macular degeneration. Invest Ophthalmol Vis Sci 48, 968-977.

Sarna, T., Burke, J.M., Korytowski, W., Rozanowska, M., Skumatz, C.M., Zareba, A., and Zareba, M. (2003). Loss of melanin from human RPE with aging: possible role of melanin photooxidation. Exp Eye Res 76, 89-98.

Sasaki, N., Fukatsu, R., Tsuzuki, K., Hayashi, Y., Yoshida, T., Fujii, N., Koike, T., Wakayama, I., Yanagihara, R., Garruto, R., et al. (1998). Advanced glycation end products in Alzheimer's disease and other neurodegenerative diseases. Am J Pathol 153, 1149-1155.

Scherer, W.F., Syverton, J.T., and Gey, G.O. (1953). Studies on the propagation in vitro of poliomyelitis viruses. IV. Viral multiplication in a stable strain of human malignant epithelial cells (strain HeLa) derived from an epidermoid carcinoma of the cervix. J Exp Med 97, 695-710.

Schmidt, S.Y., and Peisch, R.D. (1986). Melanin concentration in normal human retinal pigment epithelium. Regional variation and age-related reduction. Invest Ophthalmol Vis Sci 27, 1063-1067.

Schneider, C.A., Rasband, W.S., and Eliceiri, K.W. (2012). NIH Image to ImageJ: 25 years of image analysis. Nature methods 9, 671-675.

Schramm, E.C., Clark, S.J., Triebwasser, M.P., Raychaudhuri, S., Seddon, J.M., and Atkinson, J.P. (2014). Genetic variants in the complement system predisposing to age-related macular degeneration: a review. Mol Immunol 61, 118-125.

Schutt, F., Bergmann, M., Holz, F.G., and Kopitz, J. (2003). Proteins modified by malondialdehyde, 4-hydroxynonenal, or advanced glycation end products in lipofuscin of human retinal pigment epithelium. Invest Ophthalmol Vis Sci 44, 3663-3668.

Schutt, F., Ueberle, B., Schnolzer, M., Holz, F.G., and Kopitz, J. (2002). Proteome analysis of lipofuscin in human retinal pigment epithelial cells. FEBS Lett 528, 217-221.

Schwarz, G., Boehncke, W.H., Braun, M., Schroter, C.J., Burster, T., Flad, T., Dressel, D., Weber, E., Schmid, H., and Kalbacher, H. (2002). Cathepsin S activity is detectable in human keratinocytes and is selectively upregulated upon stimulation with interferon-gamma. J Invest Dermatol 119, 44-49.

Scivittaro, V., Ganz, M.B., and Weiss, M.F. (2000). AGEs induce oxidative stress and activate protein kinase C-beta(II) in neonatal mesangial cells. Am J Physiol Renal Physiol 278, F676-683.

Sebekova, K., Schinzel, R., Ling, H., Simm, A., Xiang, G., Gekle, M., Munch, G., Vamvakas, S., and Heidland, A. (1998). Advanced glycated albumin impairs protein degradation in the kidney proximal tubules cell line LLC-PK1. Cell Mol Biol (Noisy-le-grand) 44, 1051-1060.

Seddon, J.M., Ajani, U.A., and Mitchell, B.D. (1997). Familial aggregation of age-related maculopathy. Am J Ophthalmol 123, 199-206.

Seddon, J.M., Rosner, B., Sperduto, R.D., Yannuzzi, L., Haller, J.A., Blair, N.P., and Willett, W. (2001). Dietary fat and risk for advanced age-related macular degeneration. Arch Ophthalmol 119, 1191-1199.

Seddon, J.M., Sharma, S., and Adelman, R.A. (2006). Evaluation of the clinical age-related maculopathy staging system. Ophthalmology 113, 260-266.

Semba, R.D., Nicklett, E.J., and Ferrucci, L. (2010). Does accumulation of advanced glycation end products contribute to the aging phenotype? J Gerontol A Biol Sci Med Sci 65, 963-975.

Semkova, I., Kociok, N., Karagiannis, D., Nischt, R., Smyth, N., Paulsson, M., Strauss, O., and Joussen, A.M. (2014). Anti-angiogenic effect of the basement membrane protein nidogen-1 in a mouse model of choroidal neovascularization. Exp Eye Res 118, 80-88.

Sensi, M., Pricci, F., Pugliese, G., De Rossi, M.G., Petrucci, A.F., Cristina, A., Morano, S., Pozzessere, G., Valle, E., Andreani, D., et al. (1995). Role of advanced glycation end-products (AGE) in late diabetic complications. Diabetes Res Clin Pract 28, 9-17.

Settembre, C., Fraldi, A., Medina, D.L., and Ballabio, A. (2013). Signals from the lysosome: a control centre for cellular clearance and energy metabolism. Nat Rev Mol Cell Biol 14, 283-296.

Shamsi, F.A., and Boulton, M. (2001). Inhibition of RPE lysosomal and antioxidant activity by the age pigment lipofuscin. Invest Ophthalmol Vis Sci 42, 3041-3046.

Sharma, A., Neekhra, A., Gramajo, A.L., Patil, J., Chwa, M., Kuppermann, B.D., and Kenney, M.C. (2008). Effects of Benzo(e)Pyrene, a toxic component of cigarette smoke, on human retinal pigment epithelial cells in vitro. Invest Ophthalmol Vis Sci 49, 5111-5117.

Sheraidah, G., Steinmetz, R., Maguire, J., Pauleikhoff, D., Marshall, J., and Bird, A.C. (1993). Correlation between Lipids Extracted from Bruch Membrane and Age. Ophthalmology 100, 47-51.

Shirinifard, A., Glazier, J.A., Swat, M., Gens, J.S., Family, F., Jiang, Y., and Grossniklaus, H.E. (2012). Adhesion failures determine the pattern of choroidal neovascularization in the eye: a computer simulation study. PLoS Comput Biol 8, e1002440.

Singh, R., Phillips, M.J., Kuai, D., Meyer, J., Martin, J.M., Smith, M.A., Perez, E.T., Shen, W., Wallace, K.A., Capowski, E.E., et al. (2013). Functional analysis of serially expanded human iPS cell-derived RPE cultures. Invest Ophthalmol Vis Sci 54, 6767-6778.

Smith, W., Assink, J., Klein, R., Mitchell, P., Klaver, C.C., Klein, B.E., Hofman, A., Jensen, S., Wang, J.J., and de Jong, P.T. (2001). Risk factors for age-related macular degeneration: Pooled findings from three continents. Ophthalmology 108, 697-704.

Snell, R.S., and Lemp, M.A. (1998). Clinical anatomy of the eye, 2nd edn (Malden, MA, USA: Blackwell Science).

Sparrow, J.R., and Boulton, M. (2005). RPE lipofuscin and its role in retinal pathobiology. Exp Eye Res 80, 595-606.

Sparrow, J.R., Ueda, K., and Zhou, J. (2012). Complement dysregulation in AMD: RPE-Bruch's membrane-choroid. Mol Aspects Med 33, 436-445.

Spilsbury, K., Garrett, K.L., Shen, W.Y., Constable, I.J., and Rakoczy, P.E. (2000). Overexpression of vascular endothelial growth factor (VEGF) in the

retinal pigment epithelium leads to the development of choroidal neovascularization. Am J Pathol 157, 135-144.

Spraul, C.W., Lang, G.E., Grossniklaus, H.E., and Lang, G.K. (1999). Histologic and morphometric analysis of the choroid, Bruch's membrane, and retinal pigment epithelium in postmortem eyes with age-related macular degeneration and histologic examination of surgically excised choroidal neovascular membranes. Surv Ophthalmol 44 Suppl 1, S10-32.

Stamer, W.D., Bok, D., Hu, J., Jaffe, G.J., and McKay, B.S. (2003). Aquaporin-1 channels in human retinal pigment epithelium: role in transepithelial water movement. Invest Ophthalmol Vis Sci 44, 2803-2808.

Steinhardt, R.A., Bi, G., and Alderton, J.M. (1994). Cell membrane resealing by a vesicular mechanism similar to neurotransmitter release. Science 263, 390-393.

Stitt, A.W. (2005). The maillard reaction in eye diseases. Ann N Y Acad Sci 1043, 582-597.

Stitt, A.W., He, C., and Vlassara, H. (1999). Characterization of the advanced glycation end-product receptor complex in human vascular endothelial cells. Biochem Biophys Res Commun 256, 549-556.

Stitt, A.W., Hughes, S.J., Canning, P., Lynch, O., Cox, O., Frizzell, N., Thorpe, S.R., Cotter, T.G., Curtis, T.M., and Gardiner, T.A. (2004). Substrates modified by advanced glycation end-products cause dysfunction and death in retinal pericytes by reducing survival signals mediated by platelet-derived growth factor. Diabetologia 47, 1735-1746.

Strauss, O. (2005). The retinal pigment epithelium in visual function. Physiol Rev 85, 845-881.

Stros, M., Ozaki, T., Bacikova, A., Kageyama, H., and Nakagawara, A. (2002). HMGB1 and HMGB2 cell-specifically down-regulate the p53- and p73-dependent sequence-specific transactivation from the human Bax gene promoter. J Biol Chem 277, 7157-7164.

Stypmann, J., Glaser, K., Roth, W., Tobin, D.J., Petermann, I., Matthias, R., Monnig, G., Haverkamp, W., Breithardt, G., Schmahl, W., et al. (2002). Dilated cardiomyopathy in mice deficient for the lysosomal cysteine peptidase cathepsin L. Proc Natl Acad Sci U S A 99, 6234-6239.

Sugano, E., Tomita, H., Abe, T., Yamashita, A., and Tamai, M. (2003). Comparative study of cathepsins D and S in rat IPE and RPE cells. Experimental eye research 77, 203-209.

Suguna, K., Padlan, E.A., Smith, C.W., Carlson, W.D., and Davies, D.R. (1987). Binding of a reduced peptide inhibitor to the aspartic proteinase from Rhizopus chinensis: implications for a mechanism of action. Proc Natl Acad Sci U S A 84, 7009-7013.

Suk, K., Yeou Kim, S., and Kim, H. (2001). Regulation of IL-18 production by IFN gamma and PGE2 in mouse microglial cells: involvement of NF-kB pathway in the regulatory processes. Immunol Lett 77, 79-85.

Sun, K., Cai, H., Tezel, T.H., Paik, D., Gaillard, E.R., and Del Priore, L.V. (2007). Bruch's membrane aging decreases phagocytosis of outer segments by retinal pigment epithelium. Mol Vis 13, 2310-2319.

Sun, M., Ouzounian, M., de Couto, G., Chen, M.Y., Yan, R., Fukuoka, M., Li, G.H., Moon, M., Liu, Y., Gramolini, A., et al. (2013). Cathepsin-L Ameliorates Cardiac Hypertrophy Through Activation of the Autophagy-Lysosomal Dependent Protein Processing Pathways. J Am Heart Assoc 2.

Suter, M., Reme, C., Grimm, C., Wenzel, A., Jaattela, M., Esser, P., Kociok, N., Leist, M., and Richter, C. (2000). Age-related macular degeneration. The lipofusion component N-retinyl-N-retinylidene ethanolamine detaches proapoptotic proteins from mitochondria and induces apoptosis in mammalian retinal pigment epithelial cells. J Biol Chem 275, 39625-39630.

Szumilas, M. (2010). Explaining odds ratios. J Can Acad Child Adolesc Psychiatry 19, 227-229.

Tam, C., Idone, V., Devlin, C., Fernandes, M.C., Flannery, A., He, X., Schuchman, E., Tabas, I., and Andrews, N.W. (2010). Exocytosis of acid sphingomyelinase by wounded cells promotes endocytosis and plasma membrane repair. J Cell Biol 189, 1027-1038.

Tamatani, M., Mitsuda, N., Matsuzaki, H., Okado, H., Miyake, S., Vitek, M.P., Yamaguchi, A., and Tohyama, M. (2000). A pathway of neuronal apoptosis induced by hypoxia/reoxygenation: roles of nuclear factor-kappaB and Bcl-2. J Neurochem 75, 683-693.

Tanabe, H., Kumagai, N., Tsukahara, T., Ishiura, S., Kominami, E., Nishina, H., and Sugita, H. (1991). Changes of Lysosomal Proteinase Activities and Their Expression in Rat Cultured Keratinocytes during Differentiation. Biochimica Et Biophysica Acta 1094, 281-287.

Tang, Q., Cai, J., Shen, D., Bian, Z., Yan, L., Wang, Y.X., Lan, J., Zhuang, G.Q., Ma, W.Z., and Wang, W. (2009). Lysosomal cysteine peptidase cathepsin L protects against cardiac hypertrophy through blocking AKT/GSK3beta signaling. J Mol Med (Berl) 87, 249-260.

Tate, D.J., Jr., Miceli, M.V., and Newsome, D.A. (1995). Phagocytosis and H2O2 induce catalase and metallothionein gene expression in human retinal pigment epithelial cells. Invest Ophthalmol Vis Sci 36, 1271-1279.

Tatti, M., Motta, M., Di Bartolomeo, S., Scarpa, S., Cianfanelli, V., Cecconi, F., and Salvioli, R. (2012). Reduced cathepsins B and D cause impaired autophagic degradation that can be almost completely restored by overexpression of these two proteases in Sap C-deficient fibroblasts. Hum Mol Genet 21, 5159-5173.

Telander, D.G. (2011). Inflammation and age-related macular degeneration (AMD). Semin Ophthalmol 26, 192-197.

Terman, A., Kurz, T., Navratil, M., Arriaga, E.A., and Brunk, U.T. (2010). Mitochondrial turnover and aging of long-lived postmitotic cells: the mitochondrial-lysosomal axis theory of aging. Antioxid Redox Signal 12, 503-535.

Thallas-Bonke, V., Thorpe, S.R., Coughlan, M.T., Fukami, K., Yap, F.Y., Sourris, K.C., Penfold, S.A., Bach, L.A., Cooper, M.E., and Forbes, J.M. (2008). Inhibition of NADPH oxidase prevents advanced glycation end product-mediated damage in diabetic nephropathy through a protein kinase C-alpha-dependent pathway. Diabetes 57, 460-469.

Thannickal, V.J., and Fanburg, B.L. (2000). Reactive oxygen species in cell signaling. Am J Physiol Lung Cell Mol Physiol 279, L1005-1028.

Thornalley, P.J. (1998). Cell activation by glycated proteins. AGE receptors, receptor recognition factors and functional classification of AGEs. Cell Mol Biol (Noisy-le-grand) 44, 1013-1023.

Thorpe, S.R., and Baynes, J.W. (2003). Maillard reaction products in tissue proteins: new products and new perspectives. Amino Acids 25, 275-281.

Tien, L., Rayborn, M.E., and Hollyfield, J.G. (1992). Characterization of the interphotoreceptor matrix surrounding rod photoreceptors in the human retina. Exp Eye Res 55, 297-306.

Towbin, H., Staehelin, T., and Gordon, J. (1992). Electrophoretic transfer of proteins from polyacrylamide gels to nitrocellulose sheets: procedure and some applications. 1979. Biotechnology 24, 145-149.

Trikalinos, T.A., Salanti, G., Khoury, M.J., and Ioannidis, J.P. (2006). Impact of violations and deviations in Hardy-Weinberg equilibrium on postulated gene-disease associations. Am J Epidemiol 163, 300-309.

Tseng, W.A., Thein, T., Kinnunen, K., Lashkari, K., Gregory, M.S., D'Amore, P.A., and Ksander, B.R. (2013). NLRP3 inflammasome activation in retinal pigment epithelial cells by lysosomal destabilization: implications for age-related macular degeneration. Invest Ophthalmol Vis Sci 54, 110-120.

Turk, B., Bieth, J.G., Bjork, I., Dolenc, I., Turk, D., Cimerman, N., Kos, J., Colic, A., Stoka, V., and Turk, V. (1995). Regulation of the activity of lysosomal cysteine proteinases by pH-induced inactivation and/or endogenous protein inhibitors, cystatins. Biol Chem Hoppe Seyler 376, 225-230.

Turk, B., Dolenc, I., Turk, V., and Bieth, J.G. (1993). Kinetics of the pH-induced inactivation of human cathepsin L. Biochemistry 32, 375-380.

Turk, V., and Bode, W. (1991). The cystatins: protein inhibitors of cysteine proteinases. FEBS Lett 285, 213-219.

Turk, V., Stoka, V., and Turk, D. (2008). Cystatins: biochemical and structural properties, and medical relevance. Frontiers in bioscience : a journal and virtual library 13, 5406-5420.

Turk, V., Stoka, V., Vasiljeva, O., Renko, M., Sun, T., Turk, B., and Turk, D. (2012). Cysteine cathepsins: from structure, function and regulation to new frontiers. Biochim Biophys Acta 1824, 68-88.

Turk, V., Turk, B., Guncar, G., Turk, D., and Kos, J. (2002). Lysosomal cathepsins: structure, role in antigen processing and presentation, and cancer. Adv Enzyme Regul 42, 285-303.

Uchimoto, T., Nohara, H., Kamehara, R., Iwamura, M., Watanabe, N., and Kobayashi, Y. (1999). Mechanism of apoptosis induced by a lysosomotropic agent, L-Leucyl-L-Leucine methyl ester. Apoptosis 4, 357-362.

Untergasser, A., Cutcutache, I., Koressaar, T., Ye, J., Faircloth, B.C., Remm, M., and Rozen, S.G. (2012). Primer3--new capabilities and interfaces. Nucleic acids research 40, e115.

van's Gravesande, K.S., Layne, M.D., Ye, Q., Le, L., Baron, R.M., Perrella, M.A., Santambrogio, L., Silverman, E.S., and Riese, R.J. (2002). IFN regulatory factor-1 regulates IFN-gamma-dependent cathepsin S expression. J Immunol 168, 4488-4494.

van der Schaft, T.L., Mooy, C.M., de Bruijn, W.C., Oron, F.G., Mulder, P.G., and de Jong, P.T. (1992). Histologic features of the early stages of age-related macular degeneration. A statistical analysis. Ophthalmology 99, 278-286.

Velilla, S., Garcia-Medina, J.J., Garcia-Layana, A., Dolz-Marco, R., Pons-Vazquez, S., Pinazo-Duran, M.D., Gomez-Ulla, F., Arevalo, J.F., Diaz-Llopis, M., and Gallego-Pinazo, R. (2013). Smoking and age-related macular degeneration: review and update. J Ophthalmol 2013, 895147.

Verzijl, N., DeGroot, J., Thorpe, S.R., Bank, R.A., Shaw, J.N., Lyons, T.J., Bijlsma, J.W., Lafeber, F.P., Baynes, J.W., and TeKoppele, J.M. (2000). Effect of collagen turnover on the accumulation of advanced glycation end products. J Biol Chem 275, 39027-39031.

Vlassara, H., Brownlee, M., and Cerami, A. (1986). Novel macrophage receptor for glucose-modified proteins is distinct from previously described scavenger receptors. J Exp Med 164, 1301-1309.

Vlassara, H., and Bucala, R. (1996). Recent progress in advanced glycation and diabetic vascular disease: role of advanced glycation end product receptors. Diabetes 45 Suppl 3, S65-66.

Vlassara, H., Li, Y.M., Imani, F., Wojciechowicz, D., Yang, Z., Liu, F.T., and Cerami, A. (1995). Identification of Galectin-3 as a High-Affinity Binding-Protein for Advanced Glycation End-Products (Age) - a New Member of the Age-Receptor Complex. Mol Med 1, 634-646.

Wahlbom, M., Wang, X., Lindstrom, V., Carlemalm, E., Jaskolski, M., and Grubb, A. (2007). Fibrillogenic oligomers of human cystatin C are formed by propagated domain swapping. J Biol Chem 282, 18318-18326.

Wallin, H., Abrahamson, M., and Ekstrom, U. (2013). Cystatin C properties crucial for uptake and inhibition of intracellular target enzymes. J Biol Chem 288, 17019-17029.

Wang, A.L., Boulton, M.E., Dunn, W.A., Rao, H.V., Cai, J., Lukas, T.J., and Neufeld, A.H. (2009a). Using LC3 to monitor autophagy flux in the retinal pigment epithelium. Autophagy 5, 1190-1193.

Wang, A.L., Lukas, T.J., Yuan, M., Du, N., Tso, M.O., and Neufeld, A.H. (2009b). Autophagy and exosomes in the aged retinal pigment epithelium: possible relevance to drusen formation and age-related macular degeneration. PLoS One 4, e4160.

Wang, J., Ohno-Matsui, K., Yoshida, T., Kojima, A., Shimada, N., Nakahama, K., Safranova, O., Iwata, N., Saido, T.C., Mochizuki, M., et al. (2008). Altered function of factor I caused by amyloid beta: implication for pathogenesis of age-related macular degeneration from Drusen. J Immunol 181, 712-720.

Wang, L., Clark, M.E., Crossman, D.K., Kojima, K., Messinger, J.D., Mobley, J.A., and Curcio, C.A. (2010). Abundant lipid and protein components of drusen. PLoS One 5, e10329.

Wang, X., Yu, S., Wang, C.Y., Wang, Y., Liu, H.X., Cui, Y., and Zhang, L.D. (2015a). Advanced glycation end products induce oxidative stress and mitochondrial dysfunction in SH-SY5Y cells. In Vitro Cell Dev Biol Anim 51, 204-209.

Wang, X.L., Yu, T., Yan, Q.C., Wang, W., Meng, N., Li, X.J., and Luo, Y.H. (2015b). AGEs Promote Oxidative Stress and Induce Apoptosis in Retinal Pigmented Epithelium Cells RAGE-dependently. J Mol Neurosci.

Wang, Y.R., Qin, S., Han, R., Wu, J.C., Liang, Z.Q., Qin, Z.H., and Wang, Y. (2013). Cathepsin L Plays a Role in Quinolinic Acid- Induced NF-Kb Activation and Excitotoxicity in Rat Striatal Neurons. Plos One 8.

Wang, Z., Paik, D.C., Del Priore, L.V., Burch, R.L., and Gaillard, E.R. (2005). Nitrite-modified extracellular matrix proteins deleteriously affect retinal

pigment epithelial cell function and viability: a comparison study with nonenzymatic glycation mechanisms. Curr Eye Res 30, 691-702.

Wasselius, J., Wallin, H., Abrahamson, M., and Ehinger, B. (2003). Cathepsin B in the rat eye. Graefes Arch Clin Exp Ophthalmol 241, 934-942.

Weiter, J.J., Delori, F.C., Wing, G.L., and Fitch, K.A. (1986). Retinal pigment epithelial lipofuscin and melanin and choroidal melanin in human eyes. Invest Ophthalmol Vis Sci 27, 145-152.

Wilder, C.L., Park, K.Y., Keegan, P.M., and Platt, M.O. (2011). Manipulating substrate and pH in zymography protocols selectively distinguishes cathepsins K, L, S, and V activity in cells and tissues. Arch Biochem Biophys 516, 52-57.

Wille, A., Gerber, A., Heimburg, A., Reisenauer, A., Peters, C., Saftig, P., Reinheckel, T., Welte, T., and Buhling, F. (2004). Cathepsin L is involved in cathepsin D processing and regulation of apoptosis in A549 human lung epithelial cells. Biological Chemistry 385, 665-670.

Wille, A., Heimburg, A., Gerber, A., Reisenauer, A., Welte, T., and Buhling, F. (2002). Functional consequences of cathepsin L deficiency in human lung epithelial cells. Biol Chem 383, 1291-1296.

Winkler, B.S., Boulton, M.E., Gottsch, J.D., and Sternberg, P. (1999). Oxidative damage and age-related macular degeneration. Mol Vis 5, 32.

Wistow, G., Bernstein, S.L., Wyatt, M.K., Fariss, R.N., Behal, A., Touchman, J.W., Bouffard, G., Smith, D., and Peterson, K. (2002). Expressed sequence tag analysis of human RPE/choroid for the NEIBank Project: over 6000 non-redundant transcripts, novel genes and splice variants. Mol Vis 8, 205-220.

Wu, H.Y., and Lozano, G. (1994). Nf-Kappa-B Activation of P53 - a Potential Mechanism for Suppressing Cell-Growth in Response to Stress. Journal of Biological Chemistry 269, 20067-20074.

Wu, Y., Yanase, E., Feng, X., Siegel, M.M., and Sparrow, J.R. (2010). Structural characterization of bisretinoid A2E photocleavage products and implications for age-related macular degeneration. Proc Natl Acad Sci U S A 107, 7275-7280.

Wu, Y.L., Li, J., and Yao, K. (2013). Structures and biogenetic analysis of lipofuscin bis-retinoids. Journal of Zhejiang University Science B 14, 763-773.

Xiang, B., Fei, X., Zhuang, W., Fang, Y., Qin, Z., and Liang, Z. (2011). Cathepsin L is involved in 6-hydroxydopamine induced apoptosis of SH-SY5Y neuroblastoma cells. Brain Res 1387, 29-38.

Yang, H.A., Hreggvidsdottir, H.S., Palmblad, K., Wang, H.C., Ochani, M., Li, J.H., Lu, B., Chavan, S., Rosas-Ballina, M., Al-Abed, Y., et al. (2010). A critical cysteine is required for HMGB1 binding to Toll-like receptor 4 and activation of macrophage cytokine release. P Natl Acad Sci USA 107, 11942-11947.

Yang, Z., and Klionsky, D.J. (2010). Mammalian autophagy: core molecular machinery and signaling regulation. Curr Opin Cell Biol 22, 124-131.

Yin, D. (1996). Biochemical basis of lipofuscin, ceroid, and age pigment-like fluorophores. Free Radic Biol Med 21, 871-888.

Yorimitsu, T., and Klionsky, D.J. (2005). Autophagy: molecular machinery for self-eating. Cell Death Differ 12 Suppl 2, 1542-1552.

Young, R.W. (1967). The renewal of photoreceptor cell outer segments. J Cell Biol 33, 61-72.

Young, R.W. (1988). Solar radiation and age-related macular degeneration. Surv Ophthalmol 32, 252-269.

Young, R.W., and Bok, D. (1969). Participation of the retinal pigment epithelium in the rod outer segment renewal process. J Cell Biol 42, 392-403.

Young, R.W., and Droz, B. (1968). The renewal of protein in retinal rods and cones. J Cell Biol 39, 169-184.

Yu, B., Xu, P., Zhao, Z., Cai, J., Sternberg, P., and Chen, Y. (2014). Subcellular distribution and activity of mechanistic target of rapamycin in aged retinal pigment epithelium. Invest Ophthalmol Vis Sci 55, 8638-8650.

Zatterstrom, U.K., Felbor, U., Fukai, N., and Olsen, B.R. (2000). Collagen XVIII/endostatin structure and functional role in angiogenesis. Cell structure and function 25, 97-101.

Zdolsek, J., Zhang, H., Roberg, K., and Brunk, U. (1993). H2O2-mediated damage to lysosomal membranes of J-774 cells. Free Radic Res Commun 18, 71-85.

Zhang, L., Wang, H.D., Xu, J.G., Zhu, J.H., and Ding, K. (2014). Inhibition of cathepsin S induces autophagy and apoptosis in human glioblastoma cell lines through ROS-mediated PI3K/AKT/mTOR/p70S6K and JNK signaling pathways. Toxicol Lett 228, 248-259.

Zhang, X.J., Chen, S., Huang, K.X., and Le, W.D. (2013). Why should autophagic flux be assessed? Acta Pharmacol Sin 34, 595-599.

Zhang, Y.F., Wei, W., Li, L., Tu, G., Zhang, Y., Yang, J., and Xing, Y. (2015). Sirt1 and HMGB1 Regulate the AGE-Induced Pro-Inflammatory Cytokines in Human Retinal Cells. Clin Lab 61, 999-1008.

Zhou, J., Jang, Y.P., Kim, S.R., and Sparrow, J.R. (2006). Complement activation by photooxidation products of A2E, a lipofuscin constituent of the retinal pigment epithelium. Proc Natl Acad Sci U S A 103, 16182-16187.

Zimmerman, W.F., Godchaux, W., 3rd, and Belkin, M. (1983). The relative proportions of lysosomal enzyme activities in bovine retinal pigment epithelium. Exp Eye Res 36, 151-158.

Zinn, K.M., and Marmor, M.F. (1979). The Retinal pigment epithelium (Cambridge, Mass.: Harvard University Press).

Zorov, D.B., Juhaszova, M., and Sollott, S.J. (2014). Mitochondrial reactive oxygen species (ROS) and ROS-induced ROS release. Physiol Rev 94, 909-950.

Zurdel, J., Finckh, U., Menzer, G., Nitsch, R.M., and Richard, G. (2002). CST3 genotype associated with exudative age related macular degeneration. Br J Ophthalmol 86, 214-219.

Zuzarte-Luis, V., Montero, J.A., Kawakami, Y., Izpisua-Belmonte, J.C., and Hurle, J.M. (2007). Lysosomal cathepsins in embryonic programmed cell death. Dev Biol 301, 205-217.

Zweifel, S.A., Imamura, Y., Spaide, T.C., Fujiwara, T., and Spaide, R.F. (2010). Prevalence and significance of subretinal drusenoid deposits (reticular pseudodrusen) in age-related macular degeneration. Ophthalmology 117, 1775-1781.

Appendix 1 - Buffers and solutions

The following buffers and solutions were prepared and used in the procedures undertaken in this study.

10X Tris-Borate-EDTA (TBE) Electrophoresis Buffer

108g Tris

55g Orthoboric Acid ($B(OH)_3$)

2.92g EDTA

Solution was made up to 1L with ddH_2O. Stock solution was diluted 1:9 with ddH_2O to achieve 1X TBE working concentration.

10X Gel Loading Buffer

3X TBE

0.1% (w/v) Bromophenol Blue

0.2% (w/v) Xylene Cyanol

20% (w/v) Ficoll 400

Stock solution was diluted 1:20 with ddH_2O to achieve 0.5X loading buffer concentration.

Agarose gel electrophoresis

1.5g Analysis grade Agarose (Fisher Scientific, UK)

Solution was made up to 100ml with 1X TBE electrophoresis buffer in a flask.

Resolving gel buffer (3M Tris-HCl, pH 8.85)

33.33g Tris base

Initially, solution was made up to 80ml with ddH_2O after which the desired pH was achieved by addition of HCl. The final volume was then adjusted to 100ml with ddH_2O.

Stacking gel buffer (0.25M Tris-HCl, pH 6.8

3.028g Tris base

Initially, solution was made up to 80ml with ddH_2O after which the desired pH was achieved by addition of HCl. The final volume was then adjusted to 100ml with ddH_2O.

5X running buffer for SDS-PAGE

15.1 Tris base

94g Glycine

50ml 10% SDS stock solution

Solution final volume was adjusted to 1L with ddH_2O. The working concentration used in experiments was 1X and this was achieved by the diluting the 5X stock 1:4 with ddH_2O.

N.B. a separate 5X running buffer was also prepared in which no SDS was added for use in preparation of transfer buffer.

Transfer buffer for immunoblotting

100ml 5X running buffer (minus SDS)

233ml 100% Ethanol

667ml ddH_2O

10X TBS, pH 7.6

80g NaCl

24.2g Tris

Initially, solution was made up to 900ml with ddH_2O after which the desired pH was achieved by addition of HCl. The final volume was then adjusted to 1L with ddH_2O.

Wash buffer for immunoblotting

100ml 10X TBS

899ml ddH_2O

1ml Tween-20

Blocking Buffer for immunoblotting

5g Dried skimmed milk powder

100ml Wash Buffer

All membranes were blocked in 5% milk with antibodies diluted in either a solution of 5% milk or Bovine serum albumin (BSA) unless stated otherwise.

Stripping solution, pH 6.7

4.16ml 3M Tris (Resolving gel buffer pH 8.85)

40ml 10% SDS stock solution

Initially, 140 ml of ddH_2O was added after which the desired pH was achieved by addition of HCl. The final volume was then adjusted to 200ml with ddH_2O. Before using, 175µl of 2-β-mercaptoethanol was added to 25ml of solution which had pre-warmed to 65^oC.

Laemmli lysis buffer (for lysing cells)

10ml 10% SDS stock solution

10ml Glycerol

10ml 2-β-mercaptoethanol

16ml 0.25M Tris (Stacking gel buffer pH 6.8)

Solution was made up to 100ml with ddH_2O and a few speckles of Bromophenol blue was added to give a colour.

10X Loading buffer (Laemmli buffer)

1.6ml 10% SDS stock solution

0.8ml Glycerol

0.4ml 2-β-mercaptoethanol

2ml 0.25M Tris (Stacking gel buffer pH 6.8)

Solution was made up to 8ml with ddH_2O and a few speckles of Bromophenol blue was added to give a colour.

0.25% Potassium permanganate ($KMnO_4$)

1g $KMnO_4$ powder

400 ml of ddH_2O was added to the powder and stirred until fully dissolved.

1% Oxalic acid

4g Oxalic acid powder

400ml of ddH_2O was added to the powder and stirred until fully dissolved.

Appendix 2 - A missense variant in CST3 exerts a recessive effect on susceptibility to age-related macular degeneration resembling its association with Alzheimer's disease